Factors controlling the lipid composition of marine planktonic Thaumarchaeota

Dissertation zur Erlangung des Doktorgrades der Naturwissenschaften
Dr. rer. nat.

Am Fachbereich Geowissenschaften
der Universität Bremen

vorgelegt von

Felix J. Elling

Bremen
April 2015

1. Gutachter: Prof. Dr. Kai-Uwe Hinrichs
2. Gutachter: Prof. Dr. Ann Pearson

Datum des Promotionskolloquiums: 13.08.2015

Contents

ABSTRACT

Marine ammonia-oxidizing archaea of the phylum *Thaumarchaeota* are a cosmopolitan group of microorganisms representing a major fraction of the picoplankton in the ocean. They play a key role in the global cycles of carbon and nitrogen. *Thaumarchaeota* synthesize glycerol dibiphytanyl glycerol tetraether (GDGT) membrane lipids that are used as biomarkers for their abundance and activity in the marine water column. However, the interpretation of GDGT distributions as biomarkers of living *Thaumarchaeota* is restricted due to the paucity of direct observations in culture experiments and the limited availability of cultured thaumarchaeal representatives. Fossil GDGTs are used for the reconstruction of past sea surface temperatures, e.g., by means of the TEX_{86} paleothermometer, which is based on the empirical correlation of the degree of GDGT cyclization in core-top sediments and sea surface temperature. However, widely observed discrepancies between observed *in situ*- and predicted TEX_{86}-temperatures throughout the marine water column and multiple regional calibration lines indicate that the physiological and ecological controls on lipid composition in planktonic *Thaumarchaeota* remain poorly understood. Thus, constraining the influence of physiological and environmental parameters on membrane lipid composition in cultured marine *Thaumarchaeota* is crucial to enhance our ability to reliably reconstruct past environments based on the geologic record and to utilize GDGTs as biomarkers for thaumarchaeal distribution, seasonality and activity in the marine water column.

In this thesis, the influences of growth phase, temperature, salinity, and pH on lipid composition were investigated in pure cultures of the marine planktonic thaumarchaeon *Nitrosopumilus maritimus*. Characteristic intact polar GDGTs with hexose-phosphohexose headgroups are particularly abundant during growth of *N. maritimus* but are nearly absent under stationary conditions, demonstrating a high potential of hexose-phosphohexose GDGTs as biomarkers for active *Thaumarchaeota* in the environment. A strong increase in TEX_{86}-temperatures between growth and stationary phases suggests an influence of the metabolic state of *Thaumarchaeota* on the TEX_{86} index. In contrast, even large differences in salinity from 27 to 51‰ had no significant effect on intact polar GDGT composition and TEX_{86} values in *N. maritimus*. Variations in pH between 7.3 and 7.9 showed little influence on intact polar GDGT composition and only slightly elevated TEX_{86} values at lower pH. While these results are compelling, it remains to be determined to what extent other parameters such as seawater oxygen availability and nutrient supply/growth rate control thaumarchaeal lipid patterns. In order to investigate the influence of temperature on lipid composition, two novel thaumarchaeal strains that are phylogenetically closely related to *N. maritimus* were isolated from the South Atlantic Ocean. Disparate responses of membrane lipid composition to temperature in *N. maritimus* and the closely related strains suggest that variation in thaumarchaeal community composition in the environment may have a profound impact on TEX_{86} signatures. Overall, these growth experiments indicate that the TEX_{86} paleotemperature proxy is not solely dependent on temperature, but

amalgamates several physiological and environmental factors such as phylogenetic composition and metabolic state of marine archaeal communities.

The lipidomes of 11 thaumarchaeal pure and enrichment cultures were studied using novel, comprehensive analytical protocols aiming at identifying diagnostic lipid biomarkers for the activity and abundance of specific thaumarchaeal clades. These analyses demonstrate that *Thaumarchaeota* contain an unprecedented diversity of membrane lipids that is related to phylogeny as well as growth characteristics. Complementary analyses of 21 euryarchaeal and crenarchaeal species indicate that the novel lipid methoxy archaeol is found exclusively in *Thaumarchaeota*. The analysis of the distribution of this compound in the water column of the equatorial North Pacific Ocean highlights the significance of methoxyarchaeol as a biomarker for *Thaumarchaeota* in the marine environment.

Application of novel chromatographic protocols further enabled the identification of two respiratory quinones, i.e., lipids involved in cellular energy transfer, which are specific for *Thaumarchaeota*. Analyses of the respiratory quinone composition of 25 euryarchaeal, crenarchaeal and thaumarchaeal species indicate that i) respiratory quinones can be used to distinguish environmentally relevant archaeal clades and metabolisms, and ii) that the phylogenetic distribution of respiratory quinone types among archaea results from a combination of vertical inheritance, gene loss, and lateral gene transfer. The coherent distribution of thaumarchaeal respiratory quinones and membrane lipids in samples from the Black Sea water column suggests a high potential for respiratory quinones as biomarkers in the marine environment. A comprehensive case study in the Black Sea demonstrates that combined membrane lipid and respiratory quinone profiling allows tracing the abundances and metabolic processes of bacterial, archaeal, and eukaryotal clades involved in the cycling of carbon, nitrogen, and sulfur. The obtained respiratory quinone profiles reflect and resolve the expected microbial stratification of the Black Sea. Therefore, the simultaneous analysis of these compounds and membrane lipids appears to be a promising technique for enhancing the quantitative aspect of membrane lipid analyses with process-related information from respiratory quinones.

ZUSAMMENFASSUNG

Marine Ammoniak-oxidierende Archaeen des Phylums *Thaumarchaeota* sind eine weitverbreitete Gruppe von Mikroorganismen, die einen großen Anteil des Pikoplanktons im Ozean ausmachen. Sie spielen zudem eine Schlüsselrolle in den globalen Kohlenstoff- und Stickstoffkreisläufen. Thaumarchaeen synthetisieren Glyzerol Dibiphytanyl Glyzerol Tetraether (GDGT)-Membranlipide, die als Biomarker für ihre Verteilung und Aktivität im Ozean verwendet werden. Die Verteilungen von GDGTs im Ozean können aufgrund fehlender direkter Beobachtungen in Kulturexperimenten nur eingeschränkt interpretiert werden. Dies ist unter anderem auf die geringe Zahl an verfügbaren Kulturen planktonischer Thaumarchaeen zurückzuführen. Fossile GDGTs werden für die Rekonstruktion von Oberflächentemperaturen des Ozeans verwendet, z.B. mithilfe des TEX_{86}-Paläothermometers, das auf der empirischen Korrelation von Oberflächentemperaturen des Ozeans mit dem Zyklisierungsgrad von fossilen GDGT-Lipiden in marinen Oberflächensedimenten beruht. Weithin beobachtete Abweichungen von *in situ*- und TEX_{86}-basierten Ozeanoberflächentemperaturen und die verbreitete Verwendung regionaler statt globaler Kalibrationen weisen darauf hin, dass die physiologischen und ökologischen Einflussfaktoren auf die Lipidzusammensetzung in planktonischen Archaeen unzureichend verstanden sind. Es ist daher von großer Bedeutung, den Einfluss dieser Faktoren auf die Lipidzusammensetzung in kultivierten marinen Thaumarchaeen zu untersuchen und einzugrenzen, um die Verlässlichkeit von Rekonstruktionen vergangener Umweltbedingungen basierend auf geologischen Ablagerungen zu erhöhen sowie die Anwendung von GDGTs als Anzeiger für die Verteilung, Saisonalität and Aktivität von Thaumarchaeen im Ozean zu verbessern.

In dieser Dissertation werden die Einflüsse von Wachstumsphasen, Temperatur, Salinität und pH auf die Lipidzusammensetzung von Thaumarchaeen basierend auf Reinkulturen des marinen planktonischen Archaeons *Nitrosopumilus maritimus* untersucht. Charakteristische intakte polar GDGTs mit einer Hexose-Phosphohexose-Kopfgruppe treten besonders stark während des Wachstums von *N. maritimus* auf, sind jedoch kaum während der stationären Phase vorhanden, was auf ein hohes Potential von Hexose-Phosphohexose-GDGTs als Anzeiger von aktiven Thaumarchaeen in der Umwelt hindeutet. Ein starker Anstieg von TEX_{86}-Temperaturen von der Wachstumsphase zur stationären Phase verdeutlicht einen Einfluss der metabolischen Aktivität von Thaumarchaeen auf das TEX_{86}-Paläothermometer. Im Gegensatz dazu wiesen auch große Veränderungen der Salinität (27-51‰) keinen signifikanten Effekt auf die Zusammensetzung intakter polarer GDGTs und TEX_{86}-Werten in *N. maritimus* auf. Veränderungen des pH-Wertes im Bereich 7.3 bis 7.9 zeigten nur eine geringe Auswirkungen auf Zusammensetzung intakter polarer GDGTs, und führten zu leicht erhöhten TEX_{86}-Werten im unteren Spektrum des untersuchten pH-Bereiches. Es bleibt jedoch ungeklärt inwiefern andere Umweltfaktoren, wie zum Beispiel Sauerstoffkonzentrationen und Nährstoffzufuhr/Wachstumsrate die Lipidmuster in Thaumarchaeen beeinflussen. Um die Auswirkungen von Temperaturveränderungen auf die Lipidzusammensetzung zu

untersuchen, wurden zwei neue Stämme von Thaumarchaeen, die phylogenetisch eng mit *N. maritimus* verwandt sind, aus dem Südatlantik isoliert. Die Untersuchungen zeigen abweichende Beziehungen zwischen Wachstumstemperaturen und TEX_{86}-Werten in *N. maritimus* und den eng verwandten neuen Stämmen. Dies deutet darauf hin, dass die Zusammensetzung der mikrobiellen Gemeinschaft von Thaumarchaeen in der Umwelt eine große Auswirkung auf TEX_{86}-Signaturen haben kann. Die durchgeführten Kulturexperimente zeigen daher, dass das TEX_{86}-Paläothermometer nicht nur von Temperaturveränderungen sondern ebenso von physiologischen und ökologischen Faktoren, wie z.B. der Zusammensetzung der Mikroben-Vergesellschaftung und dem Stoffwechselzustand von marinen Thaumarchaeen, stark beeinflusst wird.

Die Lipidzusammensetzung von 11 Anreicherungskulturen und Reinkulturen von Thaumarchaeen wurde mittels neuartiger, umfassender analytischer Methoden mit der Zielsetzung untersucht, neuartige diagnostische Lipide für die Aktivität und Abundanz verschiedener Untergruppen der Thaumarchaeen zu finden. Die Analysen zeigen, dass Thaumarchaeen eine große Diversität an Membranlipiden synthetisieren, die charakteristisch für die phylogenetischen Untergruppen und Wachstumseigenschaften der jeweiligen Thaumarchaeen sind. Zusätzliche Analysen von 21 weiteren Spezies der Euryarchaeen und Crenarchaeen bestätigen, dass das neuartige Lipid Methoxyarchaeol ausschließlich von Thaumarchaeen synthetisiert wird. Die Analyse der Verteilung dieses Moleküls in Wasserproben aus dem äquatorialen Nordpazifik zeigt, dass Methoxyarchaeol in der Umwelt als Biomarker für Thaumarchaeen verwendet werden kann.

Die Anwendung der neuen chromatographischen Methoden ermöglichte außerdem die Identifizierung zweier Thaumarchaeen-spezifischer respiratorischer Chinone, d.h. Moleküle, die als Elektronenüberträger in der Atmungskette fungieren. Die Analyse der Chinonzusammensetzung von 25 Spezies der Phyla *Thaumarchaeota*, *Euryarchaeota* und *Crenarchaeota* weist darauf hin, dass 1.) umweltrelevante Gruppen der Archaeen und dazugehörige Metabolismen anhand der Verteilung von respiratorischen Chinonen unterschieden werden können, und 2.), dass die Verteilung von Chinon-Typen innerhalb der Domäne *Archaea* wahrscheinlich evolutionär aus einer Kombination von Vererbung, Genverlust, und horizontalem Gentransfer hervorgegangen sind. Die identische Verteilung von thaumarchaeellen Chinonen und Membranlipiden in Wasserproben aus dem Schwarzen Meer legt nahe, dass die identifizierten spezifischen respiratorischen Chinone ein hohes Potential als Biomarker für Thaumarchaeen besitzen. Eine ausführliche Untersuchung von Wasserproben aus dem Schwarzen Meer zeigt, dass die gemeinsame Analyse von Membranlipiden und Chinonen es ermöglicht, die Verteilung und metabolischen Eigenschaften von Bakterien, Archaeen und Eukaryoten aufzuklären, die die biogeochemischen Kreisläufe von Kohlenstoff, Stickstoff und Schwefel beeinflussen. Insgesamt reflektieren die ermittelten Chinonprofile daher die erwartete Stratifizierung mikrobieller Gemeinschaften im Schwarzen Meer. Die gleichzeitige Analyse von Chinonen und Membranlipiden erscheint daher als eine erfolgversprechende Methode um die quantitativen Informationen aus Membranlipidprofilen mit prozessbasierten Informationen aus Chinonprofilen zu hinterlegen.

ACKNOWLEDGEMENTS

Kai, thank you for the long years of supervision, for getting me started in science and giving me the freedom and resources for pursuing also my own ideas. You opened up a whole new world of opportunities to me. A special thanks to you, Martin, for mentoring me over the last three years and showing me how to cultivate and care for our single-celled pets. I learned everything I know about *Thaumarchaeota* from you. I would like to thank Ann Pearson for serving on my thesis committee and agreeing to review my thesis, I hope you will find it a worthwhile read. I would also like to thank Wolfgang Bach, Jan-Hendrik Hehemann, and Andreas Greve for their work in my thesis committee.

Julius, thank you for answering the countless questions (and your patience) about almost any aspect of lipid analysis that I have thrown at you over the past years. Kevin, thank you for contributing to many of my projects, keeping up my spirit, and sharing your ideas unconditionally. Jan, Marcos, Miri, Nadine, Xiaolei, Chun, Travis, Frauke, Marcus, Matthias, Florence and Guangchao: thank you for sharing countless ideas, data, and extensive discussions that you will find reflected in this thesis. Sarah, it was a pleasure working with you. Thank you for sharing the burden of never-ending chemostat shifts.

Thank you, Lars, Xavi, Jenny, Heidi, Evert, and Jessica for keeping the labs running smoothly and supporting all kinds of analyses that form the foundations of this thesis. Thank you to all the Hinrichs lab members that are not mentioned here for creating a wonderful and collaborative working atmosphere. You make this group a unique workplace and a second (if not first) home to me. I would also like to thank my students Nadine Smit, Andreas Greve, and Mirko Lange who greatly supported my work. I have gained as much from working with you as you might have from me.

Last but not least, thanks to my friends and family for their support and for understanding why I had to be absent for the better part of the last three years. Julka, thank you for your love and support and for reminding me that science is always fun when we keep our spirits up.

List of Abbreviations

1G	Monoglycosyl
2G	Diglycosyl
3G	Triglycosyl
amoA	Ammonia monooxygenase subunit A
AEG	Acyletherglycerol
Anammox	Anaerobic ammonium oxidation
ANME	Anaerobic methanotrophic archaea
AOA	Ammonia-oxidizing archaea
AR	Archaeol
BDTQ	Benzodithiophenoquinone
BL	Betaine lipid
C-GDGT	Core glycerol dialkyl glycerol tetraether
Cer	Ceramide (sphingosine)
ChQ	Chlorobiumquinone
CQ	Caldariellaquinone
Cren	Crenarchaeol
Cren'	Crenarchaeol regioisomer
DAG	Diacylglycerol
DEG	Dietherglycerol
deoxyG	Deoxyhexose
DMK	Demethylmenaquinone
DMMK	Dimethylmenaquinone
DPG	Diphosphatidylglycerol
FID	Flame ionization detector
GC	Gas chromatograph
GDD	Glycerol dialkanol diether
GDGT	Glycerol dibiphytanyl glycerol tetraether
GTGT	Glycerol trialkyl glycerol tetraether
HPH	Hexose-phosphohexose
HPLC	High performance liquid chromatography

HWCG-III ..... Hot Water Crenarcheotic Group III
IP-AR ..... Intact polar archaeol
IP-GDGT ..... Intact polar glycerol dibiphytanyl glycerol tetraether
IPL ..... Intact polar lipid
MeO-AR ..... Methoxy archaeol
MeO-GDGT .... Methoxy glycerol dibiphytanyl glycerol tetraether
MG-I/II/III/IV . Marine Group I/II/III/IV
MK ..... Menaquinone
MMK ..... Methylmenaquinone
MP ..... Methanophenazine
MS ..... Mass spectrometer/spectrometry
MTK ..... Methionaquinone
NP ..... Normal phase
OH-AR ..... Hydroxyarchaeol
OH-GDGT ..... Hydroxylated glycerol dibiphytanyl glycerol tetraether
OH-MP ..... Hydroxymethanophenazine
OL ..... Ornithine lipid
PC ..... Phosphatidylcholine
PDME ..... Phosphatidyldimethylethanolamine
PE ..... Phosphatidylethanolamine
PG ..... Phosphatidylglycerol
PH ..... Phosphohexose
PI ..... Phosphatidylinositol
PME ..... Phosphatidylmethylethanolamine
PQ ..... Plastoquinone
qToF-MS ..... quadrupole time-of-flight mass spectrometer
RI ..... Ring index
RP ..... Reversed phase
SAGMCG-1 .... South African Gold Mine Group 1
SQ ..... Sulfolobusquinone
TEX_{86} ..... Tetraether index of tetraethers consisting of 86 carbon atoms
TEX_{86}^{H} ..... TEX index for high temperatures
TEX_{86}^{L} ..... TEX index for low temperatures
TLE ..... Total lipid extract
UQ ..... Ubiquinone

CHAPTER 1

Introduction

1.1. *Archaea* – The third domain of life

Life on Earth is commonly classified into three domains on the basis of phenotypic and phylogenetic evidence (WOESE and FOX, 1977; WOESE et al., 1990). The two domains *Bacteria* and *Archaea*, the prokaryotes, comprise single-celled microorganisms in which cellular components such as ribosomes and DNA are enclosed together in the cytosol and that show only basic cellular compartmentalization (BROWN and DOOLITTLE, 1997). In contrast, the *Eukarya* (e.g., protists, fungi, animals, plants and algae) are single celled or multicellular organisms that show high levels of compartmentalization and in which the DNA is enclosed in a nucleus separate from other cellular components (LODISH et al., 2000).

Due to this dichotomy between simple and complex cellular organization, the *Archaea* were long regarded as a subdivision of the *Bacteria* ('archaebacteria'). However, with the advent of molecular phylogenetic techniques, the *Archaea* were re-discovered as a separate domain of life, distinct both phenotypically and genotypically from the *Bacteria* and *Eukarya* (WOESE and FOX, 1977; WOESE et al., 1978; WOESE et al., 1990). While *Archaea* share many features, such as genome organization, with *Bacteria* (BROWN and DOOLITTLE, 1997), their unique membrane lipids are distinct from *Bacteria* and *Eukarya* (Section 1.4; KATES, 1993; KOGA and MORII, 2005). In contrast, *Archaea* and *Eukarya* show high similarities in DNA transcription, messenger RNA translation, and cell division (BROWN and DOOLITTLE, 1997; LINDÅS et al., 2008; PELVE et al., 2011), which have led to the controversial proposal of a common evolutionary ancestor of *Archaea* and *Eukarya* distinct from *Bacteria* (e.g., EMBLEY and MARTIN, 2006; WILLIAMS et al., 2013; CAVALIER-SMITH, 2014; GUY et al., 2014).

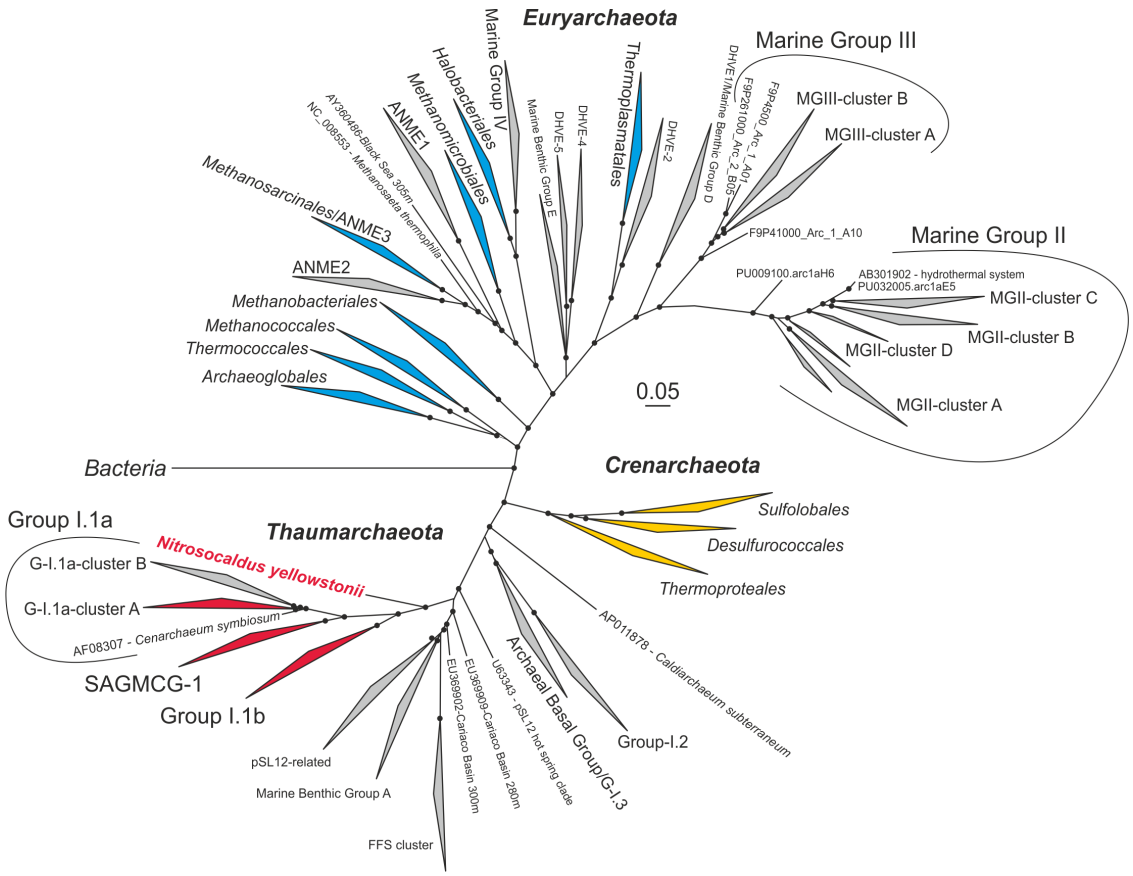

Figure 1.1. Maximum-likelihood phylogenetic tree of archaeal small sub-unit 16S rRNA gene sequences from environmental samples and cultivated species. Phylogenetic groups containing cultivated representatives are highlighted in red (*Thaumarchaeota*), yellow (*Crenarchaeota*), and blue (*Euryarchaeota*; modified from ULLOA et al., 2013). The scale bar indicates the expected changes per sequence position along the branches.

Based on 16S rRNA, a highly conserved gene found in all prokaryotes, and whole-genome sequences, the domain archaea is commonly subdivided into three major phyla, the *Crenarchaeota*, the *Euryarchaeota* and the recently proposed *Thaumarchaeota* (WOESE et al., 1990; BROCHIER-ARMANET et al., 2008; STIEGLMEIER et al., 2014a). Furthermore, the phyla *Korarchaeota* and *Nanoarchaeota* were proposed based on genome sequences of an enrichment culture and a single isolate, respectively (HUBER et al., 2002; ELKINS et al., 2008; BROCHIER-ARMANET et al., 2011). Apart from some methanogenic lineages, archaea have classically been regarded as obligate extremophiles (e.g., WOESE and FOX, 1977; DELONG, 1998, and references therein).

Extremophilic archaea inhabit a wide range of environments spanning pH gradients of -0.06 to 11 (SCHLEPER et al., 1995; KAMEKURA et al., 1997), salinities up to NaCl saturation (KAMEKURA, 1998), temperatures of up to 122 °C (KASHEFI and LOVLEY, 2003; TAKAI et al., 2008) and subsurface depths of up to 2-3 km (TAKAI et al., 2001; BIDDLE et al., 2006; CIOBANU et al., 2014). More recently however, archaea of all

three major phyla have been recognized to be particularly abundant in non-extreme habitats such as soils, lakes and the ocean (e.g., DELONG, 1998; SCHLEPER et al., 2005; AUGUET et al., 2010; STAHL and DE LA TORRE, 2012).

1.2. Archaeal life in the ocean and the phylum *Thaumarchaeota*

1.2.1. Discovery of mesophilic planktonic archaea

The ocean is considered to be Earth's largest biome and hosts a vast diversity and abundance of prokaryotes (WHITMAN et al., 1998; KALLMEYER et al., 2012). Within the ocean, redox reactions mediated by prokaryotes are major components of the cycles of carbon, nitrogen, sulfur and other biologically active elements (NEWMAN and BANFIELD, 2002; DIETRICH et al., 2006; FALKOWSKI et al., 2008). Until the 1990s, only thermophilic and methanogenic archaea had been identified in the marine environment using cultivation techniques (ZEIKUS, 1977; STETTER et al., 1990). Based on novel lipid-based, cultivation, and cultivation-independent techniques, the roles of mesophilic archaea in biogeochemical cycles became increasingly revealed during the last two decades (PACE, 1997; DELONG, 1998; SCHLEPER et al., 2005; JARRELL et al., 2011).

A major paradigm shift in archaeal ecology was the discovery of a novel group of archaea by sequencing of archaeal 16S rRNA genes from open ocean water samples (DELONG, 1992; FUHRMAN et al., 1992). This novel archaeal group was remotely related to cultivated *Crenarchaeota* and thus named Marine Group I *Crenarchaeota* (MG-I, Figure 1.1). Furthermore, DELONG (1992) identified a cluster of sequences distantly related to cultivated *Euryarchaeota* of the order *Thermoplasmatales* (Marine Group II; Figure 1.1). Sequences affiliated with these archaeal groups, in particular MG-I, were subsequently detected in a broad range of environments, such as marine sediments, lakes, rivers, and soils (BINTRIM et al., 1997; DELONG, 1998; SCHLEPER et al., 2005). Two other euryarchaeal groups were later detected in marine water samples and sediments, the MG-III (FUHRMAN and DAVIS, 1997; MUNSON and NEDWELL, 1997) which are related to the Marine Group II *Euryarchaeota*, as well as the Marine Group IV *Euryarchaeota*, which are related to the *Halobacteriales* but only rarely detected in metagenomic surveys (Figure 1.1 LÓPEZ-GARCÍA et al., 2001; BANO et al., 2004).

Molecular surveys revealed that MG-I are particularly abundant in the deep ocean below 100 m, while MG-II are the dominant archaeal group in the upper photic zone (Figure 1.2a; MASSANA et al., 1997, 1998; MASSANA et al., 2000). In addition to the ubiquitous distribution, MG-I account for up to 40% of the picoplankton in the deep ocean (KARNER et al., 2001) and about 20% of the total picoplankton in the global ocean (Figure 1.2a; SCHATTENHOFER et al., 2009), amounting to a total of 6×10^{27} to 1.3×10^{28} cells.

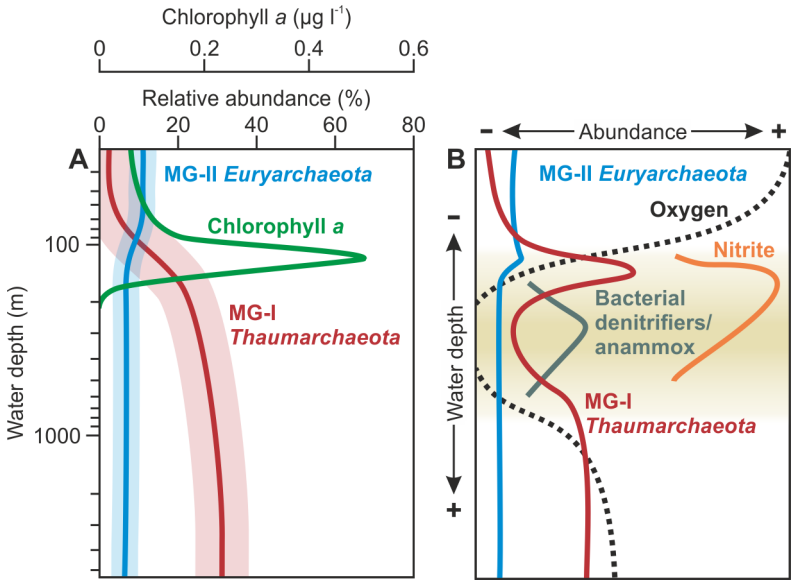

Figure 1.2. (A) Conceptual representation of abundances of Marine Group I *Thaumarchaeota* and Marine Group II *Euryarchaeota* relative to total picoplankton in the marine water column showing a maximum of *Thaumarchaeota* near the deep chlorophyll maximum and higher relative abundances of *Euryarchaeota* in surface waters (based on fluorescence *in situ* hybridization counts of KARNER et al. (2001) from the Hawaii Ocean Time Series as well as SCHATTENHOFER et al. (2009) and TEIRA et al. (2006) from the North Atlantic Ocean). Chlorophyll *a* concentrations were extracted from the Hawaii Ocean Time Series dataset[1], station ALOHA. (B) Conceptual representation of archaeal community structure as well as denitrifying and anaerobic ammonium-oxidizing (anammox) bacteria in oceanic oxygen minimum zones (based on BELMAR et al., 2011; LAM and KUYPERS, 2011; PITCHER et al., 2011b; PODLASKA et al., 2012; ULLOA et al., 2012).

Despite their high abundances and ubiquity, the metabolisms and ecology of planktonic archaea remained elusive. A major advancement was the identification of the sponge symbiont *Cenarchaeum symbiosum*, phylogenetically affiliated with the MG-I *Crenarchaeota* (PRESTON, 1996) and the detection lipid biomarkers typically found in cultivated *Crenarchaeota* in this organism (DELONG et al., 1998). The ^{13}C and ^{14}C signatures of these lipids in water column and sediment samples (HOEFS et al., 1997; KUYPERS et al., 2001; PEARSON et al., 2001) as well as uptake of ^{13}C-labeled bicarbonate into lipids in mesocosm experiments (WUCHTER et al., 2003) indicated that MG-I *Crenarchaeota* might be autotrophic. In contrast, uptake of amino acids by MG-I *Crenarchaeota* and MG-II *Euryarchaeota* indicated a potential role as heterotrophs for these clades (OUVERNEY and FUHRMAN, 2000; TEIRA et al., 2004; HERNDL et al., 2005). The detection of a gene for proteorhodopsin, a light-driven proton pump, in surface-dwelling MG-II *Euryarchaeota* (FRIGAARD et al., 2006) as well as genes coding for protein- and lipid-degrading enzymes encoded in a reconstructed MG-II genome suggested a photoheterotrophic metabolism for MG-II, consistent with their

[1]Retrieved from http://hahana.soest.hawaii.edu/hot/, April 4th, 2015

abundance in the photic zone (IVERSON et al., 2012). In contrast, the metabolisms of deep-dwelling MG-II *Euryarchaeota*, which lack proteorhodopsin (FRIGAARD et al., 2006), the rare MG-IV *Euryarchaeota* and the MG-III *Euryarchaeota* which are particularly abundant in the deep ocean (FUHRMAN and DAVIS, 1997; MARTIN-CUADRADO et al., 2008; GALAND et al., 2009b), remain unresolved.

First indications for an involvement of MG-I *Crenarchaeota* in the nitrogen cycle and a potential nitrifying metabolism came from an ammonium monooxygenase gene found on an archaeal-associated scaffold within a Sargasso Sea shotgun sequencing dataset (VENTER et al., 2004) as well as a similar archaeal monooxygenase found in a soil metagenome that was distantly related to monooxygenases of methanotrophic and ammonia-oxidizing bacteria (AOB) (TREUSCH et al., 2005). Unambiguous identification of autotrophy and ammonia-oxidizing activity ($NH_3 + 1.5\ O_2 \rightarrow NO_2^- + H_2O + H^+$, Section 1.3) was demonstrated by the cultivation of the first MG-I archaeon, *Nitrosopumilus maritimus*, from a tropical fish tank at the Seattle Aquarium (KÖNNEKE et al., 2005). The involvement of archaea in nitrification was unprecedented as ammonia-oxidation was considered to be limited to the bacterial domain since the first isolation of AOB from soil in the 1890s (WINOGRADSKY, 1890, 1891; KOWALCHUK and STEPHEN, 2001; SCHLEPER and NICOL, 2010). In fact, the technique used for the isolation of *N. maritimus* using liquid mineral medium amended with ammonium chloride and bicarbonate was similar to the method developed by Winogradsky, apart from drastically reduced ammonium concentrations that otherwise inhibit growth of AOA (e.g., KÖNNEKE et al., 2005; BOLLMANN et al., 2011; TOURNA et al., 2011, also refer to Chapter 4).

1.2.2. Phylogeny and ecology of the Thaumarchaeota

Analyses of the distribution of ammonia-monooxygenase subunit A (*amoA*) gene biomarkers and isotope tracer techniques have identified AOA as major nitrifiers in a wide range of environments such as the marine water column (WUCHTER et al., 2006; BEMAN et al., 2008), soils (LEININGER et al., 2006; PROSSER and NICOL, 2008), estuaries (CAFFREY et al., 2007), lakes (AUGUET and CASAMAYOR, 2008; POULIOT et al., 2009), and hydrothermal springs (REIGSTAD et al., 2008; DODSWORTH et al., 2011). Since the isolation of *N. maritimus*, several AOA strains have been cultivated from hydrothermal springs (DE LA TORRE et al., 2008; HATZENPICHLER et al., 2008), marine and estuarine sediments (BLAINEY et al., 2011; PARK et al., 2014), marine surface water (SANTORO and CASCIOTTI, 2011; QIN et al., 2014; SANTORO et al., 2015), and soils (e.g., LEHTOVIRTA-MORLEY et al., 2011; TOURNA et al., 2011). However, due to the slow growth and low cell densities of AOA, only three pure cultures exist besides

N. maritimus: *Nitrososphaera viennensis* isolated from a garden soil (TOURNA et al., 2011) and two strains closely related to *N. maritimus* isolated from fjord surface water (QIN et al., 2014).

The analysis of a number of AOA genomes and environmental metagenomes has resulted in the establishment of the novel archaeal phylum *Thaumarchaeota*, which comprises all cultivated AOA as well as the environmental sequences formerly affiliated with the MG-I *Crenarchaeota*. The phylum *Thaumarchaeota* can be subdivided into several subgroups based on *amoA* and 16S rRNA gene phylogenies that broadly correlate with habitat types (Figure 1.1; e.g., BROCHIER-ARMANET et al., 2008; PESTER et al., 2011; STAHL and DE LA TORRE, 2012). *N. maritimus*, *C. symbiosum*, and most marine sequences are affiliated with the shallow (i.e., <200 m water depth) cluster A of Group I.1a, while cluster B comprises sequences typically found in the deep ocean beneath 200 m water depth and has so far no cultivated representatives (Figure 1.1; e.g., FRANCIS et al., 2005; MINCER et al., 2007; LUO et al., 2014). The SAGMCG-1/*Nitrosotalea* cluster represents a sister group of the Group I.1a *Thaumarchaeota* comprising environmental sequences from soils and lakes as well as a single, acidophilic enrichment culture from soil, *Nitrosotalea devanaterra* (LEHTOVIRTA-MORLEY et al., 2011; STAHL and DE LA TORRE, 2012; AUGUET and CASAMAYOR, 2013). While Group I.1a *Thaumarchaeota* are also found in soils (e.g., PESTER et al., 2012), most sequences from soils and other terrestrial environments as well as the isolate *N. viennensis* (TOURNA et al., 2011; STIEGLMEIER et al., 2014b) are affiliated with Group I.1b (e.g., BINTRIM et al., 1997; DELONG, 1998; STAHL and DE LA TORRE, 2012, ; Figure 1.1). Additionally, Group I.1a and I.1b both contain moderate thermophiles such as *Candidatus* Nitrosotenuis uzonensis and *Nitrososphaera gargensis*, which have upper temperature limits for growth of 52 °C and 46 °C, respectively (HATZENPICHLER et al., 2008; LEBEDEVA et al., 2013). However, the only cultivated obligate thermophile known to date is *Nitrosocaldus yellowstonii* (ThAOA/HWCG III cluster; Figure 1.1), which grows in the range of 60 to 74 °C (DE LA TORRE et al., 2008). The basal character of this thermophilic branch suggests that the mesophilic *Thaumarchaeota* may originate from a thermophilic ancestor (BROCHIER-ARMANET et al., 2012).

All cultivated *Thaumarchaeota* are ammonia-oxidizers and most are neutrophilic obligate lithoautotrophs, i.e., they assimilate inorganic carbon into biomass, while only few strains have the ability for mixotrophic growth by metabolizing tricarboxylic acid cycle intermediates such as pyruvate and α-ketoglutarate (Figure 1.4; TOURNA et al., 2011; STAHL and DE LA TORRE, 2012; QIN et al., 2014). However, MUSSMANN et al. (2011) demonstrated that some *Thaumarchaeota* in a wastewater treatment plant lack the capacity to fix inorganic carbon and oxidize ammonia. Similarly, members of the uncultivated Group I.1c *Thaumarchaeota* in soil are potentially not obligate

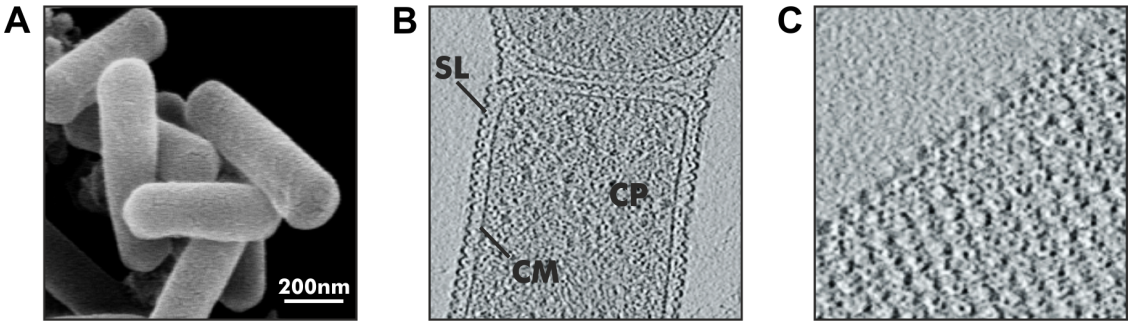

Figure 1.3. (A) Scanning electron micrograph showing rod morphology of *Nitrosopumilus maritimus*. (B) Cryo-electron tomography section of two adjacent *N. maritimus* cells showing cytoplasm (CP), cytoplasmic membrane (CM, thin dark contour, ca. 5 nm thickness), and surrounding S-layer (SL, ca. 25 nm thickness). (C) Cryo-electron tomogram showing the ultrastructure of *N. maritimus* with periodic arrangement of S-layer proteins. Cryo-electron tomograms and scanning electron micrograph courtesy of M. Könneke.

ammonia-oxidizers but metabolize organic nitrogen compounds (WEBER et al., 2015). Group I.1a *Thaumarchaeota* are among the smallest organisms in the ocean, occuring as rods of about 0.2 µm width and 0.8 to 1 µm length (PRESTON, 1996; KÖNNEKE et al., 2005). In contrast, Group I.1b *Thaumarchaeota* appear as cocci with a diameter of 0.6-0.9 µm (HATZENPICHLER et al., 2008; TOURNA et al., 2011; STIEGLMEIER et al., 2014b). A notable exception to otherwise uniformly small sizes of thaumarchaeal cells are giant *Thaumarchaeota* of about 10 µm width and 24 µm length identified in a mangrove sediment and affiliated with smaller bacterial symbionts (MULLER et al., 2010). Similar to many other archaea, the thaumarchaeal isolates *N. maritimus* and *N. viennensis* possess a protective S-layer, a porous paracrystalline layer of surface proteins enclosing the cell, which has a hexagonal p3-symmetry similar to the S-layers of the crenarchaeal *Sulfolobales* (ALBERS and MEYER, 2011; HEINZ et al., 2013; STIEGLMEIER et al., 2014b).

The physiology of *Thaumarchaeota* indicates that these archaea are particularly adapted to oligotrophy and outcompete bacteria in these environments (PESTER et al., 2011; STAHL and DE LA TORRE, 2012). *Thaumarchaeota* utilize a modified 3-hydroxypropionate/4-hydroxybutyrate cycle for CO_2 fixation, which represents the most energy-efficient aerobic CO_2 assimilation pathway (WALKER et al., 2010; KÖNNEKE et al., 2014). *Thaumarchaeota* have a much higher affinity for ammonium than AOB, indicating that AOA may effectively outcompete AOB in oligotrophic environments (MARTENS-HABBENA et al., 2009). In contrast, growth rates and maximum cell densities of cultivated *Thaumarchaeota* are lower than those of cultivated AOB and growth of thaumarchaeal cultures is inhibited at ammonium concentrations higher than 3-4 mM, indicating that AOB may be better adapted to eutrophic environments

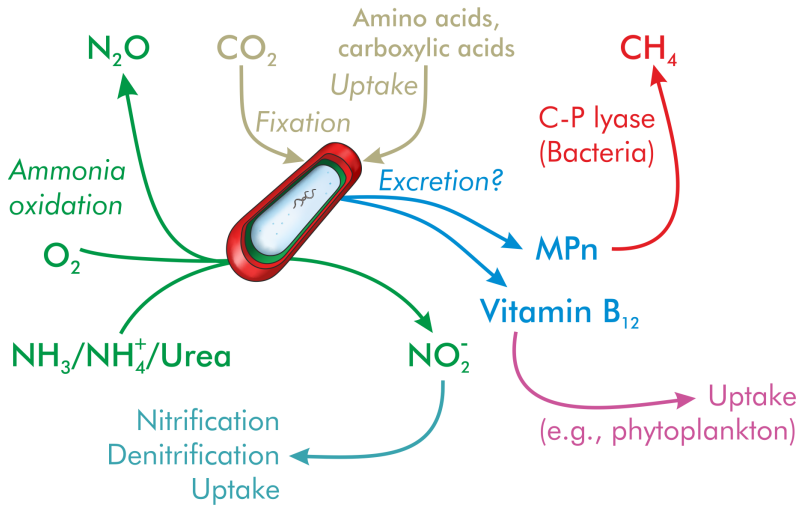

Figure 1.4. Biogeochemical processes associated with *Thaumarchaeota* and their metabolic products. *Thaumarchaeota* gain energy through the oxidation of ammonia (NH_3, which is in equilibrium with the protonated NH_4^+ in aqueous solutions) or urea (after hydrolytic cleavage into two NH_3 molecules) with oxygen to yield NO_2^- (chemotrophy) as well as the the greenhouse gas N_2O as a byproduct (KÖNNEKE et al., 2005; SANTORO et al., 2011; STAHL and DE LA TORRE, 2012). *Thaumarchaeota* take up the greenhouse gas CO_2 (lithoautotrophy; KÖNNEKE et al., 2005; STAHL and DE LA TORRE, 2012; KÖNNEKE et al., 2014) or small organic compounds such as amino acids in addition to CO_2 (mixotrophy; e.g., OUVERNEY and FUHRMAN, 2000; QIN et al., 2014) as carbon sources. NO_2^- produced by *Thaumarchaeota* may be used as a nitrogen source by planktonic bacteria and eukaryota or in bacterial nitrification (yielding NO_3^-) and denitrification (yielding N_2 or N_2O as end products). *Thaumarchaeota* synthesize methylphosphonate (MPn; METCALF et al., 2012), which may be utilized by phosphorous-starved bacteria by lysing the C-P bond yielding phosphate and as a byproduct the greenhouse gas methane (KARL et al., 2008; METCALF et al., 2012; CARINI et al., 2014). Vitamin B_{12}, a coenzyme essential for amino acid biosynthesis, is produced by *Thaumarchaeota* and may be utilized by auxotrophic planktonic bacteria and eukaryota (DOXEY et al., 2015).

than *Thaumarchaeota* (e.g., KÖNNEKE et al., 2005; MARTENS-HABBENA et al., 2009; STAHL and DE LA TORRE, 2012; STIEGLMEIER et al., 2014a). In some environments, thaumarchaeal nitrification is further sustained by hydrolytic cleavage of urea into two ammonia molecules, which may be especially important for the oligotrophic deep and high-latitude ocean as well as acidic soils (e.g., KONSTANTINIDIS et al., 2009; ALONSO-SÁEZ et al., 2012; LU et al., 2012; TULLY et al., 2012; PEDNEAULT et al., 2014). Similar to AOB, growth of *N. maritimus* is inhibited by light (MERBT et al., 2012). However, genomic analyses of *Thaumarchaeota* inhabiting the surface ocean suggest that these posess adaptive mechanisms to reduce light-induced damage (LUO et al., 2014). Cultivation as well as *amoA* and 16S rRNA gene surveys have revealed a large habitat range of *Thaumarchaeota* far exceeding that of cultured AOB (STAHL and DE LA TORRE, 2012), ranging from freshwater to hypersaline (IONESCU et al., 2009; AUGUET

et al., 2010; BERG et al., 2014; NGUGI et al., 2015), pH as low as 2-4 (NICOL et al., 2008; REIGSTAD et al., 2008; LEHTOVIRTA-MORLEY et al., 2011), and temperatures of −2 to 97 °C (DELONG et al., 1994; MURRAY et al., 1998; REIGSTAD et al., 2008). Thus, the upper temperature limit of *Thaumarchaeota* is by ca. 40 °C higher than that of AOB (LEBEDEVA et al., 2005; DE LA TORRE et al., 2008; STAHL and DE LA TORRE, 2012).

In addition to nitrification, *Thaumarchaeota* are involved in several globally relevant biogeochemical processes (Figure 1.4). For instance, *Thaumarchaeota* release the greenhouse gas N_2O as a byproduct of ammonia-oxidation through a yet unknown pathway (SANTORO and CASCIOTTI, 2011; LÖSCHER et al., 2012; STIEGLMEIER et al., 2014b). Furthermore, *Thaumarchaeota* are a potentially significant source of cobalamin (vitamin B_{12}) in the ocean, an enzyme cofactor that is not synthesized by eukaryotic phytoplankton and a large number of prokaryotes but essential for amino acid synthesis in these organisms (Figure 1.4; DOXEY et al., 2015). *Thaumarchaeota* are also regarded as a major source of methylphosphonate in the ocean (METCALF et al., 2012). Methylphosphonate is utilized as a phosphorous source by phosphate-starved planktonic bacteria and decomposed into phosphate and the greenhouse gas methane, a process accounting for the apparent supersaturation of methane in the surface ocean relative to the atmosphere and representing a cross-link between the cycles of nitrogen and methane/carbon (Figure 1.4; e.g., DAUGHTON et al., 1979; KARL et al., 2008; METCALF et al., 2012; CARINI et al., 2014). Due to the importance of oceanic OMZs and anoxic basins in global nitrogen cycling (LAM and KUYPERS, 2011), the abundances and activity of *Thaumarchaeota* in these environments as well as their interactions with denitrifying bacteria have been a focal point of recent research (Figures 1.2 and 1.4 and Section 1.3; e.g., LAM et al., 2007; WOEBKEN et al., 2007; PITCHER et al., 2011a).

1.3. The role of *Thaumarchaeota* in the marine nitrogen cycle

Nitrogen is an essential element for life as a major constituent of amino acids, proteins and nucleic acids and occurs predominantly as dinitrogen gas (N_2) in the atmosphere, which represents the largest nitrogen reservoir on Earth (BRANDES et al., 2007; CANFIELD et al., 2010). However, N_2 is chemically inert and therefore inaccessible to direct biological uptake. Nitrogen fixation, i.e., the reduction of N_2 into bioavailable ammonium (NH_4^+), is performed only by some bacterial and archaeal species (ZEHR and KUDELA, 2011; OFFRE et al., 2013). In the marine environment, phototrophic cyanobacteria are considered to be the major contributors to nitrogen fixation and thus form the basis of the marine nitrogen cycle (Figure 1.5; ZEHR, 2011). Other quan-

titatively important sources of (anthropogenic) fixed nitrogen in coastal environments are terrestrial runoff and atmospheric deposition (GALLOWAY et al., 2004). Marine phytoplankton lack the ability to fix N_2 and thus depend on uptake of dissolved NH_4^+ and other inorganic nitrogen species such as nitrate (NO_3^-) and, to a lesser degree, also nitrite (NO_2^- CANFIELD et al., 2010; ZEHR, 2011). Thus, the availability of fixed nitrogen is often a limiting factor for primary- as well as whole ecosystem productivity (ARRIGO, 2005; ZEHR, 2011; MOORE et al., 2013). The fixed nitrogen pool is replenished by the release of NH_4^+ from microbial remineralization of dead biomass (Figure 1.5; DUGDALE and GOERING, 1967; THAMDRUP, 2012).

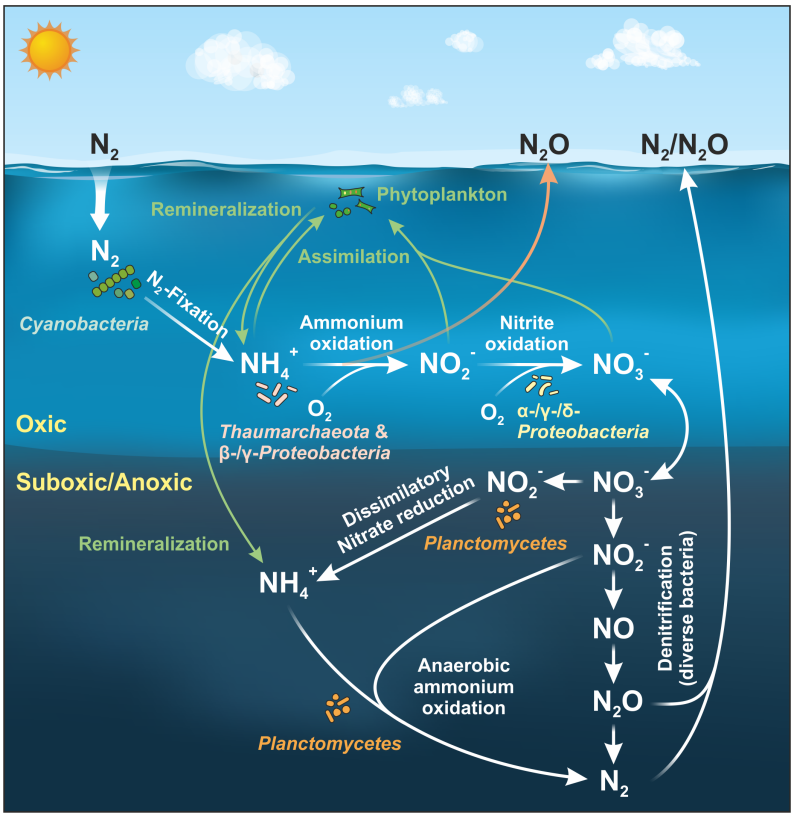

Figure 1.5. Transformation pathways of nitrogen species and mediating microorganisms in the marine microbial nitrogen cycle in oxic and suboxic/anoxic environments (based on ARRIGO, 2005; FRANCIS et al., 2007).

Fixed nitrogen is transformed via multiple microbially mediated redox reactions that ultimately result in the loss of fixed nitrogen as N_2 to the atmosphere (CANFIELD et al., 2010; THAMDRUP, 2012). Thus, the overall productivity of the ocean depends on the balance of nitrogen fixation and conversion of fixed nitrogen into N_2 (FALKOWSKI, 1997; GRUBER, 2008). Under oxic to suboxic conditions, NH_4^+ is oxidized to NO_3^- via a two-step pathway using oxygen as the terminal electron acceptor (nitrification). The first and rate-limiting step of nitrification is the oxidation of NH_3 (which is in equilibrium with the protonated form, ammonium) to NO_2^- by *Thaumarchaeota* and bacteria

affiliated with the β and γ subclasses of the phylum *Proteobacteria* (KOWALCHUK and STEPHEN, 2001; FRANCIS et al., 2007). Nitrite is then further oxidized to NO_3^- by nitrite-oxidizing α-, γ-, and δ-*Protebacteria* (SPIECK and LIPSKI, 2010). N_2O is released as a byproduct of thaumarchaeal and bacterial ammonia-oxidation, particularly under low-oxygen conditions and may thus escape from the marine nitrogen cycle into the atmosphere (LAM and KUYPERS, 2011; SANTORO and CASCIOTTI, 2011; LÖSCHER et al., 2012).

Under oxic, euphotic conditions, the nitrate derived from nitrification may again serve as a nitrogen source for primary producers (e.g., YOOL et al., 2007). Under suboxic and anoxic conditions such as in oceanic oxygen minimum zones and shallow sediments, nitrate and nitrite are transformed to N_2 via multiple pathways and intermediates (Figure 1.5; THAMDRUP, 2012). During (canonical) denitrification, NO_2^- and NO_3^- serve as terminal electron acceptors in bacterial heterotrophic respiration and are reduced to N_2 and/or N_2O via an NO intermediate (e.g., WARD et al., 2009). While some thermophilic *Cren-* and *Euryarchaeota* perform nitrate reduction, there is currently no evidence for mesophilic denitrifying archaea (CABELLO et al., 2004; OFFRE et al., 2013). In addition to canonical denitrification, autotrophic bacteria of the phylum *Planctomycetes* mediate the anaerobic oxidation of ammonium by nitrite (anammox) to N_2 (Figure 1.5; MULDER et al., 1995; STROUS et al., 1999), a process that significantly contributes to oceanic fixed nitrogen losses (e.g., KUYPERS et al., 2005; HAMERSLEY et al., 2007). Under ammonium limitation, NO_3^- and NO_2^- may also be reduced to NH_4^+ by *Planctomycetes* (KARTAL et al., 2007; LAM et al., 2009). Denitrification and anammox are particularly important in oceanic oxygen minimum zones (OMZs) and the transition zones of anoxic basins such as the Black Sea, making these zones hot-spots for nitrogen cycling and fixed nitrogen loss (Figure 1.2b; KUYPERS et al., 2003, 2005; LAM and KUYPERS, 2011). Ammonia released from biomass remineralization within OMZs and anoxic basins furthermore supports high standing stocks of nitrifying archaea and bacteria in the suboxic transition zones, which replenish the nitrite pool and thus support denitrification and anammox and consequently increased fixed nitrogen losses (Figure 1.2b; COOLEN et al., 2007; LAM et al., 2007; WAKEHAM et al., 2007; LAM and KUYPERS, 2011; YAN et al., 2012).

1.4. Structure, function and adaptation mechanisms of microbial lipid membranes

1.4.1. Structure and function of microbial lipid membranes

In all organisms, the cytoplasmic membrane serves as the mechanical and physicochemical barrier separating the interior of the cell from the environment. The membrane primarily functions as a semipermeable barrier limiting the flux of ions and other solutes in and out of the cell and thus maintaining the proton and ion gradients that are essential for microbial energy conservation and ATP generation (MADIGAN et al., 2011). The membrane further serves as a matrix for embedded proteins such as channel proteins that perform passive or active transport of solutes across the cell membrane and as an anchor for S-layer proteins in some species of archaea and bacteria (Figure 1.6a; SINGER and NICOLSON, 1972; ALBERS and MEYER, 2011; NICOLSON, 2014). Furthermore, the enzymatic machinery involved in microbial energy conservation is typically located within the cell membrane (MADIGAN et al., 2011).

The structural organization of cytoplasmic membranes is commonly described using the fluid mosaic model, which considers the membrane as a mixture of polar lipids, proteins and other components such as sterols and carbohydrates (SINGER and NICOLSON, 1972; NICOLSON, 2014). The inherent properties of these components and their interactions confer a viscous-fluid character to the membrane (NICOLSON, 2014) that is vital in various cellular processes such as cell division and membrane protein dynamics (LENAZ, 1987). Furthermore, lipids perform other vital functions such as in cell signaling and energy storage (VAN MEER et al., 2008).

All membrane lipids share the same principal structure: a glycerol backbone with two attached apolar, hydrophobic side chains forms the core lipid to which a polar, hydrophilic headgroup is bound (Figure 1.6b,c). These polar membrane lipids assemble into two-dimensional sheets consisting of polar headgroups facing the cytoplasm and the cell exterior and a hydrophobic core region formed by the apolar chains (Figure 1.6a; VAN MEER et al., 2008; LÓPEZ and KOLTER, 2010).

The types of membrane lipids and other membrane constituents differ fundamentally between the three domains of life. While all domains contain predominantly glycerol-based lipids with glycosidic or phosphatidic polar headgroups, the stereochemistry of the glycerol backbone represents a distinct difference between the *Archaea* and the other two domains. While all representatives of the domains *Bacteria* and *Eukarya* contain lipids based on *sn*-glycerol-3-phosphate, archaeal membrane lipids are without exception based on the enantiomer *sn*-glycerol-1-phosphate (Figure 1.6c; KATES, 1993; KOGA, 2011). This 'lipid divide' might represent the origin of the differentiation of

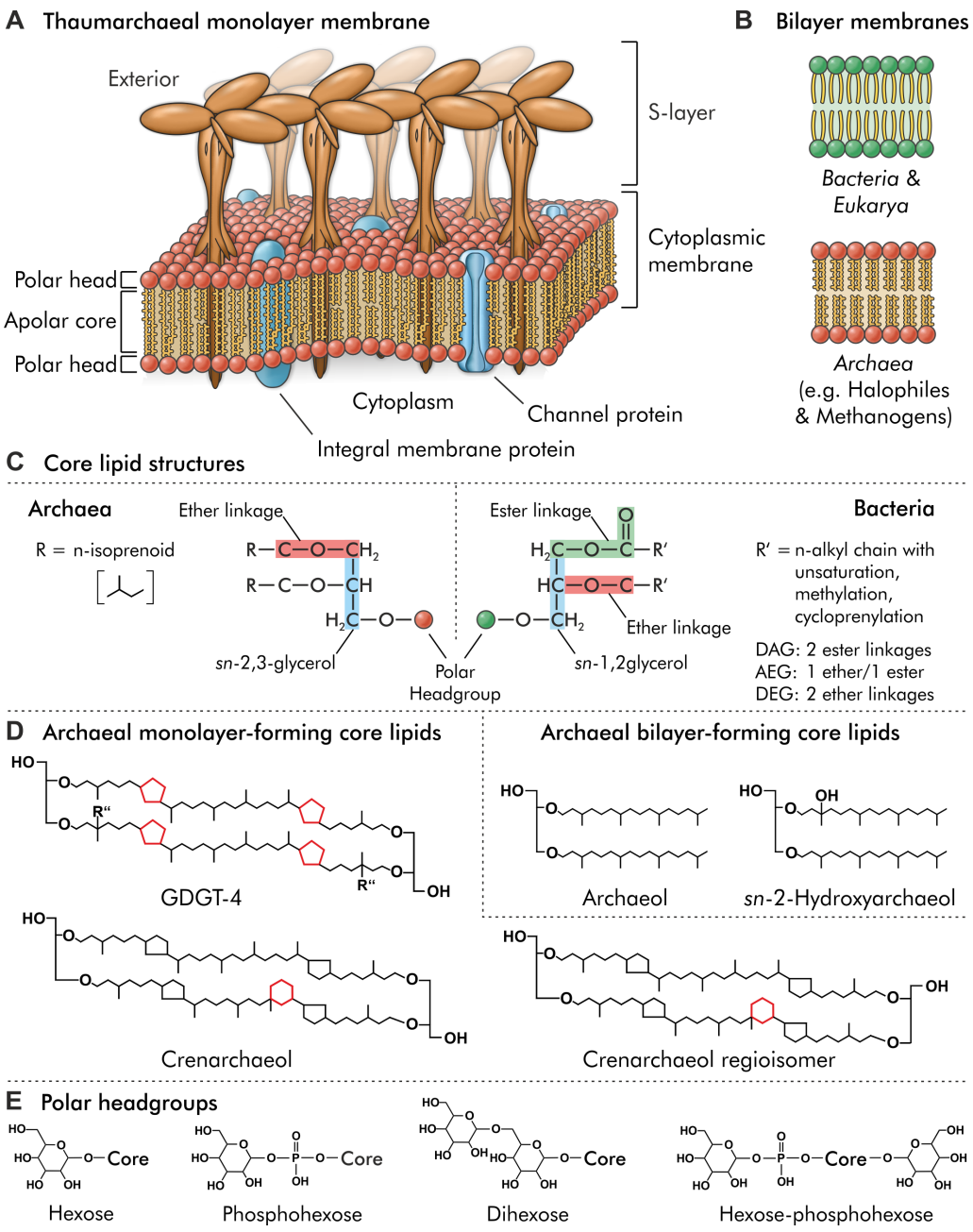

Figure 1.6. (A) Structure of the thaumarchaeal membrane consisting of a mix of mono-layer forming glycerol dibiphytanyl glycerol tetraether lipids (GDGTs) and minor amounts of bilayer-forming isoprenoid diphytanyl glycerol diethers (archaeols) connected to two and one polar headgroups, respectively, that face the cytoplasm and the cell exterior. The membrane serves as a matrix supporting integral and channel proteins and the surrounding proteinaceous cell envelope, the S-layer. Graphical representation of the S-layer is based on p3-symmetry for *Nitrososphaera viennensis* (STIEGLMEIER et al., 2014b) and *Sulfolobales* (ALBERS and MEYER, 2011). (B) Bilayer membranes typical for *Euryarchaeota* and *Bacteria*/*Eukarya*. (C) Stereochemistry as well as side chain linkage and structure of archaeal and bacterial/eukaryotal membrane lipids (based in part on VALENTINE, 2007). (D) Core structures of archaeols and GDGTs (0 to four cyclopentane rings (red) in *Thaumarchaeota*, up to two hydroxyl groups in the side chain at positions R', R''') and the *Thaumarchaeota*-specific GDGT crenarchaeol (four cyclopentane rings, one cyclohexyl ring, red) and its regioisomer. (E) Structures of headgroups (linked to the hydroxyl group of the glycerol backbone) typically found in intact polar lipids of *Thaumarchaeota* and other archaea.

the domains *Archaea* and *Bacteria* and represents one of the focal points of currently discussed models of early prokaryotic evolution (KOGA, 2011; LOMBARD et al., 2012; KOGA, 2014).

The membrane lipids of *Archaea*, *Bacteria*, and *Eukarya* are further distinguished by core lipid structure. The membranes of bacteria and eukaryota are predominantly composed of bilayers of polar lipids with ester linked fatty acid side chains (diacylglycerols). However, some bacteria also synthesize lipids with ether-linked, predominantly linear, alkyl chains (dietherglycerols) or mixed ester-/ether bonds (acyletherglycerols; Figure 1.6c). Additionally, other lipid types such as betaine- and sphingolipids occur in some eukaryota and bacteria while ornithine lipids are restricted to the bacterial domain (DEMBITSKY, 1996; OLSEN and JANTZEN, 2001; GEIGER et al., 2010). As a notable exception, hyperthermophilic bacteria of the order *Thermotogales* synthesize tetraether, tetraester and mixed ether/ester membrane spanning lipids (SINNINGHE DAMSTÉ et al., 2007). Similar tetraether lipids of supposedly bacterial origin have also been observed in soils, lakes, the marine water column and sediments (e.g., SINNINGHE DAMSTÉ et al., 2000; LIU et al., 2014). Furthermore, bacteria and eukaryota utilize hopanoids and sterols, respectively, to modulate membrane lipid ordering (SIMONS and IKONEN, 1997; SÁENZ et al., 2012), while these compounds are lacking in archaea.

In contrast to *Bacteria* and *Eukarya*, the membranes of *Archaea* are composed exclusively of ether lipids with isoprenoid alkyl side chains (Figure 1.6c,d; KATES, 1993; KOGA and MORII, 2005), while there is only limited evidence for membrane lipid-ordering agents (LANYI et al., 1974; GILMORE et al., 2013). Archaeal membrane lipids can be separated into two major classes. Archaeols, which are found in most cultivated archaea, particular in *Euryarchaeota*, consist of a glycerol ether-linked to two C_{20} isoprenoid (phytanyl) chains and form bilayer membranes (Figure 1.6a-d; DE ROSA et al., 1988; KATES, 1993; KOGA and MORII, 2005). Glycerol dibiphytanyl glycerol tetraethers (GDGTs) are found in most thermophilic archaea, some mesophilic methanogenic *Euryarchaeota*, as well as *Thaumarchaeota* and are composed of two C_{40} isoprenoid (biphytanyl) chains ether-linked to two glycerols to constitute a bipolar lipid forming monolayer membranes (Figure 1.6a,d; reviewed in DE ROSA et al., 1988; KATES, 1993; SCHOUTEN et al., 2013). Multiple variations to these basic structures exist, such as archaeols bearing an additional hydroxyl group in the side chain connected to the *sn*-2 carbon of glycerol (*sn*-2-hydroxyarchaeol), which are characteristic for methanogenic and anaerobic methanotrophic *Euryarchaeota* (Figure 1.6d; SPROTT et al., 1990; HINRICHS et al., 1999). Similarly, GDGTs may comprise up to two hydroxyl-groups within the side chains (LIU et al., 2012b) and up to eight cyclopentane rings among a number of other GDGT derivatives (Figure 1.6d; e.g., DE ROSA et al., 1988; KATES, 1993; SCHOUTEN et al., 2013). Furthermore, a number of archaeal 'orphan'-lipids, i.e., lipids

with an unknown source organism, have recently been identified in marine sediments by the use of novel, comprehensive analytical techniques (cf. BECKER et al., 2013; ZHU et al., 2013). These comprise, among others, GDGTs with unsaturations or additional methylations within the side chain, GDGTs bearing methoxy groups connected to the glycerol, as well as GDGT analogues with butanetriol and pentanetriol backbones (KNAPPY et al., 2014; ZHU et al., 2014a,b).

1.4.2. Membrane lipid composition of Thaumarchaeota

The lipid membranes of cultivated *Thaumarchaeota* are composed primarily of GDGTs with zero to four cyclopentane rings (DE LA TORRE et al., 2008; SCHOUTEN et al., 2008; PITCHER et al., 2011a; SINNINGHE DAMSTÉ et al., 2012), while only traces of archaeol have been reported to occur in *N. maritimus* (SCHOUTEN et al., 2008). In addition, a GDGT containing four cyclopentane rings and one cyclohexyl ring, crenarchaeol (Figure 1.6d), as well as a regioisomer of crenarchaeol have been found exclusively in *Thaumarchaeota* (SINNINGHE DAMSTÉ et al., 2002b; DE LA TORRE et al., 2008; SCHOUTEN et al., 2008; PITCHER et al., 2011a; SINNINGHE DAMSTÉ et al., 2012).

The membrane lipid composition of *N. maritimus* is broadly similar to that observed in cultured and enriched Group I.1a and I.1b *Thaumarchaeota* (SCHOUTEN et al., 2008; PITCHER et al., 2011a; SINNINGHE DAMSTÉ et al., 2012). However, due to limitations in the employed analytical methodology, only few lipid types have been reported from *Thaumarchaeota* and quantitative information on the relative abundances of intact polar GDGT classes is not available (cf. SCHOUTEN et al., 2008; PITCHER et al., 2011a; SINNINGHE DAMSTÉ et al., 2012). Common intact polar lipids of *Thaumarchaeota* are monoglycosidic (1G-) and diglycosidic (2G-) GDGTs as well as phosphohexose- (PH-) and hexose-phosphohexose- (HPH-) GDGTs (Figure 1.6e; SCHOUTEN et al., 2008; PITCHER et al., 2011a; SINNINGHE DAMSTÉ et al., 2012). Within the *Thaumarchaeota*, 1G- and 2G-GDGTs containing a hydroxylation in one of the side chains (Figure 1.6d; LIPP and HINRICHS, 2009; LIU et al., 2012b) have so far only been observed in marine group I.1a *Thaumarchaeota* (SCHOUTEN et al., 2008; PITCHER et al., 2011a) and thus appear to be a characteristic intact polar lipid (IPL) of this clade (cf. SINNINGHE DAMSTÉ et al., 2012). Similarly, GDGTs with a trihexose headgroup have only been observed in Group 1.1b *Thaumarchaeota* (SINNINGHE DAMSTÉ et al., 2012). The membrane lipid composition of representatives of the SAGMCG-1 cluster (e.g., *N. devanaterra*) has not been investigated, while only core lipids but not IPLs were analyzed for *N. yellowstonii* (ThAOA cluster; DE LA TORRE et al., 2008).

The most abundant GDGT core structures in Group I.1a *Thaumarchaeota* are acyclic GDGT (GDGT-0) and crenarchaeol (SCHOUTEN et al., 2008; PITCHER et al., 2011a). In

contrast, GDGT-4, crenarchaeol, and the crenarchaeol regioisomer are the main core GDGTs found in thermophilic and soil Group I.1b *Thaumarchaeota* (PITCHER et al., 2010; SINNINGHE DAMSTÉ et al., 2012). Similarly, crenarchaeol is the dominant core GDGT in *N. yellowstonii* but the crenarchaeol regioisomer is not abundant in this strain (DE LA TORRE et al., 2008). In addition, glycerol trialkyl glycerol tetraethers (GTGTs), GDGT analogues that consist of one biphytanyl and two phytanyl chains ether linked to two glycerols, have been observed in high abundances in *N. yellowstonii* as well as in traces in *N. maritimus* (DE LA TORRE et al., 2008; SCHOUTEN et al., 2008).

Due to a lack of available cultures, the membrane lipid composition of only one marine planktonic thaumarchaeon, *N. maritimus*, has been studied. Recently developed analytical methods enable to quantify relative abundances of individual IPL classes as well as their core GDGT composition simultaneously (cf. BECKER et al., 2013; ZHU et al., 2013). These methods offer high potential to re-evaluate the IPL composition of *N. maritimus* and other cultivated *Thaumarchaeota*. Furthermore, application of these methods to established and recently cultivated thaumarchaeal cultures will enable the screening for novel lipid biomarkers. The characterization of lipids in cultivated *Thaumarchaeota* will facilitate the interpretation of IPLs abundantly detected in environmental studies and their assignment to phylogenetic clades.

1.4.3. Membrane lipid adaptation in Archaea

Maintaining membrane fluidity in a narrow window is essential for optimal cell functioning and enables archaea to thrive in a wide range of environments. On the one hand, the membrane needs to be tight to minimize proton and ion leakage and maintain proton motive force, i.e., proton and ion gradients across the membrane that are essential for microbial energy conservation (VAN DE VOSSENBERG et al., 1998; BAKER-AUSTIN and DOPSON, 2007). On the other hand, the membrane must be fluid enough to enable crucial cellular processes such as cell division (MADIGAN et al., 2011). The isoprenoid bilayer and monolayer membranes of archaea are particularly well adapted for minimized ion and proton permeability, thus reducing maintenance energy and maximizing proton motive force (YAMAUCHI et al., 1993; VAN DE VOSSENBERG et al., 1998; MATHAI et al., 2001; KONINGS et al., 2002; VALENTINE, 2007). Archaea regulate membrane integrity, fluidity and permeability by altering core lipid and polar headgroup composition in response to changes in temperature, salinity, pH and other environmental parameters (ULRIH et al., 2009; KOGA, 2012; OGER and CARIO, 2013). Past research on the mechanisms of membrane lipid adaptation has nearly exclusively focused on changes in core lipid composition of cultivated extremophilic *Cren-* and

Euryarchaeota (cf. OGER and CARIO, 2013), while similar studies on *Thaumarchaeota* are lacking (cf. PEARSON and INGALLS, 2013).

As the diffusion rate of protons and other ions increases greatly with increasing temperature, archaea employ a variety of mechanisms to counteract ion leakage (VAN DE VOSSENBERG et al., 1998; OGER and CARIO, 2013). As GDGT monolayer membranes are particularly impermeable to protons, most acidophilic, thermophilic and hyperthermophilic *Cren-* and *Euryarchaeota* contain GDGTs as their major membrane lipids (VAN DE VOSSENBERG et al., 1998; BAKER-AUSTIN and DOPSON, 2007; OGER and CARIO, 2013; SCHOUTEN et al., 2013). Additionally, some thermophilic *Euryarchaeota* increase the relative abundances of GDGTs over archaeols in their membranes with increasing temperature (LAI et al., 2008; MATSUNO et al., 2009). However, some hyperthermophilic *Euryarchaeota* do not contain GDGTs at all (cf. OGER and CARIO, 2013; SCHOUTEN et al., 2013), or contain special macrocyclic archaeols, in which the phytanyl chains are linked at the terminal carbons via a covalent bond (COMITA and GAGOSIAN, 1983; DANNENMULLER et al., 2000).

A well-studied adaptation mechanism of thermophilic archaea is the increase of the average number of cyclopentane rings in GDGTs with increasing temperature (e.g., DE ROSA et al., 1980; UDA et al., 2001; BOYD et al., 2011). This promotes a tighter packing of the side chains, thus reducing the spacing of polar headgroups and limiting proton permeability (cf. CHONG, 2010; PEARSON and INGALLS, 2013). However, the relationship between GDGT cyclization and temperature is specific for each species (cf. OGER and CARIO, 2013). In contrast, the psychrophilic methanogen *Methanococcoides burtonii* adapts to low temperature by increasing the degree of unsaturation in its archaeol-based membrane lipids (NICHOLS et al., 2004). Similarly, halophilic archaea adapt to high salinities, i.e., high cross-membrane ion concentration gradients and osmotic stress, by synthesizing unsaturated archaeols (DAWSON et al., 2012) and specific anionic polar headgroups (e.g., TENCHOV et al., 2006).

Acidophilic archaea maintain intracellular pH by increasing (BOYD et al., 2011, 2013) or decreasing (SHIMADA et al., 2008) GDGT cyclization in response to decreasing pH. Furthermore, the thermoacidophile *T. acidophilum* subsitutes phosphoglycosidic GDGTs with glycosidic GDGTs in response to decreasing pH, thus decreasing proton permeability by increased hydrogen-bonding between the polar headgroups (GABRIEL and CHONG, 2000; SHIMADA et al., 2008). The influence of energy-starvation on lipid composition is less constrained, but two thermophilic euryarchaeal species, *Thermococcus kodakarensis* and *Methanothermobacter thermautotrophicus*, accumulate phospholipids in stationary phase compared to growth phase (MEADOR et al., 2014a; YOSHINAGA et al., 2015). Furthermore, *M. thermautotrophicus* accumulates glycolipids relative to phospholipids during nutrient-limited growth (YOSHINAGA et al., 2015).

The diversity of responses to temperature and other parameters in cultivated *Cren-* and *Euryarchaeota* indicates that adaptive patterns may be difficult to predict between phylogenetically distinct archaea and that these observations may therefore not be transferable to *Thaumarchaeota*. Pure culture experiments are therefore needed to constrain the adaptive mechanisms employed by *Thaumarchaeota*.

1.5. Application of archaeal lipids as biomarkers and in paleoenvironmental reconstructions

1.5.1. Use of archaeal GDGTs as biomarkers for Thaumarchaeota

The analysis of archaeal lipid biomarkers in environmental samples has been essential for establishing the ubiquitous distribution of archaea in the environment and their significance in global biogeochemical cycles (cf. BROCKS and BANFIELD, 2009).

For example, the detection of strongly ^{13}C-depleted *sn*-2-hydroxyarchaeol in marine sediments was pivotal to the establishment of archaea as the major mediating organisms of anaerobic oxidation of methane (e.g., HINRICHS et al., 1999; ORPHAN et al., 2001). Similarly, core GDGTs, i.e., lipids that are released from intact polar GDGTs after cell senescence by cleavage of the polar headgroup, have been extensively used to trace the abundance of *Thaumarchaeota* in the marine and terrestrial environment (e.g., SCHOUTEN et al., 2000; PEARSON et al., 2004; LEININGER et al., 2006; COOLEN et al., 2007). However, core GDGTs are not suitable for tracing living cells as they predominantly represent a fossil signal, which is indicated for example by mismatches of the abundances of crenarchaeol and thaumarchaeal *amoA* and 16S rRNA gene markers in the water column of the Black Sea (e.g., COOLEN et al., 2007; WAKEHAM et al., 2007).

Based on the assumption of rapid degradation of intact polar to core lipids after cell lysis, intact polar GDGTs have recently been introduced as biomarkers for tracing and quantifying living *Thaumarchaeota* in the marine water column (Figure 1.7a; e.g., SCHUBOTZ et al., 2009; INGALLS et al., 2012; SCHOUTEN et al., 2012; BASSE et al., 2014). The crenarchaeol derivatives of HPH- and 2G-GDGTs have been shown to correlate with thaumarchaeal 16S rRNA and *amoA* gene copy numbers in the Arabian Sea water column (PITCHER et al., 2011b; SCHOUTEN et al., 2012), suggesting a causal relationship between HPH- and 2G-crenarchaeol abundance and active ammonia-oxidizing *Thaumarchaeota*. Moreover, it has been suggested that glycosidic IPLs are more slowly degraded than phosphatidic IPLs (e.g., SCHOUTEN et al., 2010; XIE et al., 2013), thereby raising the question which IPLs are indicative for living *Thaumarchaeota* in the marine water column. However, with respect to archaeal lipids, which are

present exclusively as ether lipids, conclusive evidence for more rapid degradation of phosphate-based IPLs than glycosidic IPLs is still lacking (LOGEMANN et al., 2011). Interpretation of water column IPL profiles is further hindered by the lack of studies on lipid composition in cultivated marine planktonic *Thaumarchaeota* and of quantitative data on lipid composition in the only studied strain, *N. maritimus* (cf. SCHOUTEN et al., 2008).

1.5.2. Use of archaeal GDGTs in paleoenvironmental reconstructions

Fossil core GDGTs originating from planktonic AOA are ubiquitously found in marine and lacustrine sediments of up to Cretaceous and Jurassic age and are frequently used in paleoceanography as a proxy for past surface water temperatures (indexed as TEX_{86}; SCHOUTEN et al., 2002; PEARSON and INGALLS, 2013; SCHOUTEN et al., 2013). The TEX_{86} (**T**etra**E**ther inde**X** of tetraethers consisting of 86 carbon atoms) paleothermometer is based on the observation that the differences in relative abundances of core GDGTs, and specifically those containing one to three cyclizations and the crenarchaeol regioisomer, as indexed in the TEX_{86} (Eq. 1), are strongly correlated to sea surface temperature (SST; Eq. 2 and Figure 1.7; SCHOUTEN et al., 2002).

$$TEX_{86} = \frac{[\text{GDGT-2}] + [\text{GDGT-3}] + [\text{Cren'}]}{[\text{GDGT-1}] + [\text{GDGT-2}] + [\text{GDGT-3}] + [\text{Cren'}]} \quad \text{(Eq. 1)}$$

$$SST_{TEX_{86}}(^{\circ}C) = 67.5 \times TEX_{86} + 46.9 \quad \text{(Eq. 2)}$$

The calibration of the TEX_{86} ratio in globally distributed core-top sediments with satellite-derived SSTs and the derivation of distinct calibration lines for high and low temperatures, TEX_{86}^{H} (Eq. 3) and TEX_{86}^{L} (Eq. 4), subsequently laid the foundation of the TEX_{86} paleothermometer (Figure 1.7b; SCHOUTEN et al., 2002; KIM et al., 2008, 2010).

$$SST_{TEX_{86}^{H}}(^{\circ}C) = 68.4 \times \log(TEX_{86}) + 38.6 \quad \text{(Eq. 3)}$$

$$SST_{TEX_{86}^{L}}(^{\circ}C) = 67.5 \times \log\left(\frac{[\text{GDGT-2}]}{[\text{GDGT-1}] + [\text{GDGT-2}] + [\text{GDGT-3}]}\right) + 46.9 \quad \text{(Eq. 4)}$$

While TEX_{86} paleothermometry has been widely applied for reconstructing past SSTs reaching back as far as the Cretaceous and Middle Jurassic (e.g., JENKYNS et al., 2012; LINNERT et al., 2014), it has become evident that the simple assumptions underlying this paleothermometer, i.e., a sole dependence of GDGT cyclization on temperature and the provenance of sedimentary GDGTs from surface waters, are inconsistent with

the current understanding of thaumarchaeal physiology and ecology (reviewed in PEARSON and INGALLS, 2013).

Although the general concept of GDGT cyclization as a means of temperature adaptation is well established for cultivated thermophilic archaea (Section 1.4.3; e.g., CHONG et al., 2010; OGER and CARIO, 2013), direct evidence for a physiological basis of the TEX_{86} paleothermometer from planktonic thaumarchaeal cultures is still lacking. Indeed, the sole dependence of TEX_{86} on growth temperature seems unlikely given the fact that multiple additional physiological and environmental parameters may affect lipid composition in other archaea (Section 1.4.3; e.g., MORII and KOGA, 1993; KANESHIRO and CLARK, 1995; SHIMADA et al., 2008; BOYD et al., 2011; DAWSON et al., 2012). While TEX_{86}-temperatures calculated from core GDGTs in the surface ocean correlate well with actual SSTs (Figure 1.7a; e.g., WUCHTER et al., 2005), recent analyses of intact polar and core GDGT compositions of in situ planktonic assemblages show that TEX_{86} values of both fossil and living subsurface archaeal biomass do not reflect in situ water temperatures in various oceanic provinces, neither in trend nor magnitude (Figure 1.7a; WUCHTER et al., 2005; INGALLS et al., 2006; TURICH et al., 2007; SCHOUTEN et al., 2012; BASSE et al., 2014; HERNÁNDEZ-SÁNCHEZ et al., 2014; XIE et al., 2014). In addition, the TEX_{86}-temperatures reconstructed from individual IPL types are offset from each other by up to 20 °C, which has been attributed to either a biosynthetic signature of living *Thaumarchaeota* or to differential degradation rates of IPL types within the water column (Figure 1.7a; cf. LENGGER et al., 2012; BASSE et al., 2014). The discrepancies between *in situ* and TEX_{86} temperatures in the marine water column indicate that both the export depth of the TEX_{86} signal as well as the physiological and ecological controls on GDGT composition in living thaumarchaea remain poorly understood.

In particular, the mechanism coupling TEX_{86} to SST remains elusive given the fact that *Thaumarchaeota* are most abundant and active in sub-surface waters broadly coinciding with the deep chlorophyll maximum (Figure 1.2; MASSANA et al., 1997; KARNER et al., 2001; FRANCIS et al., 2005; CHURCH et al., 2010). Moreover, thaumarchaeal shallow (0-200 m) and deep water (>200 m) ecotypes live under contrasting nutrient regimes (FRANCIS et al., 2005; YAKIMOV et al., 2011; SINTES et al., 2013), which may impact GDGT cyclization (cf. PEARSON and INGALLS, 2013). Surface and deep thaumarchaeal ecotypes have also distinct GDGT biosynthetic genes (VILLANUEVA et al., 2014a), which might be associated with preferential occurrence of bicyclic over tricyclic GDGTs in deep compared to shallow waters (TAYLOR et al., 2013; KIM et al., 2015).

In addition to vertical ecological differences, thaumarchaeal assemblages in the Arctic and Antarctic oceans as well as the Red Sea are phylogenetically distinct from

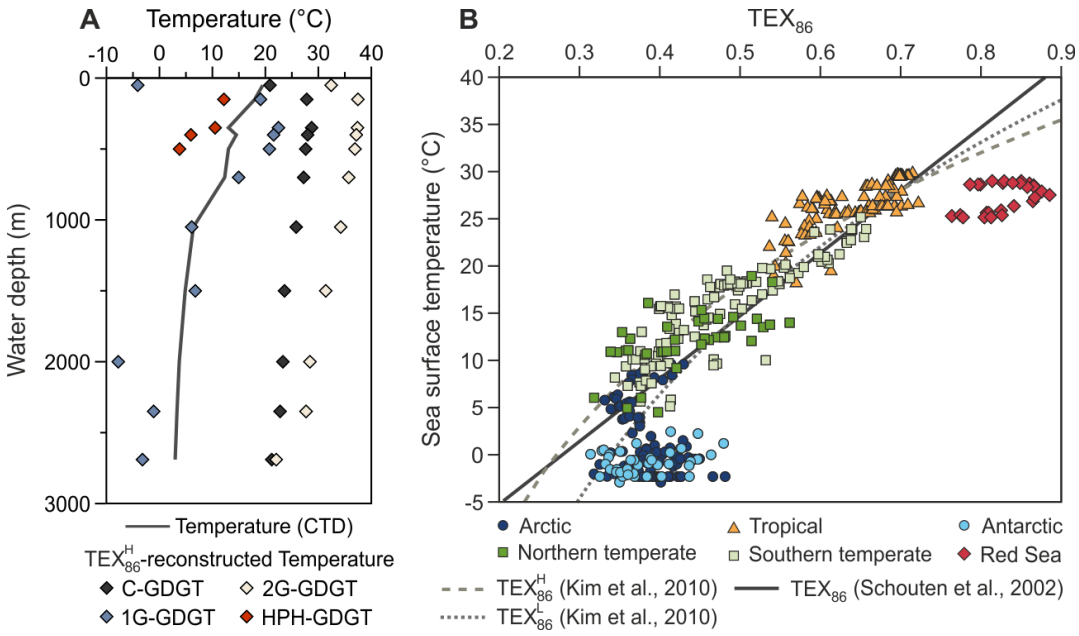

Figure 1.7. (A) Profiles of TEX_{86}^{H}-reconstructed temperatures of core and intact polar GDGTs with monoglycosidic (1G), diglycosidic (2G) and hexose-phosphohexose (HPH) headgroups in suspended particulate matter from the upwelling system off North West Africa showing subsurface divergence of in situ temperatures and reconstructed temperatures as well as systematic offsets in TEX_{86}^{H}-temperatures among different GDGT classes (data from BASSE et al., 2014, Expedition POS425, station GeoB16103-9, 20.78°N, 18.74°W). (B) Relationship of sea surface temperature and TEX_{86} in globally distributed marine core top sediments (KIM et al., 2010) distinguished by location (modified from PEARSON and INGALLS, 2013), indicating poor agreement of Arctic, Antarctic and Red Sea data with the calibration models of SCHOUTEN et al. (2002, TEX_{86}) as well as KIM et al. (2010) for low (TEX_{86}^{L}) and high temperatures (TEX_{86}^{H}; TEX_{86}^{L}, which excludes the crenarchaeol regioisomer, was fitted on the TEX_{86} scale by applying the equation $\text{GDGT-1} = 0.571\ln(TEX_{86}) - 0.776$ as described in PEARSON and INGALLS, 2013).

tropical and temperate planktonic *Thaumarchaeota* (BANO et al., 2004; GALAND et al., 2009a; IONESCU et al., 2009). Samples from these regions deviate strongly from the global TEX_{86} calibration line (Figure 1.7; KIM et al., 2008; TROMMER et al., 2009; KIM et al., 2010), indicating that phylogenetically distinct archaeal communities may have diverging TEX_{86}–temperature relationships. TEX_{86}-temperatures calculated using global regression lines have also revealed regional patterns of over- or underestimation of SSTs (e.g., HUGUET et al., 2007; LEE et al., 2008; LEIDER et al., 2010; WEI et al., 2011; TIERNEY and TINGLEY, 2014). These observations have often been interpreted to reflect regional differences in thaumarchaeal seasonality and have resulted in a plethora of regional TEX_{86} regression models (e.g., TROMMER et al., 2009; LEIDER et al., 2010; HO et al., 2014; SEKI et al., 2014). However, these differences may be equally explained by differences in the production depth of GDGTs (cf. PEARSON et al., 2001; PEARSON and INGALLS, 2013) or differences in the relative contributions of

shallow and deep thaumarchaeal clades to the overall signal (e.g., JIA et al., 2012; KIM et al., 2015). The observed spatial patterns of TEX_{86} and the wealth of regional calibration lines challenge the universal paleogeographical and temporal applicability of the TEX_{86} paleothermometer.

Additional, largely unconstrained variables are the highly debated contributions of other planktonic archaeal groups, such as MG-II *Euryarchaeota* (e.g., LINCOLN et al., 2014a,b; SCHOUTEN et al., 2014), and benthic archaea (e.g., LIPP and HINRICHS, 2009; SCHOUTEN et al., 2010; LIU, 2011; LENGGER et al., 2014) to the water column and sedimentary TEX_{86} signals, respectively. A contribution of these organisms to the environmental signal seems likely, given the wide distribution of GDGT biosynthesis in the *Archaea* (cf. PEARSON and INGALLS, 2013) and the abundance of uncultivated lineages of *Cren-* and *Euryarchaeota* in the water column and sediments (e.g., SCHLEPER et al., 2005; TESKE and SØRENSEN, 2008; AUGUET et al., 2010).

The systematic investigation of the influences of physiological and environmental parameters on lipid composition in cultivated *Thaumarchaeota* may provide a starting point for understanding the formation of thaumarchaeal biomarker signals both in the modern ocean and in ancient environments, in particular of TEX_{86}. Overcoming the impediment of only one available and investigated planktonic thaumarchaeal strain by the isolation and lipid analysis of novel planktonic *Thaumarchaeota* would provide an opportunity to test for the existence of a universal membrane lipid response to temperature and the applicability of currently used empirical TEX_{86}–temperature relationships. Collectively, these experiments could provide a mechanistic basis for the TEX_{86} paleothermometer and thus enhance our ability to reliably reconstruct past environments based on the geologic record.

1.5.3. Potential of respiratory quinones as microbial biomarkers

Besides polar lipids, cytoplasmic membranes also contain respiratory quinones bound to proteins as well as free within the lipid membrane (LENAZ et al., 2007). Respiratory quinones are an essential component of the respiratory chains in almost all organisms, except fermenting bacteria and methanogens, which shuttle electrons and protons between membrane-bound protein complexes (ANRAKU, 1988; GRAY and ELLIS, 1994). Respiratory quinones consist of a polar cyclic headgroup bearing two keto-groups and a head-to-tail linked, saturated or polyunsaturated isoprenoid side chain (Figure 1.8 COLLINS and JONES, 1981; HIRAISHI, 1999). The polar headgroup enables interaction with enzymes, while the apolar side chain facilitates rapid diffusion through the apolar core region of the membrane (LENAZ et al., 2007; NOWICKA and KRUK, 2010). The transfer of electrons and protons from quinones to enzymes is facilitated by the

reversible two-step reduction of the oxidized form, quinone, to the reduced form, quinol, via the free-radical intermediate semi-quinone and vice versa (Figure 1.9; LENAZ et al., 2007; NOWICKA and KRUK, 2010).

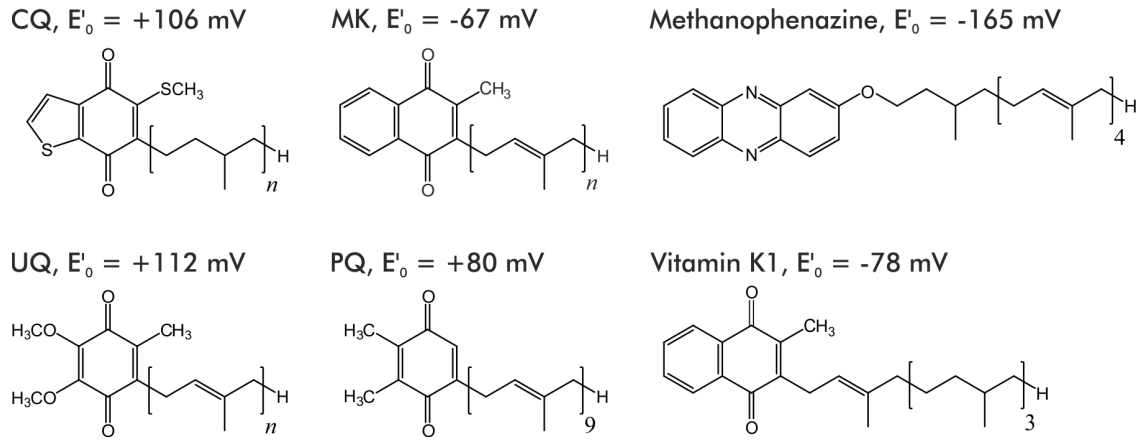

Figure 1.8. Structures and midpoint redox potentials (E'_0 at pH 7) of selected respiratory quinone classes detected in cultivated archaea (CQ, MK, MP) and bacteria/eukaryotes (MK, UQ, Vitamin K1, PQ). Caldariellaquinones (CQ) are specific for aerobic archaea of the order *Sulfolobales*, while menaquinones (MK) have been detected in a number of eury- and crenarchaeal species and anaerobic bacteria (COLLINS et al., 1981; COLLINS and JONES, 1981; HIRAISHI, 1999). Methanophenazine is a functional quinone analogue in the methanogenic archaeon *Methanosarcina mazei* (ABKEN et al., 1998). Ubiquinones (UQ) are essential in aerobic respiration of bacteria and mitochondria (NOWICKA and KRUK, 2010). Vitamin K1 (also known as phylloquinone) and plastoquinones (PQ) occur in photosystems I and II, respectively, of plants, algae, and cyanobacteria (NOWICKA and KRUK, 2010). The lengths and degrees of unsaturation of the isoprenoid side chains of quinones are chemotaxonomically significant and may vary from 4 to 14 and completely saturated to fully unsaturated, respectively (COLLINS and JONES, 1981). Chain lengths of Vitamin K1, PQ, and MP are fixed at 4, 8/9 and 5 isoprenoid units, respectively (ABKEN et al., 1998; NOWICKA and KRUK, 2010).

For proper functioning of quinones in respiratory chains, their redox potentials must be tuned to those of the interacting enzymes and thus, to the specific metabolic process of the organism and overall redox conditions of the environment (COLLINS and JONES, 1981; HIRAISHI, 1999). Therefore, a large variety quinone structural types has been detected among cultivated organisms (Figure 1.8 COLLINS and JONES, 1981; COLLINS, 1985; HIRAISHI, 1999). In all three domains of life, the distribution of respiratory quinone types depends both on metabolism as well as phylogeny and may therefore be used to i) constrain chemotaxnomy (COLLINS and JONES, 1981), ii) to delineate evolutionary relationships (NITSCHKE et al., 1995; ZHI et al., 2014), and iii) to elucidate microbial metabolisms and community composition in the environment (HEDRICK and WHITE, 1986; URAKAWA et al., 2000; VILLANUEVA et al., 2010).

In addition to their function in electron transport chains, quinones might contribute to membrane adaptation to physiological stresses similar to membrane lipids. For

instance, (SÉVIN and SAUER, 2014) observed that sustained osmotic-stress tolerance in the bacterium *Escherichia coli* depended on accumulation of ubiquinone. Therefore, characterization of the cellular quinone pool appears essential for a holistic understanding of membrane properties in microorganisms.

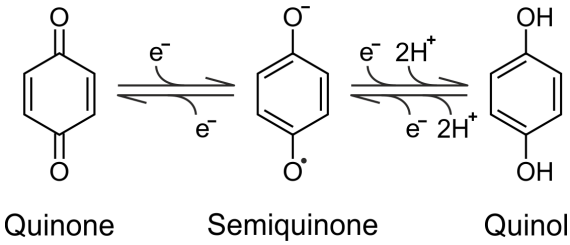

Figure 1.9. Redox transformations between the quinone, semi-quinone intermediate and the quinol forms of respiratory quinones (based on NOWICKA and KRUK, 2010).

However, the knowledge on the distribution of quinone structural types particularly in *Archaea* remains fragmentary (cf. HIRAISHI, 1999; NOWICKA and KRUK, 2010). For example, the quinone composition of *Thaumarchaeota* has not been investigated despite the presumed central role of quinones in current models of the respiratory pathway for ammonia oxidation (WALKER et al., 2010; STAHL and DE LA TORRE, 2012). Still, there is considerable diversity of quinone types with distinct redox potentials among investigated archaeal species (Figure 1.8). For instance, the obligately aerobic *Sulfolobales* synthesize characteristic sulfur-containing quinones such as caldariellaquinone (Figure 1.8; DE ROSA et al., 1977), while halophilic archaea of the order *Halobateriales* contain exclusively polyunsaturated menaquinones and menaquinone derivatives (COLLINS et al., 1981). Similarly, the thermoacidophile *Thermoplasma acidophilum* synthesizes characteristic polyunsaturated methylated menaquinones (SHIMADA et al., 2001). In contrast, methanogenic archaea lack quinones but *Methanosarcina mazei* and potentially other representatives of the order *Methanosarcinales* synthesize methanophenazine as a substitute electron carrier (Figure 1.8 ABKEN et al., 1998).

Based on the large structural diversity of respiratory quinones and their distinct redox-potentials, quinones have a high potential as process-specific biomarkers in environmental studies that remains largely unassessed for *Archaea*.

CHAPTER 2

Scope and Outline

Archaeal GDGT membrane lipids are used both as biomarkers for the abundance of living planktonic *Thaumarchaeota* and for the reconstruction of past SST using the TEX_{86} paleothermometer. However, it is generally known that archaeal membrane lipid composition responds and thus reflects a wealth of environmental (stress) factors. While TEX_{86}-reconstructed temperatures of surface ocean water- and core-top sediment samples correlate with SST, TEX_{86} does not reflect *in situ* temperatures throughout the water column. Investigating the response of thaumarchaeal membrane lipid composition to changes in physiological and environmental parameters, in particular other than temperature, may therefore yield important insights into the functioning of the TEX_{86} proxy. Furthermore, comprehensive analysis of *Thaumarchaeota* cultivated from diverse environments may reveal novel lipid biomarkers for tracing *Thaumarchaeota* independently from GDGTs. In this way, studying the membrane lipid composition of cultivated *Thaumarchaeota* will enhance our ability to reliably reconstruct past environments based on the geologic record.

This thesis is divided into two parts: In **Part I** (Chapters 3 to 5), I investigate the influences of physiological and environmental parameters on the membrane lipid composition of planktonic *Thaumarchaeota* and compare the lipidomes of planktonic, thermophilic and soil *Thaumarchaeota*. **Part I** (Chapters 6 and 7) explores the distribution of respiratory quinones in cultivated *Archaea* and their potential as biomarkers for archaeal and bacterial community structure in a case study from the Black Sea. Part I contains three first-authored manuscripts (one published, two prepared for publication) and Part II comprises two co-first-authored manuscripts (one submitted, one prepared for publication).

The main findings of this thesis are summarized in Chapter 8. Chapter 9 contains

abstracts of 7 manuscripts on microbial membrane lipids, currently in preparation (3), submitted (2), or published (2), which I contributed to as a co-author.

Part I: Membrane lipid adaptation in *Thaumarchaeota*

In **Chapter 3**, I demonstrate that the intact polar lipid composition and TEX_{86} are strongly influenced by growth phase, and therefore likely electron donor availability, in the marine planktonic thaumarchaeon *Nitrosopumilus maritimus*. These observations have important implications for the use of intact polar GDGTs as biomarkers for *Thaumarchaeota* and interpretation of environmental TEX_{86} signals. Furthermore, I show that individual polar GDGT classes have distinct TEX_{86} values. This indicates that differences in degradation rates of intact polar GDGTs may influence TEX_{86} because the intact polar lipid precursors differ for individual core GDGTs. Additionally, a range of novel membrane lipids including the apolar lipid methoxy archaeol are described for the first time.

In **Chapter 4**, I demonstrate that *N. maritimus* and two novel thaumarchaeal strains isolated from the South Atlantic Ocean have distinct intact polar lipid compositions and disparate relationships of TEX_{86} and growth temperature. This indicates that TEX_{86} signals in the environment may be strongly influenced by community composition and questions the temporal and spatial applicability of TEX_{86} paleothermometry. Additionally, I show that pH has a minor, but significant influence on TEX_{86} and lipid composition in *N. maritimus* while there are no such effects of salinity.

In **Chapter 5**, I characterize the lipid composition of 11 thaumarchaeal pure and enrichment cultures and show that these organisms contain an unprecedented diversity of membrane lipids. While the core lipid composition of the different strains reflects thaumarchaeal phylogeny, the intact polar lipid composition is related to the habitat. Complementary analysis of >20 euryarchaeal and crenarchaeal species shows that methoxy archaeol is found exclusively in *Thaumarchaeota*. I further demonstrate in a case study from the equatorial North Pacific Ocean that methoxy archaeol can be used as a biomarker for *Thaumarchaeota* in the environment.

Part II: Respiratory quinones as chemotaxonomic biomarkers

In **Chapter 6**, we describe the respiratory quinone composition of 25 archaeal species based on novel chromatographic protocols that enable the rapid characterization of archaeal respiratory quinones and membrane lipids in a single analysis. We show that respiratory quinone compositions can be used to distinguish environmentally relevant archaeal clades and metabolisms. Based on these results, we suggest that the distribution of respiratory quinone types among extant archaeal species results from a combination of vertical inheritance, gene loss, and lateral gene transfer. Furthermore,

we demonstrate in a case study from the Black Sea water column that specific respiratory quinones trace thaumarchaeal distribution and abundance, suggesting a high potential for archaeal respiratory quinones as biomarkers in the marine environment.

In **Chapter** 7, we demonstrate that combined membrane lipid and respiratory quinone profiling can be used to trace abundances and metabolic processes of bacterial, archaeal, and eukaryotal clades involved in the cycling of carbon, nitrogen, and sulfur and thus resolve the microbial stratification in the chemocline, anoxic waters and sediments of the Black Sea. Therefore, the simultaneous analysis of membrane lipids and respiratory quinones appears as a promising technique for enhancing the quantitative aspect of membrane lipid analyses with process-related information from respiratory quinones.

Contributions to publications

Chapter 3: Effects of growth phase on the membrane lipid composition of the thaumarchaeon *Nitrosopumilus maritimus* and their implications for archaeal lipid distributions in the marine environment.
Felix J. Elling, Martin Könneke, Julius S. Lipp, Kevin W. Becker, Emma J. Gagen, Kai-Uwe Hinrichs

Published in *Geochimica et Cosmochimica Acta*, 2014, Vol. 141, pages 579-597.

F.J.E, M.K., J.S.L., and K.-U.H. designed the research; F.J.E. and E.J.G. performed lab work; F.J.E. analyzed data with help from M.K., J.S.L., K.W.B, and K.-U.H.; F.J.E., M.K., and K.-U.H. wrote the manuscript with contributions from all co-authors.

Chapter 4: Differential response of membrane lipid composition to temperature, pH, and salinity in marine planktonic *Thaumarchaeota*.
Felix J. Elling, Martin Könneke, Marc Mußmann, Andreas Greve, Kai-Uwe Hinrichs

In preparation for *Geochimica et Cosmochimica Acta*

F.J.E, M.K., and K.-U.H. designed the research; F.J.E. and A.G. performed lab work; F.J.E. analyzed data with contributions of M.K., M.M., A.G., and K.-U.H.; F.J.E. and M.K. wrote the manuscript with contributions from all co-authors.

Chapter 5: Comparative analysis of the thaumarchaeal lipidome.
Felix J. Elling, Martin Könneke, Kevin W. Becker, Michaela Stieglmeier, Graeme W. Nicol, Eva Spieck, José R. de la Torre, Gerhard Herndl, Christa Schleper, Kai-Uwe Hinrichs

In preparation for *Applied and Environmental Microbiology*

F.J.E, M.K., and K.-U.H. designed the research; M.S., G.W.N, E.S., J.R.d.l.T., G.H., and C.S. provided samples; F.J.E. performed lab work; F.J.E. analyzed data with contributions from M.K., K.W.B., and K.-U.H.; F.J.E. wrote the manuscript with contributions from M.K. and K.W.B.

Chapter 6: Respiratory quinones in *Archaea*: phylogenetic distribution and application as biomarkers in the marine environment.
Felix J. Elling, Kevin W. Becker*, Martin Könneke, Jan M. Schröder, Matthias Y. Kellermann, Michael Thomm, Kai-Uwe Hinrichs*
*equal contribution

Under review for *Environmental Microbiology*

F.J.E., K.W.B., and K.-U.H. designed the research; M.T. provided samples; F.J.E., K.W.B., J.M.S., and M.Y.K. performed lab work; F.J.E. and K.W.B. analyzed data with contributions from J.M.S., M.Y.K., M.K., and K.-U.H.; F.J.E., K.W.B. and M.K. wrote the manuscript with contributions from all co-authors.

Chapter 7: Sources, distribution and fate of respiratory quinones in the water column and sediments of the Black Sea.
Kevin W. Becker, Felix J. Elling*, Jan M. Schröder, Julius S. Lipp, Matthias Zabel, Kai-Uwe Hinrichs*
*equal contribution

In preparation for *Geochimica et Cosmochimica Acta*

K.W.B., F.J.E., and K.-U.H. designed the research; K.W.B., F.J.E., and J.M.S performed lab work; M.Z. provided data; K.W.B., F.J.E., and J.M.S. analyzed data with contributions from J.S.L., M.Z., and K.-U.H.; K.W.B. and F.J.E. wrote the manuscript with contributions from all co-authors.

Part I.

Membrane lipid adaptation in *Thaumarchaeota*

CHAPTER 3

Effects of growth phase on the membrane lipid composition of the thaumarchaeon *Nitrosopumilus maritimus* and their implications for archaeal lipid distributions in the marine environment

Felix J. Elling[a], Martin Könneke[a,*], Julius S. Lipp[a], Kevin W. Becker[a], Emma J. Gagen[b]† and Kai-Uwe Hinrichs[a]

Published in *Geochimica et Cosmochimica Acta*
2014
Vol. 141, pages 579-597. doi: 10.1016/j.gca.2014.07.005

[a] Organic Geochemistry Group, MARUM - Center for Marine Environmental Sciences & Department of Geosciences, University of Bremen, 28359 Bremen, Germany
[b] Lehrstuhl für Mikrobiologie und Archaeenzentrum, Universität Regensburg, 93053 Regensburg, Germany

† Present address: E.J. Gagen, School of Earth Sciences, The University of Queensland, St. Lucia, Australia

* Corresponding author. E-mail: mkoenneke@marum.de

Abstract

The characteristic glycerol dibiphytanyl glycerol tetraether membrane lipids (GDGTs) of marine ammonia-oxidizing archaea (AOA) are widely used as biomarkers for studying their occurrence and distribution in marine environments and for reconstructing past sea surface temperatures using the TEX_{86} index. Despite an increasing use of GDGT biomarkers in microbial ecology and paleoceanography, the physiological and environmental factors influencing lipid composition in AOA, in particular the cyclization of GDGTs, remain unconstrained. We investigated the effect of metabolic state on the composition of intact polar and core lipids and the resulting TEX_{86} paleothermometer in pure cultures of the marine AOA *Nitrosopumilus maritimus* as a function of growth phase. The cellular lipid content ranged from 0.9 to 1.9 fg cell^{-1} and increased during growth but was lower in the stationary phases, indicating changes in average cell size in response to metabolic status. The relative abundances of monoglycosidic GDGTs increased from 27% in early growth phase to 60% in late stationary phase, while monohydroxylated GDGTs increased only slightly. The proportions of characteristic hexose-phosphohexose GDGTs were up to 7-fold higher during growth than in stationary phase, suggesting that they are valuable biomarkers for the metabolically active fraction of AOA assemblages in the environment. Methoxy archaeol was identified as a novel, genuine archaeal lipid of yet unknown function; it is one of the most abundant single compounds in the lipidome of *N. maritimus*. TEX_{86} values of individual intact GDGTs and total GDGTs differed substantially, were generally lower during early and late growth phases than in stationary phase, and did not reflect growth temperature. Consequently, our results strongly suggest that biosynthesis is at least partially responsible for the systematic offsets in TEX_{86} values between different intact polar GDGT classes observed previously in environmental samples. Nevertheless, differences in degradation rates of intact polar GDGTs may influence the TEX_{86} index because the intact polar lipid precursors differ for individual core GDGTs and moreover their relative abundances change with growth stage, which may result in distinct release rates of core GDGTs from their polar precursors. Overall, our findings stress the need to accurately describe the factors influencing GDGT cyclization in thaumarchaea and thus paleotemperature reconstructions.

3.1. Introduction

Marine ammonia-oxidizing archaea (AOA) are a cosmopolitan and abundant group of microorganisms in the oceans (KARNER et al., 2001; SCHATTENHOFER et al., 2009). They play a key role in the marine nitrogen cycle by catalyzing the first and rate-limiting step of nitrification, the oxidation of ammonia to nitrite, and are well adapted to the oligotrophic conditions commonly found in the open ocean (MARTENS-HABBENA et al., 2009; STAHL and DE LA TORRE, 2012; KÖNNEKE et al., 2014). The marine AOA (formerly Marine Group I *Crenarchaeota*) as well as terrestrial and thermophilic AOA are affiliated with the *Thaumarchaeota*, a recently proposed novel phylum of the domain Archaea (BROCHIER-ARMANET et al., 2008; SPANG et al., 2010).

The cytoplasmic membranes of *Archaea* consist of glycerol diphytanyl diether lipids (archaeols) and membrane-spanning glycerol dibiphytanyl glycerol tetraethers (GDGTs) containing up to four cyclopentyl moieties in their core structures (Fig. 3.1; DE ROSA and GAMBACORTA, 1988). A distinct feature of the *Thaumarchaeota* is the presence and relatively high proportion of crenarchaeol, a core lipid with one cyclohexyl and four cyclopentyl moieties (e.g., SINNINGHE DAMSTÉ et al., 2002b; DE LA TORRE et al., 2008; SCHOUTEN et al., 2008; PITCHER et al., 2010, 2011a, Fig. 3.1). In live thaumarchaeal cells, lipids occur primarily as intact polar lipids (IPLs), i.e., core lipids with one to two phosphatidic, glycosidic or glycophosphatidic headgroups attached (e.g., SCHOUTEN et al., 2008; PITCHER et al., 2011a, Fig. 3.1).

GDGTs in their core lipid form, crenarchaeol in particular, have frequently been used as biomarkers in microbial ecology to study the occurrence and distribution of thaumarchaea in the marine water column (e.g., SCHOUTEN et al., 2000; SINNINGHE DAMSTÉ et al., 2002a; INGALLS et al., 2006; HERFORT et al., 2007; WAKEHAM et al., 2007). However, core GDGTs are not suitable for tracing live cells as they predominantly represent a fossil signal. Based on the assumption of rapid degradation of intact polar to core lipids after cell death, intact polar GDGTs have recently been introduced as biomarkers for tracing and quantifying living AOA in the marine water column (e.g., SCHUBOTZ et al., 2009; PITCHER et al., 2011c; INGALLS et al., 2012; SCHOUTEN et al., 2012; WAKEHAM et al., 2012; BASSE et al., 2014; XIE et al., 2014).

The characterization of IPLs in AOA cultures facilitates the interpretation of IPLs abundantly detected in environmental studies and their assignment to phylogenetic clades. The membrane lipid composition of *Nitrosopumilus maritimus*, a cultivated marine group I.1a thaumarchaeon (KÖNNEKE et al., 2005; STAHL and DE LA TORRE, 2012) closely related to abundant phylotypes found in the open ocean, is similar to that observed in cultured and enriched sedimentary, soil and thermophilic AOA (DE LA TORRE et al., 2008; SCHOUTEN et al., 2008; PITCHER et al., 2011a). The

membranes of AOA are dominated by monoglycosidic (1G-GDGTs) and diglycosidic GDGTs (2G-GDGTs) as well as hexose-phosphohexose-GDGTs (HPH-GDGTs). Within the *Thaumarchaeota*, 1G- and 2G-GDGTs containing a hydroxylation in one of the side chains (1G- and 2G-OH-GDGTs; LIPP and HINRICHS, 2009; LIU et al., 2012b) have so far only been observed in marine group I.1a *Thaumarchaeota* (SCHOUTEN et al., 2008; PITCHER et al., 2011a) and thus appear to be a characteristic IPL of this clade.

The crenarchaeol derivatives of HPH- and 2G-GDGTs have been shown to correlate with thaumarchaeal 16S rRNA and *amoA* (ammonia monooxygenase subunit A) gene copy numbers in the Arabian Sea water column (PITCHER et al., 2011b; SCHOUTEN et al., 2012), suggesting a causal relationship between HPH- and 2G-crenarchaeol abundance and active AOA. Moreover, it has been suggested that glycosidic IPLs are more slowly degraded than phosphatidic IPLs (e.g., SCHOUTEN et al., 2010; XIE et al., 2013), thereby raising the question which IPLs can be utilized for indicating live AOA in the marine water column. However, with respect to archaeal lipids, which are present exclusively as ether lipids, conclusive evidence for more rapid degradation of phosphate-based IPLs than glycosidic IPLs is still lacking (cf. LOGEMANN et al., 2011).

Fossil core GDGTs originating from planktonic AOA are ubiquitously found in marine and lacustrine sediments of up to Cretaceous age and are frequently used in paleoceanography as a proxy for past surface water temperatures (indexed as TEX_{86}; SCHOUTEN et al., 2002; for reviews refer to PEARSON and INGALLS, 2013 and SCHOUTEN et al., 2013). The TEX_{86} paleothermometer is based on the observation that the degree of cyclization of GDGTs found in surface sediments is correlated to sea surface temperature (SST; SCHOUTEN et al., 2002). Temperature sensitivity experiments on marine enrichment cultures by WUCHTER et al. (2004) and SCHOUTEN et al. (2007a) as well as core-top calibration studies (KIM et al., 2008, 2010) indicated that the differences in relative abundance of core GDGTs, and specifically those containing one to three cyclizations and the crenarchaeol regioisomer, as indexed in the TEX_{86}, are strongly correlated to sea surface temperature. The influence of physiological and environmental parameters on TEX_{86} has not been systematically studied in cultures of AOA. This represents a major caveat in TEX_{86}-based temperature reconstructions, since parameters like growth phase, salinity and pH are known to substantially influence lipid composition in other archaea (e.g., MACALADY et al., 2004; MATSUNO et al., 2009; BOYD et al., 2011; DAWSON et al., 2012). In fact, the exact physiological and ecological controls on GDGT cyclization in living AOA remain enigmatic in the face of widely observed discrepancies between *in situ* and TEX_{86} temperatures in mesopelagic AOA assemblages (e.g., TURICH et al., 2007; SCHOUTEN et al., 2012). Thus, constraining the influence of physiological and environmental parameters on membrane lipid composition in marine planktonic AOA is crucial for

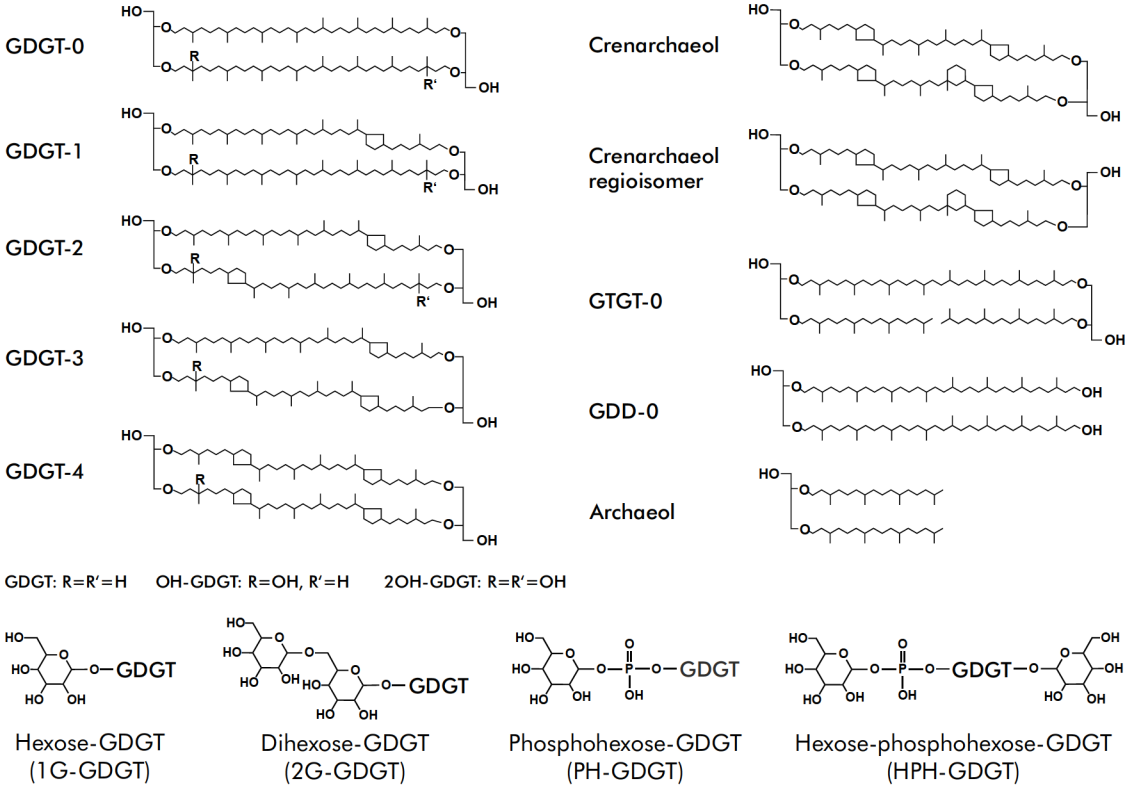

Figure 3.1. Molecular structures of glycerol dibiphytanyl glycerol tetraether (GDGT) core lipids (R=R'=H) with 0 to 4 cyclopentyl moieties and the putatively AOA-specific core lipid crenarchaeol. OH-GDGTs and 2OH-GDGTs are core structures bearing one (R=OH, R'=H) and two additional hydroxyl groups (R=R'=OH), respectively. Archaeol, glycerol trialkyl glycerol tetraether (GTGT) and zero to five ring bearing glycerol dialkanol diethers (GDDs) are minor core lipids in thaumarchaeota. Intact polar lipids consist of one or two polar headgroups attached to a core lipid. Typical intact polar lipids in *N. maritimus* are hexose- (1G-GDGTs), dihexose- (2G-GDGTs), phosphohexose- (PH-GDGTs) and hexose-phosphohexose-GDGTs (HPH-GDGTs).

comprehensively evaluating the TEX_{86} paleotemperature proxy. Furthermore, this will improve lipid-based reconstructions of the role of AOA in the past and present cycles of carbon and nitrogen.

Here, we studied the response of membrane lipid composition to growth phase in the first marine AOA available in pure culture, *N. maritimus* (KÖNNEKE et al., 2005). In contrast to environmental studies, the growth of a pure culture allows the performance of experiments under defined, reproducible conditions. While batch cultures cannot fully reflect the complexities of natural microbial assemblages, these tightly controlled experiments have proved to be fundamental to our understanding of environmental lipid fingerprints (e.g., PRAHL and WAKEHAM, 1987). We analyzed the IPL composition of *N. maritimus* in different growth phases to facilitate interpretation of IPL data from environmental samples and to identify intact polar GDGTs that are indicative for growing AOA. Our study significantly extends the range of lipid diversity

known for *N. maritimus* by using innovative analytical protocols (cf. BECKER et al., 2013; ZHU et al., 2013). Furthermore, we determined the cellular lipid content of *N. maritimus* during different growth phases to facilitate the lipid-based quantification of thaumarchaeal biomass in water column studies. The influence of growth phase on composition and cyclization of the intact and core GDGT pools of *N. maritimus* was investigated and discussed in the context of environmental lipid signatures and the TEX_{86} paleothermometer.

3.2. Materials and Methods

3.2.1. Cultivation and lipid extraction

N. maritimus strain SCM1 was grown aerobically at 28 °C in four separate 8.5-l batch cultures in pH 7.5 HEPES-buffered Synthetic Crenarchaeota Medium (SCM) as described previously (KÖNNEKE et al., 2005; MARTENS-HABBENA et al., 2009; KÖNNEKE et al., 2012). The medium was amended with 1.5 mM ammonium chloride and each bottle was inoculated with 450 ml of an *N. maritimus* culture being in the middle of the growth phase as indicated by the consumption of 0.4 mM ammonia. Cell concentrations after inoculation were between 7.0 and 8.3×10^5 cells ml^{-1} and corresponding nitrite concentrations were between 0.024 and 0.027 mM. Cultures were gently shaken by hand twice a day when they reached nitrite concentrations of about 0.1 mM. Purity of the culture was checked daily by phase contrast microscopy. Growth was monitored by measuring nitrite formation daily and by counting SYBR Green I stained cells at the beginning and the end of the experiment.

Cells were enumerated by epifluorescence microscopy of 2% formaldehyde-fixed samples using SYBR Green I staining solution as described by (LUNAU et al., 2005). Nitrite concentration was determined using diazo-colorimetry with photo- metric detection at 545 nm (STICKLAND and PARSONS, 1972). Cells were harvested at four time-points (one batch for each time-point; Fig. 3.2) using a Sartocon Slice cross-flow filtration system (Sartorius, Göttingen, Germany). In order to estimate reproducibility, samples for the early stationary phase time point were grown in triplicate batches. The cell pellets (ca. 3×10^{10} to 1.5×10^{11} cells, cf. Table 3.1) were stored at −20 °C until extraction. Lipids from each batch were extracted with dichloromethane:methanol:buffer (1:2:0.8, v:v:v) following a modified Bligh & Dyer protocol (STURT et al., 2004) using phosphate and trichloroacetic acid (CCl_3CO_2H) buffers (each 2×) and an ultrasonic probe (15 min sonication; HD2200, Bandelin electronic, Germany). The total lipid extract (TLE) was dried under a stream of N_2 and stored at −20 °C until measurement.

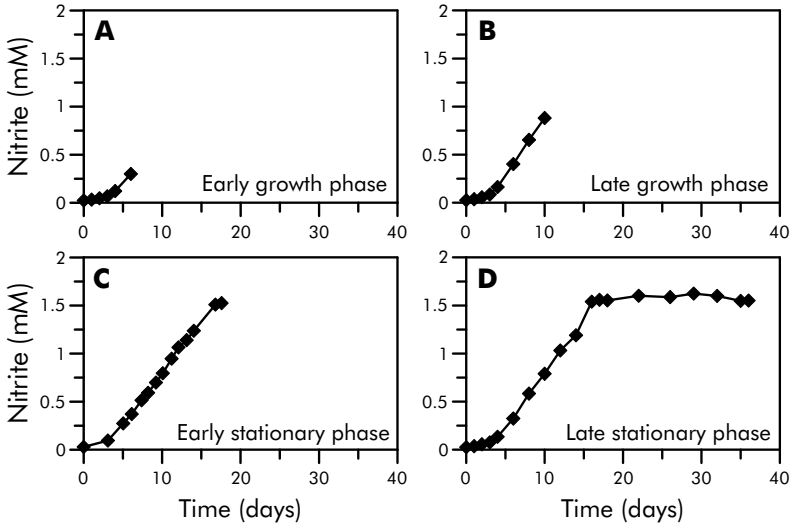

Figure 3.2. Growth of *N. maritimus* in four individual batch cultures monitored by nitrite formation. Cells were harvested in early (A) and late growth phase (B) as well as in early (C) and late (D) stationary phases.

3.2.2. Intact polar and core lipid analysis

Intact polar and core lipids were quantified by injecting 10% of the TLE dissolved in methanol on a Dionex Ultimate 3000 high performance liquid chromatography (HPLC) system connected to a Bruker maXis Ultra-High Resolution quadrupole time-of-flight tandem mass spectrometer (qTOF-MS) equipped with an ESI ion source operating in positive mode (Bruker Daltonik, Bremen, Germany). The mass spectrometer was set to a resolving power of 27,000 at m/z 1222 and every analysis was mass-calibrated by loop injections of a calibration standard and correction by lock mass, leading to a mass accuracy of better than 1-3 ppm. Ion source and other MS parameters were optimized by infusion of standards (GDGT-0, 1G-GDGT-0, 2G-GDGT-0) into the eluent flow from the LC system using a T-piece.

Analyte separation was achieved using reversed phase (RP) HPLC on an ACE3 C_{18} column (2.1 × 150 mm, 3 µm particle size, Advanced Chromatography Technologies, Aberdeen, Scotland) maintained at 45 °C as described by ZHU et al. (2013). In brief, analytes were eluted at a flow rate of 0.2 ml min^{-1} isocratically for 10 min with 100% eluent A (methanol:formic acid:14.8 M NH_4^+, 100:0.04:0.10, v:v:v), followed by a linear gradient to 24% eluent B (2-propanol:formic acid:14.8 M NH_4^+, 100:0.04:0.10, v:v:v) in 5 min, followed by a gradient to 65% B in 55 min. The column was then flushed with 90% B for 10 min and re-equilibrated with 100% A for 10 min.

Additionally, core lipids were analyzed in duplicate on the same system under different chromatographic conditions using normal phase (NP) HPLC and an APCI-II ion source operated in positive mode, as described by BECKER et al. (2013). Briefly,

5% TLE aliquots were dissolved in *n*-hexane:2-propanol (99.5:0.5, v:v) and injected onto two coupled Acquity BEH Amide columns (2.1 × 150 mm, 1.7 μm particle size, Waters, Eschborn, Germany) maintained at 50 °C. Lipids were eluted using linear gradients of *n*-hexane (eluent A) to *n*-hexane:2-propanol (90:10, v:v; eluent B) at a flow rate of 0.5 ml min^{-1}. The initial gradient was 3% B to 5% B in 2 min, followed by increasing B to 10% in 8 min, to 20% in 10 min, to 50% in 15 min and 100% in 10 min, followed by 6 min at 100% B to flush and 9 min at 3% B to re-equilibrate the columns.

To determine the TEX_{86} of total GDGTs and cellular lipid content, 10% of the TLE was hydrolyzed with 1 M HCl in methanol for 3 h at 70 °C to yield core GDGTs. Tests with varying acid strengths, reaction times and temperatures revealed a high efficiency (<5% IPLs left) and minimal formation of artifacts (<2%, e.g., unsaturated or methylated GDGTs), using these conditions. The hydrolyzed TLE was dried under a flow of N_2 at 35 °C and then analyzed as described above for the core lipids.

Lipids were identified by retention time as well as by accurate molecular mass and isotope pattern match of proposed sum formulas in full scan mode and MS^2 fragment spectra. Integration of peaks was performed on extracted ion chromatograms of ±10 mDa width and included the $[M+H]^+$ ions for NP-HPLC-MS and additionally $[M+NH_4]^+$ and $[M+Na]^+$ ions for RP-HPLC-MS. Where applicable, double charged ions were included in the integration. The areas of 1G-, 2G-, and HPH-GDGT-4 were corrected for co-elution with the respective crenarchaeol regioisomer (Cren') by subtracting the area of the +2 Da isotope peak of Cren', which was calculated from natural isotope abundances (ZHANG et al., 2006).

Lipid quantification was achieved by injecting an internal standard (HUGUET et al., 2006, C_{46}-GTGT;) along with the samples. Lipid abundances were corrected for response factors of commercially available as well as purified standards. Archaeol was purchased from Avanti Polar Lipids Inc. (Alabaster, AL, USA). Phosphatidylglycerol-hexose GDGT was obtained from Matreya LLC (Pleasant Gap, PA, USA). GDGT-0, 1G-GDGT-0, 2G-GDGT-0, monoglycosidic archaeol (1G-AR), and diglycosidic archaeol (2G-AR) were purified from extracts of *Archaeoglobus fulgidus* by orthogonal preparative liquid chromatography as described by ZHU et al. (2013). The abundances of core GDGTs, methoxy archaeol and archaeol were averaged from duplicate measurements and corrected for the response factors of purified GDGT-0 and core archaeol standards versus the C_{46}-GTGT standard. The relative discrepancy of duplicate measurements from the average was below 9%. The abundances of glycerol trialkyl glycerol tetraethers (GTGTs), hydroxy GDGTs (OH-GDGTs), glycerol dialkanol diethers (GDDs) and hydroxy GDDs (OH-GDDs) were corrected for the response factor of GDGT-0. Similarly, the abundances of IPLs were corrected for the response factors of purified

1G-AR, 1G-GDGT-0 (for 1G-, 1G-OH-, deoxy-1G-GDGTs, 1G-GDDs), and 2G-GDGT-0 (for 2G-, 2G-OH, 2G-2OH-GDGTs) standards versus the C_{46}-GTGT standard. Due to a lack of appropriate standards, the abundances of phosphohexose- and HPH-GDGTs were corrected for the response of a phosphatidylglycerol-hexose GDGT standard, respectively. For phosphohexose archaeol (PH-AR), we assumed the response factor of 2G-AR. We assumed the same response factor of GDGT-0 and MeO-GDGTs due to a lack of an authentic MeO-GDGT standard. However, the presence of the methoxy group might influence the response of MeO-GDGTs relative to GDGT-0. The relative abundance of MeO-AR was corrected by its response factor relative to AR by comparing the relative abundance of MeO-AR and AR analyzed by GC-FID; assuming unity of their FID-based response factors, we found that RP-HPLC-MS analysis resulted in a 1.6 times higher response of MeO-AR relative to AR and corrected the calculated concentrations accordingly. The C_{46}-GTGT injection standard was then used to correct for matrix effects (assuming the same ion suppression effect for all compounds of interest) and the calibration was used to correct for individual response.

The TEX_{86} index was calculated after SCHOUTEN et al. (2002) using the peak areas of GDGT-1, GDGT-2, GDGT-3 and Cren', with the number indicating the number of cyclizations within the molecule:

$$TEX_{86} = \frac{[\text{GDGT-2}] + [\text{GDGT-3}] + [\text{Cren'}]}{[\text{GDGT-1}] + [\text{GDGT-2}] + [\text{GDGT-3}] + [\text{Cren'}]} \quad \text{(Eq. 1)}$$

TEX_{86} reconstructed temperatures were calculated using the core-top calibration of KIM et al. (2010):

$$\text{SST } (^{\circ}\text{C}) = 68.4 \times \log(TEX_{86}) + 38.6 \quad \text{(Eq. 2)}$$

To evaluate GDGT cyclization we calculated the ring index (RI) according to PEARSON et al. (2004):

$$RI = \frac{[\text{GDGT-1}] + 2 \times [\text{GDGT-2}] + 3 \times [\text{GDGT-3}] + 4 \times [\text{GDGT-4}] + 5 \times [\text{Cren} + \text{Cren'}]}{[\text{GDGT-0}] + [\text{GDGT-1}] + [\text{GDGT-2}] + [\text{GDGT-3}] + [\text{GDGT-4}] + [\text{Cren} + \text{Cren'}]} \quad \text{(Eq. 3)}$$

3.2.3. Identification of novel lipids

Samples were screened for novel lipids using NP- and RP-HPLC-MS^2. For further analysis of a novel group of compounds, methoxy archaeol and methoxy GDGTs, a core lipid fraction was prepared from a *N. maritimus* extract by semi-preparative liquid chromatography using an Agilent 1200 series HPLC system connected to an Agilent

1200 series fraction collector. Core and intact polar lipids were separated on an Inertsil diol column (10 × 150 mm, 5 µm particle size, GL Sciences, Tokyo, Japan) maintained at 30 °C and using linear gradients of *n*-hexane:2-propanol (85:15, v:v; eluent A) and 2-propanol:water (90:10, v:v; eluent B) at a flow rate of 3 ml min^{-1}. The gradient program consisted of 0% B to 10% B in 5 min, increasing B to 85% at 6 min, hold at 85% B for 9 min followed by re-equilibration with 100% A for 10 min.The core lipids were collected within the time window of 0 to 5 min.

The core lipid fraction was then acetylated according to the protocol of ALUWIHARE et al. (2002) to check for the absence of primary hydroxyl groups in the tentatively assigned methoxy archaeol and GDGTs. In brief, the core lipid fraction was mixed with 100 µl of acetic anhydride and 20 µl of 1-methyl imidazole and left at room temperature. After 15 min, excess reagent was quenched with 0.5 ml of water and the mixture was left at room temperature for 10 min. The acetylated lipids were then extracted 5 times with 0.5 ml of dichloromethane. The extracts were combined, dried and dissolved in *n*-hexane:2-propanol (99.5:0.5, v:v) for NP-HPLC-MS analysis. An archaeol standard was acetylated and analyzed under the same conditions as a positive control. An aliquot of the core lipid fraction was analyzed directly by coupled gas chromatography-mass spectrometry (GC-MS) using an Agilent 7890A GC coupled to an Agilent 5975c VL MSD. A further aliquot was derivatized using bis-(trimethylsilyl) trifluoroacetamide in pyridine at 70 °C for 1 h and analyzed on the same system. The mass spectrometer was operated in electron impact mode at 70 eV with a full scan mass range of m/z 50-800. Analyte separation was achieved on an Optima 5 MS Accent capillary column (30 m × 250 µm × 0.25 µm, Macherey-Nagel, Duren, Germany) using an oven temperature program of 60 °C (held 1 min) to 150 °C at 10 °C min^{-1} and then to 320 °C (held 30 min) at 4 °C min^{-1}. The linear retention index (LRI) was determined relative to *n*-alkane standards according to VAN DEN DOOL and KRATZ (1963).

To assess artificial production of methoxy archaeol and GDGTs by methylation of core archaeol and core GDGTs during extraction or sample preparation, one half of a *N. maritimus* cell pellet was extracted using methanol:dichloromethane:buffer (2:1:0.8, v:v:v) as described above. The remaining half was extracted with ethanol substituted for methanol in the extraction mixture. Trace impurities of methanol in the ethanol (<100 ppm) contributed less than 5 µl of methanol to the extraction mix in this experiment. The TLEs were then analyzed by NP-HPLC-MS.

3.2.4. Reproducibility assessment

Reproducibility of lipid composition was evaluated on triplicate batch cultures of *N. maritimus* harvested in early stationary phase. The standard deviation of cell counts based on replicate filtration and counting was below 2%. Lipid yield per cell determined for hydrolyzed samples in these triplicates varied by up to 0.4 fg cell^{-1} (24%, including propagated errors from cell counting). The standard deviation of IPL abundance was 7.9% for 1G-GDGTs, 1.2% for 1G-OH-GDGTs, 5.9% for 2G-GDGTs, 6.8% for 2G-OH-GDGTs, and 0.3% for HPH-GDGTs (Supp. Table 3.2). The standard deviation of TEX_{86} values was 0.03 for 1G-GDGTs,<0.01 for 2G-GDGTs, 0.01 for HPH-GDGTs and 0.04 for core GDGTs and hydrolysis-derived core GDGTs (Supp. Table 3.3). Duplicate hydrolysis revealed variations of up to 0.02 in TEX_{86} of core GDGTs.

3.3. Results

3.3.1. Cellular lipid content

Growth of *N. maritimus* among independent cultures as monitored by nitrite formation was very similar (Fig. 3.2). Cell counts at the point of harvest were 3.7×10^6 cells ml^{-1} for early growth phase, 9.5×10^6 cells ml^{-1} for late growth phase, 2.4×10^7 cells ml^{-1} for early stationary phase and 1.8×10^7 cells ml^{-1} for late stationary phase (Table 3.1). The absolute abundances of GDGTs, OH-GDGTs, and archaeols were quantified before and after hydrolysis, yield- ing the abundance of IPLs by subtraction. The cellular lipid content calculated from cell counts and lipid abundance comprised nearly exclusively IPLs and changed during growth (Table 3.1). The cellular lipid content increased from 0.9 fg cell^{-1} in early growth phase to 1.6 fg cell^{-1} in late growth phase and 1.9 fg cell^{-1} in early stationary phase. In late stationary phase, cellular lipid content decreased to 0.9 fg cell^{-1}. Lipid carryover from the inoculum (equivalent to 7-8 $\times 10^5$ cells ml^{-1}) comprised <20% of the extract in early growth phase and <10% in the later time points.

3.3.2. Intact polar lipids

Intact polar GDGTs and IPL archaeols comprised 85-92% of the total lipids of *N. maritimus* (Table 3.2). The major IPLs were 1G-GDGT, 2G-GDGT and HPH-GDGT, as well as GDGTs with mono- and dihexose headgroups and monohydroxylated core structures (1G-OH-GDGT, 2G-OH-GDGT; Fig. 3.3a). IPLs of minor abundance (i.e., <1%, Table 3.2) comprised dihydroxylated 2G-GDGTs (2G-2OH-GDGT; cf. LIU et al., 2012b), phosphohexose GDGTs (PH-GDGT; cf. SCHOUTEN et al., 2008), and mono-glycosidic GDDs (1G-GDD; cf. MEADOR et al., 2014b). Furthermore, we detected a sequence of

Table 3.1. Cell densities, NO_2^- formation and cellular lipid contents in growth phases and stationary phase. Total lipids were determined on hydrolyzed samples. IPL content was determined by subtracting abundances of core lipids in the TLE from total lipids. GDGT content includes GDGTs and OH-GDGTs, archaeol content includes AR and MeO-AR.

Time interval	Early growth phase	Late growth phase	Early stationary phase	Late stationary phase
Cell density (cells ml^{-1})	3.7×10^6	9.5×10^6	2.4×10^7	1.8×10^7
NO_2^- formed (mM)	0.28	0.86	1.46	1.53
Specific cell yield (cells/mol NH_4^+)	9.57×10^{12}	9.86×10^{12}	1.23×10^{13}	1.11×10^{13}
Total lipids (fg $cell^{-1}$)	0.86	1.55	1.85	0.92
Total IPLs (fg $cell^{-1}$)	0.83	1.52	1.81	0.91
Intact polar GDGTs (fg $cell^{-1}$)	0.82	1.52	1.81	0.91
Intact polar archaeols (fg $cell^{-1}$)	<0.02	<0.01	<0.01	<0.01
Total core lipids (fg $cell^{-1}$)	0.03	0.03	0.04	0.01
Core GDGTs (fg $cell^{-1}$)	0.01	0.01	0.01	<0.01
Core archaeols (fg $cell^{-1}$)	0.02	0.02	0.03	<0.01
Total GDGTs (fg $cell^{-1}$)	0.83	1.52	1.82	0.91
Total archaeols (fg $cell^{-1}$)	0.03	0.03	0.03	0.01

compounds with identical molecular mass and MS^2 spectra as 2G-GDGTs but eluting 4 min earlier in RP-HPLC; their highest abundance among IPLs was during the early stationary phase (2.8%). We tentatively identified a series of GDGTs eluting after 1G-GDGT showing a neutral loss of 147.1 as deoxy hexose GDGTs (deoxy-1G-GDGT) based on their exact mass and proposed sum formula. Finally, we identified archaeols bearing a hexose headgroup (1G-AR, m/z 832.8 $[M+NH_4]^+$) and a phosphohexose or phosphoinositol headgroup (PH-AR, m/z 895.7 $[M+H]^+$; cf. YOSHINAGA et al., 2011) based on diagnostic losses of 179.1 (hexose plus NH_3) and 261.0 (phosphohexose or phosphoinositol), respectively. Intact polar archaeols were of low abundance in all extracts with the exception of PH-AR that accounted for 4.4% of IPLs during early growth phase.

3.3.3. Intact polar lipid composition in different growth phases

The relative abundances of major IPLs changed strongly between different growth phases and stationary phase (Fig. 3.3a). The abundance of 1G-GDGTs increased from 27% in early growth phase to 60% of total IPLs in late sta- tionary phase, while

Table 3.2. Relative abundances (in %) of intact polar and core membrane lipids in total lipid extracts of *N. maritimus* in different growth and stationary phases as determined by reversed phase HPLC-MS (b.d. = below detection). GDGT-# refers to the GDGT/GTGT core structures. Numbers in brackets refer to the abundance (in %) relative to total IPLs. IPL names in italics indicate compounds summarized under 'Other IPLs' in Fig. 3.3a. MeO-AR was grouped with core lipids as it represents an intact but apolar lipid.

	Early growth phase	Late growth phase	Early stationary phase	Late stationary phase	GDGT-#
Intact polar lipids					
1G-GDGT	23.2 (27.2)	42.5 (49.1)	46.8 (51.0)	51.2 (60.3)	0-5, 5‘
1G-OH-GDGT	1.9 (2.3)	3.4 (3.9)	2.5 (2.8)	3.4 (4.0)	0-5
2G-GDGT	9.1 (10.6)	5.4 (6.2)	10.0 (10.7)	4.1 (4.8)	0-5, 5‘
2G-OH-GDGT	27.9 (32.6)	23.6 (27.2)	20.7 (22.8)	20.2 (23.8)	0-4
2G-2OH-GDGT	0.5 (0.6)	1.1 (1.2)	1.9 (2.1)	0.9 (1.1)	0-2
HPH-GDGT	18.1 (21.1)	8.6 (9.9)	6.3 (6.8)	2.7 (3.2)	0-5, 5‘
PH-GDGT	0.4 (0.5)	0.2 (0.3)	0.1 (0.1)	0.3 (0.3)	0-2, 5
*early-2G-GDGT**	0.1 (0.2)	0.5 (0.6)	2.6 (2.8)	0.4 (0.5)	0-3, 5
*deoxy-1G-GDGT**	0.2 (0.2)	0.6 (0.7)	0.4 (0.5)	1.0 (1.2)	0-5
1G-GDD	b.d.	0.1 (0.1)	<0.1 (<0.1)	0.3 (0.3)	0-5
1G-AR	0.3 (0.4)	0.2 (0.2)	0.2 (0.2)	0.3 (0.3)	-
PH-AR	3.8 (4.4)	0.5 (0.5)	0.2 (0.3)	0.2 (0.2)	-
Total intact polar lipids	85.6	86.5	91.8	85	
Core/apolar lipids					
GDGT	4.6	4.9	3.1	6.8	0-5, 5‘
OH-GDGT	0.1	0.1	0.1	0.2	0-2
MeO-GDGT	0.1	0.1	0.2	0.2	0-3
GTGT	0.3	0.1	0.2	0.3	0, 0:1
GDD	b.d.	<0.1	<0.1	0.1	0-5
OH-GDD	b.d.	<0.1	<0.1	0.1	1, 2, 4, 5
AR	5.2	4.4	1.7	3	-
MeO-AR	4.1	3.7	2.8	4.2	-
1uns-AR	<0.1	<0.1	<0.1	<0.1	-
2uns-AR	<0.1	<0.1	<0.1	<0.1	-
Total core lipids	14.4	13.5	8.2	15	

*see section 3.3

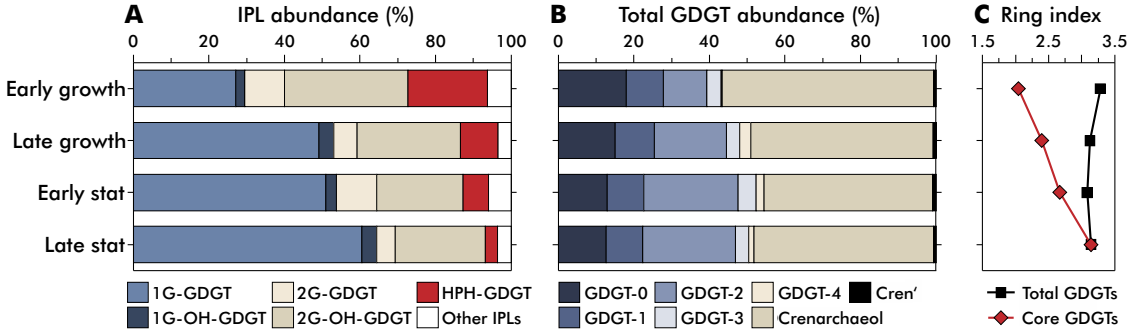

Figure 3.3. (A) Relative abundances of intact polar lipids in *N. maritimus* extracts in growth and stationary phases. (B) Relative abundance of core GDGTs in the total GDGT pool (hydrolyzed TLE). (C) Ring indices of the total GDGTs derived from hydrolysis and core GDGTs in the TLE. Cren' indicates the crenarchaeol regioisomer.

the abundance of 1G-OH-GDGTs did not change significantly. Both 2G-GDGTs and 2G-OH-GDGTs abundance decreased slightly during growth. HPH-GDGT abundance showed a strong and continuous decrease during growth from 21% in early growth phase to 3% in late stationary phase. 1G-GDDs were not detected in early growth phase but appeared in low abundance in late growth phase and increased slightly in late stationary phase. Deoxy-1G-GDGTs occurred in all growth phases and increased in abundance towards late stationary phase. PH-AR abundance decreased strongly towards late growth phase from 4.4% in early growth phase to 0.2% in late stationary phase. The abundance of 1G-AR showed no relationship with growth phase.

We hydrolyzed the TLE for all samples to investigate the changes of relative distributions and cyclization patterns of core lipids in the total GDGT pool (Fig. 3.3b). Crenarchaeol was the dominant core structure in all growth phases but decreased towards late stationary phase. Similarly, GDGT-0 continuously decreased in abundance during growth. In contrast, GDGT-2 became increasingly abundant towards late stationary phase. GDGT-1, -3, and -4 were of low abundance and did not correlate with growth phase. These changes are reflected in the ring index (Eq. 3, which indicates a decrease in overall cyclization from early growth to early stationary phase and no further change in late stationary phase (Fig. 3.3c). The ratio of GDGT-2 to GDGT-3 (TAYLOR et al., 2013) increased strongly during growth and in stationary phase for both total GDGTs and individual IPL classes (Supp. Table 3.4); the ratio of crenarchaeol to GDGT-0 (PEARSON and INGALLS, 2013) showed no apparent relationship with growth phase (Supp. Table 3.4). The abundance of the crenarchaeol regioisomer was less than 1% in all samples. Other GDGT-isomers occurred as shoulder peaks of the regular GDGT peaks and were of low abundance (Fig. 3.4).

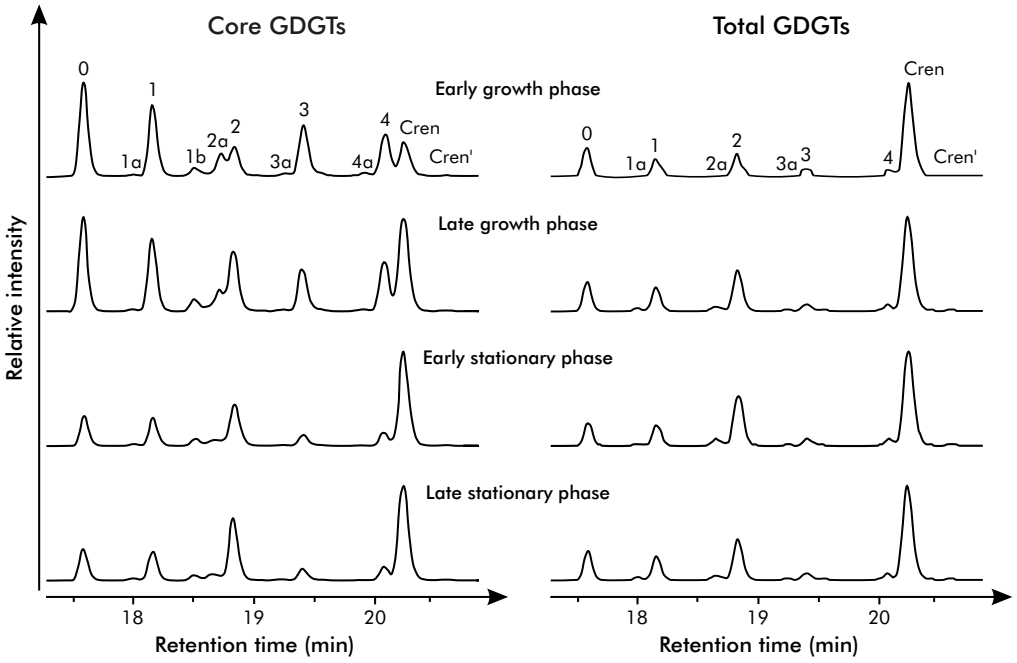

Figure 3.4. Extracted ion chromatograms of m/z 1290–1304 obtained by NP-HPLC-APCI-MS analysis showing distribution of GDGTs 0 to 4, crenarchaeol (Cren), the crenarchaeol regioisomer (Cren') and corresponding shoulder peaks (appended 'a' and 'b') in core GDGT (left) and total GDGT (right) pools.

3.3.4. Identification of novel archaeal core lipids

Several novel compounds were identified in extracts of N. maritimus based on elution time, accurate mass/proposed sum formula, MS^2 fragmentation in NP-HPLC-APCI-MS, and partly also chemical derivatization experiments.

3.3.4.1. Methoxy archaeol (MeO-AR)

We tentatively identified an abundant compound at *m/z* 667.7 $[M+H]^+$ which eluted 5 min earlier than archaeol during NP-HPLC analysis (Fig. 3.5a-c and Table 3.2). With its relative contribution of 2.8-4.2% of total glycerol-based lipids, this compound is one of the most abundant single compounds in the lipidome of *N. maritimus*. Considering the variation of core structures of intact polar GDGTs, only 2G-OH-GDGT-2 (14.9-19.3%), 1G-crenarchaeol (6.9-10.9%) and 2G-GDGT-2 (3.2-6.0%) are more abundant than MeO-AR, but these values still represent mixtures of several compounds that possess different sugars as headgroups (cf. KÖNNEKE et al., 2012). This compound was also observed in similar abundance when methanol was substituted by ethanol during extraction and sample preparation, while an ethoxy derivative was not detected, and is therefore considered to be a biosynthetic product of *N. maritimus*. Sum formula calculation from accurate mass and isotope pattern match indicated the stoichiometric formula $C_{44}H_{91}O_3^+$ for the protonated molecule. Based on mass spectrometric evidence

and chromatographic behavior during both HPLC and GC analysis we tentatively identify this compound as an *sn*-1 methylether derivative of archaeol, termed methoxy archaeol (MeO-AR).

The dominant product ion of MeO-AR during NP-HPLC-APCI-MS^2 analysis was 387.4, indicative of monophytanyl glycerol ether with an additional methylene ($C_{24}H_{51}O_3^+$; Fig. 3.5b). In comparison, archaeol exhibited a major product ion at *m/z* 373.4, corresponding to monophytanyl glycerol ether ($C_{23}H_{49}O_3^+$; Fig. 3.5c). The absence of the 373.4 fragment in the spectrum of MeO-AR indicates that the additional methylene is located in the glycerol unit rather than one of the phytanyl chains. MeO-AR exhibited minor product ions at *m/z* 369.4, 355.4, and 339.4. The product ion at *m/z* 369.4 ($C_{24}H_{49}O_2^+$) was likely generated by the loss of water and phytanyl from the molecular ion. The product ion at *m/z* 355.4 ($C_{23}H_{47}O_2^+$) is consistent with a loss of methanol from the methoxy monophytanyl glycerol ether fragment or a loss of methanol and phytanyl from the molecular ion. This strongly suggested that the additional methylene can be explained by the presence of a methoxy group at *sn*-1 position of the glycerol moiety. The product ion at *m/z* 355.4 was also abundant in the MS^2 spectrum of archaeol, but, in contrast to MeO-AR, was likely derived by a loss of water from the monophytanyl glycerol ether fragment. The product ion at *m/z* 339.4 ($C_{23}H_{47}O^+$) was possibly related to a loss of CH_2O by rearrangement from methoxy monophytanyl glycerol ether. A range of minor abundant product ions (e.g., at *m/z* 225.3 and 183.2) likely resulted from fragmentation of the phytanyl chains both in archaeol and MeO-AR. Acetylated archaeol (*m/z* 695.7 $[M+H]^+$), analyzed in the core lipid fraction and as standard, eluted before archaeol during NP-HPLC and showed diagnostic losses of 42 Da (acetyl group) and 397.4 Da (acetylated phytanyl-glycerol monoether) in MS^2. An acetylation product of MeO-AR was not observed.

During EI GC-MS analysis, MeO-AR had a linear retention index, LRI, of 3913 (Fig. 3.5d and f) while the TMS-derivative of archaeol eluted slightly later (LRI 3929; Fig. 3.5e and g). Both compounds exhibited a fragment ion at *m/z* 278.3 (phytanyl) as well as smaller fragments related to the fragmentation of the phytanyl chains (e.g., at *m/z* 57.1). Unlike TMS archaeol with its prominent fragments at *m/z* 426.4 and 130.1 related to the loss of one and two O-phytanyl chains from the molecular ion, respectively (cf. TEIXIDOR et al., 1993), MeO-AR was characterized by fragment ions at *m/z* 387.4 (loss of phytanyl), 354.4 (loss of phytanyl and CH_3O) and 343.2 (loss of phytanyl and CH_3OCH_2).

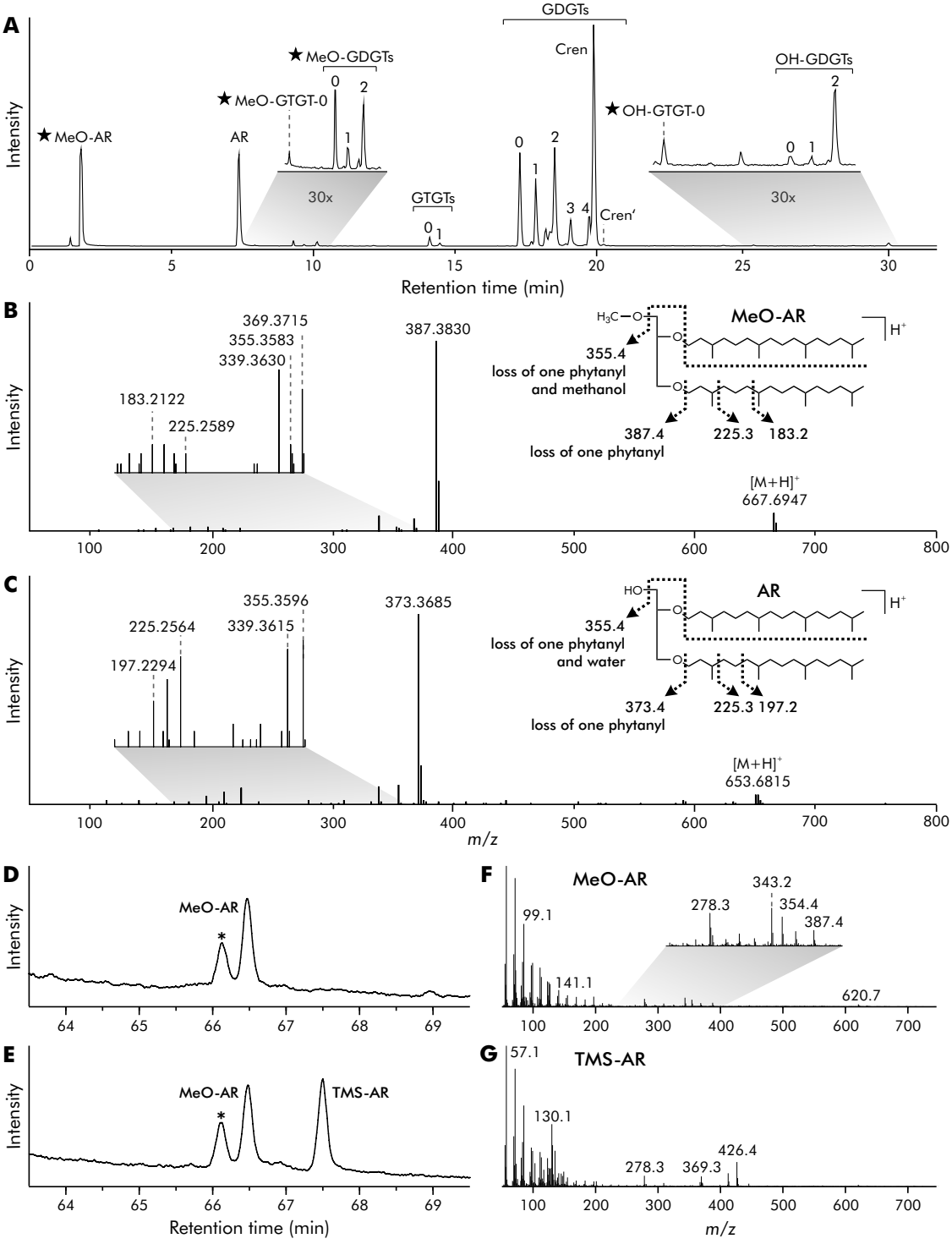

Figure 3.5. (A) Reconstructed base peak chromatogram of a late growth phase extract of *N. maritimus* showing elution of the novel compounds (stars) methoxy archaeol (MeO-AR), methoxy GTGT-0, methoxy GDGTs and OH-GTGT-0 in normal phase HPLC-APCI-MS. Panels (B) and (C) show MS^2 spectra of protonated molecules of MeO-AR (*m/z* 667.7) and archaeol (AR; *m/z* 653.7), respectively. Total ion chromatograms obtained using EI GC–MS of underivatized and trimethylsilyl-derivatized apolar fractions of *N. maritimus* extracts are shown in panels (D) and (E), respectively. Mass spectra of MeO-AR and trimethylsilyl archaeol (TMS-AR) obtained using EI GC–MS are shown in panels (F) and (G), respectively (asterisk: column contaminant).

3.3.4.2. Methoxy GDGTs (MeO-GDGTs), MeO-GTGT, and unsaturated GTGT

In addition to MeO-AR, we detected a series of three isoprenoidal GDGTs in the *m/z* range 1310-1316 $[M+H]^+$ that eluted earlier than core GDGTs in NP-HPLC (Fig. 3.5a and Supp. Fig. 3.1) and showed mass spectrometric behavior analogous to MeO-AR. We tentatively identified these compounds based on exact mass information, retention time and fragmentation pattern as *sn*-1 MeO-GDGTs with 0 to 3 cycloalkyl moieties. As in the case of MeO-AR, these compounds were present independent of the extraction solvent used. The compound at *m/z* 1316.3 exhibited major product ions related to the loss of a biphytanyl moiety at *m/z* 757.7 and glycerol biphytanyl ether plus two molecules of water at *m/z* 615.6 (Fig. 3.6a). A minor abundant product ion at *m/z* 1284.3 was likely related to the loss of methanol. This indicated the presence of one methoxy group at the *sn*-1 position of glycerol moiety; doubly methoxylated GDGTs on the other hand were not detected. MeO-AR and MeO-GDGTs were also detected using the RP-HPLC-MS protocol of (ZHU et al., 2013).

Analogously to MeO-GDGTs we detected a methoxy derivative of GTGT-0 at *m/z* 1318.3 (Fig. 3.5a and 3.6b). This compound generated major product ions at *m/z* 373.4 and 387.4, relating to monophytanyl glycerol ether and methoxy monophytanyl glycerol ether. This indicated that the methylation did not occur in the biphytanyl chain of GTGT-0 but rather in one of the glycerol moieties or phytanyl chains. Furthermore, product ions at *m/z* 1038.0 (loss of one phytanyl moiety) and 757.3 (loss of two phytanyl moieties) indicated that the additional methylene was not located in one of the phytanyl chains. Finally, a product ion at *m/z* 355.4 was related to the loss of methanol from a methoxy monophytanyl glycerol, confirming a methoxy ether structure of this compound. Mono- and di-acetylated MeO-GDGTs were not detected, likely owing to their low concentrations in the core lipid fraction.

Additionally, we tentatively identified a monounsaturated phytane-containing glycerol trialkyl glycerol tetraether (GTGT-0:1) with *m/z* 1302.3 $[M+H]^+$ ($C_{86}H_{173}O_6^+$) that eluted shortly after GTGT-0 in NP-HPLC analysis (Fig. 3.5a). As GTGT-0, the compound exhibited a major product ion at *m/z* 373.4 (Supp. Fig. 3.2a, b). Additional peaks at *m/z* 371.4 and 929.9 suggested the presence of a ring- or double bond-bearing phytanyl side chain (Supp. Fig. 3.2b, d). The peak disappeared after hydrogenation of the TLE, confirming the presence of a double bond. However, since the loss of signal due to hydrogenation was generally very high, it is possible that monocyclic GTGT was still present but below the detection limit after hydrogenation. We also detected OH-GTGT-0, the hydroxylated analogue of GTGT-0, at *m/z* 1320.3 ($C_{86}H_{175}O_7^+$; Fig. 3.5a and 3.2c). The compound exhibited in-source fragmentation to *m/z* 1302.3 $[M+H]^+$ ($C_{86}H_{173}O_6^+$), related to a loss of water from the molecule and subsequent formation

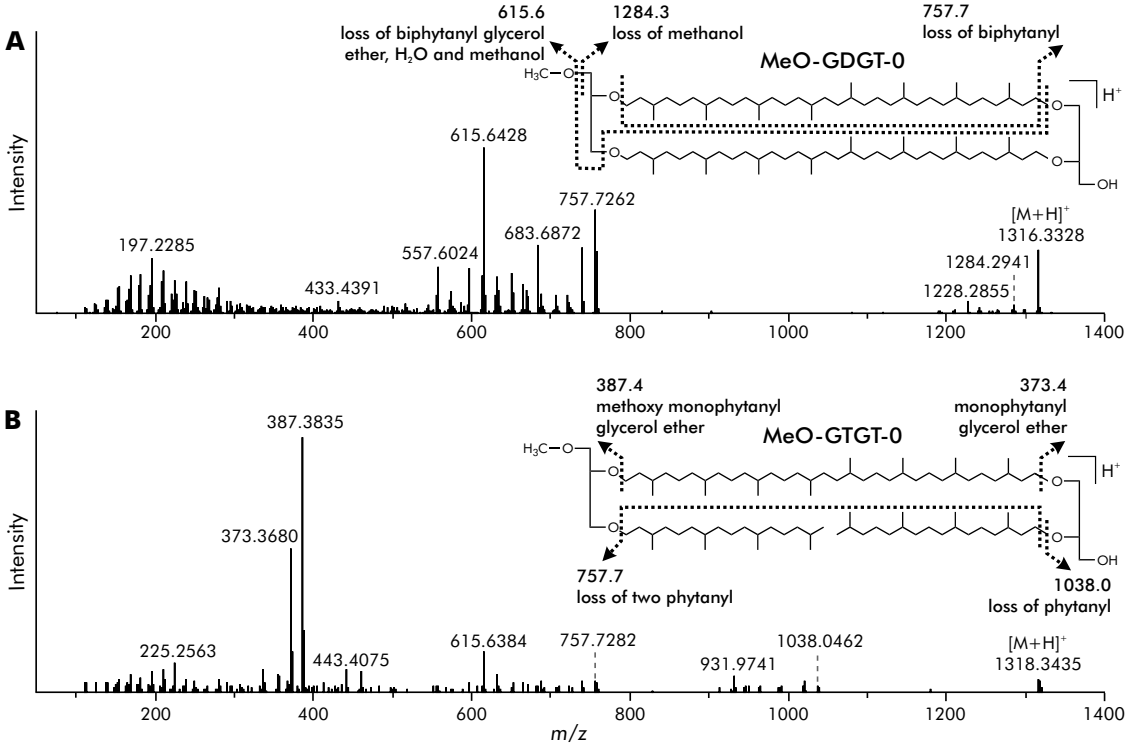

Figure 3.6. MS^2 spectra of protonated molecules of (A) methoxy GDGT-0 (*m/z* 1316.3) and (B) methoxy GTGT-0 (*m/z* 1318.3) in late growth phase extract of *N. maritimus*.

of a double bond, as described previously for OH-GDGTs (cf. LIU et al., 2012b). The fragmentation pattern of the in-source fragment was highly similar to that of GTGT-0:1 (Supp. Fig. 3.2d). The occurrence of product ions at *m/z* 371.4 and 929.9 as well as the absence of product ions indicative of an additional double bond in the biphytane moiety suggested that the additional OH-moiety was located in one of the phytanyl chains prior to in-source dehydration.

3.3.5. Core lipid composition during growth

Core and apolar lipids, including methoxylated compounds, comprised 8-15% of the total lipids of *N. maritimus* (Table 3.2). The most abundant core and apolar lipids were GDGTs, MeO-AR and archaeol. Minor compounds (i.e., <1%) comprised mono- (1uns-AR) and di-unsaturated archaeol (2uns-AR), MeO-GDGTs with 0-3 rings, GTGTs with 0-1 rings or double bonds, MeO-GTGT-0, OH-GTGT-0, GDDs as well as alkyl-hydroxylated GDDs (OH-GDDs; cf. LIU et al., 2012a,b) and GDGTs (OH-GDGTs). AR decreased in relative abundance with growth, while the abundance of MeO-AR was similar in all growth phases. Core GDGTs increased slightly from 5% in early growth phase to 7% in late stationary phase. In contrast, MeO-GDGT and GTGT abundance showed no apparent relationship with growth phase. GDDs were not detected in early growth phase but appeared in low abundance in late growth phase and stationary

phase. The cyclization of core GDGTs increased strongly during growth, reflected by an increase in the ring index from ~2 to 3, reaching equivalence with the ring index of the total GDGTs in early stationary phase (Fig. 3.3c). In early growth phase, GDGT-0 and GDGT-1 were the most abundant core GDGTs; towards stationary phase, the GDGT distribution gradually transformed to a predominance of GDGT-2 and crenarchaeol (Fig. 3.4 and Supp. Table 3.4). Shoulder peaks were of high abundance relative to the regular GDGT peaks during early growth phase but decreased significantly during growth. In late stationary phase, the abundance of shoulder peaks was similar to that of total GDGTs (Fig. 3.4).

Table 3.3. TEX_{86} values of major lipid classes of *N. maritimus* in different growth phases and stationary phase.

	Early growth phase	Late growth phase	Early stationary phase	Late stationary phase
1G-GDGTs	0.59	0.62	0.66	0.64
2G-GDGTs	0.95	0.97	0.97	0.98
HPH-GDGTs	0.49	0.62	0.63	0.67
Core GDGTs	0.56	0.67	0.69	0.72
Core GDGTs incl. shoulders	0.59	0.64	0.63	0.68
Total GDGTs	0.62	0.69	0.75	0.75
Total GDGTs incl. shoulders	0.62	0.7	0.76	0.76

3.3.6. Relation of core GDGTs to their polar precursors and IPL-specific TEX_{86}

TEX_{86} values were calculated for all compounds with non-hydroxylated GDGT core structure, i.e., 1G-GDGTs, 2G-GDGTs, HPH-GDGTs and core GDGTs in the TLE and total GDGTs in the hydrolyzed TLE, representing the integrated signal of intact polar and core GDGTs (Table 3.3). The TEX_{86} of total GDGTs increased gradually with growth phase, peaking in early stationary phase and remaining constant in late stationary phase (Fig. 3.7). The TEX_{86} values of core, 1G- and 2G-GDGTs followed this trend, while TEX_{86} of HPH-GDGTs also increased in late stationary phase. The temperatures reconstructed from TEX_{86} showed marked differences from actual incubation temperature (28 °C; Fig. 3.7). The temperatures reconstructed for total GDGTs were up to 4 °C below incubation temperature during growth and up to 2 °C above incubation temperature in stationary phase. The TEX_{86} temperatures calculated from 1G- and HPH-GDGTs were by 2-5 and 1-11 °C lower than incubation temperature, respectively, while 2G-GDGTs indicated temperatures that were ~10 °C higher. In contrast, the

TEX_{86} temperatures derived from core GDGTs were up to 7 °C lower than incubation temperature during growth but matched incubation temperature in stationary phase. Including the GDGT shoulder peaks in the calculation did not significantly alter TEX_{86} values of total GDGTs (≤0.01 TEX_{86}) and core GDGTs (∼0.04 TEX_{86}, Table 3.3).

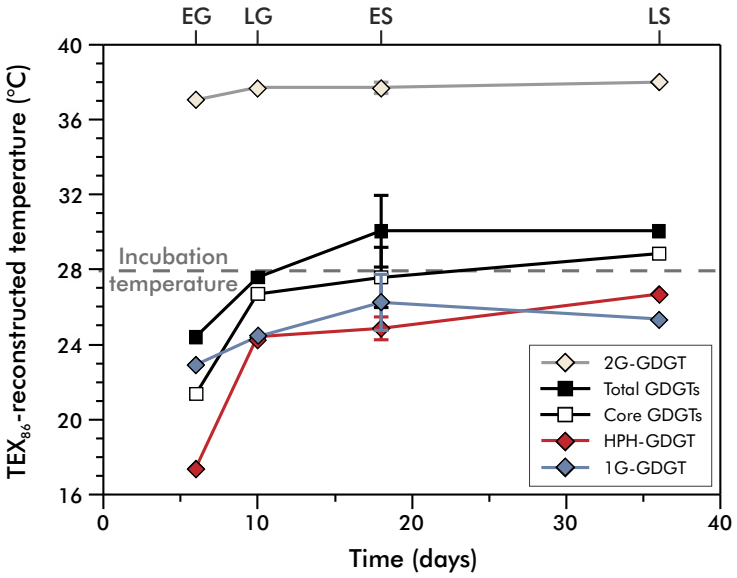

Figure 3.7. Reconstructed TEX_{86} temperatures for individual IPLs (diamonds) and core GDGTs in the TLE and total GDGTs derived by hydrolysis (squares) showing temperature increase during batch growth compared to the actual incubation temperature (28 °C, dashed line). Error bars represent the deviation of the mean for triplicate cultures harvested in early stationary phase. EG: Early growth phase; LG: Late growth phase; ES: Early stationary phase; LS: Late stationary phase.

Since established GDGT-based paleo proxies are exclusively based on core GDGTs, we examined the distribution of individual core GDGTs as a function of their affiliation with the major IPLs and growth stage (Fig. 3.8 and Supp. Table 3.1). The major polar precursors of non-hydroxylated core GDGTs in *N. maritimus*, accounting for ∼99% of the total intact polar GDGTs, are 1G-GDGTs, 2G-GDGTs and HPH-GDGTs (Table 3.2). The two major core GDGTs, GDGT-0 and crenarchaeol, were primarily associated with the major IPL type 1G-GDGT, even though especially in early growth phase their occurrence as HPH derivatives was substantial. GDGT-1 behaved similarly, i.e., its major sources were monoglycosides with the exception of early growth phase. The situation was more complex for the other minor GDGTs that are included in the TEX_{86} ratio, i.e., GDGT-2, GDGT-3, and crenarchaeol regioisomer, as well as for GDGT-4. These compounds were to a substantial degree also associated with the diglycosidic IPL 2G-GDGT. For GDGT-2, GDGT-3 and GDGT-4, the contribution of 2G-GDGT and HPH-GDGT declined with growth in favor of higher proportions of 1G-GDGT. For the crenarchaeol regioisomer, on the other hand, 2G-GDGT was the major polar derivative

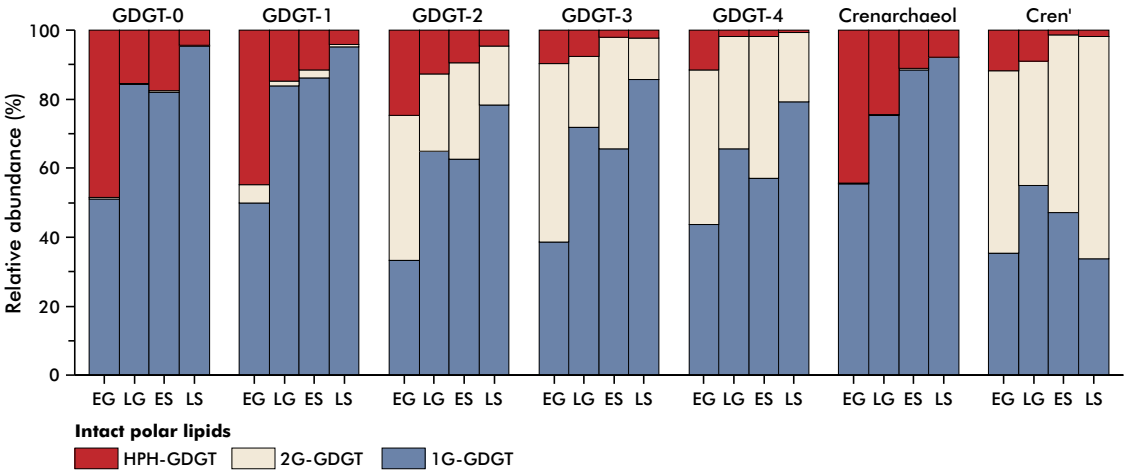

Figure 3.8. Relative contribution of the intact polar lipids 1G-, 2G- and HPH-GDGTs to specific core GDGT classes during growth and stationary phases of *N. maritimus*. Values were calculated using IPL abundances (Table 3.2) and IPL-specific core GDGT compositions (Supp. Table 3.4). Cren' indicates the crenarchaeol regioisomer. EG: Early growth phase; LG: Late growth phase; ES: Early stationary phase; LS: Late stationary phase.

with the exception of late growth phase. For all GDGTs, the association with HPH declined strongly towards stationary phase.

3.4. Discussion

3.4.1. Cellular lipid content

Membrane lipid analysis has been utilized to assess cell numbers and quantify microbial biomass in sedimentary and aquatic systems (e.g., BIDDLE et al., 2006; LIPP et al., 2008; ZINK et al., 2008; HUGUET et al., 2010). Due to a paucity of direct measurements on pure cultures, the conversion of archaeal lipid abundance into cells or biomass relies on assumptions of cell size and theoretical conversion factors of cell volume to lipid abundance. To enhance membrane lipid-based biomass quantification of planktonic archaea, we determined the cellular lipid content of *N. maritimus* experimentally by relating bulk lipid concentrations to cell counts.

The lipid content of *N. maritimus* of 0.9-1.9 fg cell^{-1} is in the lower range of previous estimates derived from archaeal gene abundances in correlation with intact polar GDGT concentrations in marine suspended organic matter and *N. maritimus* (0.1-8.5 fg cell^{-1}; HUGUET et al., 2010). Assuming a dry mass of 20 fg cell^{-1} (MARTENS-HABBENA et al., 2009), GDGTs accounted for 4-9% of the dry mass in our experiment, which is within the range of cellular lipid quota reported from other archaea (e.g., LANGWORTHY et al., 1974; TORNABENE et al., 1979; FERRANTE et al., 1990).

For further evaluation of our results, we calculated the theoretical lipid content of *N. maritimus* cells using the model of SIMON and AZAM (1989) modified for the cell geometry of *N. maritimus* (rods of 0.5-0.9 μm length, 0.2 μm width; KÖNNEKE et al., 2005), a protein content of 50% (MARTENS-HABBENA et al., 2009) and a membrane thickness of 5 nm (HEINZ et al., 2013). Our experimentally determined cellular lipid abundances of 0.9-1.9 fg cell^{-1} deviate only slightly from the modeled values of 0.9 and 1.5 fg cell^{-1} for rods sized 0.5 × 0.2 and 0.9 × 0.2 μm, respectively. However, our experimental and modeled values are high in comparison to theoretical estimates for larger thaumarchaeal cells by SINNINGHE DAMSTÉ et al. (2002a, 1 fg cell^{-1}, 0.8×0.5 μm rod) and those calculated by (SCHOUTEN et al., 2012) of 0.25 fg cell^{-1} (0.5 × 0.15 μm rod) for a similar cell geometry using the model of See SINNINGHE DAMSTÉ et al. (2002a, based on GABRIEL and CHONG, 2000). To further compare our results with existing environmental data, we estimated cell volumes of 0.02-0.06 μm^3 for *N. maritimus* based on cellular lipid content. These fit closely to cell volumes of 0.03-0.06 μm^3 determined for marine group I archaea in the Atlantic Ocean (SCHATTENHOFER et al., 2009). The agreement of experimentally and theoretically determined lipid content in *N. maritimus* suggests that our model is a robust representation of the relation of cell size to lipid content.

The slow growth rates characteristic for *N. maritimus* (cf. KÖNNEKE et al., 2005; MARTENS-HABBENA et al., 2009) may lead to the accumulation of several effects during batch growth, e.g., the accumulation of core lipids via degradation of IPLs due to cell lysis. While core lipids were abundant during growth and in stationary phase, no accumulation during the course of the experiment was observed. Indeed, core lipid abundance and intact polar lipid composition did not change significantly during 20 days of stationary conditions between early and late stationary phase (Table 3.1 and 3.2). Furthermore, the abundant GDGT isomers in the TLE were not observed in the hydrolyzed extract and changed in abundance during the course of the experiment (Fig. 3.4). Therefore, core GDGTs are not reflecting the IPL pool and were therefore likely not directly derived from IPLs in *N. maritimus*. Collectively, this suggests that the contribution of lysed cells to the total GDGT pool was generally low and therefore did not significantly affect our cellular GDGT estimates (Table 3.1). In contrast, high cellular GDGT contents (analyzed as core GDGTs) of up to 30 fg cell^{-1} in environmental samples and enrichment cultures (e.g., WUCHTER, 2006; HERFORT et al., 2007; PITCHER et al., 2009) vastly exceed the range of cellular lipid quota anticipated from variations in cell size and lipid packing (cf. SIMON and AZAM, 1989; GABRIEL and CHONG, 2000). Estimates based on core GDGTs may instead have included a contribution of fossil core GDGTs relative to IPL-derived GDGTs (cf. LIPP and HINRICHS, 2009).

The abundance of lipids per cell was highest in late growth and early stationary phases compared to early growth phase and late stationary phase. These differences are likely caused by larger average cell size during growth and early stationary phase, which decreased in stationary phase due to substrate-depletion (e.g., KJELLEBERG et al., 1987; NYSTRÖM, 2004). Analogously, variations in cell size and therefore cellular lipid content are likely to be constrained by nutrient dynamics in the typically energy-limited marine environment (e.g., SCHUT et al., 1997). Assuming one copy of the 16S rDNA gene per cell (WALKER et al., 2010), the variation in cell size with metabolic status may therefore explain discrepancies between thaumarchaeal 16S rDNA and intact polar GDGTs in water column profiles (PITCHER et al., 2011b; SCHOUTEN et al., 2012). In addition, these discrepancies may also be attributed to employment of filters with different pore sizes for genetic (0.2 μm) and lipid biomarker analyses (0.7 μm) as previously suggested by INGALLS et al. (2012). Therefore, our results support previous suggestions that cellular GDGT content may be used as an indicator of metabolic status (cf. HUGUET et al., 2010).

3.4.2. Intact polar GDGTs as biomarkers for live thaumarchaea

The significant changes in the membrane lipid composition in *N. maritimus* during growth have implications for the use of intact polar GDGTs in tracing live thaumarchaea in the marine environment.

The abundance of HPH-crenarchaeol is thought to be the best indicator for live thaumarchaea in the marine environment due to its specificity to the phylum *Thaumarchaeota* and the assumed reactivity of its phosphorous ester bond relative to glycosidic bonds (e.g., SCHOUTEN et al., 2008; PITCHER et al., 2011a). The high abundance of HPH-GDGT during growth and its decrease to near absence in late stationary phase in our experiment indicates its capacity for tracing not only live but especially growing thaumarchaea (Fig. 3.3).

In contrast to HPH-GDGTs, glycosidic GDGTs are assumed to be more refractory and may therefore overestimate the living biomass (e.g., HARVEY et al., 1986; SCHOUTEN et al., 2010). This notion can be challenged on the basis of results by LOGEMANN et al. (2011) which suggested about equal degradation rates of phospho- and glycosidic archaeal diethers. Nevertheless, SCHOUTEN et al. (2012) attributed peaks in 1G-GDGT abundance in the Arabian Sea water column that were not correlated to HPH-GDGT abundance to preferential degradation of HPH-GDGTs. Our results demonstrate that low HPH-GDGT abundance does not correspond to low thaumarchaeal biomass. On the basis of our experiments (cf. Fig. 3.3), we suggest that varying ratios of the abundance of HPH-GDGTs over 1G-GDGTs in environmental samples are reflective of

the metabolic status of the thaumarchaeal community rather than being solely caused by selective degradation.

We anticipate that a dormant thaumarchaeal population has a higher ratio of 1G-GDGTs to HPH-GDGTs compared to a metabolically active community. Indeed, PITCHER et al. (2011b) showed that HPH-crenarchaeol abundance correlated more strongly with transcribed 16S rRNA and *amoA* mRNA than with 16S rDNA and *amoA* gene copy numbers. This observation is consistent with our argument that an absence of HPH-crenarchaeol does not necessarily imply an absence of living thaumarchaeal biomass but corresponds to lower metabolic activity. Therefore, we propose that HPH-crenarchaeol abundance is linked to growing and metabolically active cells rather than to abundance of viable cells. Based on our experiments, we propose that lipids that do not change significantly in abundance during growth, e.g., 2G-and 2G-OH-GDGTs (Fig. 3.3a), have the highest suitability for quantification of live thaumarchaeal biomass in aquatic (non-sedimentary) samples.

3.4.3. Influence of growth phase and core structure distribution in IPLs on the TEX_{86} paleotemperature proxy

The inverse correlation of *in situ* TEX_{86} and water temperature observed in several water column studies (e.g., TURICH et al., 2007; SCHOUTEN et al., 2012) is in contrast to the positive correlation of SST and TEX_{86} in core-top sediments (SCHOUTEN et al., 2002; KIM et al., 2008), suggesting the influence of additional parameters on the TEX_{86} proxy. In environmental systems, the entanglement of environmental and physiological parameters (e.g., temperature, salinity, metabolic status) hampers the evaluation of their separate influence on TEX_{86} (PEARSON and INGALLS, 2013). *N. maritimus* may serve as a useful model for studying the influence of growth parameters on lipid composition and the TEX_{86} proxy since most planktonic thaumarchaeal sequences found in the Global Ocean Sampling database are closely related to *N. maritimus* (WALKER et al., 2010; STAHL and DE LA TORRE, 2012), although environmental lipid distributions might be influenced by parameters that are not captured in pure culture experiments.

Under the controlled conditions of our pure culture experiment, we observed a dependence of TEX_{86} on growth phase, resulting in an increase in TEX_{86} temperature of 6 °C in the total GDGT pool and 1-9 °C for individual IPLs from early growth to stationary phase (Fig. 3.7). The total GDGTs (96-99% IPL-derived, Table 3.1) show a TEX_{86} temperature of 30 °C in stationary phase, while the core GDGTs in the TLE match the incubation temperature of 28 °C. A similar offset of TEX_{86} between IPL-derived and core GDGTs has been observed in water column and sediment profiles (LIPP and

HINRICHS, 2009; LIU et al., 2011; LENGGER et al., 2012; SCHOUTEN et al., 2012). LIPP and HINRICHS (2009) and LIU et al. (2011) explained this offset in sediments by GDGT production by benthic archaea, while others suggested that this offset was caused by selective degradation of IPLs (LENGGER et al., 2012; SCHOUTEN et al., 2012; LENGGER et al., 2013). However, both explanations do not apply to our pure culture experiment and therefore the observed offset, along with the remark- able differences in the GDGT shoulder compounds, is likely a biosynthetic signature. In the present study, this offset is also not an artifact caused by co-elution of core GDGTs with unsaturated GDGTs that may have been formed by dehydration of OH-GDGTs during hydrolysis (cf. LIU et al., 2012b) because unsaturated GDGTs were not detected in the hydrolyzed extract when analyzed using the RP-HPLC-MS protocol of ZHU et al. (2013, 2014b).

LENGGER et al. (2012) showed that 1G- and 2G-GDGTs exhibited higher TEX_{86} values compared to HPH-GDGTs in sediment from the Arabian Sea, and speculated that preferential degradation of HPH-GDGTs caused elevated IPL-derived TEX_{86} values. We found that TEX_{86} values are inherently variable between different IPLs (Table 3.3; cf. BASSE et al., 2014) but the specific stratification of TEX_{86} values is only observed during early growth while during the other examined growth phases 1G- and HPH-GDGTs exhibited similar values. When converted to temperatures, the TEX_{86} of 2G-GDGTs indicates ~38 °C, overestimating incubation temperature by 10 °C, while 1G- and HPH-GDGTs underestimate incubation temperature by 2-5 and 1-11 °C, respectively (Fig. 3.7). This divergence indicates that the correlation of TEX_{86} with temperature is distinct for specific IPLs and different from that of total GDGTs, which overestimate incubation temperature by 2 °C in stationary phase.

Overall, the strong increase of TEX_{86} values from growth to stationary phase suggests that growth phase exerts substantial influence on GDGT ring distribution. Since growth phase corresponds to conditions of higher ammonia availability and stationary phase to ammonia depletion, our results imply that nutrient conditions may influence the TEX_{86} signal in the environment. Therefore, our findings suggest that the seasonality of TEX_{86} values of marine AOA assemblages may not only reflect seasonal temperature variability (e.g., WUCHTER et al., 2005; LEIDER et al., 2010; TURICH et al., 2013) but also nutrient availability (cf. TURICH et al., 2007).

The 6 °C variability of TEX_{86} temperatures observed for different growth phases of *N. maritimus* is significantly higher than the analytical error of the TEX_{86} temperature proxy of 0.7 °C (SCHOUTEN et al., 2007b). Assuming that *N. maritimus* serves as a useful model for environmental planktonic communities, nutrient dynamics are likely recorded in TEX_{86}-paleotemperature records and need to be considered for confidently interpreting the TEX_{86} signal. For example, TEX_{86} values obtained from nutrient-replete near-shore and oceanic upwelling environments systematically un-

derestimate water temperature (HUGUET et al., 2007; LEE et al., 2008; LEIDER et al., 2010; WEI et al., 2011). This bias towards colder temperatures has been interpreted as a shift in the depth of GDGT production (KIM et al., 2008; cf. TAYLOR et al., 2013). This interpretation may need to be revised in light of several more recent reports of increasing TEX_{86} values with water depth (SCHOUTEN et al., 2012; HERNÁNDEZ-SÁNCHEZ et al., 2014; XIE et al., 2014). In contrast, the cold bias observed during growth of *N. maritimus* suggests a potential causal link between low TEX_{86} values and high nutrient availability in upwelling systems and reconciles these contradictions. This notion is further supported by strongly increasing ratios of GDGT-2 to GDGT-3 in *N. maritimus* between early growth and late stationary phase (Supp. Table 3.4). An increase of similar magnitude with water depth has been observed in water column suspended particulate matter (cf. TAYLOR et al., 2013), indicating that deep-water thaumarchaea might be increasingly nutrient-limited or non- growing compared to shallow-water assemblages.

The TEX_{86} SST proxy is based on the distributions of core GDGTs in sediments; these compounds are presumably released from their IPL precursors during early diagenesis. Our data show that the four compounds used for calculation of the TEX_{86} derive from three principal IPL precursors, whose relative importance changes with growth (Fig. 3.8). Even though the differences in reactivity of the various glycosidic and phosphatidic bonds that need to be cleaved to release the respective core GDGTs from these IPLs are not constrained (cf. LOGEMANN et al., 2011), it is plausible that their diagenetic fates in the environment differ given their differences in chemical structure and polarity. For example, the low abundance of the crenarchaeol regioisomer in *N. maritimus* and similar observations in enrichment cultures and mesocosms (WUCHTER et al., 2004; SCHOUTEN et al., 2007a; PITCHER et al., 2011a) are in contrast to higher abundances observed in marine suspended particulate matter and sediments (e.g., INGALLS et al., 2012; SCHOUTEN et al., 2012). The fact that the crenarchaeol regioisomer (Cren') originates from a different distribution of IPL precursors than the other three compounds (GDGT-1 to -3; Fig. 3.8) raises the possibility that inclusion of the former compound in the TEX_{86} may complicate its utility as a SST proxy and endorses the use of TEX_{86} derivatives such as the TEX_{86}^{L} that omit this compound (cf. SHAH et al., 2008; KIM et al., 2010).

3.4.4. Identification of methoxy diether and tetraether lipids in N. maritimus

Diether lipids have hitherto not been reported in cultivated representatives of the *Thaumarchaeota* except for minor abundances in *N. maritimus* (SCHOUTEN et al., 2008). In contrast, we observed that archaeols account for up to 13% of the total

glycerol-based lipids in *N. maritimus*. However, archaeols were only a minor fraction of the IPLs and were predominantly present as apolar MeO-AR and core archaeol. These two compounds each comprised about 4% of the total glycerol-based membrane lipids of *N. maritimus*, respectively.

Similar methoxy di- and tetraether lipids have previously been observed as artifacts arising from acid methanolysis of archaeal lipids (FERRANTE et al., 1988; EKIEL and SPROTT, 1992; KNAPPY et al., 2009). However, the presence of these compounds in non-hydrolyzed, ethanol extracted TLE of *N. maritimus* and the distinct ring distribution of MeO-GDGTs in comparison to core GDGTs strongly suggest that these methoxylated ether lipids are of biosynthetic origin. The retention times, mass spectra and acetylation products of methoxy GDGTs are also distinct from those of the butanetriol tetraethers recently identified by ZHU et al. (2014a) and the alkyl-methylated GDGTs observed by KNAPPY et al. (2009) and GALLIKER et al. (1998).

Methoxy di- and tetraether lipids are equally abundant in all growth phases of *N. maritimus*, while the ratio of methoxy archaeol to archaeol increases throughout growth due to a relative decrease in archaeol abundance. This indicates that methoxy archaeol may be required in similar amounts irrespective of growth phase and may serve a different biological function than archaeol. Elucidating the exact function of these methoxy ether lipids in physiological and/or biosynthetic process will require more research. The biosynthesis of methoxy di- and tetraether lipids has not been previously reported from other archaea. Thus, it seems possible that these novel lipids are restricted to planktonic archaea. Given the high abundance of *Nitrosopumilus*-like thaumarchaea in the ocean, a considerable fraction of the intact and core archaeols found in environmental samples might in fact be derived from thaumarchaea. Likewise, we expect that MeO-AR and MeO-GDGTs may also be found in the marine water column and surface sediments. Therefore, this suite of lipids might have a high potential to serve as novel biomarkers in the marine environment.

3.5. Conclusions

In summary, the present study demonstrates that the lipid composition of *N. maritimus* changes markedly with growth phase. This observation likely applies to other marine AOA and impacts both the use of GDGTs and the corresponding IPLs as biomarkers for thaumarchaea and of GDGTs in TEX_{86} paleothermometry. While results from batch culture experiments might not be directly transferable to the environment, the ability to perform reproducible batch culture experiments with *N. maritimus* opens new avenues towards a mechanistic understanding of the formation of archaeal lipid signatures in the environment. Our data do not support the notion that high abundances of

1G-GDGTs relative to HPH-GDGTs in the water column indicate "fossil" intact polar lipids originating from unviable biomass. Instead, HPH-GDGT abundance seems to be linked to growing and metabolically active cells rather than to the abundance of viable cells. We therefore propose that a high ratio of 1G- to HPH-GDGTs indicates thaumarchaeal communities at steady state, e.g., under oligotrophic conditions (cf. KJELLEBERG et al., 1987; NYSTRÖM, 2004), while relatively high HPH proportions indicate metabolically active AOA assemblages, for example at the onset of seasonal blooms. Consequently, lipids such as 2G- and 2G-OH-GDGTs, i.e., compounds whose relative proportions do not change significantly during growth, have the greatest potential for quantification of viable thaumarchaeal biomass in aquatic samples. The novel methoxy derivatives of archaeol and GDGTs may serve as additional biomarkers for marine thaumarchaea; studies of their occurrence among archaeal taxa as well as their distribution in the environment will shed light on their taxonomic specificity and relevance.

The TEX_{86}-temperatures of specific IPLs and total GDGTs increased by up to 9 °C between growth and stationary phase. This shows that metabolic state has a profound effect on GDGT cyclization and thus TEX_{86}-derived temperatures. Moreover, the relative contributions of individual IPLs as potential sources of individual core GDGTs change during growth, and the four core GDGTs included in the TEX_{86} are generally sourced in different proportions from the principal IPL precursors. Consequently, diagenetic processes (cf. LIPP and HINRICHS, 2009; LENGGER et al., 2012; SCHOUTEN et al., 2012; LENGGER et al., 2013) may distinctly affect the individual core GDGTs during their hydrolytic release from polar precursors. Collectively, our results suggest that a complex interplay of processes independent of temperature influences the formation of the TEX_{86} signal. Our observations emphasize the need to accurately describe the factors influencing GDGT cyclization in thaumarchaea and potentially affecting TEX_{86} paleotemperature reconstructions.

Acknowledgements

We thank L. Wörmer for supporting HPLC-MS analysis. The study was funded by the European Research Council under the European Union's Seventh Framework Programme–'Ideas' Specific Programme, ERC Grant agreement No. 247153 (Advanced Grant DARCLIFE; PI: K.-U.H.) and by the Deutsche Forschungsgemeinschaft through the Gottfried Wilhelm Leibniz Prize awarded to Kai-Uwe Hinrichs and instrument grant Inst 144/300-1 (LC-qTOF system) and the DFG-Research Center/Cluster of Excellence MARUM.

3.6. Supporting Information

3.6.1. Hydrogenation

Presence of double bonds in GTGT-1 was assessed by performing platinum oxide catalyzed hydrogenation on a *N. maritimus* TLE aliquot with squalene as an internal standard (cf. BECKER et al., 2013). A standard mix containing *cis*- and *trans*-phytol as well as squalene was hydrogenated in parallel to serve as a control. In brief, 10 mg of PtO_2 were filled into a self-made glass ampoule, 100 µl of *n*-hexane were added and the mixture was purged with hydrogen gas. The sample was dissolved in 50 µl *n*-hexane and added to the ampoule. Subsequently, the ampoule was flushed with hydrogen and sealed. After 1 hour at 60 °C, the samples were evaporated to dryness and prepared for GC-MS and NP-HPLC-APCI-MS analysis.

3.6.2. Theoretical cell volume

We assumed a power-law relationship of cellular lipid content and cell volume based on Simon and Azam (1989): Cell volume (μm^3) = 0.027 $x^{1.48}$ with x = lipid/cell in fg.

Supplementary Table 3.1 Affiliation of GDGT core structures to the three major lipid classes of *N. maritimus* (in %) in different growth and stationary phases.

Time interval	GDGT-0	GDGT-1	GDGT-2	GDGT-3	GDGT-4	Cren	Cren'
Early growth phase							
1G-GDGTs	51.1	50	33.2	38.6	43.8	55.4	35.3
2G-GDGTs	0.3	5.3	42.1	51.7	44.7	0.3	53
HPH-GDGTs	48.5	44.7	24.7	9.7	11.5	44.3	11.7
Late growth phase							
1G-GDGTs	84.4	84	64.9	71.8	65.7	75.4	55
2G-GDGTs	0.1	1.2	22.4	20.5	32.4	0.1	36
HPH-GDGTs	15.4	14.8	12.7	7.7	1.9	24.5	8.9
Early stationary phase							
1G-GDGTs	82	86.2	62.5	65.5	57.1	88.5	47.2
2G-GDGTs	0.4	2.3	28.1	32.3	41.2	0.4	51.5
HPH-GDGTs	17.6	11.6	9.4	2.2	1.7	11.2	1.3
Late stationary phase							
1G-GDGTs	95.5	95.2	78.3	85.7	79.2	92.1	33.8
2G-GDGTs	0.1	0.7	17.2	12.1	20	0.1	64.4
HPH-GDGTs	4.4	4.1	4.5	2.3	0.8	7.8	1.8

Supplementary Table 3.2 Means and standard deviations of relative lipid abundances determined for extracts of *N. maritimus* grown in triplicate and harvested in early stationary phase.

	Mean abundance (%)	Standard deviation (%)
Intact polar lipids		
1G-GDGT	46.8 (51.0)	8.1 (7.9)
1G-OH-GDGT	2.5 (2.8)	0.9 (1.2)
2G-GDGT	10.0 (10.7)	5.9 (5.9)
2G-OH-GDGT	20.7 (22.8)	5.1 (6.8)
2G-2OH-GDGT	1.9 (2.1)	0.7 (0.7)
HPH-GDGT	6.3 (6.8)	0.5 (0.3)
PH-GDGT	0.1 (0.1)	0.1 (0.2)
early-2G-GDGT	2.6 (2.8)	2.0 (2.0)
deoxy-1G-GDGT	0.4 (0.5)	0.3 (0.4)
1G-GDD	<0.1 (<0.1)	<0.1 (<0.1)
1G-AR	0.2 (0.2)	<0.1 (<0.1)
PH-AR	0.2 (0.3)	0.3 (0.3)
Total intact polar lipids	91.8	5.5
Core/apolar lipids		
C-GDGT	3.1	2.8
C-OH-GDGT	0.1	0.1
Me-C-GDGT	0.2	0.2
GTGT	0.2	0.2
GDD	<0.1	<0.1
OH-GDD	<0.1	<0.1
C-AR	1.7	1.3
Me-AR	2.8	1.2
1uns-C-AR	<0.1	<0.1
2uns-C-AR	<0.1	<0.1
Total core lipids	8.2	5.5

Supplementary Table 3.3 Means and standard deviations of TEX_{86} values determined for extracts of *N. maritimus* grown in triplicate and harvested in early stationary phase.

	Mean TEX_{86}	Standard deviation
1G-GDGTs	0.66	0.03
2G-GDGTs	0.97	<0.01
HPH-GDGTs	0.63	0.01
C-GDGTs	0.69	0.04
C-GDGTs incl. shoulders	0.63	0.01
Total GDGTs	0.75	0.04
Total GDGTs incl. shoulders	0.76	0.05

Supplementary Table 3.4 Relative abundance of GDGT core structures of major lipid classes of *N. maritimus* (in %) in different growth and stationary phases.

Time interval	GDGT-0	GDGT-1	GDGT-2	GDGT-3	GDGT-4	Cren	Cren'	GDGT-2/ GDGT-3	Cren/(Cren + GDGT-0)
Early growth phase									
1G-GDGTs	23.7	17.2	17.3	6.5	5	29.6	0.7	2.7	0.6
2G-GDGTs	0.4	4.7	56.3	22.3	13.1	0.4	2.7	2.5	0.5
HPH-GDGTs	29	19.8	16.6	2.1	1.7	30.5	0.3	7.9	0.5
C-GDGTs	29.3	19.3	9	15.5	15.4	11.2	0.3	0.6	0.3
C-GDGTs incl. shoulders	26.2	19.9	13.5	14.5	15.4	10.3	0.2	0.9	0.3
Total GDGTs	18	9.9	11.5	3.7	0.3	55.9	0.7	3.1	0.8
Total GDGTs incl. shoulders	16.9	10.2	12.2	4.1	2.1	53.9	0.6	3	0.8
Late growth phase									
1G-GDGTs	25.8	17.7	21.5	7.2	5	22.3	0.5	3	0.5
2G-GDGTs	0.3	2	59	16.3	19.6	0.3	2.6	3.6	0.5
HPH-GDGTs	23.21	15.4	20.7	3.8	0.7	35.7	0.4	5.4	0.6
C-GDGTs	19.5	15.1	18.7	12	15.6	18.6	0.6	1.6	0.5
C-GDGTs incl. shoulders	17.3	18.2	21.4	11	14.8	16.8	0.5	1.9	0.5
Total GDGTs	15.1	10.3	19.2	3.5	3	48.3	0.7	5.5	0.8
Total GDGTs incl. shoulders	14.4	10.6	20.7	3.8	3.4	46.3	0.7	5.4	0.8
Early stationary phase									
1G-GDGTs	18	16.6	23.1	8.9	7	25.9	0.5	2.6	0.6
2G-GDGTs	0.4	2.1	49.5	20.9	24.1	0.5	2.6	2.4	0.6
HPH-GDGTs	29	16.7	26	2.2	1.6	24.5	b.d.	11.8	0.5
C-GDGTs	15.3	11.9	20.9	5	6.9	39.3	0.6	4.2	0.7
C-GDGTs incl. shoulders	16.8	16.4	20.9	6.3	8.3	30.9	0.5	3.3	0.6
Total GDGTs	14.2	11.2	24.3	7.4	3.8	38.2	0.9	3.3	0.7
Total GDGTs incl. shoulders	13.2	11.5	26	7.7	4.3	36.4	0.9	3.4	0.7
Late stationary phase									
1G-GDGTs	24.5	17.8	23.4	7.6	5.4	21.2	0.1	3.1	0.5
2G-GDGTs	0.4	1.6	64.8	13.5	17.2	0.2	2.4	4.8	0.3
HPH-GDGTs	21.18	14.4	25.6	3.8	1	33.9	b.d.	6.7	0.6
C-GDGTs	12.9	10.5	21.7	4.2	5.9	44.3	0.6	5.2	0.8
C-GDGTs incl. shoulders	11.9	13	23	4.3	6	41.3	0.5	5.3	0.8
Total GDGTs	12.7	9.6	24.5	3.5	1.5	47.5	0.7	7	0.8
Total GDGTs incl. shoulders	11.9	9.8	25.9	3.7	1.9	46.1	0.6	7	0.8

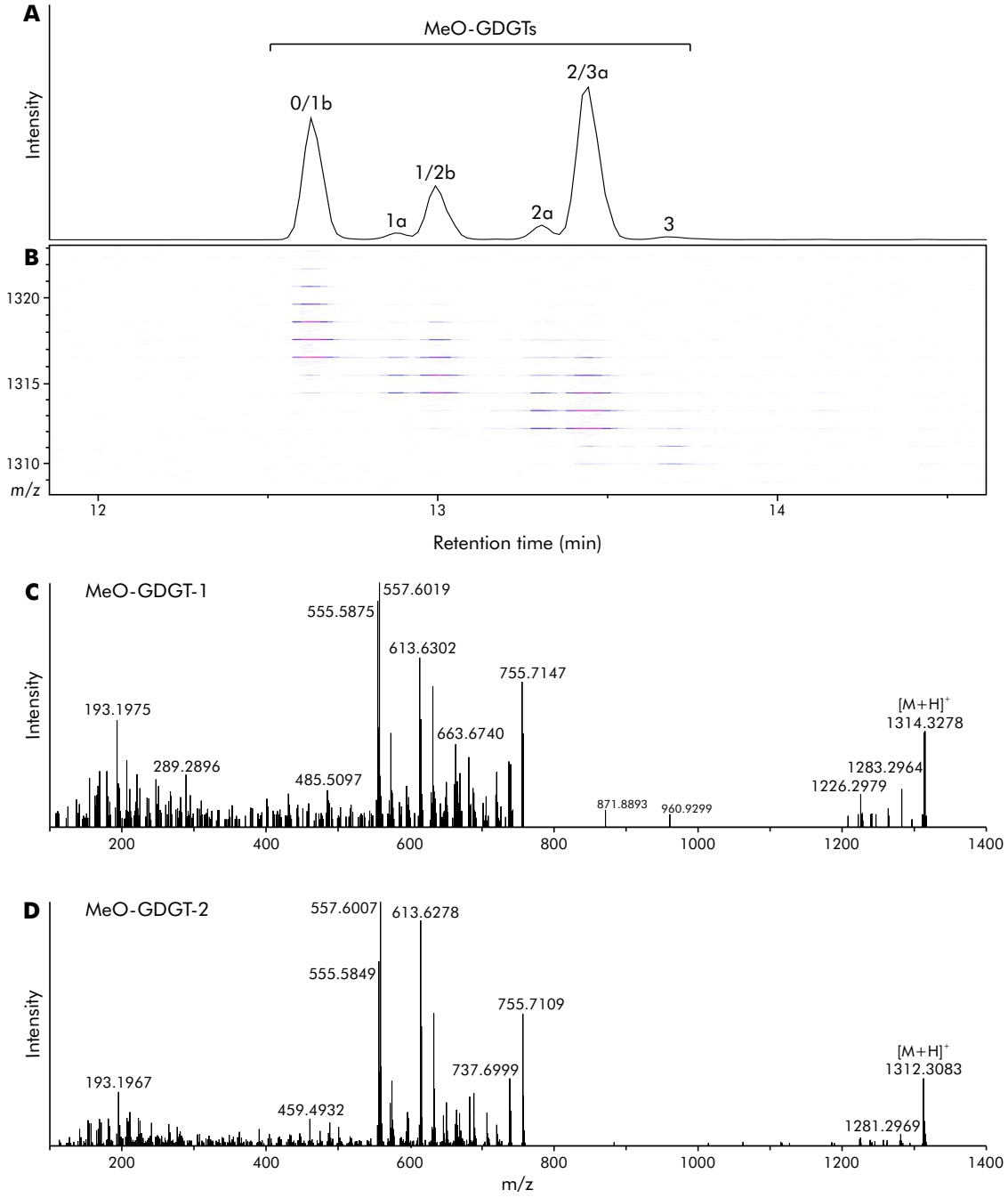

Supplementary Figure 3.1 Reconstructed base peak chromatogram (A) and density map (B) of late growth phase extract of *N. maritimus* obtained by normal phase HPLC-MS showing elution of methoxy GDGTs (MeO-GDGTs) with 0 to 3 rings and associated isomers 1a, 1b, 2a, 2b, and 3a. Panels (C) and (D) show MS^2 spectra of MeO-GDGT-1 (*m/z* 1314.3 $[M+H]^+$) and MeO-GDGT-2 (*m/z* 1312.3 $[M+H]^+$), respectively.

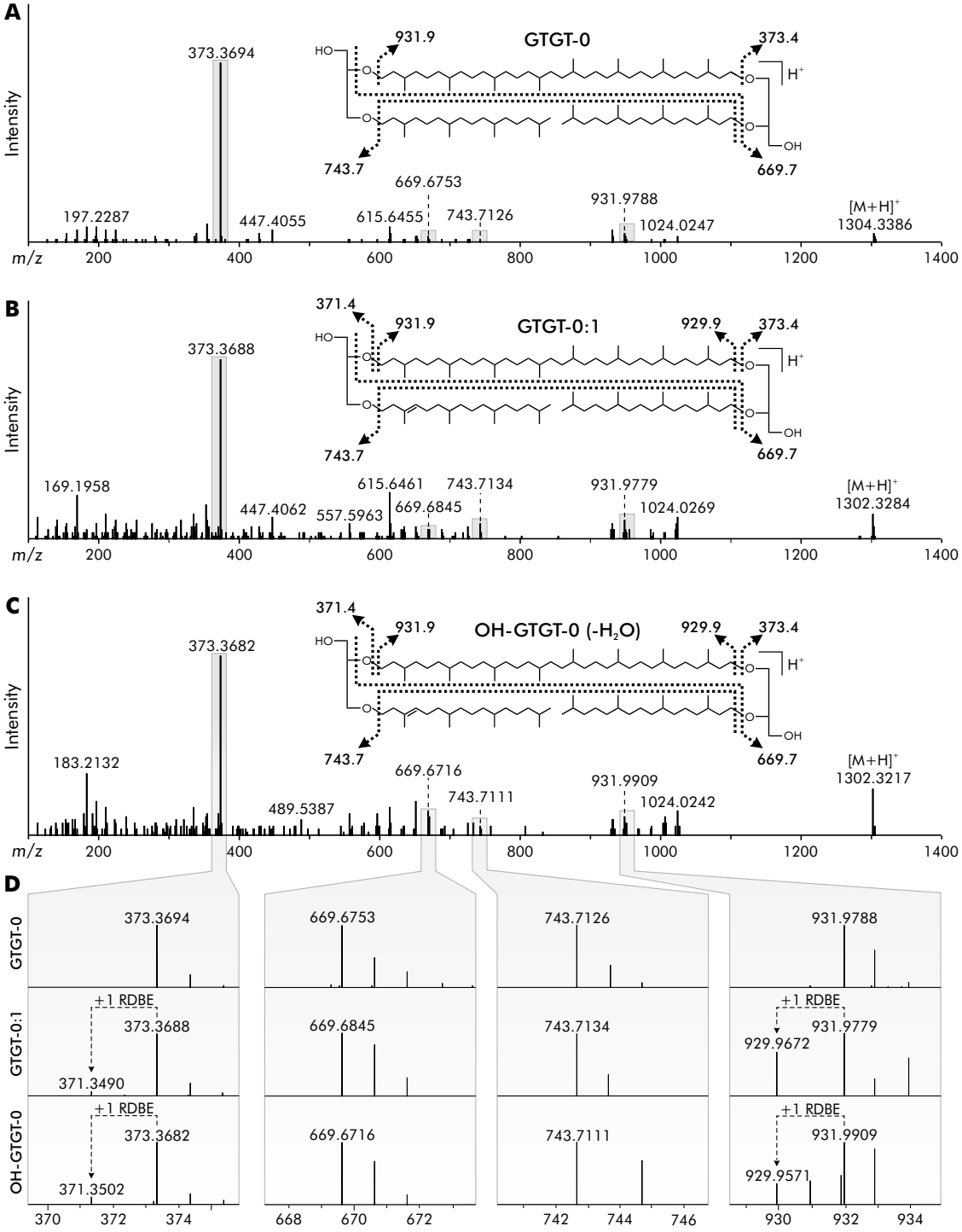

Supplementary Figure 3.2 MS^2 spectra of (A) GTGT-0 (*m/z* 1304.3 $[M+H]^+$), (B) GTGT-1 (*m/z* 1302.3 $[M+H]^+$) and (C) the in-source fragment (*m/z* 1302.3 $[M+H]^+$) of OH-GTGT-0 (*m/z* 1320.3 $[M+H]^+$) obtained by normal phase HPLC-APCI-MS of late growth phase extract of *N. maritimus*. Lower panels in (D) show detailed views of fragments containing only biphytane as side chain (*m/z* 669.7 and 743.7), fragments containing either phytane (*m/z* 373.4), monocyclic phytane or phytene (*m/z* 371.4; RDBE = ring or double bond equivalent), as well as fragments containing biphytane plus phytane (*m/z* 931.4) and biphytane plus monocyclic phytane or phytene (*m/z* 929.9). Please note that the exact position of the ring in GTGT-1 and the double bond (hydroxyl group) in OH-GTGT-0 cannot be inferred from the spectra.

CHAPTER 4

Differential response of membrane lipid composition to temperature, pH, and salinity in marine planktonic *Thaumarchaeota*

Felix J. Elling[a], Martin Könneke[a,*], Marc Mußmann[b], Andreas Greve[a] and Kai-Uwe Hinrichs[a]

In preparation for *Geochimica et Cosmochimica Acta*

[a] Organic Geochemistry Group, MARUM - Center for Marine Environmental Sciences & Department of Geosciences, University of Bremen, 28359 Bremen, Germany
[b] Max Planck Institute for Marine Microbiology, Celsiusstraße 1, 28359 Bremen, Germany

[*] Corresponding author. E-mail: mkoenneke@marum.de

Abstract

Marine ammonia-oxidizing archaea of the phylum *Thaumarchaeota* are a cosmopolitan group of microorganisms representing a major fraction of the picoplankton in the ocean. The cytoplasmic membranes of *Thaumarchaeota* consist predominantly of intact polar isoprenoid glycerol dibiphytanyl glycerol tetraether (GDGT) lipids, which may be used as biomarkers for living *Thaumarchaeota*. Thaumarchaeal GDGTs accumulate as core lipids in marine sediments and serve as the basis for geochemical proxies such as the TEX_{86} paleothermometer, which is based on the empirical correlation of the degree of GDGT cyclization in core-top sediments and sea surface temperature. However, discrepancies between in situ and TEX_{86}-reconstructed temperatures in the marine water column indicate that the physiological and ecological controls on GDGT composition in *Thaumarchaeota* remain poorly understood. Here, we demonstrate that the responses of membrane lipid compositions and resulting TEX_{86} values to growth temperature strongly diverge in three closely related thaumarchaeal pure cultures, including *Nitrosopumilus maritimus* and two novel strains isolated from South Atlantic surface water. While the intact polar and core lipid inventories of the three strains were overall similar, *N. maritimus* and the closest related strain NAOA6 showed linear relationships of TEX_{86} and growth temperature in comparison to non-linear temperature response in the more distantly related strain NAOA2. This disparate relationship of TEX_{86} to growth temperature among closely related *Thaumarchaeota* suggests that the TEX_{86} signal in natural samples may include an ecological component that requires further attention. In contrast, differences in salinity between 27‰ and 51‰ had no significant effect on intact polar GDGT composition and TEX_{86} values in *N. maritimus*. Similarly, variations of pH from 7.3 to 7.9 showed little influence on intact polar GDGT composition but slightly elevated TEX_{86} values at lower pH. In sum, our pure culture studies promote the understanding of intact polar GDGTs as biomarkers of *Thaumarchaeota* in the marine water column and suggest that the TEX_{86} paleotemperature proxy is not solely dependent on growth temperature, but amalgamates several physiological and environmental factors such as metabolic state, pH, and phylogenetic composition of marine thaumarchaeal assemblages. The disparate relationships of TEX_{86}-derived and actual growth temperature among closely related *Thaumarchaeota* suggests that changes in community composition may exert a strong control on TEX_{86} signatures.

4.1. Introduction

Archaeal membrane lipids are found ubiquitously in the environment. In particular, glycerol dibiphytanyl glycerol tetraether lipids (GDGTs) are abundant in the marine water column and sediments and are thought to originate primarily from planktonic Thaumarchaeota (HOEFS et al., 1997; DELONG et al., 1998; SCHOUTEN et al., 2000). Archaea of the recently established phylum *Thaumarchaeota* (formerly Marine Group I Crenarchaeota, BROCHIER-ARMANET et al., 2008; SPANG et al., 2010) are globally abundant aerobic chemolithoautotrophs that generate energy by oxidizing ammonia to nitrite (KÖNNEKE et al., 2005; WALKER et al., 2010; KÖNNEKE et al., 2014) and account for up to 20 % of the total picoplankton in the ocean (KARNER et al., 2001; SCHATTENHOFER et al., 2009). Similarly, ammonia-oxidizing *Thaumarchaeota* have been recognized as the predominant nitrifiers in a wide range of terrestrial habitats (FRANCIS et al., 2005; LEININGER et al., 2006; AUGUET and CASAMAYOR, 2008; DE LA TORRE et al., 2008) and their GDGTs are abundant in soils, lakes, and hydrothermal springs (e.g. PEARSON et al., 2004; POWERS et al., 2004; LEININGER et al., 2006).

Physiological, genetic, and biochemical studies of the first thaumarchaeal isolate, *Nitrosopumilus maritimus*, revealed that marine planktonic *Thaumarchaeota* are well adapted to the oligotrophic conditions typically encountered in the pelagic ocean by having high substrate-affinities and using an energy-efficient carbon fixation pathway (MARTENS-HABBENA et al., 2009; WALKER et al., 2010; KÖNNEKE et al., 2014). In addition, their GDGT monolayer membranes have been suggested to be particularly adapted for minimized ion and proton permeability, thus reducing maintenance energy and maximizing proton motive force (VAN DE VOSSENBERG et al., 1998; MATHAI et al., 2001; KONINGS et al., 2002; VALENTINE, 2007).

In living *Thaumarchaeota*, GDGTs occur as intact polar lipids (IPLs), i.e., with a polar headgroup attached to the GDGT core lipid. Typical IPLs of cultivated *Thaumarchaeota* comprise monoglycosidic, diglycosidic or glycophosphatidic headgroups attached to GDGTs with zero to four cyclopentyl rings and crenarchaeol, a GDGT with four cyclopentyl and one cyclohexane ring that has been exclusively found in *Thaumarchaeota* (SINNINGHE DAMSTÉ et al., 2002b; SCHOUTEN et al., 2008; PITCHER et al., 2011a; ELLING et al., 2014).

Intact polar GDGTs, particularly with crenarchaeol as the core lipid, are commonly used as biomarkers for thaumarchaeal abundance and archaeal community structure in the water column (e.g. SCHUBOTZ et al., 2009; SCHOUTEN et al., 2012; BASSE et al., 2014). After loss of the polar headgroup following cell lysis, GDGTs of planktonic archaea accumulate as core lipids in sediments and may be preserved over geologic timescales (e.g. CARRILLO HERNANDEZ, 2004; JENKYNS et al., 2012). Sedimentary

core GDGTs thus represent molecular fossils indicative of past archaeal activity and membrane lipid adaptation. In particular, the degree of cyclization of GDGTs in marine surface sediments, especially of the GDGTs with one to three cyclizations and the crenarchaeol regioisomer (Fig. 4.1) as indexed in the TEX_{86} ratio, was found to correlate with sea surface temperature (SST; SCHOUTEN et al., 2002). The calibration of the TEX_{86} ratio in globally distributed core-top sediments with satellite-derived SSTs (SCHOUTEN et al., 2002; KIM et al., 2008, 2010) subsequently laid the foundation of the TEX_{86} paleothermometer. While TEX_{86} paleothermometry has been widely applied for reconstructing past SSTs reaching back as far as the Cretaceous and Middle Jurassic (e.g. JENKYNS et al., 2012; LINNERT et al., 2014), it has become evident that the simple assumptions underlying this paleothermometer, i.e., a sole dependence of GDGT cyclization on temperature and the provenance of sedimentary GDGTs from surface waters, are inconsistent with the current understanding of thaumarchaeal physiology and ecology (reviewed in PEARSON and INGALLS, 2013).

While the general concept of GDGT cyclization as a means of temperature adaptation is well established for cultivated thermophilic archaea (CHONG, 2010; KOGA, 2012; OGER and CARIO, 2013), direct evidence for a physiological basis of the TEX_{86} paleothermometer from planktonic thaumarchaeal cultures is still lacking. Indeed, the sole dependence of TEX_{86} on growth temperature seems unlikely given the fact that multiple additional factors such as pH (SHIMADA et al., 2008; BOYD et al., 2011), salinity (DAWSON et al., 2012) and pressure (KANESHIRO and CLARK, 1995) have been shown to affect lipid composition in other archaea. So far, observational evidence has only documented the significant influence of growth phase and thus energy limitation on lipid composition and TEX_{86} in cultivated *Thaumarchaeota* (ELLING et al., 2014).

Recent analyses of intact polar and core GDGT compositions of in situ planktonic assemblages show that TEX_{86} values of both fossil and living subsurface archaeal biomass do not reflect in situ water temperatures in various oceanic provinces, neither in trend nor magnitude (WUCHTER et al., 2005; INGALLS et al., 2006; TURICH et al., 2007; SCHOUTEN et al., 2012; BASSE et al., 2014; HERNÁNDEZ-SÁNCHEZ et al., 2014; XIE et al., 2014). The discrepancies between *in situ* and TEX_{86} temperatures in the marine water column indicate that both the export depth of the TEX_{86} signal as well as the physiological and ecological controls on GDGT composition in living *Thaumarchaeota* remain poorly understood.

In particular, the mechanism coupling TEX_{86} to sea surface temperature remains elusive given the fact that *Thaumarchaeota* are most abundant and active in subsurface waters broadly coinciding with the deep chlorophyll maximum (MASSANA et al., 1997; KARNER et al., 2001; FRANCIS et al., 2005; CHURCH et al., 2010). Moreover, thaumarchaeal shallow (0-200 m) and deep water (>200 m) ecotypes live under

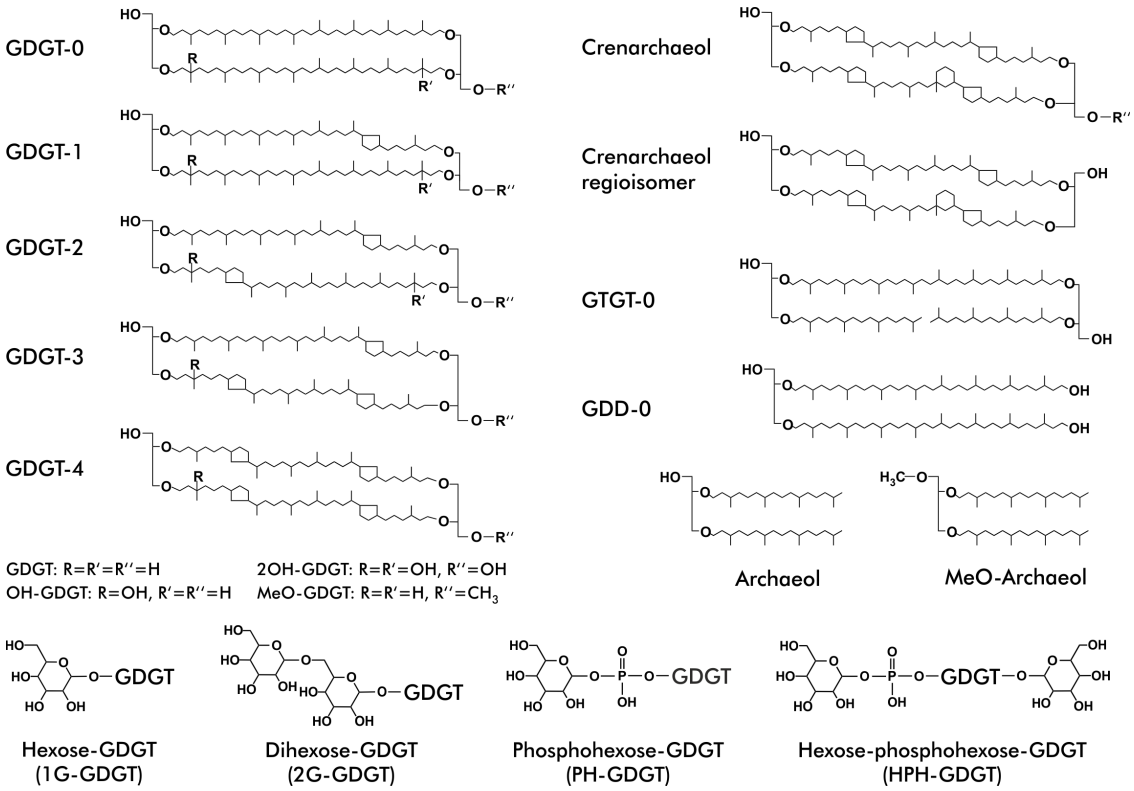

Figure 4.1. Structures of thaumarchaeal glycerol dibiphytanyl glycerol tetraether (GDGT) and glycerol diphytanyl diether (archaeol) core lipids. GDGTs may contain up to four cyclopentane rings or one cyclohexane and four cyclopentane rings (crenarchaeol). Derivatives of basic lipid structures comprise GDGTs containing one (OH-GDGT) or two (2OH-GDGT) additional hydroxyl groups and zero to four cyclopentane rings in the biphytanyl side chain, acyclic or monocyclic glycerol trialkyl glycerol tetraether (GTGT), zero to five ring bearing glycerol dialkanol diethers (GDDs) as well as GDGT and archaeol containing a methoxy group at the sn-1 position of the glycerol moiety (MeO-GDGT and MeO-AR). Thaumarchaeal intact polar lipids consist of one or two glycosidic or glycophosphatidic headgroups attached to the glycerol *sn*-1 hydroxyl position of a diether or tetraether core lipid.

contrasting nutrient regimes (FRANCIS et al., 2005; YAKIMOV et al., 2011; SINTES et al., 2013), which may increase or decrease TEX_{86} under nutrient-limited or nutrient-replete conditions, respectively, as suggested by culture experiments (ELLING et al., 2014). Surface and deep thaumarchaeal ecotypes have also distinct GDGT biosynthetic genes (VILLANUEVA et al., 2014a), which might be associated with preferential occurrence of bicyclic over tricyclic GDGTs in deep compared to shallow waters (TAYLOR et al., 2013; KIM et al., 2015). In addition to vertical ecological differences, thaumarchaeal assemblages in the Arctic and Antarctic oceans and the Red Sea are phylogenetically distinct from tropical and temperate planktonic *Thaumarchaeota* (BANO et al., 2004; GALAND et al., 2009a; IONESCU et al., 2009). Samples from these regions deviate strongly from the global TEX_{86} calibration line (KIM et al., 2008; TROMMER et al., 2009; KIM et al., 2010), indicating that phylogenetically distinct archaeal communities

may have diverging TEX_{86}–temperature relationships. This observation as well as regionally distinct thaumarchaeal seasonality inferred from core-top analyses have resulted in a plethora of regional TEX_{86} regression lines (TROMMER et al., 2009; LEIDER et al., 2010; HO et al., 2014; SEKI et al., 2014) which challenge the paleogeographical and temporal applicability of the TEX_{86} paleothermometer

In order to better understand the influence of environmental and physiological parameters on thaumarchaeal lipid composition and to enhance our ability to reliably reconstruct past environments based on the geologic record, we assessed the influence of temperature, salinity, and pH on intact polar and core lipid composition of the first ammonia-oxidizing pure culture *Nitrosopumilus maritimus*. We demonstrate that membrane lipid composition in *N. maritimus* responds to changes in temperature and pH, but not to salinity, and thus forms a part of thaumarchaeal homeostasis. Moreover, we report the isolation of two novel thaumarchaeal ammonia oxidizers from the southern Atlantic Ocean that share close relatedness to *N. maritimus* with respect to their 16S rRNA and *amoA* genes as well as their membrane lipid compositions. Disparate responses of membrane lipid composition to temperature in *N. maritimus* and the closely related strains suggest that thaumarchaeal community composition may have a profound impact on TEX_{86} signatures.

4.2. Experimental procedures

4.2.1. Isolation of ammonia-oxidizing archaea from marine surface water

Two strains of ammonia-oxidizing archaea were isolated from surface water samples from the Benguela upwelling system (Fig. 4.2) at stations GeoB 12802 (NAOA2; 5 m water depth; in situ temperature (14.9 °C; 25°30'S, 13°27'E) and GeoB 12806 (NAOA6; 5 m; 13.6 °C; 25°S, 14°23'E) taken during R/V Meteor cruise M76/1 in 2008 (ZABEL et al., 2008). Surface ocean water (200 ml) was passed through a 0.45 µm pore size filter to exclude particles and larger biota. The filtered water was supplemented with 0.5 mM NH_4^+ and 100 mg l^{-1} streptomycin to select for archaeal ammonia-oxidizers. After incubation at 15 °C for 3 years, significant amounts of nitrite had accumulated in the samples. The enrichments were transferred to Synthetic Crenarchaeota Medium (SCM, KÖNNEKE et al., 2005) containing 1 mM NH_4^+ as well as 100 mg l^{-1} streptomycin. The enrichment was then incubated at 28 °C and purified by filtration through a 0.45 µm pore size filter followed by serial dilutions in SCM using 10 % inoculum for each transfer. Purity of the cultures was checked using phase contrast microscopy and plating on agar SCM medium containing 1 g l^{-1} yeast extract, glucose, and peptone incubated at 28 °C. Remaining bacterial contaminations (<1 %

of total cells) were removed using serial dilutions in SCM with 100 mg l^{-1} gentamicin (NAOA2) or kanamycin (NAOA6).

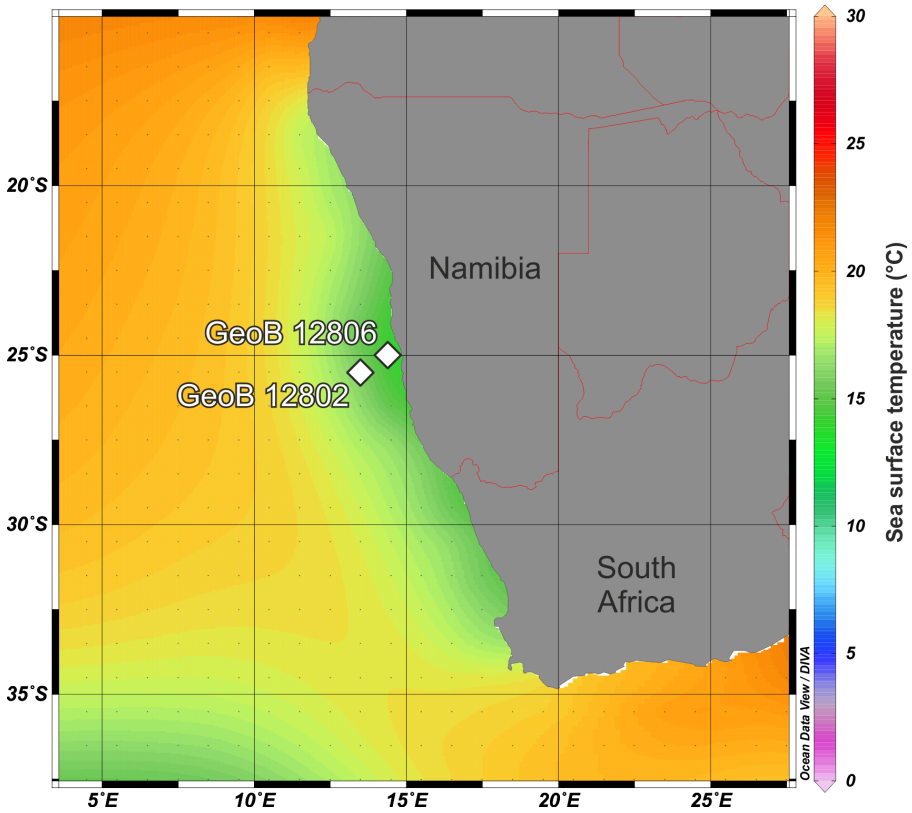

Figure 4.2. Annual mean sea surface temperatures in the Benguela upwelling region (World Ocean Atlas 2009; LOCARNINI et al., 2010). Diamonds indicate sampling sites of surface water samples and used for isolating the novel strains NOA2 (GeoB 12802) and NAOA6 (GeoB 12806) R/V Meteor cruise M76/1 in 2008.

The growth temperature range of the isolated strains was determined at 12 equally spaced temperature intervals in the range of 12 to 40 °C by using a temperature gradient block (KALLMEYER et al., 2003). For this purpose, 8 ml aliquots of freshly inoculated (10 % exponential-phase cells) SCM media were distributed into screw-capped hungate tubes, leaving 8 ml headspace. Nitrite concentrations were then monitored for up to 40 days.

4.2.2. DNA extraction, gene amplification and phylogenetic reconstructions

Cell pellets for 16S rRNA and ammonia monooxygenase subunit A (*amoA*) gene sequencing were collected by centrifugation (20,000 x g, 30 min) of 100 ml culture aliquots. Cells were lysed in 40 µl MilliQ H_2O using micropistils and stored at −20 °C. The archaeal 16S rRNA and *amoA* genes were amplified using the primers Arch20F/Univ1492 (KANE et al., 1993; ALM et al., 1996) and amoA19F/616r (PESTER et al., 2012), respectively. PCR reactions (100 µl) were set up as follows: 10 µl 10x

reaction buffer (5 Prime GmbH, Hamburg), 10 µl desoxynucleotides, 2.5 mM each (Roche Diagnostic GmbH, Mannheim), 0.25 µl Taq Polymerase, 5 u/µl (5 Prime GmbH, Hamburg), 1 µl of each primer (0 µM), 1 µl template, and 100 µl with PCR-grade water.

Amplification of the 16S rRNA genes was performed under the following conditions: initial denaturation at 94 °C for 5 min, 30 cycles of 94 °C for 1 min, 58 °C for 1 min and 72 °C for 3 min, and a final extension of 72 °C for 10 minutes. Likewise, *amoA* genes were amplified with the following modifications: annealing at 53 °C for 1 min and extension at 73 °C for 1 min.

For phylogenetic analyses of *amoA* and 16S rRNA gene sequences the ARB program package was used (LUDWIG et al., 2004). For the *amoA* gene a termini-filter considering 576 nucleotide positions and for the 16S rRNA gene a 50 % conservation filter were used. After manual refinement of the sequence alignment maximum parsimony, distance-matrix (ARB Neighbour-Joining with the Jukes-Cantor factor) and maximum-likelihood calculations (Rax-ML) were calculated and consensus trees were generated manually.

4.2.3. Cultivation and lipid extraction

For lipid analysis, *N. maritimus* strain SCM1 as well as strains NAOA2 and NAOA6 were grown aerobically in 8.5-l batch cultures of pH 7.5 HEPES-buffered Synthetic Crenarchaeota Medium (SCM; 1.5 mM NH_4Cl, 5 % inoculum) as described previously (KÖNNEKE et al., 2005; MARTENS-HABBENA et al., 2009; KÖNNEKE et al., 2012; ELLING et al., 2014). For the temperature experiment, cultures were grown in duplicate or triplicate at incubation temperatures of 2 °C, 25 °C, 28 °C for *N. maritimus*, 18 °C, 22 °C, 28 °C, 35 °C for strain NAOA2 and 18 °C, 22 °C, 28 °C for strain NAOA6. For the salinity experiment, *N. maritimus* was grown at 28 °C in a modified medium containing the same proportions of inorganic salts as SCM at total salt concentrations of 27‰, 37‰, 44‰, and 51‰ (44‰ and 51‰ in duplicate). For the pH experiment, *N. maritimus* was grown at 28 °C and pH 7.3, 7.6 and 7.9 (pH 7.3 and 7.9 in duplicate). The pH of each bottle was checked daily and adjusted with sterile 1 M HCl or NaOH when pH changed by more than 0.05.

Purity of the cultures was checked daily by phase contrast microscopy. Growth was monitored by measuring nitrite formation. Nitrite concentrations were determined using diazo-colorimetry with photometric detection at 545 nm (STICKLAND and PARSONS, 1972).

Cells were harvested in early stationary phase (temperature and pH experiments) or mid to late growth phase (salinity experiment) using a Sartocon Slice cross-flow

filtration system (Sartorius, Göttingen, Germany). The cell pellets (ca. 1010 to 1011 cells) were stored at −20 °C until extraction. Lipids from each batch were extracted following a modified Bligh & Dyer protocol (STURT et al., 2004) using phosphate and trichloroacetic acid (CCl_3CO_2H) buffers (each 2x) and an ultrasonic probe (15 min sonication; HD2200, Bandelin Electronic, Berlin, Germany). The total lipid extract (TLE) was dried under a stream of N2 and stored at −20 °C until measurement.

4.2.4. Intact polar and core lipid analysis

Intact polar and core lipids were quantified by injecting 5 to 10 % of the TLE dissolved in methanol on a Dionex Ultimate 3000 high performance liquid chromatography (HPLC) system connected to a Bruker maXis Ultra-High Resolution quadrupole time-of-flight tandem mass spectrometer (qToF-MS) equipped with an ESI ion source operating in positive mode (Bruker Daltonik, Bremen, Germany). The mass spectrometer was set to a resolving power of 27000 at m/z 1222 and every analysis was mass-calibrated by loop injections of a calibration standard and correction by lock mass, leading to a mass accuracy of better than 1-3 ppm. Ion source and other MS parameters were optimized by infusion of standards (GDGT-0, 1G-GDGT-0, 2G-GDGT-0) into the eluent flow from the LC system using a T-piece.

Analyte separation was achieved using reversed phase (RP) HPLC on an ACE3 C_{18} column (2.1 x 150 mm, 3 µm particle size, Advanced Chromatography Technologies, Aberdeen, Scotland) maintained at 45 °C as described by (ZHU et al., 2013). In brief, analytes were eluted at a flow rate of 0.2 ml min^{-1} isocratically for 10 min with 100 % eluent A (methanol:formic acid:14.8 M NH_4, 100:0.04:0.10, v:v:v), followed by a linear gradient to 24 % eluent B (2-propanol:formic acid:14.8 M NH_4^+, 100:0.04:0.10, v:v:v) in 5 min, followed by a gradient to 65 % B in 55 min. The column was then flushed with 90 % B for 10 min and re-equilibrated with 100 % A for 10 min.

To determine the TEX_{86} and ring indices of total GDGTs, 10 % of the TLE was hydrolyzed with 1 M HCl in methanol for 3 h at 70 °C to yield core GDGTs (ELLING et al., 2014). The hydrolyzed TLE was then analyzed on the same system under different chromatographic conditions using normal phase (NP) HPLC and an APCI-II ion source operated in positive mode, as described by (BECKER et al., 2013). Briefly, 5 % TLE aliquots were dissolved in *n*-hexane:2-propanol (99.5:0.5, v:v) and injected onto two coupled Acquity BEH Amide columns (2.1 x 150 mm, 1.7 µm particle size, Waters, Eschborn, Germany) maintained at 50 °C. Lipids were eluted using linear gradients of *n*-hexane (eluent A) to *n*-hexane:2-propanol (90:10, v:v; eluent B) at a flow rate of 0.5 ml min^{-1}. The initial gradient was 3 % B to 5 % B in 2 min, followed by increasing B to 10 % in 8 min, to 20 % in 10 min, to 50 % in 15 min and 100 % in

10 min, followed by 6 min at 100 % B to flush and 9 min at 3 % B to re-equilibrate the columns.

Lipids were identified by retention time as well as accurate molecular mass and isotope pattern match of proposed sum formulas in full scan mode and MS2 fragment spectra. Integration of peaks was performed on extracted ion chromatograms of ±10 mDa width and included the $[M+H]^+$ ions for NP-HPLC-MS and additionally $[M+NH_4]^+$ and $[M+Na]^+$ ions for RP-HPLC-MS. Where applicable, double charged ions were included in the integration. The areas of 1G-, 2G-, and HPH-GDGT-4 were corrected for co-elution with the respective crenarchaeol regioisomer (Cren') by subtracting the area of the +2 Da isotope peak of Cren', which was calculated from natural isotope abundances (ZHANG et al., 2006).

Lipid abundances were corrected for response factors of commercially available as well as purified standards as described in (ELLING et al., 2014). Archaeol was purchased from Avanti Polar Lipids Inc. (Alabaster, AL, USA). Phosphatidylglycerol-hexose GDGT was obtained from Matreya LLC (Pleasant Gap, PA, USA). GDGT-0, 1G-GDGT-0, 2G-GDGT-0, monoglycosidic archaeol (1G-AR), and diglycosidic archaeol (2G-AR) were purified from extracts of Archaeoglobus fulgidus by orthogonal preparative liquid chromatography as described by (ZHU et al., 2013). The abundances of core GDGTs, methoxy archaeol and archaeol were averaged from duplicate measurements and corrected for the response factors of purified GDGT-0 and core archaeol standards versus the C46-GTGT standard. The relative discrepancy of duplicate measurements from the average was below 5 %. The abundances of glycerol trialkyl glycerol tetraethers (GTGTs), hydroxy GDGTs (OH-GDGTs), glycerol dialkanol diethers (GDDs) and hydroxy GDDs (OH-GDDs) were corrected for the response factor of GDGT-0. Similarly, the abundances of IPLs were corrected for the response factors of purified 1G-AR, 1G-GDGT-0 (for 1G-, 1G-OH-, deoxy-1G-GDGTs, 1G-GDDs), and 2G-GDGT-0 (for 2G-, 2G-OH, 2G-2OH-GDGTs) standards versus the C46-GTGT standard. Due to a lack of appropriate standards, the abundances of phosphohexose-GDGTs (PH-GDGTs) and HPH-GDGTs were corrected for the response of a phosphatidylglycerol-hexose GDGT standard, respectively. For phosphohexose archaeol (PH-AR), we assumed the response factor of 2G-AR. We assumed the response factor of GDGT-0 for MeO-GDGTs due to a lack of an authentic standard. However, the presence of the methoxy group might influence the response of MeO-GDGTs relative to GDGT-0. The relative abundance of MeO-AR was corrected by its response factor relative to AR by comparing the relative abundance of MeO-AR and AR analyzed by GC-FID (ELLING et al., 2014).

The TEX_{86} index was calculated after SCHOUTEN et al. (2002) using the peak areas of GDGT-1, GDGT-2, GDGT-3 and Cren', with the number indicating the number of

cyclizations within the molecule:

$$\mathrm{TEX}_{86} = \frac{[\text{GDGT-2}] + [\text{GDGT-3}] + [\text{Cren'}]}{[\text{GDGT-1}] + [\text{GDGT-2}] + [\text{GDGT-3}] + [\text{Cren'}]} \quad \text{(Eq. 1)}$$

TEX_{86} reconstructed temperatures were calculated using the core-top calibration of KIM et al. (2010) recommended for temperatures above 15 °C ($\mathrm{TEX}_{86}^{\mathrm{H}}$):

$$\mathrm{SST}\ (^{\circ}\mathrm{C}) = 68.4 \times \log(\mathrm{TEX}_{86}) + 38.6 \quad \text{(Eq. 2)}$$

To evaluate GDGT cyclization we calculated the ring index (RI) according to PEARSON et al. (2004):

$$\mathrm{RI} = \frac{[\text{GDGT-1}] + 2 \times [\text{GDGT-2}] + 3 \times [\text{GDGT-3}] + 4 \times [\text{GDGT-4}] + 5 \times [\text{Cren} + \text{Cren'}]}{[\text{GDGT-0}] + [\text{GDGT-1}] + [\text{GDGT-2}] + [\text{GDGT-3}] + [\text{GDGT-4}] + [\text{Cren} + \text{Cren'}]} \quad \text{(Eq. 3)}$$

4.3. Results

4.3.1. Isolation and characterization of novel thaumarchaeal strains

Enrichment cultures of marine ammonia-oxidizing archaea were inoculated with from surface water from the Benguela upwelling system and showed significant nitrite formation after three years of incubation in the dark at 15 °C. Stable ammonia-oxidizing cultures were obtained by transferring the initial enrichments to synthetic medium containing 1 mM NH_4^+ and incubating at 28 °C. After repeated serial dilutions by a factor of 108 for about two years, only one morphotype per enrichment was observed by phase-contrast microscopy. Bacterial contaminants were not observed during microscopy but evident on solid medium for heterotrophs incubated at 28 °C for two weeks. These contaminants accounted for <1 % of cells and were subsequently removed from the enrichments using additional serial dilutions with SCM containing 100 mg l^{-1} gentamicin (NAOA2) or kanamycin (NAOA6).

The morphology of strains NAOA2 and NAOA6 was similar to *N. maritimus* occurring as rods of approximately 0.5 to 1 µm length and 0.2 µm width. Growth of the isolates was not stimulated by addition of 100 to 250 µM of organic carbon in the form of glyoxylate, oxaloacetate, or α-ketoglutarate to the medium. Nitrite production and growth of the novel strains was not observed when grown in media containing urea as the sole energy source. Nitrite was formed by the strains NAOA2 and NAOA6 between 14 and 37 °C, but significant growth occurred only between 17 and 35 °C for strain NAOA2 and 17 and 32 °C for strain NAOA6. The highest nitrite production rates were achieved at 22 °C for strain NAOA2 and at 27 °C for strain NAOA6. In

comparison,*N. maritimus* strain SCM1 exhibited nitrite production between 12 and 40 °C, with an optimum between 25 and 32 °C, but significant growth occurred only between 22 and 32 °C.

Figure 4.3. 16S rRNA (A) and ammonia-monooxygenase subunit A (*amoA*; B) gene consensus phylogeny of the novel thaumarchaeal isolates NAOA2 and NAOA6 (red), representative cultivated thaumarchaeal strains and selected environmental sequences showing close relationship of the isolates with *N. maritimus* and the thaumarchaeal group I.1a. The scale bars represent 10% estimated sequence divergence.

Phylogenetic analysis of the *amoA* and 16S rRNA genes of strains NAOA2 and NAOA6 indicated that both strains are phylogenetically affiliated with the thaumarchaeal group I.1a. Strain NAOA2 shares 98 % 16S rRNA and 92 % *amoA* gene sequence identity with*N. maritimus* SCM1, indicating that this strain may represent a novel species of the genus *Nitrosopumilus* (Fig. 4.3). Strain NAOA6 shares 100 % 16S rRNA and 98 % *amoA* gene sequence identity with *N. maritimus* SCM1 as well as 98 % 16S rRNA and 92 % *amoA* gene sequence identity with strain NAOA2. This indicates that strain NAOA6 represents a novel strain of the species *N. maritimus*.

The 16S rRNA and *amoA* genes of the novel strains are also distinct from those of the group I.1a *Thaumarchaeota Nitrosoarchaeum limnia* (97 % and 87 %, respectively) and *Cenarchaeum symbiosum* (94 % and 78 %, respectively), supporting the affiliation with the genus *Nitrosopumilus*. Similarly, the 16S rRNA and *amoA* genes are distinct from those of cultivated representatives of major thaumarchaeal groups from soil and hydrothermal environments (Fig. 4.3), sharing less than 90 % 16S rRNA and <77 %

amoA sequence identity with the genes of *Nitrosotalea devanaterra* (SAGMCG-I/Group I.1a associated), *Nitrososphaera viennensis* (group I.1b), and *Nitrosocaldus yellowstonii* (HWCG-III/ThAOA).

4.3.2. *Lipid composition of Nitrosopumilus maritimus and strains NAOA2 and NAOA6 at different growth temperatures*

The novel strains NAOA2 and NAOA6 contained a similar suite of core lipids and IPLs as *N. maritimus* but the relative abundances of IPL classes and core lipid structures varied between the three strains (Fig. 4.4). The dominant IPLs in *N. maritimus* grown at 28 °C were 1G-GDGTs, 2G-GDGTs and 2G-OH-GDGTs while HPH-GDGTs were less abundant (Fig. 4.4a). Strain NAOA6 (28 °C) had a different IPL composition with about equal proportions of 1G-, 2G-, 2G-OH- and HPH-GDGTs (Fig. 4.4b). In contrast, the IPL pool of strain NAOA2 consisted of about equal parts 2G-, 2G-OH- and HPH-GDGTs at 28 °C while 1G-GDGTs abundances were minor. Other lipids detected in all strains were the IPL-archaeols 1G-AR and PH-AR as well as 1G-OH-GDGTs, PH-GDGTs, core, hydroxylated, and monoglycosidic GDDs (cf. LIU et al., 2012b; MEADOR et al., 2014b), core GDGTs, core archaeol and methoxy archaeol (MeO-AR, Table 4.1).

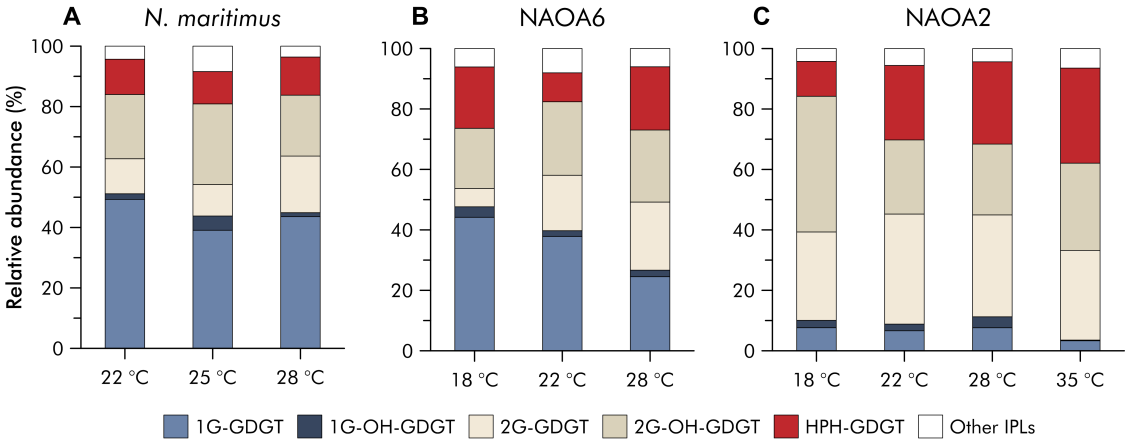

Figure 4.4. Relative abundances of intact polar lipids in extracts of *N. maritimus* (A) and the novel thaumarchaeal isolates NAOA6 (B) and NAOA2 (C) grown at different temperatures.

The lipid composition of all three strains varied considerably with incubation temperature. An increase in incubation temperature resulted in an increase of the relative abundance of HPH-GDGTs at the expense of 1G-GDGTs and minor increase or decrease of other IPL classes in all strains (Fig. 4.4). In strain NAOA2, decreasing growth temperature additionally resulted in increase in 2G-and 2G-OH-GDGTs. The ring indices of individual IPL classes were positively correlated with growth temperature while the abundance of MeO-AR relative to total lipids was inversely correlated with growth

temperature in strain NAOA2 but did not change significantly in strain NAOA6 and *N. maritimus*. The TEX_{86} values of IPLs were positively correlated with growth temperature in *N. maritimus* and strain NAOA6 but showed different slopes. In contrast, TEX_{86} of IPLs showed no correlation with growth temperature in strain NAOA2.

Table 4.1. Abundances of archaeol (AR) and methoxy archaeol (MeO-AR) in thaumarchaeal cultures relative to total lipids derived by acid hydrolysis as well as ring index (RI), TEX_{86} and TEX_{86}^{H}-temperature in total hydrolysis-derived GDGTs (measured using normal phase HPLC-APCI-MS).

	Growth temp. (°C)	AR (%)	MeO-AR (%)	RI	TEX_{86}	TEX_{86}^{H}-temp. (°C)
Nitrosopumilus maritimus	22	1.4	3.5	2.4	0.60	23.2
	25	2.3	3.9	2.9	0.70	28.0
	28	0.2	2.1	3.4	0.86	34.0
Strain NAOA2	18	3.3	13.2	2.9	0.80	32.0
	22	3.4	4.7	2.8	0.83	33.2
	28	1.5	2.3	3.1	0.86	34.4
	35	4.1	0.6	4.0	0.78	31.2
Strain NAOA6	18	2.4	5.5	2.2	0.54	20.3
	22	2.7	4.2	3.2	0.83	33.1
	28	0.4	4.5	3.4	0.89	35.3

The relative abundances of core GDGT types in the hydrolysis-derived total GDGT pool were overall similar between the three strains (Fig. 4.5). Crenarchaeol was the most abundant GDGT in all strains at 28 °C but was less abundant in strain NAOA2 (∼30 % of GDGTs) compared to strain NAOA6 (∼45 %) and *N. maritimus* (∼50 %). The relative abundances of GDGT-2 and GDGT-3 were significantly higher in strain NAOA2 than in strain NAOA6 and *N. maritimus*. The relative abundances of core GDGTs changed with growth temperature in all three strains. An increase in growth temperature was associated with an increase in crenarchaeol abundance and a decrease in GDGT-0 and GDGT-1. The influence of growth temperature on the abundance of other GDGTs was different between the three strains. In *N. maritimus* and strain NAOA6, the abundance of GDGT-2 increased with increasing growth temperature, while GDGT-4 abundance remained similar and GDGT-3 abundance decreased. In strain NAOA2, the abundances of GDGT-3 and GDGT-4 decreased with increasing growth temperature while the abundance of GDGT-2 increased from 18 to 28 °C but decreased at 35 °C. The crenarchaeol regioisomer increased in abundance in strain NAOA2 from 0.7 % at 18 °C to 2.8 % at 35 °C but was generally below 1 % in strain NAOA6 and *N. maritimus* and did not change significantly with growth temperature in these strains (Fig. 4.5).

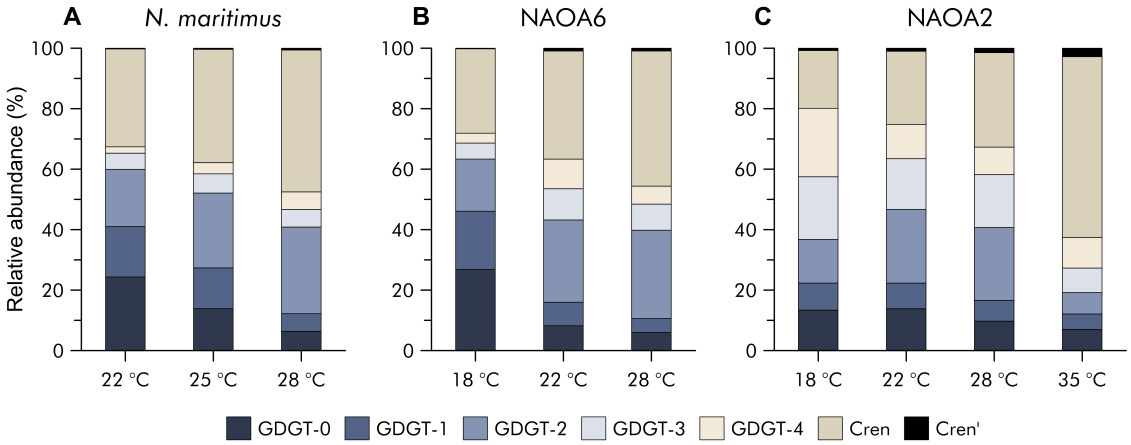

Figure 4.5. Relative abundances of hydrolysis-derived total GDGTs in extracts of *N. maritimus* (A) and the novel thaumarchaeal isolates NAOA6 (B) and NAOA2 (C) grown at different temperatures.

The ring index of the total GDGT pool increased with growth temperature in all strains, but each strain exhibited a different relationship between temperature and GDGT cyclization (Fig. 4.6). Changes in ring index were primarily driven by the relative abundances of crenarchaeol and GDGT-0 in all investigated strains. TEX_{86} values increased linearly with increasing growth temperature in *N. maritimus* and strain NAOA6 though following different slopes. In contrast, TEX_{86} values in strain NAOA2 increased between 18 and 28 °C and decreased again at 35 °C, indicating a quadratic polynomial relationship with temperature (Fig. 4.6).

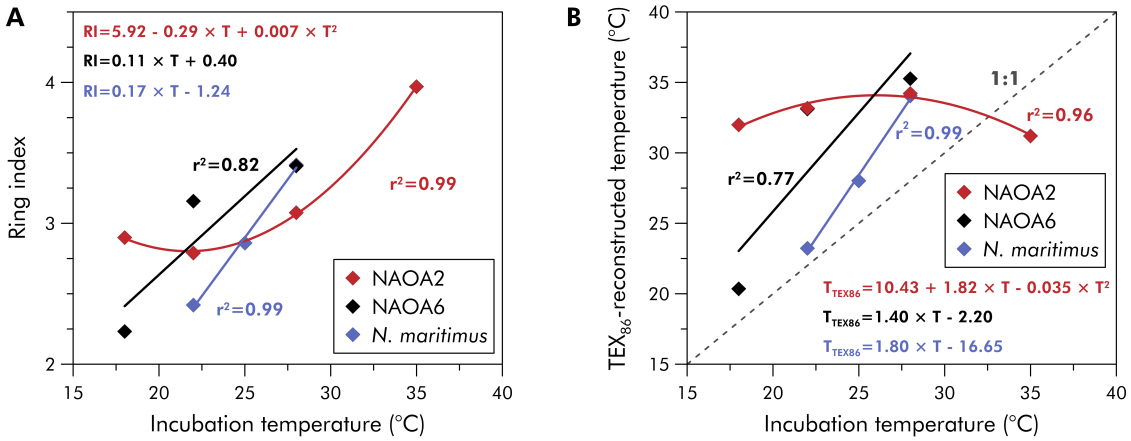

Figure 4.6. (A) Ring indices and (B) TEX_{86} temperatures reconstructed from hydrolysis-derived total GDGTs of *N. maritimus* and the novel thaumarchaeal isolates NAOA2 and NAOA6 grown at different temperatures. The dashed line (1:1) indicates identity between TEX_{86}-reconstructed temperatures and the global core-top calibration model for temperatures over 15 °C (TEX_{86}^{H}) by KIM et al. (2010).

4.3.3. *Growth and lipid composition of Nitrosopumilus maritimus at different salinities*

Growth of *N. maritimus* SCM1 was observed over a wide range of growth medium salinities from 16‰ to 96‰. The highest nitrite production and optimal growth rate was achieved at a growth medium salinity of 37‰ and was only slightly lower at 26‰. Growth rates decreased gradually towards higher salinities but more rapidly towards lower salinities. Growth was partially inhibited below 16‰ and above 96‰ but completely inhibited at 3‰.

The intact polar and core lipid composition of *N. maritimus* was reproducible in duplicate cultures but did not differ significantly between various salinities (Fig. 4.7a). The main components were 1G- and 2G-GDGTs and their hydroxylated derivatives. Minor lipids were HPH-GDGTs and intact polar archaeols with PH and 1G headgroups as well as core archaeol and MeO-AR. The relative abundance of 2G-GDGTs was slightly elevated at 37‰ salinity compared to 27‰, 44‰ and 51‰ at the expense of 1G-GDGT abundance. The TEX_{86} temperatures reconstructed from individual intact polar GDGTs were either lower (1G-, HPH-GDGTs) or higher (2G-GDGTs) than incubation temperature by up to 10 °C. The TEX_{86}-temperatures calculated from total hydrolysis-derived GDGTs underestimated incubation temperature only slightly by 0.5 to 2 °C. However, the TEX_{86}-temperatures derived from total and individual intact polar GDGTs as well as their ring indices did not vary significantly between different growth medium salinities (Fig. 4.7b).

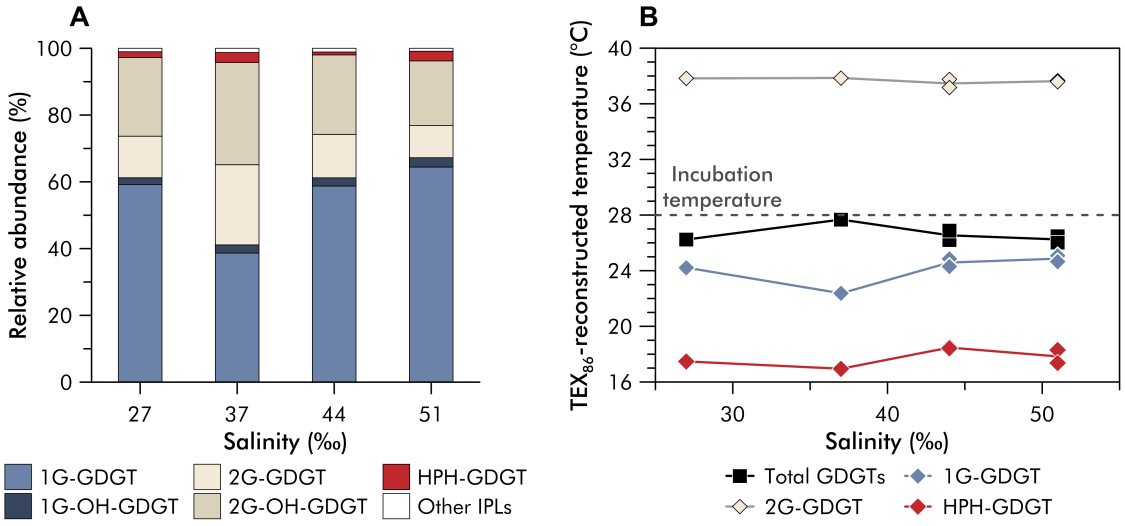

Figure 4.7. (A) Relative abundances of intact polar lipids in extracts of *N. maritimus* grown at different growth medium salinities and harvested in late growth stage. (B) Reconstructed TEX_{86} temperatures for individual IPLs (diamonds) and total GDGTs derived by hydrolysis (squares) at different growth medium salinities. Dashed line indicates actual incubation temperature of 28 °C.

4.3.4. *Growth and lipid composition of Nitrosopumilus maritimus at different growth medium pH*

Growth of *N. maritimus* was observed at growth medium pH of 6.8 to 8.2 with an optimum between pH 7.4 and 7.9. However, the lag phase was significantly longer with up to 10 days below pH 7.4 and above pH 8.

Similar to the other experiments, the major IPLs were 1G- and 2G-, and HPH-GDGTs and their hydroxylated derivatives (Fig. 4.8a). Minor IPLs were intact polar archaeols with PH and 1G headgroups and early eluting isomers of 2G- and 2G-OH-GDGTs. These isomers have similar MS^2 fragmentation spectra as the respective later eluting compounds and may represent constitutional isomers, e.g., having one monoglycosidic headgroup connected to each glycerol moiety versus a diglycosidic moiety linked to only one of the glycerols. Intact polar lipid composition changed between different growth medium pH in the range 7.3 to 7.9. The abundances of PH-AR, HPH-, 2G- and 2G-OH-GDGTs as well as their early eluting isomers decreased with increasing pH. In contrast, the abundances of 1G-GDGTs, 1G-AR and early eluting 2G-GDGTs increased with increasing pH (Fig. 4.1a). The ring indices of individual intact polar GDGT classes and total GDGTs did not change significantly. The TEX_{86}-temperatures reconstructed from individual intact polar and hydrolysis-derived total GDGTs showed patterns of lower and higher TEX_{86}-temperatures similar to the other experiments. The TEX_{86}-temperatures derived from total GDGTs varied by up to 2 °C between different growth medium pH (Fig. 4.8b). TEX_{86} temperatures derived from total GDGTs were highest at pH 7.3 (31.5 to 32.5 °C) and lower at pH 7.6 and 7.9 (30.5 to 30.7 °C). TEX_{86}-temperatures of 2G-GDGTs were constant but those of 1G-GDGTs increased slightly at pH 7.3. TEX_{86}-temperatures of HPH-GDGTs were minimal at pH 7.6 and elevated at pH 7.3 and 7.9 (Fig. 4.8b).

4.4. Discussion

4.4.1. *Novel thaumarchaeal isolates from the temperate Atlantic Ocean*

The cultivation of the thaumarchaeal ammonia oxidizer *N. maritimus* was essential for unraveling the physiology and ecology as well as the lipid inventory of this globally abundant archaeal clade (STAHL and DE LA TORRE, 2012). While *N. maritimus* was first discovered in a tropical aquarium (KÖNNEKE et al., 2005), the thaumarchaeal strains reported here were isolated from temperate surface water sampled from the South Atlantic Ocean, off the coast of Namibia. The strains NAOA2 and NAOA6 share high phylogenetic relatedness with *N. maritimus* and numerous environmental 16S rRNA and *amoA* sequences (Fig. 4.3), thus confirming the ubiquitous distribution of the genus

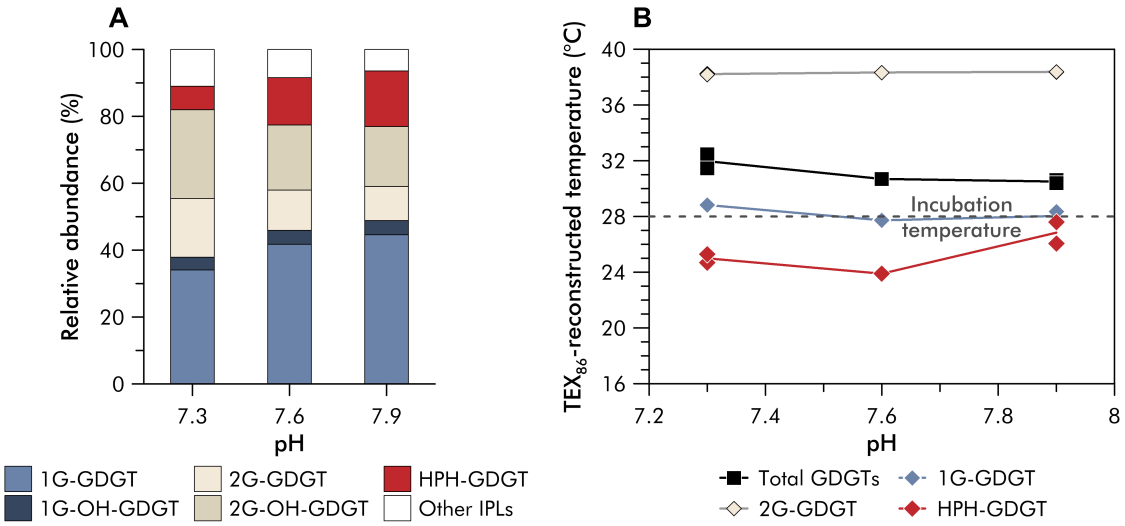

Figure 4.8. (A) Relative abundances of intact polar lipids in extracts of *N. maritimus* grown at different growth medium pH and harvested in early stationary phase. (B) Reconstructed TEX_{86} temperatures for individual IPLs (diamonds) and total GDGTs derived by hydrolysis (squares) at different growth medium pH. Dashed line indicates actual incubation temperature of 28 °C.

Nitrosopumilus and its use as a model organism for studying marine *Thaumarchaeota*. In contrast to *N. maritimus*, both strains grew over a broader temperature range and thus were well suited to investigate the response of lipid composition to temperature in marine planktonic *Thaumarchaeota*.

4.4.2. Lipid composition at different growth temperatures and implications for TEX_{86}

The dominant membrane lipids in *N. maritimus*, the novel strains NAOA2 and NAOA6 as well as all other characterized *Thaumarchaeota* are crenarchaeol and GDGTs with zero to four cyclizations in the biphytanyl side chains (PITCHER et al., 2011a; SINNINGHE DAMSTÉ et al., 2012; ELLING et al., 2014). Similar to thermophilic *Crenarchaeota* and *Euryarchaeota*, the three mesophilic *Thaumarchaeota* adapt their membranes to increasing growth temperatures by increasing the average number of cyclopentane rings in GDGTs (e.g. DE ROSA et al., 1980; UDA et al., 2001; CHONG, 2010; KOGA, 2012; OGER and CARIO, 2013). The introduction of cyclopentane rings into GDGTs has been suggested to promote dense packing of the monolayer membrane, thus maintaining optimal membrane fluidity and lowering proton permeability at high temperatures (GLIOZZI et al., 1983; GABRIEL and CHONG, 2000; ZHAI et al., 2012). The additional cyclohexyl moiety of crenarchaeol, on the other hand, has been suggested to cause loose packing of GDGT membranes based on molecular dynamics simulations, thus allowing *Thaumarchaeota* to adapt to low temperature habitats

(SINNINGHE DAMSTÉ et al., 2002b). However, the pronounced increase in relative abundance of crenarchaeol with increasing growth temperature (Fig. 4.5) in all three investigated strains suggests that crenarchaeol is involved in membrane lipid adaptation to high instead of low temperatures. This observation is supported by the fact that crenarchaeol is the most abundant GDGT in cultivated thermophilic *Thaumarchaeota* (DE LA TORRE et al., 2008; PITCHER et al., 2010) and occurs in terrestrial hot springs (PEARSON et al., 2004; ZHANG et al., 2006).

In contrast to core lipid structure, the effect of polar headgroups on membrane properties and fluidity in archaea is less constrained. The three thaumarchaeal isolates *N. maritimus*, strain NAOA2 and strain NAOA6 share the same suite of polar headgroups (Fig. 4.4). In these strains, membrane lipid adaptation to higher temperatures involves increased relative abundances of HPH- and 2G-GDGTs compared to 1G-GDGTs. Additionally, HPH-GDGT abundances show the same trend in strain NAOA2 but the abundances of the other IPLs do not seem to vary systematically, but there is a maximum of 2G-GDGT and 2G-OH-GDGT abundances at 18 °C (Fig. 4.4). The increase in phospholipid over glycolipid abundances with increasing temperature in the three thaumarchaeal strains contrasts with the inverse observation in the thermoacidophilic euryarchaeon *Thermoplasma acidophilum* (SHIMADA et al., 2008), indicating that the roles of headgroups in membrane lipid adaptation may diverge between different archaea.

Similar to crenarchaeal and euryarchaeal species, ring index of total GDGTs is linearly correlated with growth temperature in *N. maritimus* and strain NAOA6 (Fig. 4.6). In contrast, the ring index in strain NAOA2 increases only above 22 °C, suggesting that changes in GDGT cyclization as a mode of homeoviscous adaptation in *Thaumarchaeota* might be limited to a certain temperature range and species-specific. The slopes of the ring index-temperature function diverge between *N. maritimus* (0.16 $°C^{-1}$), strain NAOA6 (0.12 $°C^{-1}$) and strain NAOA2 (22-35°C: 0.09 $°C^{-1}$), which is in agreement with species-specific relationships of ring index and temperature in cultivated thermophilic *Crenarchaeota* and Euryarchaeota (e.g. DE ROSA et al., 1980; UDA et al., 2004). Our results therefore suggest that the distinct relationships between GDGT cyclization and temperature observed in different oceanic provinces may in fact be related to variations in archaeal community composition (cf. PEARSON and INGALLS, 2013). However, the significantly higher slopes of the ring index versus temperature relationship in *N. maritimus* and strain NAOA6 compared to most thermophiles (cf. OGER and CARIO, 2013) indicate that GDGT cyclization in marine *Thaumarchaeota* is very sensitive to changes in growth temperature, which is in agreement with previous observations from mesocosm studies (WUCHTER et al., 2004; SCHOUTEN et al., 2007a) and environmental data (SCHOUTEN et al., 2002).

While the cyclization of most IPL-GDGTs increases with growth temperature, the ring indices also differ between the various IPL classes at a given growth temperature. Therefore, shifts in the relative abundances of IPL-GDGTs appear to be additional drivers of increasing cyclization in total GDGTs. The dependency of core GDGT cyclization on the attached polar headgroups might be related to interactions of the hydrophilic headgroups with the hydrophobic core regions. These may influence membrane density and proton permeability by controlling the overall conformation of the lipid molecule and the orientation of headgroups relative to the membrane surface (cf. GABRIEL and CHONG, 2000). Overall, the individual IPL profiles of the three thaumarchaeal strains indicate that the membranes of planktonic *Thaumarchaeota* grown at the same temperature are composed of the same suite of IPLs but differ in the relative abundances of these IPLs and their core GDGT compositions.

In addition to regular and hydroxylated GDGTs, *N. maritimus* contains multiple additional lipids that are also present in the strains NAOA2 and NAOA6. The abundance of most of these compounds, except MeO-AR (cf. ELLING et al., 2014), is relatively low and their function in archaeal cells and influence on membrane structure remain unconstrained (ELLING et al., 2014; MEADOR et al., 2014a). These lipids comprise, among others, archaeol with 1G and PH headgroups as well as core, hydroxylated, and monoglycosidic GDDs (Fig. 4.1). The abundances of these compounds were not correlated with growth temperatures, salinity or pH in all three strains, suggesting that they are not primarily involved in membrane lipid homeostasis. The apolar lipid MeO-AR (Fig. 4.1), a *sn*-1 methylether derivative of archaeol that has so far only been observed in *N. maritimus* (ELLING et al., 2014), is also present in strain NAOA2 and strain NAOA6. The abundance of MeO-AR relative to total lipids did not change significantly with growth temperature in strain NAOA6 and *N. maritimus*. However, MeO-AR abundance decreased with increasing growth temperature in strain NAOA2 from 13 % to 0.6 % between 18 and 35 °C (Table 4.1). This suggests that MeO-AR is involved in homeoviscous adaptation at least in some *Thaumarchaeota*. While the exact function of this lipid remains unknown, MeO-AR might be involved in increasing membrane fluidity at low temperatures in a similar way as squalene may increase membrane fluidity in halophilic archaea by spacing polar lipids further apart (LANYI et al., 1974; LANYI, 1974).

4.4.3. Influence of community composition on TEX_{86}-temperature relationships and implications for paleoenvironmental reconstructions

The systematic change in GDGT cyclization and TEX_{86} values in response to growth temperature in the three studied thaumarchaeal strains *N. maritimus*, strain NAOA2,

and strain NAOA6 confirms a physiological basis of the TEX_{86} paleothermometer, i.e., temperature-dependent adjustment of membrane fluidity by altering GDGT cyclization (SCHOUTEN et al., 2002). However, the disparate relationships of TEX_{86} with growth temperature among these closely related thaumarchaeal strains contrast with the global calibration curves that form the basis of most published TEX_{86} temperature records (SCHOUTEN et al., 2002; KIM et al., 2008, 2010). This suggests that multiple physiological and ecological factors (cf. PEARSON and INGALLS, 2013) might amalgamate into the global calibration.

The diverging TEX_{86}–temperature responses of *N. maritimus* and strains NAOA2 and NAOA6 imply that community composition may exert an important control on the TEX_{86} signal in the environment. Non-linearity of TEX_{86} functions has been shown before in mesocosm incubations of North Sea water (WUCHTER et al., 2004) incubated at 5 to 35 °C. In these experiments, the form of the TEX_{86}–temperature function was dependent on whether the mesocosms were pre-incubated at 13 °C (concave up) or 27 °C (concave down). While this trend was neither described nor discussed by WUCHTER et al. (2004), it suggests that pre-incubation conditions were selective for different thaumarchaeal ecotypes and thus distinct temperature responses. Given that planktonic *Thaumarchaeota* exhibit considerable diversity (FERNÀNDEZ-GUERRA and CASAMAYOR, 2012) and that multiple thaumarchaeal phylotypes coexist in the environment (e.g. TULLY et al., 2012; HOLLIBAUGH et al., 2014), it seems likely that the TEX_{86} signal recorded in sediments integrates activities of a mixture of different thaumarchaeal eco-/phylotypes with different responses to temperature.

To illustrate this ecological effect, we devised a simple model describing the TEX_{86} signal of a hypothetical mixed community composed of *N. maritimus*, strain NAOA2 and strain NAOA6 (Fig. 4.9). Hereby, we varied the relative abundance of each strain in 10 %-intervals relative to the other two strains and calculated the integrated TEX_{86} temperature as a fractional contribution of the three strains to the total TEX_{86} signal. The results from the mixing model indicate that numerous combinations of the three thaumarchaeal strains may explain a broad range of TEX_{86} signals (Fig. 4.9). However, the closest approximation of the model for the range 21 to 33 °C exceeds incubation temperatures by up to 5 °C. This deviation may in part be explained by sensitivity of TEX_{86} to growth phase, which has been shown to account for deviations of TEX_{86} temperatures from growth temperatures of up to 6 °C (-4 to +2 °C, ELLING et al., 2014). As illustrated in Fig. 4.9, changes in community composition could additionally account for positive TEX_{86}-temperature deviations of up to 10 to 15 °C (Fig. 4.9), suggesting that these may override temperature signals and the influence of growth phase. Therefore, environmental TEX_{86} signals likely integrate the effects of temperature adaptation and community dynamics, which might also explain the

subsurface decoupling of TEX_{86} and in situ temperature observed in marine water column profiles (e.g. TURICH et al., 2007; SCHOUTEN et al., 2012; HERNÁNDEZ-SÁNCHEZ et al., 2014; XIE et al., 2014).

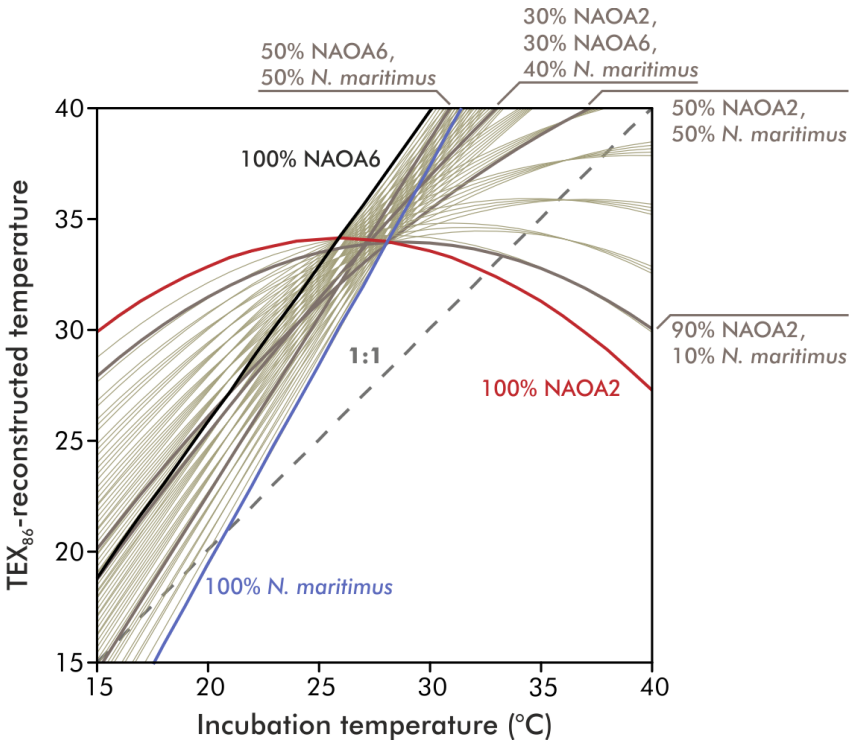

Figure 4.9. Influence of community composition on TEX_{86}-temperatures as estimated by a three end-member mixing model assuming a hypothetical community composed of *N. maritimus* and strains NAOA2 and NAOA6 (varying relative abundance in 10%-steps). The dashed line (1:1) indicates identity between TEX_{86}-reconstructed temperatures and the global core-top calibration model for temperatures over 15 °C (TEX_{86}^{H}) by KIM et al. (2010). Bold lines indicate integrated TEX_{86} functions for selected community compositions.

The absence of a common membrane lipid response to growth temperature in cultivated *Thaumarchaeota* has important implications for the applicability of the TEX_{86} paleothermometer in the geologic record. Similar to other paleoceanographic proxies TEX_{86} relies on the actualism principle, i.e., the applicability of modern observations/core-top calibrations to ancient environments. As other paleotemperature proxies such as U_{37}^{K} are often affected by diagenesis or absent from ancient sediments (BRASSELL, 2014), TEX_{86} paleothermometry has been frequently applied for reconstructing Mesozoic and Paleogene SSTs (e.g. HOLLIS et al., 2009; JENKYNS et al., 2012; LINNERT et al., 2014). A remarkably consistent feature of these ancient TEX_{86} records are extraordinarily high sea surface temperatures and very weak meridional temperature gradients, e.g., for the Eocene, that are not supported by $\delta^{18}O$, planktonic foraminifer Mg/Ca and modeling data (HUBER and CABALLERO, 2011;

TAYLOR et al., 2013; TIERNEY and TINGLEY, 2014). TEX_{86}–temperature relationships of thaumarchaeal assemblages from the Eocene and other epochs may have differed from those of modern assemblages, resulting in an underestimation of meridional temperature gradients and suggesting overestimation of regional SST.

Given the inferred influence of community composition on TEX_{86}, the applicability of modern global calibrations for reconstructing paleotemperatures using TEX_{86} in ancient, e.g., Mesozoic and early Cenozoic, environments seems questionable. However, our observations imply that specifically adapted archaeal communities may be recognizable by distinct GDGT distributions. Knowledge of the ecological significance of distinct GDGT signatures may then be used to develop alternative calibration models using modern analogue environments as suggested by (TIERNEY and TINGLEY, 2014).

4.4.4. Influence of salinity on TEX_{86}

In contrast to temperature, varying growth medium salinity in the range of 27‰ to 51‰ did not systematically affect cyclization of total GDGTs in *N. maritimus*, consistent with previous observations in the range 27‰ to 35‰ in mesocosm experiments (WUCHTER et al., 2004). Indeed, the salinity range studied here is much larger than the spatial and vertical variability of salinity in the modern open ocean between ca. 33‰ and 38‰ (ANTONOV et al., 2010) as well as reconstructed changes for the deep ocean over the last glacial-interglacial cycle (<3‰; ADKINS et al., 2002). Therefore, our observations indicate that TEX_{86}-based paleotemperature reconstructions in pelagic environments are likely not compromised by changes in paleosalinity if phenotypes similar to *N. maritimus* prevailed during the geologic past.

Furthermore, IPL composition showed no systematic relationship with growth medium salinity, indicating that the lipid membrane of *N. maritimus* is per se adapted to low ion permeability. Therefore, the supposedly low permeability of the thaumarchaeal membrane in addition to the potential for biosynthesis of the osmolyte hydroxyectoine (WALKER et al., 2010) may explain the large growth range (ca. 16 to 96‰) observed here for *N. maritimus*. Furthermore, the S-layer of *N. maritimus* and other *Thaumarchaeota* (KÖNNEKE et al., 2005; STIEGLMEIER et al., 2014b) might confer additional osmoprotection as hypothesized by ENGELHARDT (2007). However, salinity was implicated as one of the most important factors governing the niche partitioning of thaumarchaeal lineages (BILLER et al., 2012; BOUSKILL et al., 2012; CAO et al., 2013). Indeed, specially adapted thaumarchaeal ecotypes have been described for extremely hypersaline (NGUGI et al., 2015), brackish (BLAINEY et al., 2011; MOSIER et al., 2012), and freshwater environments (AUGUET et al., 2012; FRENCH et al., 2012). These ecotypes may possess different physiology, such as the lack of

osmolyte biosynthesis in the low-salinity thaumarchaeon *Candidatus* Nitrosoarchaeum limnia, and therefore may also express different IPL composition and GDGT cyclization. This notion is supported by anomalous TEX_{86}-temperatures of −0.6 °C in the low salinity group I.1a thaumarchaeon *Ca.* Nitrosoarchaeum limnia grown at 22 °C (PITCHER et al., 2011a). An ecological effect rather than a direct effect of salinity has also been implicated to explain the unique GDGT cyclization systematics in Red Sea sediments (TROMMER et al., 2009), which might be related to a local, phylogenetically distinct I.1a *Thaumarchaeota* population (cf. IONESCU et al., 2009). Therefore, any influence of salinity on GDGT composition in environmental samples may be related to ecological rather than physiological factors.

4.4.5. Influence of pH on TEX_{86}

Thaumarchaeota live at neutral to basic pH in the ocean, which may vary spatially and vertically between ca. 7.5 and 8.2 (MILLERO, 2007). Indeed, *N. maritimus* grows in the range of pH 6.8 to 8.2, indicating that it is capable of growing in the full pH range observed in the ocean. Acidophilic archaea, i.e., archaea that have a growth optimum below pH 3, adjust membrane permeability to protons by either increasing (BOYD et al., 2011) or decreasing (SHIMADA et al., 2008) GDGT cyclization in response to decreasing pH. In contrast, the ring index of total GDGTs in the three thaumarchaeal strains studied here did not vary significantly between pH 7.3 and 7.9. However, an increase in the relative abundances of glycosidic over glycophosphatidic GDGTs with decreasing pH (Fig. 4.8a) is consistent with observations from *T. acidophilum* (SHIMADA et al., 2008) and might confer enhanced stability to the membrane by increasing hydrogen bonding between outward-facing glycosidic headgroups (MORII and KOGA, 1994; GABRIEL and CHONG, 2000; SHIMADA et al., 2008). Overall, the small influence of pH on lipid composition in the three strains studied here suggests that *Thaumarchaeota* are able to adapt to the full pH range observed in the ocean by making subtle modifications to their membrane composition. However, pH might influence environmental GDGT distribution indirectly by selecting for specific thaumarchaeal lineages with distinct lipid compositions, which might be of particular importance in environments that exhibit large variability in pH such as lakes, soils or hydrothermal springs (NICOL et al., 2008; ZHANG et al., 2008; GUBRY-RANGIN et al., 2011; AUGUET et al., 2012).

We observed an increase of 2 °C in TEX_{86} temperatures over the range of pH 7.3 to 7.9 in *N. maritimus* (Fig. 4.8). This increase in TEX_{86} can be attributed to a slight increase in relative abundance of GDGT-2 caused by an increase in abundance of 1G-GDGT-2 and 2G-GDGTs, which contain predominantly GDGT-2 as core lipid (ELLING

et al., 2014). While the surface ocean has a pH of ca. 8.2, organic carbon respiration causes pH to decrease by up to 0.5 pH units over a depth of ca. 500-1000 m (MILLERO, 2007). This effect is especially pronounced in oxygen-deficient waters such as oxygen minimum zones associated with coastal upwelling (CAPONE and HUTCHINS, 2013). The decrease in pH broadly coincides with the depth interval of TEX_{86} subsurface warming observed in water column profiles, most of which are from OMZs (e.g. SCHOUTEN et al., 2012; BASSE et al., 2014; XIE et al., 2014). However, the magnitude of TEX_{86} increase observed in the water column (up to 5 to 10 °C; e.g. SCHOUTEN et al., 2012; HERNÁNDEZ-SÁNCHEZ et al., 2014) is larger than the increase in TEX_{86} observed at low pH in *N. maritimus* (Fig. 4.8), suggesting that the contribution of water column pH variations to observed increases in subsurface TEX_{86} temperatures may be low.

In the Phanerozoic, pH varied by not more than one unit (PALMER et al., 1998; HÖNISCH et al., 2012) while events such as the Paleocene-Eocene Thermal Maximum (PETM) have been suggested to be accompanied by strong ocean acidification by up to 0.5 pH units (ZACHOS et al., 2008; HÖNISCH et al., 2012). Since these variations in ocean pH are within the range tested for *N. maritimus*, pH likely only had a small direct effect on TEX_{86} in these settings. However, the influence of strong changes in pH on marine thaumarchaeal community composition remains unconstrained. Similar to salinity, pH might be a strong discriminator determining niche differentiation of *Thaumarchaeota* as suggested for lakes (AUGUET and CASAMAYOR, 2013) and soils (NICOL et al., 2008; GUBRY-RANGIN et al., 2011) and may thus indirectly influence TEX_{86} signatures.

4.5. Conclusions

Our pure culture study demonstrates that marine planktonic *Thaumarchaeota* respond sensitively to changing growth temperatures by adjusting their membrane lipid composition, in particular the content of crenarchaeol, while influences of salinity and pH are less pronounced. In contrast to previous hypotheses suggesting that crenarchaeol increases membrane fluidity and might therefore be an adaptation to cold environments, we observed higher crenarchaeol abundances at higher growth temperatures. We conclude that crenarchaeol likely increases the phase transition temperature of thaumarchaeal lipid membranes and thus appears essential in maintaining membrane functioning at elevated temperatures. Significantly different IPL compositions in the three closely related marine thaumarchaeal isolates imply that the IPL composition of environmental samples might be driven not only by physiological and environmental factors but also by thaumarchaeal diversity.

In the three studied thaumarchaeal strains, changes of TEX_{86} signatures with temperature result primarily from changes in the relative abundances of the major IPL classes 1G-, HPH- and 2G-GDGTs, each of which are affiliated with distinct core GDGT compositions. The disparate relationships of TEX_{86} and growth temperature that we observed among the three closely related thaumarchaeal strains suggests that changes in community composition may exert a strong control on TEX_{86}. Therefore, environmental TEX_{86} signals may represent a mixture of temperature adaptation, nutrient conditions and community dynamics, which might account for the subsurface decoupling of TEX_{86} and *in situ* temperature observed in marine water column profiles.

Comprehensive investigations of TEX_{86}–temperature relationships in yet to be cultivated *Thaumarchaeota* from a wide range of environments are needed to enhance our mechanistic understanding of the influence of community composition on TEX_{86} signals and to reliably interpret the geologic GDGT record. Our results further imply that specifically adapted archaeal communities may be recognizable by distinct GDGT distributions. Careful investigation of these patterns might allow delineating archaeal community structure from characteristic GDGT signatures and might ultimately lead to improved, ecosystem-specific calibration models.

Acknowledgements

We are grateful to the crew, chief scientist M. Zabel, and the scientific shipboard party of R/V Meteor cruise M76/1. We thank J.S. Lipp and L. Wörmer for supporting HPLC-MS analyses. J. Wulf, M. Lange, N.T. Smit, and J. Arndt are thanked for laboratory assistance. The study was funded by the European Research Council under the European Union's Seventh Framework Programme–'Ideas' Specific Programme, ERC grant agreement No. 247153 (Advanced Grant DARCLIFE; PI: K.-U.H.) and by the Deutsche Forschungsgemeinschaft through the Gottfried Wilhelm Leibniz Prize awarded to Kai-Uwe Hinrichs (Hi 616-14-1) and instrument grant Inst 144/300-1 (LC-qToF system).

CHAPTER 5

Comparative analysis of the thaumarchaeal lipidome

Felix J. Elling[a], Martin Könneke[a,*], Kevin W. Becker[a], Michaela Stieglmeier[b], Graeme W. Nicol[c], Eva Spieck[d], José R. de la Torre[e], Gerhard Herndl[f,g], Christa Schleper[b] and Kai-Uwe Hinrichs[a]

In preparation for *Applied and Environmental Microbiology*

[a] Organic Geochemistry Group, MARUM - Center for Marine Environmental Sciences & Department of Geosciences, University of Bremen, 28359 Bremen, Germany
[b] Department of Microbial Ecology, University of Vienna, 1090 Vienna, Austria
[c] Institute of Biological and Environmental Sciences, University of Aberdeen, Aberdeen AB24 3UU, United Kingdom
[d] Biozentrum Klein Flottbek, Abteilung für Mikrobiologie und Biotechnologie, Universität Hamburg, 22609 Hamburg, Germany.
[e] Department of Biology, San Francisco State University, San Francisco, CA, USA
[f] Department of Limnology and Oceanography, University of Vienna, 1090 Vienna, Austria
[g] Department of Biological Oceanography, Royal Netherlands Institute for Sea Research, 1790 AB Den Burg, Netherlands

[*] Corresponding author. E-mail: mkoenneke@marum.de

Abstract

Archaea of the phylum *Thaumarchaeota* are globally distributed and abundant microorganisms mediating the oxidation of ammonia to nitrite in the ocean, soil, as well as in geothermal systems and represent a major source of archaeal lipids in these environments. However, interpretation of environmental lipid profiles is mainly hindered by the lack of comparative and quantitative studies on the membrane lipid composition of cultivated representatives of this phylum. Here, we describe the core and intact polar lipid (IPL) composition of 11 thaumarchaeal pure and enrichment cultures representing all four characterized thaumarchaeal clades. In general, all thaumarchaeal strains synthesize similar lipid types conFsisting of consisting mainly of glycerol dibiphytanyl glycerol tetraethers with monoglycosidic, diglycosidic, phosphoxehose and hexose-phosphoxose headgroups. However, the relative abundances of these lipids as well as their core lipid composition differ significantly among the thaumarchaeal phylogenetic subgroups. While the core lipid composition of cultivated *Thaumarchaeota*, such as the content of the characteristic biomarker crenarchaeol, appears to be determined by their phylogenetic affiliation, the IPL composition reflects their habitat or growth conditions. Based on comparison of the thaumarchaeal lipidome with analyses of 21 eury- and crenarchaeal strains and environmental samples from the equatorial North Pacific Ocean, we further demonstrate that the apolar lipid methoxy archaeol is synthesized exclusively by *Thaumarchaeota* and thus represents a diagnostic chemotaxonomic biomarker for this archaeal phylum. The description of the thaumarchaeal lipidome comprised of 100 structurally different lipid types supports the interpretation of archaeal lipid signatures in environmental samples and provides useful characteristics to identify distinct thaumarchaeal clades.

5.1. Introduction

Archaea of the recently proposed phylum *Thaumarchaeota* are globally distributed microorganisms accounting for up to 20 to 40 % of the picoplankton in the oceans and 1 to 5 % of the prokaryotes in soil (KARNER et al., 2001; OCHSENREITER et al., 2003; BROCHIER-ARMANET et al., 2008; LEHTOVIRTA et al., 2009; SCHATTENHOFER et al., 2009; STAHL and DE LA TORRE, 2012). Since the isolation of the first representative *Nitrosopumilus maritimus* (KÖNNEKE et al., 2005), *Thaumarchaeota* have been recognized as major ammonia-oxidizers in a wide range of habitats including the marine water column and sediment as well as soil, lakes, and geothermal systems (FRANCIS et al., 2005; LEININGER et al., 2006; AUGUET and CASAMAYOR, 2008; DE LA TORRE et al., 2008; PROSSER and NICOL, 2008; REIGSTAD et al., 2008; DODSWORTH et al., 2011; LEHTOVIRTA-MORLEY et al., 2011). The phylum *Thaumarchaeota* is commonly subdivided into several subgroups based on concatenated ribosomal protein sequence alignments as well as ammonia-monooxygenase subunit A and 16S rRNA gene phylogenies that broadly correlate with habitat types (e.g., BROCHIER-ARMANET et al., 2008; SPANG et al., 2010; PESTER et al., 2011; STAHL and DE LA TORRE, 2012). *N. maritimus* as well as most marine thaumarchaeal sequences, and to a lesser extent also soil and lacustrine sequences, are affiliated with Group I.1a (FRANCIS et al., 2005; KÖNNEKE et al., 2005; PESTER et al., 2012; STAHL and DE LA TORRE, 2012). The SAGMCG-1/*Nitrosotalea* cluster represents a sister group of the Group I.1a *Thaumarchaeota* comprising environmental sequences from soils and lakes as well as a single, acidophilic enrichment culture from soil, *Nitrosotalea devanaterra* (LEHTOVIRTA-MORLEY et al., 2011; STAHL and DE LA TORRE, 2012; AUGUET and CASAMAYOR, 2013). While Group I.1a *Thaumarchaeota* are also found in soils (e.g., PESTER et al., 2011), most sequences from soils and other terrestrial environments as well as the isolate *Nitrososphaera viennensis* (TOURNA et al., 2011; STIEGLMEIER et al., 2014b) are affiliated with Group I.1b (BINTRIM et al., 1997; DELONG, 1998; STAHL and DE LA TORRE, 2012). Additionally, Group I.1a and I.1b both contain moderate thermophiles such as *Candidatus* Nitrosotenuis uzonensis and *Nitrososphaera gargensis*, which have upper temperature limits for growth of 52 °C and 46 °C, respectively (HATZENPICHLER et al., 2008; LEBEDEVA et al., 2013). However, the only cultivated obligate thermophile is *Nitrosocaldus yellowstonii* (ThAOA/HWCG-III cluster), which was enriched from a Yellowstone hot spring and grows in the temperature range of 60 to 74 °C (DE LA TORRE et al., 2008). Furthermore, cultivation-independent surveys indicate that several additional lineages of *Thaumarchaeota* occur in the environment for which no cultivated representatives and limited observational data exist (SCHLEPER et al., 2005; NICOL and SCHLEPER, 2006; STAHL and DE LA TORRE, 2012).

Detection of *Thaumarchaeota* in the environment is commonly achieved by PCR-based marker gene surveys or metagenomic approaches and the analysis of characteristic glycerol dibiphytanyl glycerol tetraether (GDGT, Fig. 5.1) membrane lipids (DELONG et al., 1998; SCHOUTEN et al., 2000; SCHUBOTZ et al., 2009; PITCHER et al., 2011b; SCHOUTEN et al., 2012; WAKEHAM et al., 2012). While providing lower taxonomic resolution than metagenomic techniques, lipid analysis offers PCR-independent, qualitative and quantitative analysis of major clades of archaea and bacteria (STURT et al., 2004). Additionally, carbon isotopic analysis of lipids enables insights into predominant metabolisms and activity of microorganisms (HINRICHS et al., 1999; WUCHTER et al., 2003; SCHUBOTZ et al., 2011; KELLERMANN et al., 2012). Core GDGTs also accumulate and are preserved in sediments and are used in organic geochemistry and paleoceanography for reconstructing past sea surface temperatures using the TEX_{86} paleothermometer, which is based on temperature-dependent variations in GDGT side-chain cyclization (SCHOUTEN et al., 2002). Application of these lipid-based approaches to complex environmental samples relies on detailed knowledge of the phylogenetic distribution of characteristic marker lipids as well as functional and ecological constraints. However, only a limited set of lipids, consisting mainly of monoglycosidic, diglycosidic and glycophosphatidic GDGTs was reported from cultivated marine and terrestrial *Thaumarchaeota* (SCHOUTEN et al., 2008; PITCHER et al., 2011a; SINNINGHE DAMSTÉ et al., 2012). The relative abundances of these intact polar lipid (IPL) classes as well as their detailed core lipid compositions were so far not examined in *Thaumarchaeota*, partly due to methodological and instrumental limitations.

Hitherto, the membrane lipid composition of only one marine planktonic thaumarchaeon, *N. maritimus*, has been studied in detail by recently developed analytical methods that allow the simultaneous quantification of relative abundances of individual IPL classes as well as their core GDGT composition (BECKER et al., 2013; ZHU et al., 2013). For example, the *N. maritimus* lipidome analyzed using these methods revealed higher lipid diversity than previously reported for any thaumarchaeon, including major abundances of diether lipids as well as a novel potential biomarker for *Thaumarchaeota*, methoxy archaeol (ELLING et al., 2014, cf. Chapter 3). Application of these methods to established and recently cultivated thaumarchaeal cultures will enable the screening for novel lipid biomarkers. Furthermore, the characterization of lipids in cultivated *Thaumarchaeota* will facilitate the interpretation of IPLs abundantly detected in environmental studies and their assignment to source organisms.

Here, we applied coupled ultra-high performance liquid chromatography–mass spectrometry to unravel the lipidome of *Thaumarchaeota* cultivated from soils, hydrothermal springs and the surface ocean. The lipid inventories of six previously analyzed strains were significantly expanded and the lipid compositions of five novel

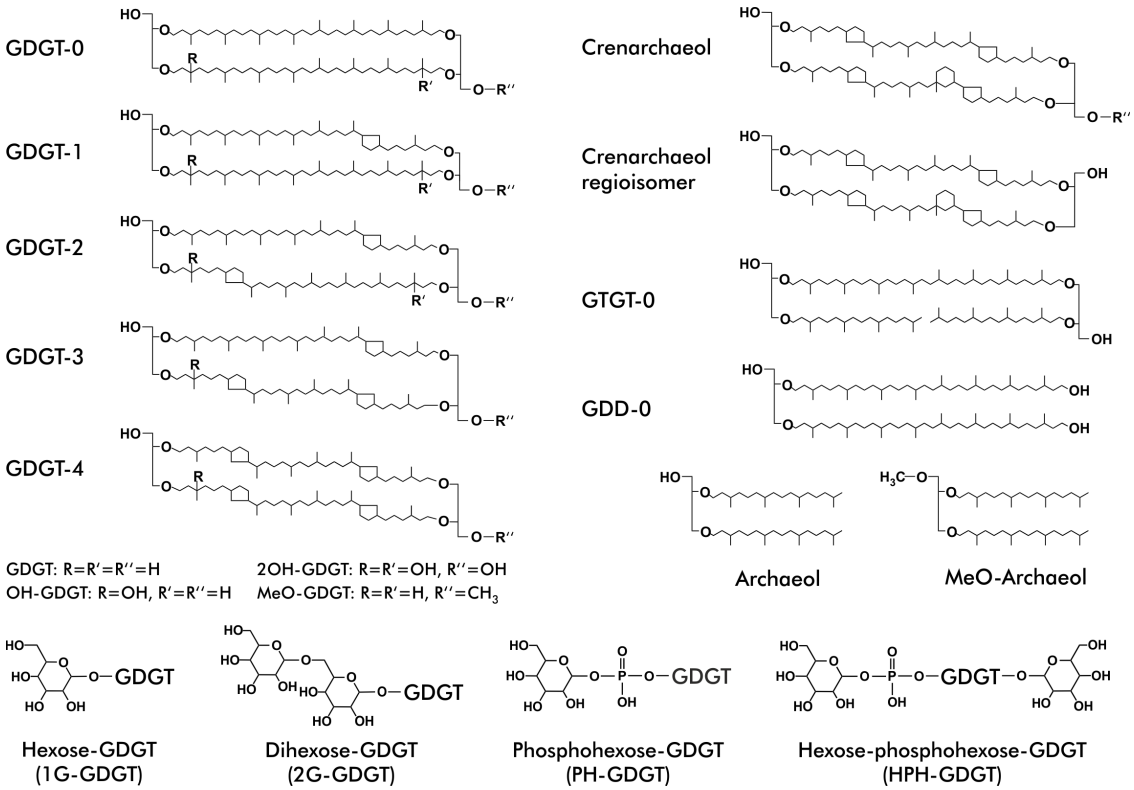

Figure 5.1. Structures of thaumarchaeal glycerol dibiphytanyl glycerol tetraether (GDGT) and glycerol diphytanyl diether (archaeol) core lipids. GDGTs may contain up to four cyclopentane rings or one cyclohexane and four cyclopentane rings (crenarchaeol). Derivatives of basic lipid structures comprise GDGTs containing one (OH-GDGT) or two (2OH-GDGT) additional hydroxyl groups and zero to four cyclopentane rings in the biphytanyl side chain, acyclic or monocyclic glycerol trialkyl glycerol tetraether (GTGT), zero to five ring bearing glycerol dialkanol diethers (GDDs) as well as GDGT and archaeol containing a methoxy group at the *sn*-1 position of the glycerol moiety (MeO-GDGT and MeO-AR). Thaumarchaeal intact polar lipids consist of one or two glycosidic or glycophosphatidic headgroups attached to the glycerol *sn*-1 hydroxyl position of a diether or tetraether core lipid.

strains cultivated from the surface ocean and hydrothermal springs were described for the first time. The data indicate distinct intact polar and core lipid compositions of Group I.1a, Group I.1b, and hyperthermophilic *Thaumarchaeota* of the HWCG-III cluster that appear to be related to phylogeny as well as habitat type.

5.2. Materials and Methods

5.2.1. Cultivation and lipid extraction

Nitrosopumilus maritimus strain SCM1, NAOA2, and NAOA6 were grown at 28 °C in 8.5 l of pH 7.5 HEPES-buffered Synthetic Crenarchaeota Medium (SCM) supplemented with 1.5 mM NH_4Cl as described previously (KÖNNEKE et al., 2005; MARTENS-HABBENA

et al., 2009; KÖNNEKE et al., 2012). *N. maritimus* was harvested in early stationary phase.

Nitrosopumilus strains D3C and N2F, isolated from surface waters of the northern Adriatic Sea (99 % 16S rRNA gene sequence identity to *N. maritimus*, B. Bayer, C. Schleper, G. Herndl et al., unpublished), were grown at 30 °C in pH 7.3 HEPES-buffered SCM supplemented with 1 mM NH_4Cl and harvested in the exponential phase.

Nitrososphaera gargensis strain Ga9.2 (HATZENPICHLER et al., 2008) was grown at 35 °C and 46 °C in 5 l of a pH 7.8 medium modified from KÖNNEKE et al. (2005) and KRÜMMEL and HARMS (1982) and harvested in stationary phase. The medium contained 5 g l^{-1} NaCl, 1.55 g l^{-1} $CaCl_2$ x 2 H_2O, 1 g l^{-1} KCl, 0.5 g l^{-1} $MgCl_2$ x 6 H_2O, 0.5 g l^{-1} $MgSO_4$ x 7 H_2O, 2 g l^{-1} KH_2PO_4, 2 mM $NaHCO_3$, 7.5 µM FeNaEDTA, 1 mM NH_4Cl and 1 ml l^{-1} of a trace element solution (WIDDEL and BAK, 1992). Cresol red was added at a concentration of 1 mg l^{-1} as a pH indicator (PITCHER et al., 2010). The pH was checked daily and adjusted to pH 7.8 using 1 M $NaHCO_3$. The NH_4Cl concentration was readjusted to 1 mM until a total of 3 to 4 mM of ammonium was consumed.

Nitrososphaera viennensis strains EN76 and EN123 were grown at 37 °C in 15-l batch cultures in pH 7.5 HEPES-buffered freshwater medium modified from TOURNA et al. (2011) by addition of 1.5 mM pyruvate and 3 mM NH_4Cl and slight stirring (150 rpm). *N. viennensis* biomass was harvested in the exponential phase.

Strain SCU2A, isolated from the Cava Scura, Ischia, Italy (95 % 16S rRNA gene sequence identity to *N. yellowstonii*, M. Stieglmeier, C. Schleper et al., unpublished), was grown at 70 °C in 120 ml of a pH 7 freshwater medium of a freshwater medium (TOURNA et al., 2011) containing 0.5 mM NH_4Cl, 2 mM $NaHCO_3$, 7.5 µm FeNaEDTA as well as 1 ml l^{-1} of a trace element and a vitamin solution. Strain SCU2A biomass was harvested in the exponential phase.

Nitrosotalea devanaterra was grown in batch culture at 25 °C and pH 5.4 in a synthetic medium modified from LEHTOVIRTA-MORLEY et al. (2011) by addition of 0.08 g l^{-1} of casamino acids and 1 µM phthalate buffer solution. *N. devanaterra* biomass was harvested in stationary phase.

Nitrosocaldus yellowstonii was grown in batch culture at 72 °C and pH ~7 in 3 l of a synthetic freshwater medium, modified from DE LA TORRE et al. (2008) by addition of 1 mM pH 7.5 MOPS buffer, with a headspace of 80 % N_2, 80 % CO_2, and 80 % O_2. *N. yellowstonii* biomass was harvested by centrifugation after 167 hours of growth, corresponding to stationary phase.

N. maritimus, NAOA2, NAOA6 and *N. gargensis* cultures were harvested using a Sartocon Slice cross-flow filtration system (Sartorius, Göttingen, Germany) and

centrifugation. *N. devanaterra*, *N. viennensis*, strain N2F, strain D3C, strain SCU2A and *N. yellowstonii* were harvested by centrifugation and subsequently lyophilized.

The cell pellets were stored at −20 °C until extraction. Lipids from each batch were extracted following a modified Bligh & Dyer protocol (STURT et al., 2004) using phosphate and trichloroacetic acid (CCl_3CO_2H) buffers (each 2x) and an ultrasonic probe (15 min sonication; HD2200, Bandelin electronic, Germany). The total lipid extract (TLE) was dried under a stream of N_2 and stored at −20 °C until measurement.

Cultivation and extraction of crenarchaeal and euryarchaeal species is described in Chapter 6.

5.2.2. Suspended particulate matter and sediment sampling

Suspended particulate matter samples were collected in the Costa Rica Dome perennial upwelling area of the equatorial North Pacific Ocean during the R/V *Seward Johnson* cruise in November 2007 (Station 8; 9°N, 90°W; XIE et al., 2014). Suspended particulate matter was recovered at 13 depths (3, 10, 25, 50, 125, 200, 350, 450, 550, 650, 750, 1000, 1250 m) by pumping 387 to 1417 liters of seawater through a 53 µm pore-size pre-filter and double pre-combusted 0.7 µm pore-size glass fiber filters using McLane Research in situ pumps (WTS-142) deployed on the conducting cable of the CTD rosette (XIE et al., 2014). Recovered filters were stored at −20 °C and extracted as described in (XIE et al., 2014). Due to the use of 0.7 µm pore-size filters, membrane lipid concentrations should be regarded as minimum estimates (cf. XIE et al., 2014). Water column profiles of temperature and dissolved oxygen were measured using a CTD rosette as described previously (XIE et al., 2014).

5.2.3. Intact polar and core lipid analysis

Intact polar and core lipids were quantified by injecting 10 to 20 % of the TLE dissolved in methanol on a Dionex Ultimate 3000 high performance liquid chromatography (HPLC) system connected to a Bruker maXis Ultra-High Resolution quadrupole time-of-flight tandem mass spectrometer (qToF-MS) equipped with an electrospray ionization (ESI) ion source operating in positive mode (Bruker Daltonik, Bremen, Germany). The mass spectrometer was set to a resolving power of 27,000 at m/z 1,222 and every analysis was mass-calibrated by loop injections of a calibration standard and correction by lock mass, leading to a mass accuracy of better than 1-3 ppm (ZHU et al., 2013). Ion source and other MS parameters were optimized by infusion of standards (GDGT-0, 1G-GDGT-0, 2G-GDGT-0) into the eluent flow from the HPLC system using a T-piece.

Analyte separation was achieved using reversed phase HPLC on an ACE3 C_{18} column (2.1 x 150 mm, 3 µm particle size, Advanced Chromatography Technologies, Aberdeen, Scotland) maintained at 45 °C as described previously (ZHU et al., 2013). In brief, analytes were eluted at a flow rate of 0.2 ml min^{-1} isocratically for 10 min with 100 % eluent A (methanol:formic acid:14.8 M NH_4^+, 100:0.04:0.10, v:v:v), followed by a linear gradient to 24 % eluent B (2-propanol:formic acid:14.8 M NH_4^+, 100:0.04:0.10, v:v:v) in 5 min, followed by a gradient to 65 % B in 55 min. The column was then flushed with 90 % B for 10 min and re-equilibrated with 100 % A for 10 min.

To determine abundances of core lipid structures relative to total lipids as well as ring index and TEX_{86} of total GDGTs, 10 % of the TLE was hydrolyzed with 1 M HCl in methanol for 3 h at 70 °C to yield core lipids (ELLING et al., 2014, cf. Chapter 3). The hydrolyzed TLE was then analyzed on the same system under different chromatographic conditions using normal phase HPLC and an APCI-II (atmospheric pressure chemical ionization) ion source operated in positive mode, as described previously (BECKER et al., 2013). Briefly, 1 to 5 % TLE aliquots were dissolved in *n*-hexane:2-propanol (99.5:0.5, v:v) and injected onto two coupled Acquity BEH Amide columns (2.1 x 150 mm, 1.7 µm particle size, Waters, Eschborn, Germany) maintained at 50 °C. Lipids were eluted using linear gradients of *n*-hexane (eluent A) to *n*-hexane:2-propanol (90:10, v:v; eluent B) at a flow rate of 0.5 ml min^{-1}. The initial gradient was 3 % B to 5 % B in 2 min, followed by increasing B to 10 % in 8 min, to 20 % in 10 min, to 50 % in 15 min and 100 % in 10 min, followed by 6 min at 100 % B to flush and 9 min at 3 % B to re-equilibrate the columns.

Lipids were identified by retention time as well as accurate molecular mass and isotope pattern match of proposed sum formulas in full scan mode and MS^2 fragment spectra. Integration of peaks was performed on extracted ion chromatograms of ±10 mDa width and included the $[M+H]^+$ ions for NP-HPLC-MS and additionally $[M+NH_4]^+$ and $[M+Na]^+$ ions for RP-HPLC-MS. Where applicable, double charged ions were included in the integration. The areas of 1G-, 2G-, and HPH-GDGT-4 were corrected for co-elution with the respective crenarchaeol regioisomer (Cren') by subtracting the area of the +2 Da isotope peak of Cren', which was calculated from natural isotope abundances (cf. Chapter 3, ZHANG et al., 2006; ELLING et al., 2014).

Lipid abundances were corrected for response factors of commercially available as well as purified standards as described in ELLING et al. (2014). The TEX_{86} index was calculated after SCHOUTEN et al. (2002) using the peak areas of GDGT-1, GDGT-2, GDGT-3 and Cren', with the digit indicating the number of cyclopentyl rings within the molecule:

$$TEX_{86} = \frac{[\text{GDGT-2}] + [\text{GDGT-3}] + [\text{Cren'}]}{[\text{GDGT-1}] + [\text{GDGT-2}] + [\text{GDGT-3}] + [\text{Cren'}]} \qquad \text{(Eq. 1)}$$

TEX_{86} reconstructed temperatures were calculated using the core-top calibration of KIM et al. (2010):

$$SST\ (°C) = 68.4 \times \log(TEX_{86}) + 38.6 \quad \text{(Eq. 2)}$$

To quantify GDGT cyclization we calculated the ring index (RI) according to PEARSON et al. (2004):

$$RI = \frac{[\text{GDGT-1}] + 2 \times [\text{GDGT-2}] + 3 \times [\text{GDGT-3}] + 4 \times [\text{GDGT-4}] + 5 \times [\text{Cren} + \text{Cren'}]}{[\text{GDGT-0}] + [\text{GDGT-1}] + [\text{GDGT-2}] + [\text{GDGT-3}] + [\text{GDGT-4}] + [\text{Cren} + \text{Cren'}]} \quad \text{(Eq. 3)}$$

5.3. Results

The lipidomes of the 11 analyzed thaumarchaeal strains contained a total of 100 individual lipids that represent either core lipids found in the TLE or intact polar lipids consisting of combinations of polar headgroups and core structures (Figs. 5.2 and 5.3). Forty compounds were common to all thaumarchaeal strains, while 10 lipids were unique to Group I.1b *Thaumarchaeota*, 21 compounds were found only in Group I.1a *Thaumarchaeota* and 4 compounds were unique to the HWCG-III (Fig. 5.2).

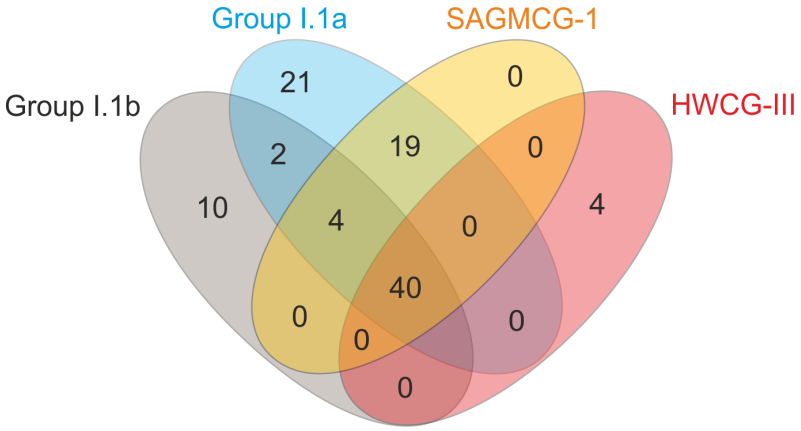

Figure 5.2. Distribution of 100 detected lipid types among the lipidomes of the four major phylogenetic subgroups of *Thaumarchaeota* with cultivated representatives (based on analyses of eleven thaumarchaeal cultures).

5.3.1. Core and apolar lipids

Analysis of the core lipid fractions derived from hydrolysis using normal phase HPLC-APCI-MS revealed distinct distributions of glycerol diphytanyl diethers (archaeols, AR), GDGTs and glycerol trialkyl tetraethers (GTGTs, Fig. 5.1; DE ROSA et al., 1983) among the investigated cultures. Major core lipid types found in all thaumarchaeal strains

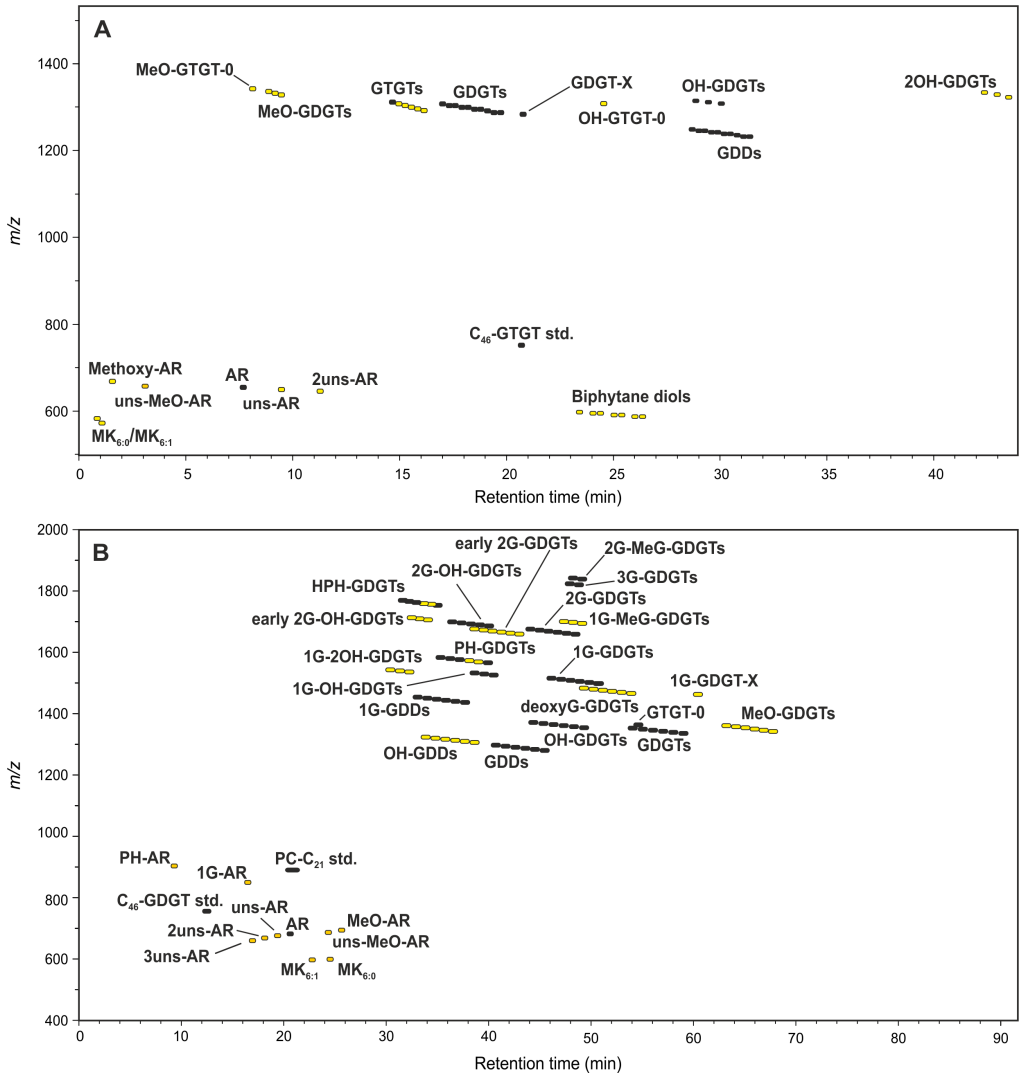

Figure 5.3. Reconstructed density maps showing elution time and mass-to-charge ratio (m/z) of membrane lipids identified in eleven thaumarchaeal cultures using normal phase HPLC-APCI-MS (a) and reversed phase HPLC-ESI-MS (b).

were GDGTs with zero to four cyclopentyl rings (GDGT-0 to GDGT-4), crenarchaeol as well as methoxy archaeol (MeO-AR). MeO-GDGTs were detected in all strains but were always trace components (<0.1 %). Acyclic GTGT (GTGT-0) as well as monounsaturated GTGT-0 (GTGT-0:1; ELLING et al., 2014, cf. Chapter 3) were detected in all thaumarchaeal strains. Differentiation between GTGTs bearing cyclizations and GDGTs containing double bonds was achieved by comparing retention behavior in normal phase HPLC-MS to retention during reversed phase HPLC-MS (cf. ZHU et al., 2014b).

Hydroxy (OH-) GTGT-0 and MeO-GTGT-0, monounsaturated methoxy archaeol (MeO-$AR_{0:1}$), as well as mono-, di-, and triunsaturated AR were detected in trace amounts in *N. maritimus* and *N. viennensis* EN76 but were not considered in relative abundance calculations due to their low concentrations («0.1 % of total lipids,

(Fig. 5.3). Similarly, low amounts of biphytane diols detected in these strains were not considered in relative abundance calculations.

The degree of GDGT cyclization as well as TEX_{86} calculated from total (hydrolysis-derived) GDGTs differed significantly between the cultures (Table 5.1). Group I.1b *Thaumarchaeota* showed the highest ring indices (4.3-4.8) and TEX_{86} values (0.97-0.99). The lowest ring index and TEX_{86} values were observed in strain NAOA6 (2.7) and *Nitrosocaldus yellowstonii*, respectively (0.61).

Table 5.1. Abundances of archaeol (AR) and methoxy archaeol (MeO-AR) in thaumarchaeal cultures relative to total lipids derived by acid hydrolysis as well as ring index (RI), TEX_{86} and TEX_{86}^{H}-temperature in total hydrolysis-derived GDGTs (measured using normal phase HPLC-APCI-MS).

	Growth temp. (°C)	Growth pH	AR (%)	MeO-AR (%)	RI	TEX_{86}	TEX_{86}^{H}-temp. (°C)
Nitrosotalea devanaterra	25	5.4	0.3	20.9	3.7	0.90	35.5
Nitrosopumilus maritimus	22	7.5	1.4	3.5	2.4	0.60	23.2
	25	7.5	2.3	3.9	2.7	0.70	28.0
	28	7.5	0.2	2.1	3	0.86	34.0
Strain NAOA2	18	7.5	3.3	13.2	2.9	0.80	32.0
	22	7.5	3.4	4.7	2.8	0.83	33.2
	28	7.5	1.5	2.3	2.8	0.86	34.4
	35	7.5	4.1	0.6	4.0	0.78	31.2
Strain NAOA6	18	7.5	2.4	5.5	2.2	0.54	20.3
	22	7.5	2.7	4.2	2.7	0.83	33.1
	28	7.5	0.4	4.5	3.1	0.89	35.3
Strain D3C	30	7.3	2.4	5.3	3	0.82	32.5
Strain N2F	30	7.3	4.2	11.5	3	0.78	31.2
Nitrososphaera viennensis EN76	37	7.5	1.5	1.9	4.3	0.99	38.2
Nitrososphaera viennensis EN123	37	7.5	0.3	1.6	4.3	0.99	38.4
Nitrososphaera gargensis	35	7.8	2.1	<0.01	4.4	0.92	36.1
	46	7.8	1.1	0.2	4.8	0.97	37.6
Strain SCU2A	70	7	4	<0.01	3.6	0.64	25.5
Nitrosocaldus yellowstonii	72	7	6.2	0.1	3.8	0.61	24.1

In all strains affiliated with Group I.1a, GDGT-0 to -4 and crenarchaeol contributed 80 to 90 % to the total lipids, while the crenarchaeol regioisomer was a minor compound (<3 %; Fig. 5.4). Among the Group I.1a *Thaumarchaeota*, AR and MeO-AR were especially abundant in strains N2F and D3C with up to 5 % and 11 %, respectively (Fig. 5.4,Table 5.1). Glycerol dialkanol diethers (GDDs, Fig. 5.1) occurred in relatively high abundances in strains NAOA2 and strain N2F with 9 and 7 %, respectively. In *N. devanaterra*, MeO-AR accounted for about 20 % of total lipids, while archaeol

was only present in trace amounts (0.3 %) and GDDs accounted for less than 4 % of the total lipids. In contrast to Group I.1a *Thaumarchaeota*, *N. devanaterra* contained high amounts of GDGT-4 (28 %). OH-GDGTs were detected in small amounts in *N. devanaterra* as well as all Group I.1a strains (Fig. 5.4).

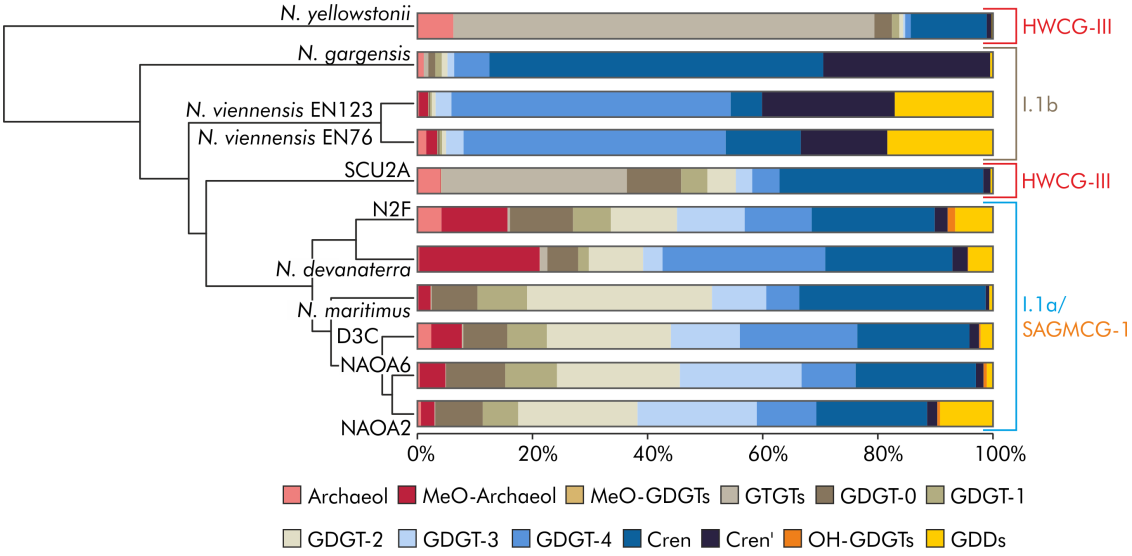

Figure 5.4. Cluster analysis of the relative abundances of major core lipid types in eleven thaumarchaeal strains from the four phylogenetic groups I.1a, I.1b, SAGMCG-1 and HWCG-III (calculated using the Euclidean distance metric from full lipid diversity including individual cyclized GTGTs, MeO-GDGTs and GDDs). Cren: crenarchaeol. Cren': crenarchaeol regioisomer.

Group I.1b *Thaumarchaeota* were characterized by low abundances of AR and MeO-AR (<2 %) as well as high abundances of the crenarchaeol regioisomer, which were in the range of 15 to 20 % in the two *N. viennensis* strains EN76 and EN123 and about 30 % in *N. gargensis* (Fig. 5.4). While highly abundant in both *N. viennensis* strains (22 to 23 %), GDGT-4 was only a minor lipid in *N. gargensis* (6 %). Crenarchaeol was the dominant lipid in *N. gargensis*, contributing 58 % to the total lipids (Fig. 5.4). *N. gargensis* additionally contained the GDGT-X core lipid (PITCHER et al., 2010) in trace amounts (not included in abundance calculations). OH-GDGTs were not detected in Group I.1b *Thaumarchaeota*.

Similar to *N. gargensis*, crenarchaeol was a major lipid in the HWCG-III *Thaumarchaeota N. yellowstonii* and strain SCU2A (Fig. 5.4). However, GTGTs with up to four rings (GTGT-0 to GTGT-4; Table 5.2) were the dominant lipids in *N. yellowstonii* (cf. DE LA TORRE et al., 2008) and equally abundant as crenarchaeol in strain SCU2A (Fig. 5.4). AR contributed 4 to 6 % to the total lipids in *N. yellowstonii* and strain SCU2A while MeO-AR was detected only in trace amounts (<0.1 %) in these strains (Table 5.1). OH-GDGTs were not detected in *N. yellowstonii* and strain SCU2A.

Table 5.2. Abundances of $MK_{6:0}$ and $MK_{6:1}$ relative to total menaquinones, abundances of GTGTs relative to total GTGTs, and abundances of GDGTs relative to total GDGTs in eleven cultivated thaumarchaeal strains as determined by normal phase HPLC-APCI-MS (n.d., not detected; *GTGT-0:1 occurred in trace amounts in these strains, but could not be quantified separately due to co-elution with GTGT-1 in normal phase HPLC). Cren: crenarchaeol. Cren': crenarchaeol regioisomer.

	MK		GTGT						GDGT						
	6:0	6:1	0	0:1	1	2	3	4	0	1	2	3	4	Cren	Cren'
Nitrosotalea devanaterra	72.4	27.6	86.2	13.8	n.d.	n.d.	n.d.	n.d.	7.4	2.5	12.9	4.6	38.7	30.2	3.6
Nitrosopumilus maritimus	91.0	9.0	19.7	7	n.d.	n.d.	n.d.	n.d.	8.2	8.9	33.2	9.7	5.9	33.4	0.7
Strain NAOA2	77	23	20.1	9.8	n.d.	n.d.	n.d.	n.d.	9.5	7	23.7	23.8	11.8	22	2.1
Strain NAOA6	85.7	14.3	4.2	<0.1	n.d.	n.d.	n.d.	n.d.	11	9.6	22.9	22.6	10.1	22.4	1.4
Strain D3C	88.6	11.4	5.5	2.2	n.d.	n.d.	n.d.	n.d.	8.5	7.7	24	13.4	22.8	21.7	1.9
Strain N2F	92.5	7.5	1.4	0.2	n.d.	n.d.	n.d.	n.d.	14.4	8.6	15.1	15.5	15.3	28.1	3
Nitrososphaera viennensis EN76	76.1	23.9	3.8	n.d.*	5.1	n.d.	n.d.	n.d.	0.5	0.5	0.9	3.9	58.3	16.7	19.2
Nitrososphaera viennensis EN123	85.4	14.6	0.2	<0.1	n.d.	n.d.	n.d.	n.d.	0.4	0.3	0.8	3.4	59.9	6.7	28.5
Nitrososphaera gargensis	85.8	14.2	31.3	n.d.*	7	2.1	1.1	2.3	1.2	1.2	1	1.2	6.3	59.4	29.7
SCU2A	92.1	7.9	65.2	n.d.*	5.5	1.8	1	0.3	14.9	7.2	7.8	4.5	7.5	56	2
Nitrosocaldus yellowstonii	96.5	3.5	84.8	n.d.*	6.5	0.6	0.2	0.1	15	6.1	3.5	1.6	4.8	64.6	4.3

5.3.2. Intact polar lipids and respiratory quinones

Analysis of the intact polar lipids using reversed phase HPLC-MS revealed a high diversity of IPLs among the investigated thaumarchaeal strains (Fig. 5.3). The major IPLs in all strains were GDGTs with monoglycosyl (1G), diglycosidic (2G), phosphoxehose (PH) and hexose-phosphoxose (HPH) headgroups. However, small amounts of intact polar archaeols with 1G and PH headgroups were detected in all thaumarchaeal strains, while no intact polar GTGTs were observed. 2G-GDGTs and 2G-OH-GDGTs each consisted of two series of isomers that were separated by 3-5 min in reversed phase HPLC and yielded similar MS^2 fragmentation spectra (Fig.3; ELLING et al., 2014, cf. Chapters 3 and 4). These isomers may represent constitutional isomers, e.g., having one glycosidic headgroup connected to each glycerol moiety versus a diglycosidic moiety linked to only one of the glycerols. In addition, minor amounts of OH-GDDs were detected in the total lipid extracts of all investigated Group I.1a *Thaumarchaeota* as well as *N. devanaterra*, which were below detection in the hydrolyzed lipid extracts analyzed using normal phase HPLC-APCI-MS. Two isoprenoid naphthoquinones were detected in all thaumarchaeal strains and were identified as menaquinones with fully unsaturated ($MK_{6:0}$) and monounsaturated ($MK_{6:1}$) side chains composed of six isoprenoid units (C_{30}; cf. Chapter 6). While the relative abundances of these quinones varied between different strains, $MK_{6:0}$ was always more abundant than $MK_{6:1}$ in all thaumarchaeal strains (Table 5.2).

Group I.1a *Thaumarchaeota* contained predominantly 1G-, 1G-OH-, 2G- and 2G-OH-GDGTs in varying amounts (Fig. 5.5). Strain NAOA2 was characterized by relatively low amounts of 1G-GDGTs and high abundances of 2G-, 2G-OH, and HPH-GDGTs. In contrast, the IPL pool of *N. maritimus* consisted mostly of 1G-GDGTs (47 %) and 2G-OH-GDGTs (33 %), but only low amounts of 2G- and HPH-GDGTs and other IPLs. Intact polar GTGTs reported by SCHOUTEN et al. (2008) were not detected in *N. maritimus*. The IPL composition of NAOA6 was similar to *N. maritimus*, but was characterized by higher relative abundances of early eluting 2G- and 2G-OH-GDGTs and lower abundances of 1G-OH-GDGTs (Fig. 5.5). Strain N2F exhibited the highest relative abundances of 2G-OH-GDGTs (44 %) among all thaumarchaeal strains as well as and comparatively low amounts of 1G-GDGTs (24 %). In addition, this strain contained trace amounts of monoglycosidic dihydroxylated GDGTs (1G-2OH-GDGTs). Strain D3C showed high relative abundances of 2G-GDGTs (46 %) and equal abundances of 1G-GDGTs and 2G-OH-GDGTs (∼25 % each).

N. devanaterra contained predominantly 1G-GDGTs (50 %) as well as 2G-GDGTs and early eluting 2G-GDGTs (30 %; Fig. 5.5). Only minor amounts of 2G-OH-GDGTs and HPH-GDGTs as well as 1G-GDDs and intact polar archaeols were detected.

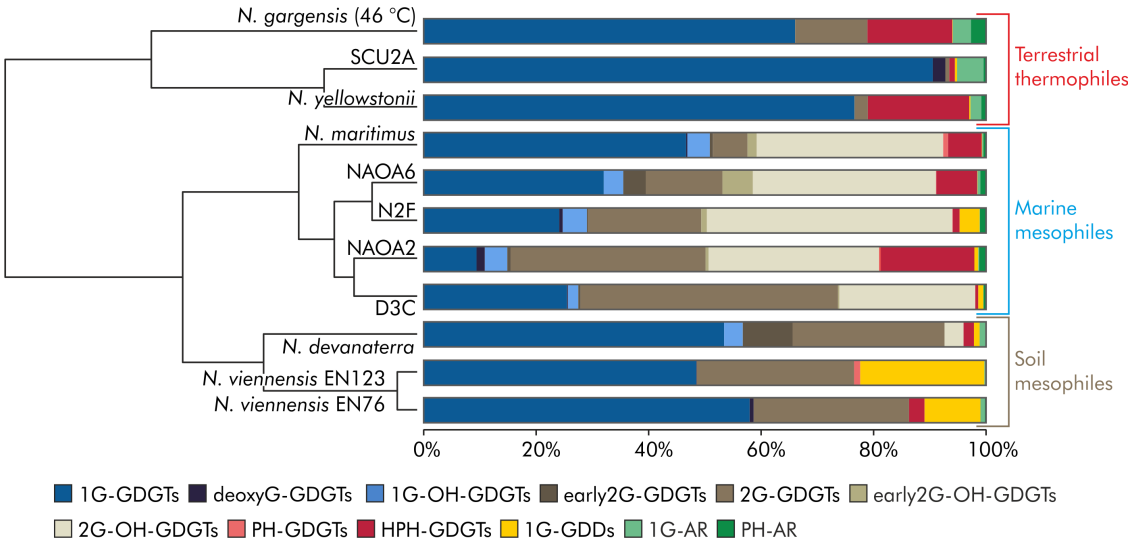

Figure 5.5. Cluster analysis of the relative abundances of intact polar lipid types in eleven thaumarchaeal strains (calculated using the Euclidean distance metric from full lipid diversity including individual cyclized intact polar GDGTs). Cultures from similar habitats show close relatedness in their intact polar lipid compositions.

Both *N. viennensis* EN76 and EN123 contained high abundances of 1G-GDGTs (~50 to 60 %) as well as 2G-GDGTs (~20 %; Fig. 5.5). The relative abundances of HPH-GDGTs were low in strain EN76 while these IPLs were completely absent in strain EN123. However, strain EN123 contained low amounts of PH-GDGTs, which were not detected in strain EN76. In contrast to all other thaumarchaeal strains, both *N. viennensis* strains contained relatively high abundances of 1G-GDDs (Fig. 5.5). *N. gargensis* contained over 60 % 1G-GDGTs, approximately 10 % each of 2G- and HPH-GDGTs as well as the highest amounts of intact polar archaeols among all thaumarchaeal strains (6 %). All Group I.1b *Thaumarchaeota* contained trace amounts of triglycosidic (3G-) GDGTs. In addition, *N. gargensis* contained trace amounts of 1G- and 2G-GDGTs bearing additional methylated sugars (1G-MeG- and 2G-MeG-GDGTs). No IPLs with OH-GDGT core structures were observed in Group I.1b *Thaumarchaeota*.

N. yellowstonii and strain SCU2A contained the highest relative abundances of 1G-GDGTs among the investigated thaumarchaeal strains with 77 % and 91 %, respectively (Fig. 5.5). Strain SCU2A contained only minor amounts of 2G-, PH, and HPH-GDGTs. Similarly, *N. yellowstonii* contained only low amounts of 2G-GDGTs but relatively high abundances of HPH-GDGTs (18 %). Furthermore, these strains contained higher relative abundances of intact polar archaeols than most other thaumarchaeal strains (up to 5 %; Fig. 5.5). Both, *N. yellowstonii* and strain SCU2A did not contain IPLs with OH-GDGT core structures.

The different intact polar GDGT classes as well as total GDGTs exhibited distinct distributions of GDGT core structural types (Fig. 5.6). Furthermore, these patterns

differed between the thaumarchaeal strains. In *N. viennensis*, the main core lipid of 1G-, 2G-, and total GDGTs were GDGT-4, while the other GDGT core structures were of minor abundance (Fig. 5.6). However, the major core lipid of HPH-GDGTs was crenarchaeol.

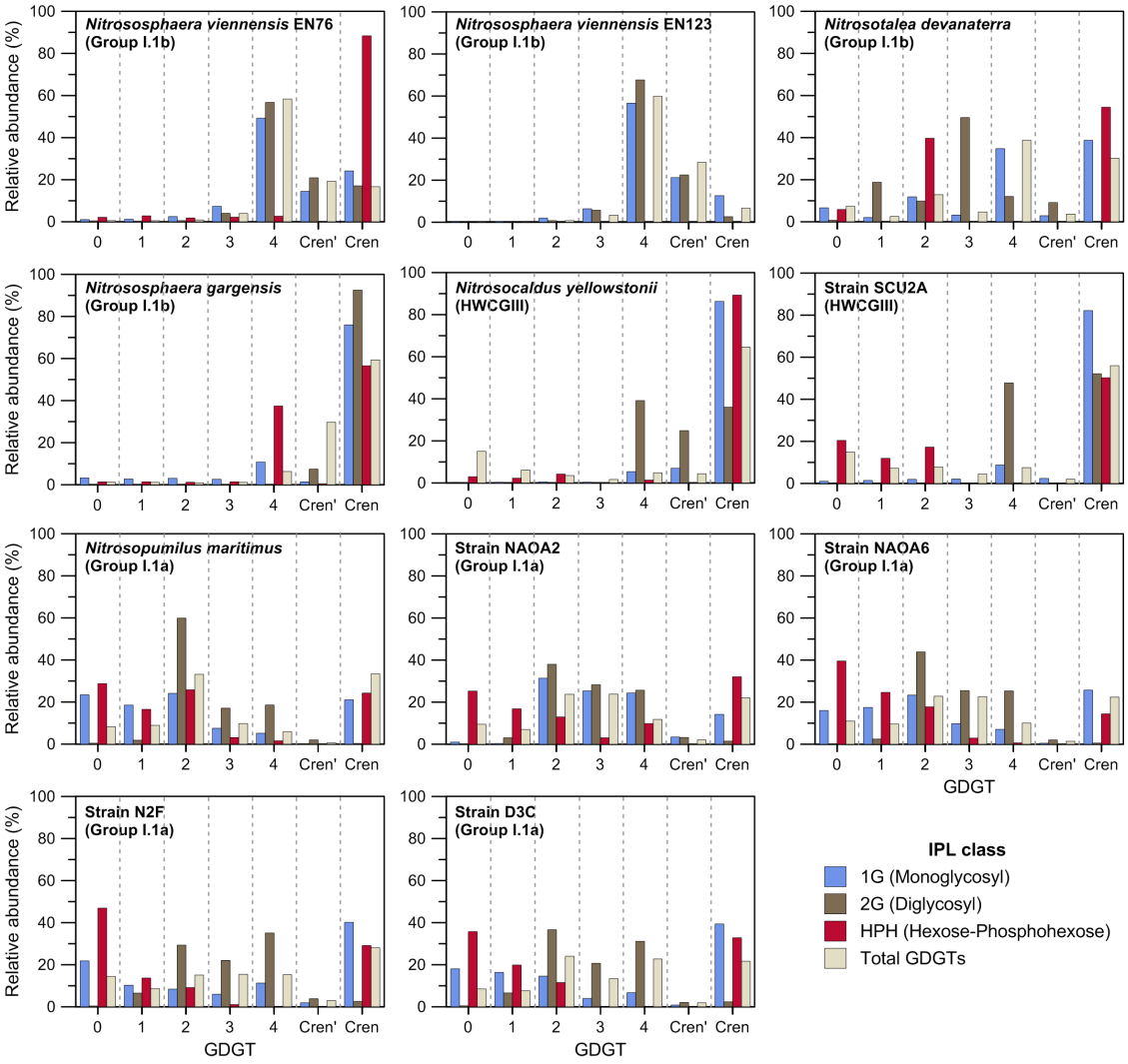

Figure 5.6. Distribution of GDGT structural types in the major thaumarchaeal intact polar lipid classes 1G-GDGT, 2G-GDGT, and HPH-GDGT as well as total GDGTs derived from hydrolysis in eleven cultivated thaumarchaeal strains. Cren: crenarchaeol. Cren': crenarchaeol regioisomer.

In *N. gargensis*, crenarchaeol was the main core lipid of total, 1G-, 2G- and HPH-GDGTs, while the latter also contained GDGT-4 as a major core structure (Fig. 5.6). Similarly, crenarchaeol was the major lipid of 1G-, HPH-, and total GDGTs in *N. yellowstonii* and strain SCU2A (Fig. 5.6). In contrast, 2G-GDGTs were affiliated to nearly equal amounts with GDGT-4, crenarchaeol and the crenarchaeol regioisomer in *N. yellowstonii* and to equal amounts with GDGT-3 and crenarchaeol in strain SCU2A. GDGT core structural types were overall more similarly distributed among the Group I.1a

Thaumarchaeota (Fig. 5.6). 2G-GDGTs were mostly affiliated with GDGT-2, GDGT-3, and GDGT-4 in all strains. While most strains showed about equal abundances of these GDGT core structures, GDGT-2 was more dominant within 2G-GDGTs in *N. maritimus* and strain NAOA6. 1G-GDGTs were affiliated mostly with GDGT-0 to GDGT-2 and crenarchaeol in *N. maritimus* and strains NAOA6, while crenarchaeol was more abundant in strains N2F and D3C. In contrast, 1G-GDGTs consisted mostly of GDGT-2 to GDGT-4 in strain NAOA2, similar to 2G-GDGTs. In all Group I.1a strains, HPH-GDGTs comprised mostly GDGT-0 and crenarchaeol core structures, but the relative abundances differed for each strain (Fig. 5.6).

5.3.3. *Distribution of thaumarchaeal biomarkers in the equatorial North Pacific Ocean*

Methoxy archaeol was detected throughout the oxic water column and the oxygen minimum zone (OMZ, approximately 50-800 m water depth) of the equatorial North Pacific Ocean between 3 and 1250 m water depth (Fig. 5.7). MeO-AR concentrations peaked in the suboxic zone in the uppermost part of the OMZ between 50 and 125 m, which coincided with a maximum in intact polar GDGTs (IP-GDGTs, derived from hydrolysis; data from XIE et al. 2014), and decreased throughout the OMZ and the deeper water column. Archaeol concentrations showed a maximum within the anoxic core of the OMZ. The ratio of MeO-AR and AR showed two maxima at the upper and lower boundaries, respectively and a minimum within the anoxic core of the OMZ (Fig. 5.7).

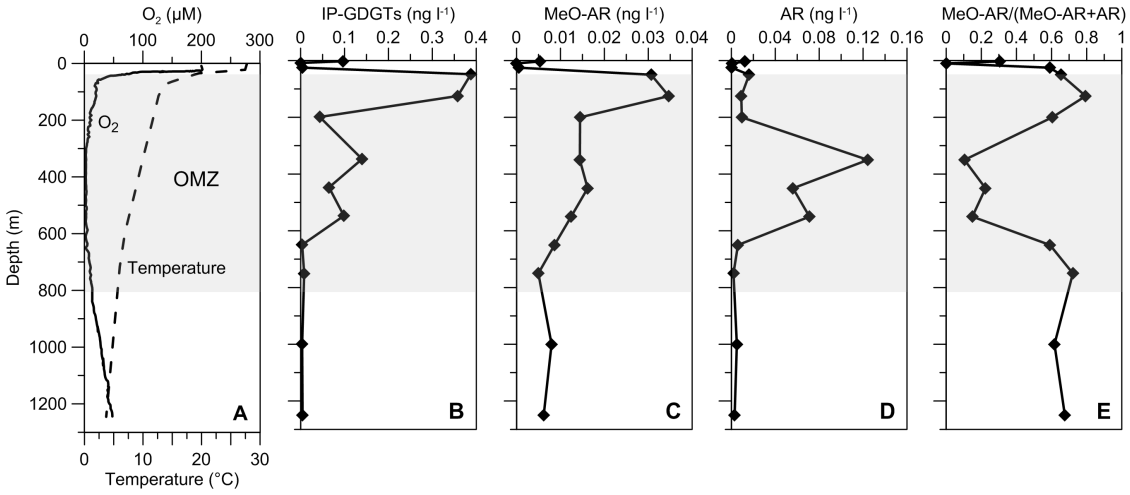

Figure 5.7. Depth profiles through the water column of the oxygen minimum zone (OMZ) in the equatorial North Pacific Ocean of (a) dissolved oxygen (O_2) and temperature, (b) intact polar GDGTs (IP-GDGTs, derived from hydrolysis, data from XIE et al. 2014), methoxy archaeol (MeO-AR), archaeol (AR), and the ratio of MeO-AR and to the sum of AR and MeO-AR.

5.4. Discussion

5.4.1. Common patterns in the lipidomes of cultivated Thaumarchaeota

Membrane lipids common to all thaumarchaeal strains investigated here comprise, among others, acyclic and cyclized GDGTs, GDDs and archaeols bearing 1G, 2G, HPH, and PH headgroups. (Figs. 5.3 to 5.5) Hierarchical cluster analysis was performed on lipid abundances of all 100 identified compounds to investigate the relationships between the lipidomes of the eleven thaumarchaeal strains (Figs. 5.4 and 5.5).

The cluster analysis indicates that the distribution of core lipid types among *Thaumarchaeota* is in part determined by phylogeny (Fig. 5.4). The core lipid compositions of all Group I.1a *Thaumarchaeota* are closely related to each other and distinct from the other thaumarchaeal lineages by the relatively similar distributions of GDGT-0 to GDGT-4 and crenarchaeol, low crenarchaeol regioisomer contents and the occurrence of OH-GDGTs. Similarly, MeO-AR contents are higher in Group I.1a than in most other *Thaumarchaeota*. The low abundance of OH-GDGT core lipids in contrast to high abundances of IPLs with OH-GDGT core structures is likely related to the loss of the hydroxyl group during acid hydrolysis (cf. LIU et al., 2012b; SINNINGHE DAMSTÉ et al., 2012). The core lipid composition of the soil thaumarchaeon *N. devanaterra* is very similar to that of Group I.1a strains and thus reflects the phylogenetic position of this thaumarchaeon in a sister clade of Group I.1a, SAGMCG-1. However, *N. devanaterra* is distinct from I.1a *Thaumarchaeota* by exhibiting higher abundances of GDGT-4 and MeO-AR. In contrast to Group I.1a, Group I.1b *Thaumarchaeota* do not exhibit a coherent lipidome. The two investigated Group I.1b *Thaumarchaeota* from soil, *N. viennensis* EN76 and EN123 are characterized by high abundances of GDGT-4 and the crenarchaeol regioisomer as well as GDDs. In contrast, the lipidome of the moderately thermophilic Group I.1b thaumarchaeon *N. gargensis* is almost exclusively composed of crenarchaeol and its regioisomer. The thermophilic *Thaumarchaeota* of the HWCG-III cluster are distinct from all other thaumarchaeal clades in containing GTGTs as their dominant core lipids as well as relatively high amounts of crenarchaeol compared to the other GDGTs.

In contrast to the core lipids, cluster analysis of the IPLs indicates that the IPL composition is related to habitat type rather than phylogeny (Fig. 5.5). According to their IPL composition, the thaumarchaeal strains can be divided into three major groups: terrestrial thermophiles, marine mesophiles, and soil mesophiles. The terrestrial thermophiles are characterized by very high abundances of 1G-GDGTs and HPH-GDGTs as well as intact polar archaeols. All marine mesophiles share high abundances of 2G-GDGTs and 2G-OH-GDGTs compared to the other archaea, while HPH-GDGTs are abundant only in some strains. The soil *Thaumarchaeota* (*N. viennensis* EN76 and

EN123, *N. devanaterra*) are characterized by high relative abundances of 1G-GDGTs and 2G-GDGTs as well as 1G-GDDs in *N. viennensis*. While these groupings are in part related to phylogeny (e.g., all investigated marine mesophiles are Group I.1a *Thaumarchaeota*), the distinct clustering indicates that IPL composition in *Thaumarchaeota* is reflective of environmental parameters and adaptation patterns, similar to the observation of ecological patterns in the polar lipid compositions of bacteria (cf. BAY et al., 2015).

5.4.2. Implications for the use of thaumarchaeal GDGTs as biomarkers

Comparison of the lipidomes of the eleven thaumarchaeal strains investigated here indicates that the core and intact polar lipid compositions of *Thaumarchaeota* reflect both phylogenetic affiliation and habitat and may thus be used to differentiate the major thaumarchaeal clades in environmental samples.

In all thaumarchaeal strains investigated here, 1G-GDGTs are the most abundant IPLs. Similarly, 1G-GDGTs and in particular 1G-crenarchaeol are often the most abundant archaeal lipids detected in the marine water column (SCHUBOTZ et al., 2009; SCHOUTEN et al., 2012). However, 1G-GDGTs are often assumed to be more refractory than 2G- and HPH-GDGTs after cell lysis, and are therefore often considered unsuitable for tracing living biomass (e.g. SCHOUTEN et al., 2012). HPH-GDGTs are often not abundant and therefore not detected in the marine water column (e.g., BASSE et al., 2014; XIE et al., 2014). Furthermore, relatively high abundances of HPH-GDGTs during growth of *N. maritimus* compared to stationary phase suggest that HPH-GDGTs might be indicators of metabolically active *Thaumarchaeota* (ELLING et al., 2014, cf. Chapter 3). Our study of five marine planktonic thaumarchaeal strains indicates that HPH-GDGT abundances are highly variable in Group I.1a *Thaumarchaeota* (Fig. 5.5), which represent the dominant thaumarchaeal clade in the ocean. Therefore, changes in HPH-GDGT abundances in the marine water column might not only be related to thaumarchaeal abundances and metabolic activity but may also reflect changes in thaumarchaeal community composition. Thus, 2G-GDGTs and 2G-OH-GDGTs seem to be more suitable for tracing thaumarchaeal biomass due to their high relative abundances in all strains. OH-GDGTs appear to be exclusively synthesized by Group I.1a (Figs. 5.4 and 5.5), consistent with previous investigations in soil and sedimentary thaumarchaeal cultures (PITCHER et al., 2011a; SINNINGHE DAMSTÉ et al., 2012), and might thus be well suited for tracing this thaumarchaeal clade in the environment. However, OH-GDGTs have also been detected in the thermophilic methanogenic euryarchaeon Methanothermococcus thermolithotrophicus (LIU et al., 2012b)and thus might be synthesized also by other thermophilic and mesophilic archaea.

Thaumarchaeal communities in soil are commonly dominated by Group I.1b *Thaumarchaeota* related to *N. viennensis* (e.g., PESTER et al., 2012), but *Thaumarchaeota* related to *N. devanaterra* (SAGMCG-1 cluster) may form a major part of the microbial community especially in acidic soils (e.g., GUBRY-RANGIN et al., 2011). These clades may be distinguishable in environmental samples by their distinct lipid compositions. While both groups synthesize predominantly 1G-GDGTs with GDGT-4 and crenarchaeol as core lipids, *N. devanaterra* synthesizes 2G-GDGTs predominantly with GDGT-3 as the core lipid in contrast to GDGT-4 in *N. viennensis* (Figs. 5.4 and 5.6). Furthermore, *N. viennensis* contains high abundances of the crenarchaeol regioisomer connected to 1G- and 2G- headgroups as well as 1G-GDDs, while *N. devanaterra* is distinct by having high abundances of MeO-AR (Figs. 5.4 to 5.6). Additionally, 3G-GDGTs appear to be synthesized exclusively by Group I.1b *Thaumarchaeota*. However, the abundance of these compounds is very low in *N. viennensis*, limiting their potential as biomarkers in environmental samples.

Thermophilic *Thaumarchaeota* associated with the HWCG-III cluster and Group I.1b have overall similar IPL profiles but might be distinguished by the high abundance of the crenarchaeol regioisomer in Group I.1b *Thaumarchaeota* as well as high abundances of GTGTs in HWCG-III *Thaumarchaeota*. While GTGTs have previously been detected in the thermophilic crenarchaeon Sulfolobus solfataricus, their biological function remains unconstrained. The high abundances of GTGTs in HWCG-III *Thaumarchaeota* are unprecedented among cultivated archaea and suggest an involvement in the adaptation of the membrane to high temperatures. Furthermore, *N. gargensis* synthesizes trace amounts of intact polar GDGTs containing methylated sugar headgroups, which were not detected in other thaumarchaeal strains.

GDD core lipids have been suggested to represent either intermediates of GDGT biosynthesis (LIU et al., 2012b; VILLANUEVA et al., 2014b) or degradation products of GDGTs resulting from the loss of one glycerol moiety (KNAPPY and KEELY, 2012; LIU et al., 2012a; YANG et al., 2014). They have so far only been reported from soils and marine sediments as well as *N. maritimus* (cf. Chapter 3, ELLING et al., 2014; MEADOR et al., 2014b) and *Methanothermococcus thermolithotrophicus* (LIU et al., 2012a). The detection of monoglycosidic GDDs in *N. maritimus* suggests that these compounds may indeed be membrane components of *Thaumarchaeota* (MEADOR et al., 2014b). The high abundances of core and 1G-GDDs observed in *N. viennensis* underline a potential role of these compounds as membrane lipids and their use as biomarkers for Group I.1b *Thaumarchaeota*. Core GDDs abundantly detected in marine sediments (KNAPPY and KEELY, 2012; LIU et al., 2012a,c) and soils (YANG et al., 2014; COFFINET et al., 2015) may thus be sourced directly by *Thaumarchaeota* in addition to possible degradation of GDGTs.

Fossil core GDGTs of marine and lacustrine planktonic *Thaumarchaeota* preserved in sediments form the basis of the TEX_{86} paleothermometer, which is based on the empirical correlation between sea surface temperature and the specific ratio indexed in TEX_{86}, i.e., the relative abundances of GDGT-2 and GDGT-3 versus GDGT-1 to GDGT-3 and the crenarchaeol regioisomer found in core-top sediments (Eq. Eq. 1; SCHOUTEN et al., 2002). While the TEX_{86} values of total GDGTs in *N. maritimus* and NAOA2 increase with increasing temperature (Chapter 4, Table 5.1), there is no universal correlation between growth temperature and TEX_{86} across the thaumarchaeal strains studied here. This indicates that the relationship between TEX_{86} and temperature is likely species-specific and that the environmental TEX_{86} signal may thus represent a community-averaged response to temperature. Moreover, specific intact polar GDGT classes are preferentially associated with specific core GDGTs in the marine mesophilic thaumarchaea studied here (Fig. 5.6; ELLING et al., 2014, cf. Chapter 3). Therefore, differences in degradation rates of intact polar GDGTs as well as community composition may influence the TEX_{86} index as the intact polar lipid precursors differ for individual core GDGTs, which may result in distinct release rates of core GDGTs from their polar precursors.

5.4.3. Patterns in thaumarchaeal membrane lipid adaptation

Thaumarchaeota contain relatively high abundances of GDGTs compared to other mesophilic archaea (cf. SCHOUTEN et al., 2013). In fact, all other archaea that contain cyclized GDGTs as the dominant membrane lipids are (hyper)thermophiles (cf. OGER and CARIO, 2013). Moreover, the ring indices of total GDGTs in mesophilic *Thaumarchaeota* such as *N. maritimus* and strain D3C are as high or higher as ring indices of (hyper)thermophiles (e.g., DE ROSA et al., 1980; UDA et al., 2001; UDA et al., 2004; SHIMADA et al., 2008). This lends further support to the hypothesis that mesophilic *Thaumarchaeota* originate from thermophilic ancestors that have adapted to low temperature habitats (cf. DELONG et al., 1998; SCHOUTEN et al., 2000; FORTERRE et al., 2002; SPANG et al., 2010). Thermophilic *Cren-* and *Euryarchaeota* adapt to high temperatures by increasing the cyclization of their GDGT membrane lipids, which increases GDGT packing density and reduces proton permeability (KOGA, 2012; OGER and CARIO, 2013). Similarly, ring indices in thaumarchaeal strains increase with increasing growth temperature (Chapter 4, Table 5.1). However, the ring indices and relative abundances of crenarchaeol are not highest in the thaumarchaeal strains grown and isolated from the highest temperatures, *N. yellowstonii* (72 %) and strain SCU2A (70 %), but in *N. viennensis* and *N. gargensis*, which have optimal growth temperatures of 37 and 46 %, respectively. This indicates, along with the distinct ring

indices of the investigated thaumarchaeal strains (Table 5.1), that membrane lipid adaptation to high temperatures is specific for distinct thaumarchaeal clades. Adaptation to high temperatures in *Thaumarchaeota* may thus involve additional mechanisms such as high abundances of 1G-GDGTs, which promote low proton permeability (e.g., MORII and KOGA, 1994; GABRIEL and CHONG, 2000; SHIMADA et al., 2008), and high abundances of GTGTs.

The mechanisms how mesophilic thaumarchaea adapt their thermophile-like lipid membranes to the low temperatures encountered in the marine environment and soil remain poorly studied. However, the abundance of MeO-AR in *Thaumarchaeota* appears to be temperature-dependent. MeO-AR is only a trace compound in thermophilic *Thaumarchaeota*, while it is most abundant in the strain grown at the coldest temperature, *N. devanaterra*. In addition, *N. gargensis* produces relatively more MeO-AR when grown at 35 °C than at 46 °C and similarly MeO-AR content increases with decreasing growth temperature in strain NAOA2 (Chapter 4), indicating that synthesis of MeO-AR might be a mechanism of adaptation to cold temperatures. Incorporation of MeO-AR into the membrane might lead to increased membrane fluidity at low temperatures in a similar way as squalene may increase membrane fluidity in halophilic archaea by spacing polar lipids further apart (cf. Chapter 4; LANYI et al., 1974; LANYI, 1974).

5.4.4. Lipid biomarkers specific for Thaumarchaeota

Comparison of the thaumarchaeal lipidome with analyses of 21 crenarchaeal and euryarchaeal species revealed that *Thaumarchaeota* harbor distinct biomarkers as well as lipids common to all archaea. All investigated *Thaumarchaeota* contained at least minor amounts of archaeol (Fig. 5.4), in contrast to prior studies on thaumarchaeal lipid composition (PITCHER et al., 2011a; SINNINGHE DAMSTÉ et al., 2012) that did not report the occurrence of archaeol in cultivated *Thaumarchaeota*. Similarly, VILLANUEVA et al. (2014b) suggested that most of the crenarchaeal and euryarchaeal species investigated here do not produce archaeol, which is not consistent with our observations as well as literature data (e.g., SHIMADA et al., 2002; KOGA and MORII, 2005; TARUI et al., 2007). Indeed, the occurrence of archaeol in all investigated strains (Table 5.3) suggests that it is a universal lipid in Archaea.

Table 5.3. Phylogenetic distribution of archaeol (AR), hydroxyarchaeol (OH-AR), methoxy archaeol (MeO-AR) and crenarchaeol (Cren) biosynthesis among cultivated representatives of the *Archaea*

Phylum	Order/Group	Genus/Species	Habitat	AR	OH-AR	MeO-AR	Cren	$MK_{6:0}$	$MK_{6:1}$
Thaumarchaeota	Group I.1a	*Nitrosopumilus maritimus*	Marine water	+	-	+	+	+	+
		Strain NAOA2	Marine water	+	-	+	+	+	+
		Strain NAOA6	Marine water	+	-	+	+	+	+
		Strain D3C	Marine water	+	-	+	+	+	+
		Strain N2F	Marine water	+	-	+	+	+	+
	Group I.1b	*Nitrososphaera viennensis* EN76	Soil	+	-	+	+	+	+
		Nitrososphaera viennensis EN123	Soil	+	-	+	+	+	+
		Nitrososphaera gargensis	Terrestrial hydrothermal	+	-	+	+	+	+
	HWCG-III/*Nitrosocaldus* cluster	*Nitrosocaldus yellowstonii*	Terrestrial hydrothermal	+	-	+	+	+	+
		SCU2A	Terrestrial hydrothermal	+	-	+	+	+	+
	SAGMCG-1/*Nitrosotalea* cluster	*Nitrosotalea devanaterra*	Acidic soil	+	-	+	+	+	+
Crenarchaeota	*Desulfurococcales*	*Ignicoccus hospitalis*	Marine hydrothermal	+	-	-	-	+	+
		Staphylothermus marinus	Marine hydrothermal	+	-	-	-	-	-
		Aeropyrum pernix	Marine hydrothermal	+	-	-	-	+	+
		Pyrolobus fumarii	Marine hydrothermal	+	-	-	-	+	-
	Sulfolobales	*Metallosphaera prunae*	Heated mine tailings	+	-	-	-	-	-
		Sulfolobus acidocaldarius	Terrestrial hydrothermal	+	(+)*	-	-	-	-
		Sulfolobus solfataricus	Terrestrial hydrothermal	+	-	-	-	-	-
		Sulfolobus islandicus	Terrestrial hydrothermal	+	-	-	-	-	-
Euryarchaeota	*Thermococcales*	*Pyrococcus furiosus*	Marine hydrothermal	+	-	-	-	-	-
		Thermococcus kodakarensis	Terrestrial hydrothermal	+	-	-	-	-	-
	Methanopyrales	*Methanopyrus kandleri*	Marine hydrothermal	+	-	-	-	-	-
	Methanobacteriales	*Methanothermobacter thermautotrophicus*	Terrestrial hydrothermal	+	-	-	-	-	-
	Methanococcales	*Methanothermococcus thermolithotrophicus*	Marine hydrothermal	+	+	-	-	-	-
	Thermoplasmatales	*Thermoplasma acidophilum*	Terrestrial hydrothermal	+	-	-	-	-	-
	Archaeoglobales	*Archaeoglobus fulgidus*	Marine hydrothermal	+	-	-	-	+	+
		Archaeoglobus profundus	Marine hydrothermal	+	-	-	-	+	+
	Halobacteriales	*Haloferax volcanii*	Terrestrial hypersaline	+	-	-	-	-	-
		Halorubrum lacusprofundi	Terrestrial hypersaline	+	-	-	-	-	-
	Methanosarcinales	*Methanosarcina acetivorans*	Marine sediment	+	+	-	-	-	-
		Methanosarcina barkeri	Terrestrial & marine sediment, soil	+	+	-	-	-	-
		Methanosarcina mazei	Terrestrial sediment & soil	+	+	-	-	-	-

*Hydroxyarchaeol was not detected in *Sulfolobus acidocaldarius* in the present study but reported as a trace component by (Sprott et al., 1997).

The apolar lipid MeO-AR (ELLING et al., 2014, cf. Chapter 3) occurs in all investigated thaumarchaeal strains but not in any analyzed crenarchaeal or euryarchaeal species (Table 5.3). MeO-AR therefore appears to be a lipid specific to archaea of the phylum *Thaumarchaeota*. Similarly, crenarchaeol was only detected in *Thaumarchaeota* (Table 5.3), in agreement with previous studies (SINNINGHE DAMSTÉ et al., 2002b; PITCHER et al., 2011a; SINNINGHE DAMSTÉ et al., 2012), and thus represents a biomarker specific for *Thaumarchaeota*.

In order to test whether MeO-AR might be used as a biomarker for *Thaumarchaeota* in the environment, we analyzed its abundance in a water column profile covering the OMZ in the equatorial North Pacific Ocean as well as the oxic and suboxic waters over- and underlying the OMZ. The distribution of MeO-AR indicates a maximum in thaumarchaeal abundance in the upper suboxic zone of the OMZ (Fig. 5.7), which is in agreement with a peak in abundance of IPL-derived GDGTs (XIE et al., 2014) at this depth. This maximum in MeO-AR concentrations is consistent with maxima in thaumarchaeal abundances commonly observed in the suboxic zones in oceanic OMZs and in the suboxic transition zones of anoxic basins (e.g., COOLEN et al., 2007; ERGUDER et al., 2009; STEWART et al., 2012; XIE et al., 2014). In contrast to MeO-AR, the abundance of AR peaked within the anoxic core of the OMZ suggesting an anaerobic archaeal source (Fig. 5.7). Since all archaea contain at least minor amounts of AR (Table 5.3), the ratio of MeO-AR to AR might serve as a semi-quantitative measure of thaumarchaeal contributions to the total archaeal population in environmental samples. In the equatorial North Pacific Ocean, the ratio of MeO-AR to AR was low within the upper oxic waters and the anoxic core of the OMZ and peaked in the suboxic zones in the upper and lower part of the OMZ (Fig. 5.7) in agreement with the anticipated distribution of *Thaumarchaeota* in the water column (e.g., KARNER et al., 2001; STEWART et al., 2012). This indicates that MeO-AR is a suitable biomarker for tracing thaumarchaeal abundance in the marine environment that might prove to be useful for constraining the highly disputed relative contributions of planktonic *Thaumarchaeota* and *Euryarchaeota* to the marine GDGT signal (LINCOLN et al., 2014a,b; SCHOUTEN et al., 2014).

All analyzed thaumarchaeal strains synthesize the same suite of respiratory quinones, the menaquinones $MK_{6:0}$ and $MK_{6:1}$ (Table 5.2). The utilization of menaquinones in *Thaumarchaeota* is distinct from the utilization of ubiquinones in ammonia-oxidizing bacteria (WHITTAKER et al., 2000), which is in line with the emerging view of phylogenetically and biochemically distinct ammonia-oxidation pathways and respiratory chains of ammonia-oxidizing archaea and bacteria (WALKER et al., 2010; STAHL and DE LA TORRE, 2012; VAJRALA et al., 2013). While $MK_{6:0}$ and $MK_{6:1}$ are minor quinones in some thermophilic *Crenarchaeota* and *Euryarchaeota*, they are not detected in other

cultivated mesophilic archaea (Table 5.2; discussed in detail in Chapter 6). Therefore, these menaquinones may be regarded as biomarkers specific for the phylum *Thaumarchaeota* in low-temperature marine and terrestrial habitats (cf. Chapters 6 and 7).

5.5. Conclusions

We characterized the lipidome of the phylum *Thaumarchaeota* based on the core and IPL compositions of 11 thaumarchaeal pure and enrichment cultures cultivated from soil, geothermal habitats, and the surface ocean. We described 100 structurally different lipid types, which indicates that *Thaumarchaeota* harbor an unprecedented diversity of membrane lipids. While all thaumarchaeal strains synthesize similar intact polar GDGT classes, the relative abundances of these lipids as well as their core lipid composition differ among the thaumarchaeal phylogenetic subgroups. The relative abundances of core lipids in cultivated *Thaumarchaeota* are determined by phylogeny, while the IPL composition is reflective of the habitat or growth conditions. Therefore, the core lipid and IPL profiles described here may help to interpret the IPL signatures observed in environmental samples and may be used to identify specific thaumarchaeal clades. While all thaumarchaeal strains synthesize crenarchaeol as a major core lipid, OH-GDGTs are only found in Group I.1a as well as the sister group SAGMCG-1. High abundances of GDGT-4, GDDs, and the crenarchaeol regioisomer are characteristic for group I.1b *Thaumarchaeota*, while the apolar lipid methoxy archaeol is particularly abundant in SAGMCG-1 but is also a major lipid in other mesophilic *Thaumarchaeota*. Thermophilic *Thaumarchaeota* of the HWCG-III cluster are distinct from the other thaumarchaeal groups by synthesizing large amounts of GTGTs. Complementary analysis of >20 euryarchaeal and crenarchaeal species shows that methoxy archaeol is found exclusively in *Thaumarchaeota*. The characteristic distribution of methoxy archaeol and intact polar GDGTs along a depth profile through the OMZ in the equatorial North Pacific Ocean suggests that methoxy archaeol may be used as a biomarker for *Thaumarchaeota* in the environment and potentially for estimating thaumarchaeal contributions to total GDGT production in the marine environment.

Acknowledgements

We thank J.S. Lipp and L. Wörmer for assistance with HPLC-MS analysis. R. Bittner (University of Vienna), J. McWilliam (University of Aberdeen), V. Russell (San Francisco State University), and X. Liu (University of Bremen) are thanked for assistance

with cultivation and lipid analysis. The study was funded by the European Research Council under the European Union's Seventh Framework Programme–'Ideas' Specific Programme, ERC grant agreement No. 247153 (Advanced Grant DARCLIFE; PI: K.-U.H.) and by the Deutsche Forschungsgemeinschaft through the Gottfried Wilhelm Leibniz Prize awarded to Kai-Uwe Hinrichs (Hi 616-14-1) and grant Inst 144/300-1 (LC-qToF system).

Part II.

Respiratory quinones as chemotaxonomic biomarkers

CHAPTER 6

Respiratory quinones in *Archaea*: phylogenetic distribution and application as biomarkers in the marine environment

Felix J. Elling[a,+,*], Kevin W. Becker[a,+], Martin Könneke[a], Jan M. Schröder[a], Matthias Y. Kellermann[b], Michael Thomm[c] and Kai-Uwe Hinrichs[a]

Submitted to *Environmental Microbiology*

[+]These authors contributed equally to this work.

[a] Organic Geochemistry Group, MARUM - Center for Marine Environmental Sciences & Department of Geosciences, University of Bremen, 28359 Bremen, Germany
[b] Department of Earth Science and Marine Science Institute, University of California, Santa Barbara, California, 93106 USA
[c] Lehrstuhl für Mikrobiologie und Archaeenzentrum, Universität Regensburg, 93053 Regensburg, Germany

[*] Corresponding author. E-mail: felling@marum.de

Abstract

Isoprenoid quinones are membrane-bound lipids functioning as electron carriers in respiratory chains of almost all organisms. However, knowledge of the quinone composition particularly in *Archaea* is still fragmentary. Using novel protocols that enable simultaneous detection of quinones and glycerol-based membrane lipids we investigated the quinone inventories of 25 species belonging to the archaeal phyla *Eury-*, *Cren-* and *Thaumarchaeota*. Saturated and monounsaturated menaquinones with six isoprenoid units forming the alkyl chain may represent chemotaxonomic markers for *Thaumarchaeota*. Other diagnostic biomarkers are thiophene-bearing quinones for *Sulfolobales* and methanophenazines as functional quinone analogs of the *Methanosarcinales*. The ubiquity of saturated menaquinones in the *Archaea* in comparison to *Bacteria* suggests that these compounds may represent an ancestral and diagnostic feature of the *Archaea*. Overlap between quinone compositions of distinct thermophilic and halophilic archaea and bacteria may indicate lateral gene transfer. The biomarker potential of thaumarchaeal quinones was exemplarily demonstrated on a water column profile of the Black Sea. Both, thaumarchaeal quinones and membrane lipids showed similar distributions with maxima at the chemocline. In conclusion, the structural variations of quinones and their distribution among the *Archaea* bear significant chemotaxonomic information and high biomarker potential for classification and quantification of distinct archaeal orders in the environment.

6.1. Introduction

Isoprenoid quinones are a structurally diverse group of membrane-bound lipids that act as electron carriers in the respiratory chains of organisms from all domains of life (NOWICKA and KRUK, 2010). Quinones are commonly classified based on the structure of a polar cyclic headgroup and can be further distinguished by the length and degree of unsaturation of the head-to-tail linked isoprenoid side chain (COLLINS and JONES, 1981; HIRAISHI, 1999). The major classes of quinones include ubiquinones (UQs), plastoquinones (PQs) and derivatives (benzoquinones), which occur exclusively in *Bacteria* and mitochondria of *Eukarya*, as well as menaquinones (MKs, also known as vitamin K2) and related compounds (naphthoquinones), which occur only in *Archaea* and *Bacteria*, except for phylloquinone ($MK_{4:1}$, also known as vitamin K1; Quinone nomenclature ($Q_{m:n}$) indicates headgroup type (Q), number of isoprenoid units in the side chain (m) and number of double bonds (n)), which is involved in electron transferin the photosystem I of cyanobacteria and phototrophic eukaryotes (COLLINS and JONES, 1981; HIRAISHI, 1999; NOWICKA and KRUK, 2010). The side chains usually comprise 4 to 10 isoprenoid units and typically contain one double bond per isoprenoid unit in *Bacteria* (hereafter termed fully unsaturated), while in *Archaea* partially unsaturated and fully saturated side chains are more common (COLLINS and JONES, 1981; TINDALL et al., 1989; HIRAISHI, 1999).

The different quinone types have distinct redox potentials that depend on headgroup structures, while the influence of length of the side chain and degree of its unsaturation has not been systematically studied (Supp. Table 6.1; NOWICKA and KRUK, 2010). The only organisms that do not contain quinones are fermentative *Bacteria* and methanogens. However, *Methanosarcina mazei* and potentially other representatives of the order *Methanosarcinales* synthesize methanophenazine as a substitute electron carrier (Supp. Fig. 6.1; ABKEN et al., 1998). Complementary to polar membrane lipid analysis, quinone profiling offers PCR-independent taxonomic characterization and quantification of microbial biomass in environmental samples (COLLINS and JONES, 1981; HIRAISHI, 1999; HIRAISHI et al., 2003). Furthermore, redox conditions and metabolism are major controls on the occurrence and relative abundance of specific quinones in microorganisms due to their distinct redox potentials (Supp. Table 6.1; HEDRICK and WHITE, 1986; WISSENBACH et al., 1990; BEKKER et al., 2007; NOWICKA and KRUK, 2010). Therefore, quinone distributions in the environment likely contain an additional functional dimension related to microbial metabolisms and redox conditions.

In addition to their function in electron transport chains, quinones might contribute to membrane adaptation to physiological stresses similar to membrane lipids. For

instance, SÉVIN and SAUER (2014) observed that sustained osmotic-stress tolerance in *Escherichia coli* depended on accumulation of ubiquinone. Therefore, characterization of the cellular quinone pool appears essential for a holistic understanding of membrane properties in microorganisms.

Structural characterization and quantification of respiratory quinones facilitates the elucidationof microbial electron transport chains (WHITTAKER et al., 2000; STAMS and PLUGGE, 2009; COATES et al., 2013). Similarly, interpretation of quinone profiles in environmental samples is facilitated by detailed description of quinone diversity in cultivated organisms (COLLINS and JONES, 1981; HIRAISHI, 1999; URAKAWA et al., 2000; URAKAWA et al., 2005).Comprehensive analysis of the occurrence of respiratory quinones in *Archaea* furthermore supports genetic investigations on the evolutionary history of quinone biosynthesis (cf. SOUSA et al., 2013; ZHI et al., 2014). However, the knowledge on the distribution of quinone structural types particularly in the *Archaea* remains fragmentary. For example, the quinone composition of representatives of the ammonia-oxidizing *Thaumarchaeota*, possibly among the most abundant *Archaea* on Earth (cf. STAHL and DE LA TORRE, 2012), has not been explored yet, despite the presumed central role of quinones in current models of the respiratory pathway for ammonia oxidation (WALKER et al., 2010; STAHL and DE LA TORRE, 2012).

Conventional methods used for quinone analysis are based on thin-layer or high performance liquid chromatography (HPLC) coupled to UV spectrophotometric detection. These methods do not allow precise quantification of quinones in complex mixtures and structural identification of unknown compounds (HIRAISHI, 1999). Moreover, UV-based techniques require work-intensive preparative steps such as the prior separation of ubiquinones from menaquinones (HIRAISHI, 1999).The coupling of HPLC to mass spectrometry (MS) provides a powerful framework to explore the taxonomic and process-related information contained in the structural diversity and abundance ofquinones (HIRAISHI, 1999; GEYER et al., 2004; KAISER et al., 2012).

Here, we performed an in-depth analysis of respiratory quinones in cultured representatives of three archaeal phyla originating from a wide range of environments including soils, hypersaline lakes, geothermal systems, and the surface ocean. These analyses were facilitated by modifying recently developed HPLC-MS methods to feature simultaneous detection and quantification of archaeal and bacterial respiratory quinones as well as core and intact polar glycerol-based membrane lipids. We explored the phylogenetic implications of respiratory quinone distribution in *Archaea* and evaluated the potential of quinones as chemotaxonomic markers. For the first time, we report the quinone inventories of soil and planktonic representatives of the phylum *Thaumarchaeota* as well as the crenarchaeal species *Ignicoccus hospitalis*, *Pyrolobus fumarii*, and *Sulfolobus islandicus*. Additionally, *M. acetivorans* and *M. barkeri*

were analyzed for their methanophenazine composition. In order to demonstrate the strength of simultaneous quinone and membrane lipid profiling in the environment, we investigated thaumarchaeal abundance in suspended particulate matter samples from the southern Black Sea, where archaeal community composition is linked to the distinctly stratified water column chemistry (COOLEN et al., 2007; WAKEHAM et al., 2007).

6.2. Results

6.2.1. Chromatographic separation and mass spectrometric characterization of respiratory quinones

Reversed phase (RP)-HPLC-MS analysis of different archaeal culture extracts yielded chromatographic separation of respiratory quinones as well as core and intact polar glycerol diphytanyl diether (archaeols) and glycerol dibiphytanyl glycerol tetraether lipids (GDGTs; Fig. 6.1). Retention of quinones was dependent on headgroup type and isoprenoid alkyl chain length and its degree of unsaturation (Fig. 6.1 & Supp. Fig. 6.2) to the effect that compounds of a given headgroup type were baseline-separated when they possessed a different number of isoprenoid units and/or double bonds in the alkyl chain. The retention time increased with increasing length of the isoprenoid chain but decreased with increasing number of double bonds. Similarly, archaeal membrane lipids were separated by headgroup type and side chain structures as described previously (ZHU et al., 2013, Fig. 6.1). For quinones with identical side chain structure, the elution order was UQs, PQs, demethylmenaquinone (DMKs), MKs, methionaquinones (MTKs), and methylmenaquinones (MMKs; Supp. Fig. 6.2 & Supp. Fig. 6.6). Co-elution was observed for several structurally distinct quinones (e.g., $DMK_{7:7}$, $MTK_{6:5}$, $MMK_{6:6}$; Supp. Fig. 6.2) but did not interfere with their quantification due to the MS-based detection. Application of the RP-HPLC-MS method from WÖRMER et al. (2013) to a marine sediment sample also yielded chromatographic separation of respiratory quinones, with the same elution order as described for the protocol by ZHU et al. (2013). The method by WÖRMER et al. (2013) additionally allowed the detection of bacterial intact polar membrane lipids and reduced analysis time from 90 to 30 min (Supp. Fig. 6.6). While archaeal lipids could be detected using this method, differences in tetraether side chain cyclization could not be fully resolved (WÖRMER et al., 2013).

Respiratory quinones were identified based on exact molecular mass and fragmentation patterns in MS2 mode. The systematic fragmentation in MS^2 spectra was primarily related to the structural properties of the headgroup and in part to the isoprenoid side

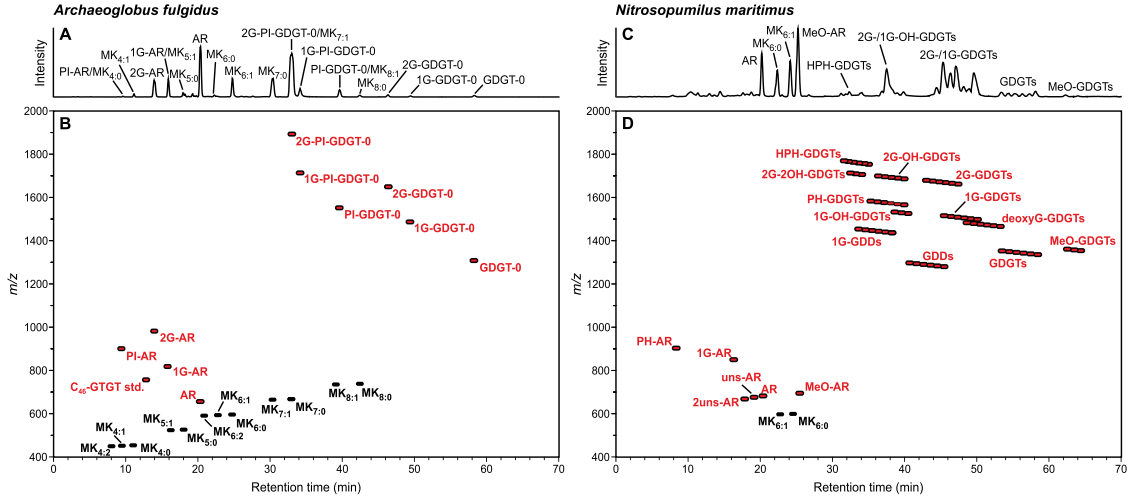

Figure 6.1. Reversed phase HPLC-MS analyses of archaeal cultures demonstrating simultaneous detection of respiratory quinones as well as core and intact polar lipids. Examples for reconstructed base peak chromatograms and density maps obtained from *Archaeoglobus fulgidus* (A, B) and *Nitrosopumilus maritimus* (C, D). Density map color code: red, glycerolipids; black, quinones. Lipid nomenclature designates combinations of core lipid types (GDGT-0, acyclic GDGT; OH-GDGT, hydroxy-GDGT; GDD, glycerol dialkanol diether; MeO-GDGT, methoxy GDGT; AR, archaeol; MeO-AR, methoxy AR) and headgroups (PI, phosphatidylinositol; PH, phosphohexose; HPH, hexose phosphohexose; 1G, monoglycosyl; 2G, diglycosyl). For chemical structures of lipids see Supp. Fig. 6.5.

chain (Fig. 6.2, Fig. 6.3, Supp. Table 6.1). For example, saturated menaquinones (MKs) showed a dominant product ion at m/z 187. This ion represents the naphthoquinone moiety after loss of the isoprenoid side chain (TINDALL et al., 1989). Similarly, the major product ions of demethylmenaquinones (DMKs), methylmenaquinones (MMKs, i.e., thermoplasmaquinones), sulfolobusquinones (SQs), caldariellaquinones (CQs), benzodithiophenoquinones (BDTQs), UQs, PQs, and methanophenazine (MP) were also related to the loss of the quinone headgroup. Fragmentation of polyunsaturated quinones often showed additional product ions related to the loss of parts of the isoprenoid chain while methylthiol-based quinones produced fragments resulting from the loss of this moiety (Fig. 6.2, Supp. Table 6.1).

6.2.2. Occurrence of respiratory quinones in distinct archaeal species

Respiratory quinones were analyzed in 25 cultured representatives of 14 archaeal orders spanning the three archaeal phyla *Euryarchaeota*, *Crenarchaeota*, and *Thaumarchaeota* (Table 6.1; Fig. 6.3). Seven respiratory quinone classes were identified in the investigated archaeal strains containing fully unsaturated to completely saturated side chains comprised of four to eight isoprenoid units. No respiratory quinones were detected in *Staphylothermus marinus*, *Thermococcus kodakarensis*, *Pyrococcus furiosus*,

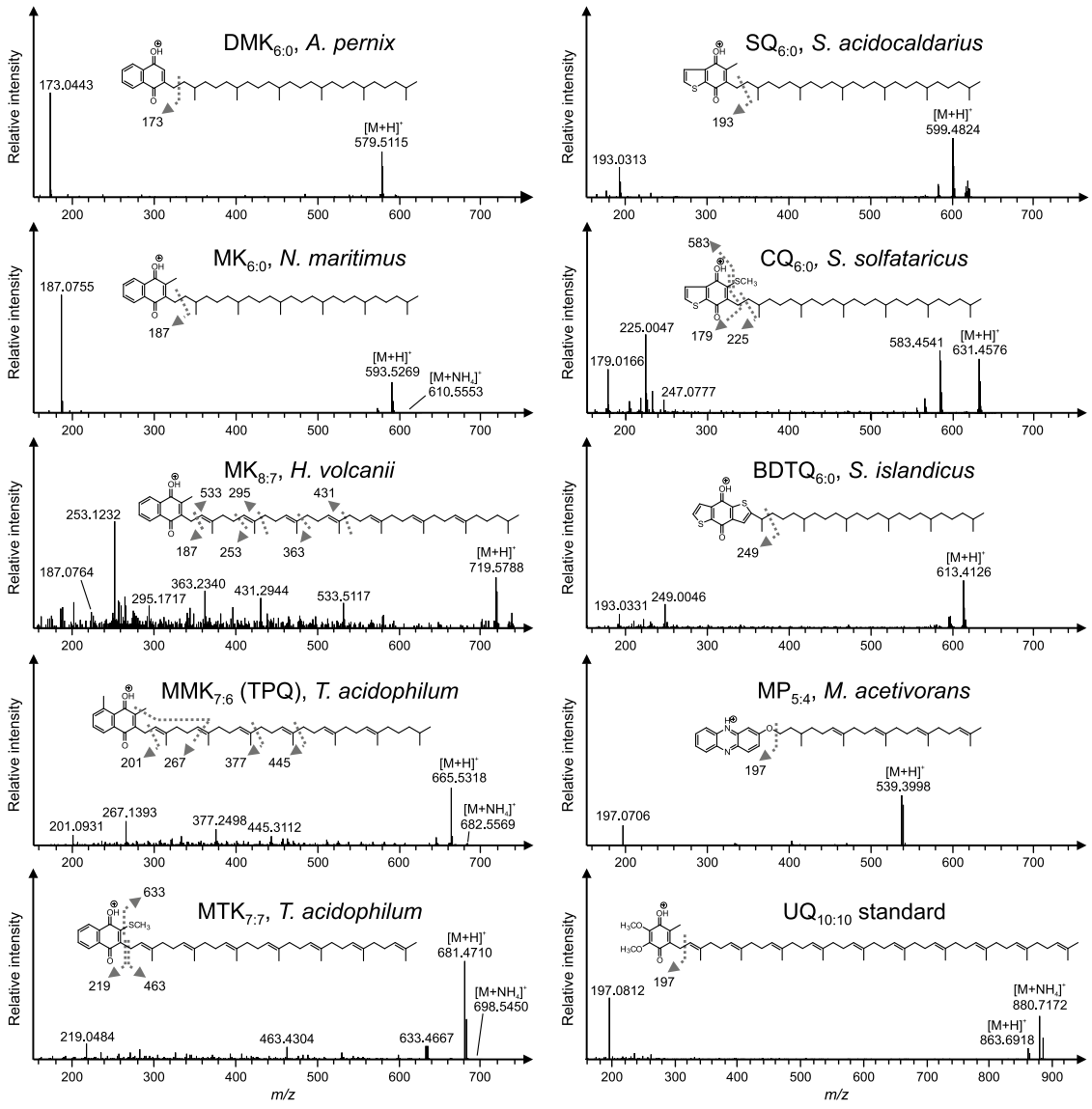

Figure 6.2. Structures and MS^2 spectra of protonated molecules of respiratory quinones (DMK, MK, MMK, MTK, SQ, CQ, BDTQ) and methanophenazine (MP), an electron carrier in Methanosarcinales, from lipid extracts of archaeal cultures and ubiquinone ($UQ_{10:10}$; available as commercial standard). The length and degree of unsaturation of the isoprenoid side chains of quinones may vary from 4 to 14 and completely saturated to fully unsaturated, respectively. Quinone nomenclature ($Q_{m:n}$) with headgroup type (Q), number of isoprenoid units in the side chain (m) and number of double bonds (n). DMK: Demethylmenaquinone. MK: Menaquinone. MMK: Methylmenaquinone. MTK: Methionaquinone. BDTQ: Benzodithiophenoquinone. SQ: Sulfolobusquinone. CQ: Caldariellaquinone. UQ: Ubiquinone.

Methanopyrus kandleri, *Methanothermobacter thermautotrophicus*, and *Methanothermococcus thermolithotrophicus*.

Fully saturated quinones were dominant in most of the archaeal strains while partially unsaturated quinones were less abundant. Fully unsaturated side chains were only detected in the euryarchaeal acidophile *Thermoplasma acidophilum*, and the euryarchaeal halophiles *Haloferax volcanii* and *Halorubrum lacusprofundi*. Menaquinones were detected in all quinone-producing strains except for members of the order *Sulfolobales*. Representatives of this order contained exclusively the sulfur-bearing quinones CQ, SQ and BDTQ with fully saturated, monounsaturated, or diunsaturated side chains comprised of five to six isoprenoid units (DE ROSA et al., 1977; THURL et al., 1986; NICOLAUS et al., 1992).

Table 6.1. Occurrence and relative abundance (% of total quinones, quinone abundances below 0.1 % were rounded to 0.1 %) of respiratory quinones in archaeal strains investigated in this study. Quinone nomenclature ($Q_{m:n}$) indicates headgroup type (Q), number of isoprenoid units in the side chain (m) and number of double bonds (n). DMK: Demethylmenaquinone. MK: Menaquinone. MMK: Methylmenaquinone. MTK: Methionaquinone. BDTQ: Benzodithiophenoquinone. SQ: Sulfolobusquinone. CQ: Caldariellaquinone. MP: Methanophenazine. OH-MP: Hydroxymethanophenazine.

Phylum	Order/Group	Species	Strain	Habitat	Major quinones (relative abundance in %)	Minor quinones (relative abundance in %)
Thaumarchaeota	Group I.1a	*Nitrosopumilus maritimus*	SCM1	Marine water	$MK_{6:0}$ (91.0)	$MK_{6:1}$ (9.0)
	Group I.1b	*Nitrososphaera viennensis*	EN76	Soil	$MK_{6:0}$ (76.1), $MK_{6:1}$ (23.9)	-
		Nitrososphaera gargensis	Ga9.2	Terrestrial hydrothermal	$MK_{6:0}$ (68.0), $MK_{6:1}$ (32.0)	-
	SAGMCG-1	*Nitrosotalea devanaterra*	Nd1	Acidic soil	$MK_{6:0}$ (72.4), $MK_{6:1}$ (27.6)	-
Crenarchaeota	*Desulfurococcales*	*Ignicoccus hospitalis*	KIN4/1	Marine hydrothermal	$DMK_{6:0}$ (62.1), $DMK_{6:1}$ (14.1), $MK_{6:0}$ (13.7)	$MK_{6:1}$ (8.6), $DMK_{5:0}$ (0.5), $MK_{7:0}$ (0.2), $MK_{5:1}$ (0.2), $DMK_{6:2}$ (0.2), $MK_{7:1}$ (0.1), $MK_{5:0}$ (0.1), $DMK_{5:1}$ (0.1)
		Staphylothermus marinus	F1	Marine hydrothermal	-	-
		Aeropyrum pernix	K1	Marine hydrothermal	$MMK_{6:0}$ (74.8), $MK_{6:0}$ (15.0)	$MMK_{6:1}$ (5.7), $MK_{6:1}$ (1.6), $MMK_{5:0}$ (1.2), $MTK_{6:0}$ (1.0), $MK_{5:0}$ (0.3), $MTK_{6:1}$ (0.3), $DMK_{5:0}$ (0.1), $DMK_{5:1}$ (0.1)
		Pyrolobus fumarii	1A	Marine hydrothermal	$DMK_{6:0}$ (92.4)	$DMK_{5:0}$ (5.5), $DMK_{6:1}$ (1.1), $MK_{6:0}$ (0.6), $MK_{5:0}$ (0.1), $DMK_{7:0}$ (0.1), $DMK_{5:1}$ (0.1),
	Sulfolobales	*Metallosphaera prunae*	Ron 12/II	Heated mine tailings	$CQ_{6:0}$ (86.1), $CQ_{6:1}$ (12.2)	$CQ_{6:2}$ (1.4), $CQ_{5:0}$ (0.1), $SQ_{6:0}$ (0.1)
		Sulfolobus acidocaldarius	98-3	Terrestrial hydrothermal	$CQ_{6:0}$ (80.9)	$SQ_{6:0}$ (9.7), $CQ_{6:1}$ (9.2), $CQ_{6:2}$ (0.2)
		Sulfolobus solfataricus	P1	Terrestrial hydrothermal	$CQ_{6:0}$ (85.8), $CQ_{6:1}$ (13.7)	$SQ_{6:0}$ (0.5)
		Sulfolobus islandicus	Y.N.15.51	Terrestrial hydrothermal	$SQ_{6:0}$ (42.9), $CQ_{6:0}$ (36.4), $CQ_{6:1}$ (14.6)	$CQ_{6:2}$ (3.2), $SQ_{5:0}$ (1.5), $CQ_{5:0}$ (0.9), $BDTQ_{6:0}$ (0.4), $CQ_{5:1}$ (0.1)
Euryarchaeota	*Thermococcales*	*Pyrococcus furiosus*	Vc 1	Marine hydrothermal	-	-
		Thermococcus kodakarensis	KOD1	Terrestrial hydrothermal	-	-
	Methanopyrales	*Methanopyrus kandleri*	AV19	Marine hydrothermal	-	-
	Methanobacteriales	*Methanothermobacter thermautotrophicus*	Delta H	Terrestrial hydrothermal	-	-
	Methanococcales	*Methanothermococcus thermolithotrophicus*	SN-1	Marine hydrothermal	-	-
	Thermoplasmatales	*Thermoplasma acidophilum*	122-1B2	Terrestrial hydrothermal	$MK_{7:7}$ (40.1), $DMK_{7:7}$ (24.0), $MTK_{7:7}$ (17.3)	$MK_{7:6}$ (6.4), $DMK_{7:6}$ (3.4) $MK_{7:5}$ (3.2), $MMK_{7:7}$ (2.1), $DMK_{6:6}$ (1.0), $MK_{6:6}$ (0.7), $MTK_{7:5}$ (0.4), $MTK_{7:4}$ (0.2), $MTK_{7:6}$ (0.2), $MMK_{7:0}$ (0.1), $MMK_{7:1}$ (0.1), $MK_{7:4}$ (0.1), $MK_{6:5}$ (0.1), $MTK_{8:8}$ (0.1), $MTK_{6:4}$ (0.1), $MTK_{6:5}$ (0.1), $DMK_{7:4}$ (0.1), $DMK_{7:5}$ (0.1), $DMK_{6:5}$ (0.1)
	Archaeoglobales	*Archaeoglobus fulgidus*	VC-16	Marine hydrothermal	$MK_{7:0}$ (68.9), $MK_{7:1}$ (25.0)	$MK_{6:0}$ (2.1), $MK_{8:0}$ (1.1), $MK_{4:2}$ (1.1), $MK_{6:2}$ (0.9), $MK_{8:1}$ (0.2), $MK_{6:1}$ (0.2), $MK_{4:0}$ (0.2), $MK_{4:1}$ (0.2), $MK_{5:0}$ (0.1), $MK_{5:1}$ (0.1)
		Archaeoglobus profundus	AV18	Marine hydrothermal	$MK_{7:0}$ (61.1), $MK_{7:1}$ (36.5)	$MK_{5:1}$ (0.8), $MK_{6:0}$ (0.8), $MK_{5:0}$ (0.5), $MK_{5:1}$ (0.3)
	Halobacteriales	*Haloferax volcanii*	DS2	Terrestrial hypersaline	$MK_{8:7}$ (67.3), $MK_{8:8}$ (22.9)	$MK_{7:7}$ (7.1), $MK_{7:6}$ (0.7)
		Halorubrum lacusprofundi	ACAM34	Terrestrial hypersaline	$MK_{8:7}$ (54.4), $MK_{8:8}$ (45.1)	$MK_{7:6}$ (0.5), $MK_{7:7}$ (0.1)
	Methanosarcinales	*Methanosarcina acetivorans*	C2A	Marine sediment	$MP_{5:4}$ (57.0), OH-$MP_{5:4}$ (18.4), OH-$MP_{5:5}$ (12.6)	OH-$MP_{5:3}$ (7.9), $MP_{5:3}$ (4.2)
		Methanosarcina barkeri	MS	Terrestrial & marine sediment	$MP_{5:2}$ (67.2), $MP_{5:3}$ (25.1)	$MP_{5:1}$ (3.1), $MP_{5:0}$ (1.6), $MP_{5:4}$ (0.6), OH-$MP_{5:3}$ (1.1), OH-$MP_{5:5}$ (0.7), OH-$MP_{5:4}$ (0.5)
		Methanosarcina mazei	S-6	Soils & sediments	$MP_{5:4}$ (93.1)	$MP_{5:3}$ (2.7), OH-$MP_{5:4}$ (2.2), OH-$MP_{5:5}$ (1.5), OH-$MP_{5:3}$ (0.5)

The major quinone found in all investigated representatives of the phylum *Thaumarchaeota* was a fully saturated menaquinone with six isoprenoid units ($MK_{6:0}$) while a less abundant monounsaturated analog ($MK_{6:1}$) was also detected. Similarly, the major quinones in *Archaeoglobus fulgidus* and *Archaeoglobus profundus* were saturated and monounsaturated MKs with the dominant compounds containing seven isoprenoid units as their side chain. Fully unsaturated MKs occurred only in euryarchaeal species, the thermoacidophile *T. acidophilum* as well as the halophiles *H. volcanii* and *H. lacusprofundi*, while the length of the isoprenoid side chains differed. The halophiles contained predominantly $MK_{8:7}$ and $MK_{8:8}$, whereas *T. acidophilum* contained mainly $MK_{7:7}$ (COLLINS et al., 1981). Representatives of the crenarchaeal order *Desulfurococcales* contained minor amounts of MKs and in the case of *Aeropyrum pernix* also minor proportions of MTKs. The dominant quinone of *I. hospitalis* and *P. fumarii* were saturated MMKs with $MMK_{6:0}$ being most abundant in both strains. These saturated MMKs were not detected in other archaeal strains. In contrast, *A. pernix* was characterized by a high abundance of $DMK_{6:0}$. Minor amounts of DMKs but with seven isoprenoid units were exclusively detected in *T. acidophilum*. Additionally, *T. acidophilum* contained several polyunsaturated MMKs that were not detected in the *Desulfurococcales* or any other archaeal strain.

In contrast to the archaeal strains described above, respiratory quinones were not detected in the *Methanosarcinales*; instead, representatives of this order contained the functional quinone analogue methanophenazine, an electron carrier directly involved in methanogenesis (ABKEN et al., 1998). The degree of unsaturation of methanophenazine was specific for *M. acetivorans*, *M. barkeri*, and *M. mazei* (Table 6.1; Fig. 6.3). A previously not described compound in *Methanosarcinales* was tentatively identified as triunsaturated methanophenazine ($MP_{5:3}$), which occurred in all three analyzed strains. In M. barkeri, di- and monounsaturated MPs ($MP_{5:2}$, $MP_{5:1}$, respectively), and a fully saturated MP ($MP_{5:0}$) were additionally identified. Furthermore, novel hydroxymethanophenazines (OH-MP), i.e., methanophenazines with an hydroxylated isoprenoid side chain, were tentatively identified in *M. acetivorans* and *M. mazei* (Supp. Fig. 6.4).

6.2.3. Chemotaxonomic patterns

Complementing the quinone distribution in the 25 investigated archaeal cultures with published distributions from 11 additional strains (Fig. 6.3; supplementary information) revealed several major chemotaxonomic groupings. The orders *Sulfolobales* and *Methanosarcinales* formed distinct clusters based on the exclusive occurrence of SQs, CQs and BDTQs, and MPs/OH-MPs, respectively. While menaquinones occurred in

all quinone-producing archaeal orders, the menaquinone producing archaeal species could be separated into three groups based on the degree of side-chain unsaturation and the co-occurrence of other quinone types. The first group comprised exclusively *Halobacteriales* strains and was characterized by polyunsaturated MKs with predominantly 7 or 8 isoprenoid units. In contrast, the two other groups, the *Thaumarchaeota* on the one hand and the *Thermoproteales* as well as most of the *Desulfurococcales* strains on the other hand, were characterized by fully saturated side chains. The *Thaumarchaeota* were further distinguished by the sole occurrence of $MK_{6:0}$ and $MK_{6:1}$, while menaquinone diversity in *Thermoproteales* and most *Desulfurococcales* strains was higher. The *Archaeoglobales* showed a similar quinone composition as *Thaumarchaeota*, *Thermoproteales* and *Desulfurococcales* but were the only *Euryarchaeota* containing saturated quinones. Similarly, *T. acidophilum* could be distinguished from other *Euryarchaeota* by the occurrence of a large range of unsaturated menaquinones and other naphthoquinone derivatives such as DMKs, MTKs, and MMKs.

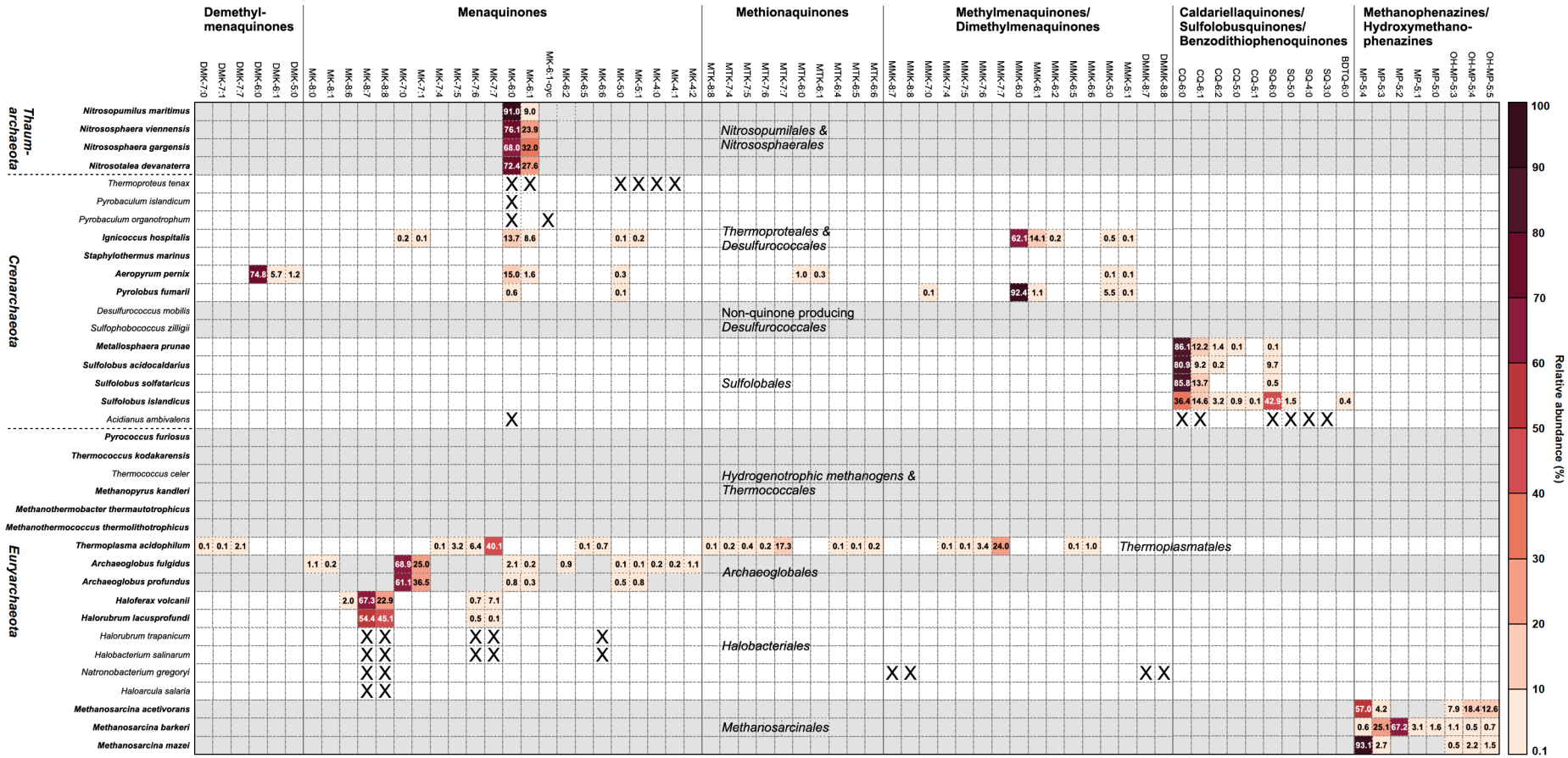

Figure 6.3. Relative abundances of respiratory quinones and methanophenazines in cultivated strains of the phyla *Thaumarchaeota*, *Crenarchaeota*, and *Euryarchaeota*. Major chemotaxonomic groupings are labeled and highlighted in grey/white. Compiled from strains investigated in this study (bold) and published data (indicating occurrence, (X) and absence/not reported (blank) of quinone types; sources listed in supplementary information). Quinone abundances below 0.1 % were rounded to 0.1 %.

6.2.4. *Thaumarchaeal quinones and glycerolipids in marine suspended particulate matter*

In order to validate the biomarker potential of archaeal quinones, we investigated thaumarchaeal quinone in concert with membrane lipid abundances in the water column of the southern Black Sea (Supp. Table 6.2). Suspended particulate matter was sampled at nine depth intervals covering all major geochemical zones from oxic water (40 m water depth) to the suboxic chemocline (90, 120, 150 m) and the underlying anoxic (sulfidic) zone (300, 500, 700, 900, 1200 m).

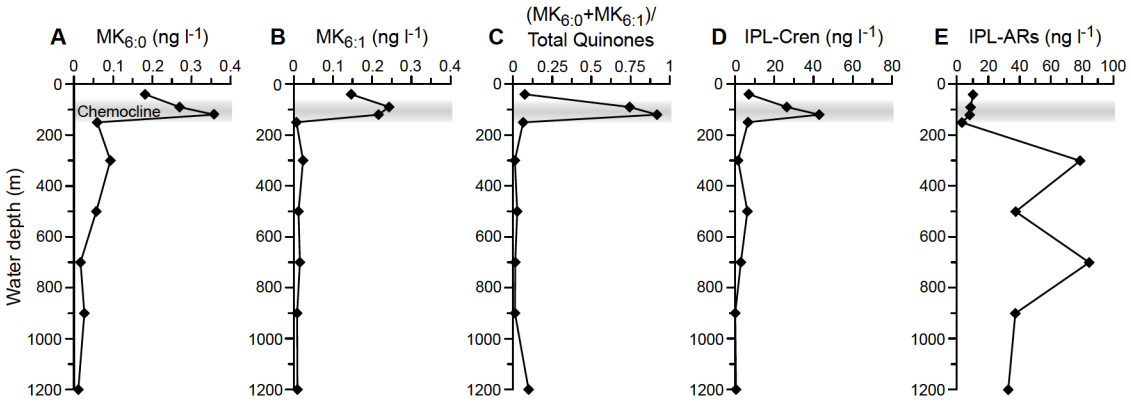

Figure 6.4. Distribution of $MK_{6:0}$ (**A**) and $MK_{6:1}$ (**B**), abundance of $MK_{6:0}$ and $MK_{6:1}$ relative to total quinones (**C**) intact polar crenarchaeol lipids (**D**), as well as intact polar archaeols (**E**) in the water column of the southern Black Sea. The location of the chemocline, indicating the transition from shallow oxic to deep anoxic water, is shaded in grey.

The concentrations of the *Thaumarchaeota*-specific quinones $MK_{6:0}$ and $MK_{6:1}$ were quantified in comparison to monoglycosidic, diglycosidic and hexose-phosphohexose crenarchaeol derivatives, i.e., major membrane lipids of marine *Thaumarchaeota* (Supp. Fig. 6.5). The concentration of $MK_{6:0}$ increased from oxic waters (0.18 ng l^{-1}) to the suboxic waters of the chemocline at 120 m (0.36 ng l^{-1}; Fig. 6.4a). $MK_{6:1}$ was similarly concentrated in the oxic waters (0.14 ng l^{-1}) but showed a shallower maximum at the chemocline at 90 m (0.24 ng l^{-1}; Fig. 6.4b). The concentrations of both $MK_{6:0}$ and $MK_{6:1}$ were one order of magnitude lower in the anoxic part of the water column below 150 m (0.01 ng l^{-1}). In contrast, total quinone concentrations, i.e., the sum of ubiquinones, menaquinones, plastoquinones, peaked in the oxic part (40 m, 4.3 ng l^{-1}) as well as in the anoxic zone below the chemocline at 300 m (9.4 ng l^{-1}; Supp. Table 6.3) but were minimal between 90-150 m. The ratio of $MK_{6:0}$ to $MK_{6:1}$ relative to total quinones showed a sharp maximum between 90-120 m (Fig. 6.4c). Similar to the $MK_{6:0}$ and $MK_{6:1}$ profiles, the distribution of total intact polar crenarchaeol showed a peak between 90 and 120 m in the suboxic waters of the chemocline with 42.8 ng l^{-1} and minimal concentrations in the fully oxic and anoxic parts of the water column

(Fig. 6.4d). Intact polar archaeols, i.e., all glycolipids and phospholipids with an archaeol core structure (Supp. Fig. 6.5; Supp. Table 6.3), showed a maximum in the anoxic zone at 300 m water depth and below but were also detected in significant amounts in the chemocline.

6.3. Discussion

6.3.1. Phylogenetic significance of quinone biosynthesis in Archaea

A major taxonomic divide among the *Archaea* is the occurrence of menaquinones. Their presence in the archaeal phylum *Thaumarchaeota* (Table 6.1; Fig. 6.3) as well as other deeply branching archaeal (Table 6.1) and bacterial lineages (Supp. Table 6.1; NITSCHKE et al., 1995; SCHÜTZ et al., 2000; SCHOEPP-COTHENET et al., 2009) suggests that menaquinone biosynthesis was present in the last common ancestor of *Archaea* and *Bacteria* (SCHOEPP-COTHENET et al., 2013; ZHI et al., 2014). In particular, the low mid-point redox potentials of menaquinones (−67 mV; WAGNER et al., 1974) support an origin of the last common ancestor in a reducing habitat (NITSCHKE et al., 1995; SCHÜTZ et al., 2000; SCHOEPP-COTHENET et al., 2009). However, the discovery of two independent biosynthetic pathways (HIRATSUKA et al., 2008) suggests that menaquinone biosynthesis has evolved at least twice (ZHI et al., 2014). While the 'classical' pathway operates in most *Bacteria* and *Halobacteriales*, the alternative futalosine pathway is employed by other *Archaea* and some *Bacteria* (SOUSA et al., 2013; ZHI et al., 2014). The respiratory quinone composition of the *Halobacteriales* is indeed remarkably similar to that of halophilic *Bacteria* (COLLINS et al., 1981; SCHOEPP-COTHENET et al., 2009) and appears to result from massive lateral gene transfer from bacterial donors to an ancestral methanogenic recipient (BOUCHER et al., 2003; NELSON-SATHI et al., 2012; ZHI et al., 2014). The acquisition of polyunsaturated menaquinone biosynthesis might have been advantageous in extremely saline habitats (cf. SÉVIN and SAUER, 2014), in analogy to the high abundances of unsaturated isoprenoid membrane lipids biosynthesized by *Halobacteriales* in response to high salinity (GIBSON et al., 2005; STIEHL et al., 2005; DAWSON et al., 2012). In contrast, saturated menaquinones occur in those archaeal clades (Table 6.1; Fig. 6.3) that have also predominantly saturated polar membrane lipids, such as the *Thaumarchaeota* and most thermophilic *Crenarchaeota* and *Euryarchaeota* (THURL and SCHÄFER, 1988; TRINCONE et al., 1992; VÖLKL et al., 1993; MORII et al., 1999; JAHN et al., 2004; TARUI et al., 2007; ELLING et al., 2014). Given the absence of saturated menaquinones in *Bacteria*, these compounds may represent an ancestral and diagnostic feature of the *Archaea*.

Methylated naphthoquinone derivatives (MMKs) are likely derived from methylation of menaquinones and are found in *Bacteria* (COLLINS and JONES, 1981), thermophilic *Archaea* (Fig. 6.3), and the haloalkaliphile *Natronobacterium gregoryi*, which also contains dimethylated menaquinones (DMMKs; Fig. 6.3; COLLINS and TINDALL, 1987). Similar to menaquinones, DMKs are found in *Bacteria* as well as *A. pernix* (Fig. 6.3; NISHIDA et al., 1999) and *T. acidophilum* (Fig. 6.3) and are precursors in menaquinone biosynthesis in the 'classical' pathway (BENTLEY and MEGANATHAN, 1982) and potentially in the futalosine pathway (HIRATSUKA et al., 2008). In addition to DMKs, *A. pernix* and *T. acidophilum* appear to be the only archaeal species to produce MTKs, methylthio-derivatives of naphthoquinones, which otherwise have only been observed in aerobic thermophilic, sulfur-metabolizing *Bacteria* belonging to the genera *Aquifex* and *Hydrogenobacter* (HIRAISHI, 1999). The biosynthesis of MTKs in both *Aquificae* as well as *A. pernix* and *T. acidophilum* may represent either convergent development due to their shared preference for oxic, sulfur-rich geothermal habitats or may have been acquired via lateral gene transfer, which is thought to occur frequently among thermophiles (NELSON et al., 1999; RUEPP et al., 2000; KOONIN et al., 2001).

As reduced menaquinones (menaquinols) may become spontaneously oxidized in the presence of oxygen (KRÖGER and DADÁK, 1969), the biosynthesis of CQs, SQs and BDTQs featuring higher midpoint redox potentials (Supp. Table 6.1) by the *Sulfolobales* likely occurred as an adaptation to aerobic metabolism (NITSCHKE et al., 1995; SCHÜTZ et al., 2000; SCHOEPP-COTHENET et al., 2009, 2013) similar to the occurrence of ubiquinone biosynthesis in proteobacteria and plastoquinones in cyanobacteria (SCHÜTZ et al., 2000). This shift to a high-redox-potential bioenergetic chain does not seem to have occurred in the obligate aerobic, ammonia-oxidizing *Thaumarchaeota*. In addition to the high affinity of *Thaumarchaeota* to both oxygen and ammonium (MARTENS-HABBENA et al., 2009), their menaquinone-based respiratory chains may facilitate persistence of *Thaumarchaeota* in oceanic redoxclines and other hypoxic environments compared to ubiquinone-utilizing ammonia-oxidizing *Bacteria* (e.g. STEWART et al., 2012). Assuming that side chain length and unsaturation have only minor effects on quinone redox potentials, the large difference between the redox potentials of menaquinone/menaquinol ($MK_{6:6}$: $E'_0 = -67\,mV$; WAGNER et al., 1974) and the NO_2/NH_3 redox couple ($E'_0 = +340\,mV$; SIMON, 2002) suggests that thaumarchaeal respiratory chains differ fundamentally from those of ammonia-oxidizing *Bacteria*.

Despite the central role of quinones in most studied archaeal respiratory chains, a considerable number of cultivated species does not synthesize quinones and hence appear to harbor distinct respiratory systems. The absence of quinones and functional quinone analogs as well as cytochromes in hydrogenotrophic methanogens (THAUER

et al., 2008) in favor of a sole dependence on chemiosmosis appears to be a simpler, more ancient metabolic configuration than quinone-based energy metabolism and has been regarded as testimony for a methanogenic ancestor of the *Archaea* (MARTIN, 2012; SOUSA et al., 2013). The occurrence of methanophenazines as quinone analogs as well as of cytochromes in *Methanosarcinales* thus appears to be a more recent evolutionary trait and might be linked to the diversification of methanogenic substrates and increased substrate utilization efficiency of the *Methanosarcinales*. In contrast, a 'menaquinone-first' hypothesis of archaeal metabolism implies repeated loss of menaquinone-biosynthetic capacities during archaeal radiation after separation from the common ancestor of *Archaea* and *Bacteria* (SCHOEPP-COTHENET et al., 2013; ZHI et al., 2014), resulting in the patchy distribution of quinone biosynthesis in the crenarchaeal order *Desulfurococcales* (Fig. 6.3). Based on current phylogenetic models (SPANG et al., 2010; BROCHIER-ARMANET et al., 2011) and the occurrence of menaquinones in *Archaea* (Fig. 6.3), a 'menaquinone-first' scenario would imply the conservation of menaquinone biosynthesis in *Thaumarchaeota* and in a considerable fraction of (cultivated) *Crenarchaeota* as well as loss of biosynthetic capability in the ancestor of *Euryarchaeota*. Menaquinone biosynthesis in *Archaeoglobales* and *Thermoplasmatales* would then need to have been acquired through lateral gene transfer from other microbes, as evidently happened to the ancestor of the *Halobacteriales* (NELSON-SATHI et al., 2012). This scenario seems likely given the isolated occurrence of menaquinone biosynthesis in *Archaeoglobales* and *Thermoplasmatales* as well as high proportions of laterally acquired genes from *Bacteria* and other *Archaea* in these thermophilic archaeal orders (RUEPP et al., 2000; BOUCHER et al., 2001; NELSON-SATHI et al., 2014). Analysis of the occurrence of respiratory quinones in additional, especially basally branching, archaeal representatives may help to further resolve the evolutionary history of quinone biosynthesis.

In contrast to numerous thermophilic and halophilic archaeal cultures, only few non-methanogenic mesophilic isolates exist, which are exclusively ammonia-oxidizing *Archaea* of the phylum *Thaumarchaeota*. Based on the high abundance and diversity of uncultured mesophilic planktonic (DELONG, 1992; FUHRMAN et al., 1992; KARNER et al., 2001) and benthic archaeal groups (BIDDLE et al., 2006; TESKE and SØRENSEN, 2008), the majority of the archaeal quinone diversity currently remains unconstrained. The analysis of archaeal respiratory quinones in environmental samples could therefore yield additional insights into diversity and respiratory pathways of uncultured *Archaea*.

In conclusion, the heterogeneous taxonomic distribution of quinone types among the *Archaea* observed in this study yields insights into the evolutionary history of quinone biosynthesis. Specifically, the distribution of menaquinones in *Archaea* suggests an ancestral origin of menaquinone biosynthesis in *Cren-* or *Thaumarchaeota*. In

contrast, the highly divergent quinone distribution in *Euryarchaeota* may result from a combination of vertical inheritance, lateral gene transfer and gene loss.

6.3.2. Biomarker potential of archaeal respiratory quinones

In ecosystems that are not amenable to cultivation-dependent approaches, lipidomics and metagenomics are routinely applied to describe microbial community composition and potential function. The approach applied in this study provides streamlined analytical protocols for highly sensitive, detailed and simultaneous profiling of quinones and membrane lipids in environmental samples. This facilitates direct comparison of archaeal glycerolipids and quinone derivatives (Fig. 6.1, Supp. Fig. 6.6) to (*i*) estimate microbial biomass and (*ii*) to characterize microbial diversity and community structure. Overall, the high abundance of saturated and partially unsaturated quinones in *Archaea* observed in this study contrasts the dominance of fully unsaturated or terminally saturated side chains in *Bacteria* and *Eukarya* (e.g. COLLINS and JONES, 1981; NOWICKA and KRUK, 2010). Even though some quinones occur in multiple archaeal species described here, the relative proportions of quinones are considerably different for each species. In particular, $MK_{6:0}$ and $MK_{6:1}$ in *Thaumarchaeota* are the first quinones to be described in mesophilic *Archaea* and are therefore promising biomarkers for tracing this globally abundant archaeal clade. Similarly, SQs, CQs and BDTQs are distinct for *Sulfolobales*, as are MPs and OH-MPs for *Methanosarcinales* (Fig. 6.3). Considering the widespread occurrence of *Methanosarcinales* in the marine environment, in particular subseafloor sediments (LEVER, 2013), MPs and OH-MPs have potential to be used as biomarkers for this archaeal order. Additionally, methanophenazines might also be synthesized by uncultivated anaerobic methane-oxidizing *Archaea* (ANME-2), which are phylogenetically closely related to the *Methanosarcinales*.

The considerably different quinone inventories of the investigated archaeal strains may be attributed to different habitats, adaptive strategies and metabolism. For instance, cultured thaumarchaeal strains have a limited temperature and pH range, are obligate ammonia-oxidizing aerobes (STAHL and DE LA TORRE, 2012) and contain only two respiratory quinones (Fig. 6.3). In contrast, the high diversity of quinones found in *T. acidophilum* may reflect the wide range of conditions to which this archaeon can adapt, such as aerobic and anaerobic growth as well as high temperature and low pH. Since the quinone composition in *Archaea* as well as *Bacteria* may change in response to growth conditions (TRINCONE et al., 1989; NICOLAUS et al., 1992; SHIMADA et al., 2001; SÉVIN and SAUER, 2014), it is likely that the response to environmental properties such as oxygenation, abundance of electron acceptors, temperature, or salinity is also encoded in environmental quinone profiles. Exploring the environmental quinone

diversity may therefore help to constrain redox conditions as well as adaptation pathways of microbes (cf. HEDRICK and WHITE, 1986; HIRAISHI, 1999). This might be especially applicable to the study of environments with high microbial diversity and strong geochemical gradients such as microbial mats and hydrothermal systems, and might complement membrane lipid-based and gene-based approaches.

6.3.3. Tracing thaumarchaeal abundance in the Black Sea using quinones and intact polar lipids

The concentrations of intact polar crenarchaeol derivatives indicate a maximum in thaumarchaeotal abundance in the suboxic zone of the southern Black Sea. This result is in agreement with previous observations based on the abundances of thaumarchaeal 16S rRNA and *amoA* (ammonia monooxygenase subunit A) gene biomarkers (COOLEN et al., 2007; LAM et al., 2007). The water column profiles of the menaquinones $MK_{6:0}$ and $MK_{6:1}$ trace the profile of intact polar crenarchaeol closely (Fig. 6.4), suggesting that these quinones are primarily sourced from *Thaumarchaeota* in the marine environment. This conclusion is supported by the observation that $MK_{6:0}$ and $MK_{6:1}$ abundances are not correlated with intact polar archaeols, which are the major archaeal lipids in the anoxic zone (Fig. 6.4e). These archaeols are likely sourced from Euryarchaeota such as methanogens (KOGA and MORII, 2005) and ANME (ROSSEL et al., 2008), which are abundant in the anoxic zone of the Black Sea (VETRIANI et al., 2003; SCHUBERT et al., 2006; WAKEHAM et al., 2007). Among our selection of cultures including literature data, $MK_{6:0}$ and $MK_{6:1}$ are only abundant in *Thaumarchaeota* (Fig. 6.3) and may thus serve as biomarkers for tracing thaumarchaeal abundance in aquatic environments. Vertical offsets in quinone vs. lipid abundances such as observed in the oxic zone of the Black Sea (Fig. 6.4) may reflect adaptations to environmental conditions (e.g., oxygen and ammonia availability) or changes in thaumarchaeal community composition.

The ratio of $MK_{6:0}$ and $MK_{6:1}$ to total quinones indicates that *Thaumarchaeota* likely dominate the microbial assemblages in a narrow interval of 90-120 m at the chemocline but are not quantitatively important in the oxic and anoxic part of the water column (Fig. 6.4; Supp. Table 6.3). Previous studies suggested that crenarchaeol core lipid maxima in the anoxic zone are related to metabolically adapted thaumarchaeal communities (COOLEN et al., 2007; WAKEHAM et al., 2007). However, our intact polar lipid and quinone profiles strongly suggest that *Thaumarchaeota* are confined to a narrow interval in the oxic and suboxic zone. Since crenarchaeol core lipids represent a predominantly fossil signal (INGALLS et al., 2012), quinone profiles appear to be better suited for tracing living Thaumarchaeota. Thus, the profiles of $MK_{6:0}$ and $MK_{6:1}$

suggest that previous crenarchaeol-based detection of Thaumarchaeota in the anoxic zone of the Black Sea may have been false positives. Considering the ubiquity of planktonic and benthic Thaumarchaeota in the oceans and other environments (STAHL and DE LA TORRE, 2012), $MK_{6:0}$ and $MK_{6:1}$ may have a high potential to serve as biomarkers for thaumarchaeal activity.

6.4. Experimental procedures

Archaeal strains described in this study were cultivated according to standard conditions. For detailed information please refer to supplementary information.

6.4.1. Suspended particulate matter sampling

Suspended particulate matter samples were collected in the southern Black Sea (41°31.70'N, 30°53.10'E, 1227 m water depth) in February 2011 at GeoB15105 during cruise M84/1 of R/V *Meteor* ("DARCSEAS I"; ZABEL and CRUISE PARTICIPANTS, 2011). Particulate matter was recovered at nine depths (40, 90, 120, 150, 300, 500, 700, 900, 1200 m) by pumping 6 to 204 liters of sea water through double pre-combusted 0.7 µm pore-size glass fiber filters using insitu pumps (for chemical zonation and corresponding CTD data refer to Supp. Table 6.2). Recovered filters were immediately wrapped in combusted aluminum foil and stored at −20 °C. Due to the use of 0.7 µm pore-size filters, membrane lipid and quinone concentrations should be regarded as minimum estimates (INGALLS et al., 2012).

6.4.2. Lipid and quinone extraction and analysis

Lipids and quinones were ultrasonically extracted from filters and biomass pellets following a modified Bligh & Dyer protocol (STURT et al., 2004) with dichloromethane:methanol:buffer (1:2:0.8, v:v:v) using phosphate and trichloroacetic acid (CCl_3CO_2H) buffers (each 2 times). The total lipid extract (TLE) was dried under a stream of N_2 and stored at −20 °C until measurement. Exposure to light was minimized during sample processing.

Respiratory quinones and intact polar membrane lipids were quantified by injecting an aliquot of the TLE dissolved in methanol on a Dionex Ultimate 3000 ultra-high performance liquid chromatography (UHPLC) system connected to a Bruker maXis Ultra-High Resolution quadrupole time-of-flight tandem mass spectrometer (qToF-MS) equipped with an ESI ion source operating in positive mode (Bruker Daltonik, Bremen, Germany). The mass spectrometer was set to a resolving power of 27,000 at m/z 1,222 and every analysis was mass-calibrated by loop injections of a calibration standard and

correction by lock mass, leading to a mass accuracy of <1-3 ppm. Ion source and other MS parameters were optimized by infusion of standards into the eluent flow from the LC system using a T-piece. Analyte separation was achieved using RP-HPLC on an ACE3 C18 column (2.1 x 150 mm, 3 µm particle size, Advanced Chromatography Technologies, Aberdeen, Scotland) maintained at 45 °C as described previously (ZHU et al., 2013). In brief, analytes were eluted at a flow rate of 0.2 ml/ min isocratically for 10 min with 100 % eluent A (methanol:formic acid:14.8 M NH_4^+, 100:0.04:0.10, v:v:v), followed by a linear gradient to 24 % eluent B (2-propanol:formic acid:14.8 M NH_4^+, 100:0.04:0.10, v:v:v) in 5 min, followed by a gradient to 65 % B in 55 min. The column was then flushed with 90 % B for 10 min and re-equilibrated with 100 % A for 10 min.

In order to demonstrate the simultaneous analysis of bacterial and archaeal quinones and membrane lipids, the samples were additionally analyzed on the same UHPLC-qToF-MS system under different chromatographic conditions using RP chromatography as described by WÖRMER et al. (2013). Briefly, 1 % TLE aliquots were dissolved in methanol:dichloromethane (9:1, v:v) and injected onto an Acquity UPLC BEH C18 column (1.7 µm, 2.1 x 150 mm, Waters, Eschborn, Germany) maintained at 65 °C. Analytes were eluted at a flow rate of 0.4 ml/ min using linear gradients of methanol:water (85:15, v:v, eluent A) to methanol:isopropanol (50:50, v:v, eluent B) both with 0.04 % formic acid and 0.1 % NH_3. The initial condition was 100 % A held for 2 min, followed by a gradient to 15 % B in 0.1 min and a gradient to 85 % B in 18 min. The column was then washed with 100 % B for 8 min.

Quinones and lipids were identified by retention time, molecular mass, and MS^2 fragmentation (cf. YOSHINAGA et al., 2011). Integration of peaks was performed on extracted ion chromatograms of ±10 mDa width and included the $[M+H]^+$, $[M+NH_4]^+$, and $[M+Na]^+$ ions. Where applicable, doubly charged ions were included in the integration. Quantification was achieved by injecting an internal standard (C_{46}-GTGT) along with the samples. The quinone abundances were corrected for the relative response of commercially available menaquinone ($MK_{4:4}$) and ubiquinone ($UQ_{10:10}$) standards (Sigma Aldrich, St. Louis, MO, USA) versus the C_{46}-GTGT standard. Analysis of quinone standard mixtures showed elution of $MK_{4:4}$ at 6.2 and $UQ_{10:10}$ at 23.6 min (Supp. Fig. 6.7a). Calibration curves of $MK_{4:4}$ and $UQ_{10:10}$ standards were established by injecting 1 pg to 10 ng quinone on column (Supp. Fig. 6.7b). The lower limit of detection was determined as <1 pg, considering a signal-to-noise ratio of greater than 3. Archaeal lipid abundances were corrected for response factors of commercially available and purified standards. Purified standards were gained from extracts of *A. fulgidus* by orthogonal semi-preparative liquid chromatography as described by ZHU et al. (2013). The abundances of mono- and diglycosidic crenarchaeol were corrected

for the response of the purified acyclic analogs. Due to the lack of an identical standard, the abundances of hexose-phosphohexose crenarchaeol were corrected for the response of a commercially available phosphatidylglycerol-hexose GDGT standard (Matreya LLC, Pleasant Gap, PA, USA). The abundances of mono- and diglycosidic archaeol were corrected for the respective purified standard, while phosphatidylglycerol, phosphatidylinositol and phosphatidylethanolamine archaeol abundances were corrected for the response of a commercial phosphatidylethanolamine archaeol standard (Avanti Polar Lipids Inc., Alabaster, AL, USA).

Acknowledgements

We thank C. Schleper, M. Stieglmeier (University of Vienna) for providing *N. viennensis*, E. Spieck (University of Hamburg) for providing *N. gargensis*, and G.W.Nicol, J.I. Prosser, and J. Ross (University of Aberdeen) for providing *N. devanaterra*. R.J. Whitaker (University of Illinois), A. Treusch, and S. Jensen (University of Southern Denmark) are thanked for providing *S. islandicus* strain Y.N.15.51. H. Huber and E.J. Gagen (University of Regensburg), C. House (Pennsylvania State University), M.W. Bowles, T.B. Meador, M.Y.Yoshinaga, X.-L. Liu, and C.A. Peters (University of Bremen) are thanked for providing biomass samples and lipid extracts of crenarchaeal and euryarchaeal strains.We thank A.-L. Ducluzeau for helpful discussions. We are grateful to the crew, chief scientist M. Zabel, and the scientific shipboard party of R/V *Meteor* cruise M84/1 (DARCSEAS I). We thank L.Wörmer and J.S.Lipp for supporting HPLC-MS analysis. This study was funded by the European Research Council under the European Union's Seventh Framework Programme–'Ideas' Specific Programme, ERC grant agreement No. 247153 (Advanced Grant DARCLIFE; PI: K.-U.H.) and by the Deutsche Forschungsgemeinschaft through the Gottfried Wilhelm Leibniz Prize awarded to K.-U.H. (Hi 616-14-1) and instrument grant Inst 144/300-1 (LC-qToF system).

6.5. Supporting Information

6.5.1. Cultivation of thaumarchaeal strains

Nitrosopumilus maritimus strain SCM1 was grown aerobically at 28 °C in 8.5-l batch cultures in pH 7.5 HEPES-buffered Synthetic Crenarchaeota Medium (SCM, 1.5 mM NH_4Cl) as described previously (KÖNNEKE et al., 2005; MARTENS-HABBENA et al., 2009; ELLING et al., 2014). Cultures were slightly shaken by hand twice a day when cultures reached a nitrite concentration of about 0.1 mM. Biomass was harvested in early stationary phase using cross-flow filtration and centrifugation.

Nitrososphaera gargensis strain (HATZENPICHLER et al., 2008) was grown at 46 °C in a 5-l batch culture in pH 7.8 SCM modified from KÖNNEKE et al. (2005) and KRÜMMEL and HARMS (1982) and harvested in early stationary phase. The medium contained 5 g l^{-1} NaCl, 1.5 g l^{-1} $CaCl_2$ x 2 H_2O, 1 g l^{-1} KCl, 0.5 g l^{-1} $MgCl_2$ x 6 H_2O, 0.5 g l^{-1} $MgSO_4$ x 7 H_2O, 2 g l^{-1} KH_2PO_4, 2 mM $NaHCO_3$, 7.5 µM FeNaEDTA, 1 mM NH_4Cl and 1 ml l^{-1} of a trace element solution (WIDDEL and BAK, 1992).

Nitrososphaera viennensis strain EN76 was grown at 37 °C in a 15-l batch culture in pH 7.5 HEPES-buffered freshwater medium modified from TOURNA et al. (2011) by addition of 1.5 mM pyruvate and 3 µM NH_4Cl and slight shaking (150 rpm). *N. viennensis* biomass was harvested in late exponential phase using centrifugation.

Nitrosotalea devanaterra strain Nd1 was grown 25 °C in a 6-l batch culture and pH 5.4 modified from LEHTOVIRTA-MORLEY et al. (2013) by addition of 0.08 g l^{-1} of CAS amino acids and 1 µM phthalate buffer solution. Cells were harvested in stationary phase using centrifugation.

6.5.2. Cultivation of crenarchaeal and euryarchaeal strains

Methanosarcina mazei (DSM 2053) and *Methanosarcina barkeri* (DSM 800) were grown at 35 °C in 100 ml of a freshwater medium (WIDDEL and BAK, 1992) supplemented with methanol, acetate and yeast extract. *Methanosarcina acetivorans* (DSM 2834) was grown at 35 °C in DSMZ medium 304 with methanol as the carbon source. All strains were harvested in stationary phase using centrifugation. *Sulfolobus islandicus* strain Y.N.15.51 (RENO et al., 2009) was grown at 80 °C and pH 4.2 in 1.5 L of DSMZ medium 182 amended with 5 g L^{-1} glucose. *S. islandicus* biomass was harvested by centrifugation at OD600 1.68, corresponding to stationary phase, and lyophilized before lipid extraction. *Haloferax volcanii* strain DS2 (ATCC 29605) and *Halorubrum lacusprofundi* strain ACAM34 (ATCC 49238) were grown at 17 °C using ATCC medium 974. *Methanothermococcus thermolithotrophicus* (DSM 2095) and *Methanopyrus kandleri* (DSM 6324) were grown at 85 °C in enamel-protected fermentors with stirring

(400 rpm) and continuous gassing (H_2/CO_2, 80/20). *Thermococcus kodakarensis* strain KOD1 (JCM 12380) was grown at 85 °C in JCM medium 280 as described previously (MEADOR et al., 2014a). *Methanothermobacter thermautotrophicus* strain Delta H (DSM 1053) was grown at 65 °C in 65-l bioreactors containing 50 l medium as described previously (YOSHINAGA et al., 2015). Biomass of *M. thermolithotrophicus*, *M. thermautotrophicus*, *M. kandleri*, and *T. kodakarensis* were harvested using centrifugation and subsequently lyophilized.

Freeze-dried biomass samples of *Aeropyrum pernix*, *Archaeoglobus fulgidus*, *Ignicoccus hospitalis*, *Metallosphaera prunae*, *Sulfolobus acidocaldarius*, *Sulfolobus solfataricus*, *Pyrococcus furiosus*, *Pyrolobus fumarii*, *Staphylothermus marinus*, and *Thermoplasma acidophilum* were provided by M. Thomm, E.J. Gagen, and H. Huber from the Archaeenzentrum, University of Regensburg, Germany. *A. pernix* (DSM 11879) was grown at 90 °C and pH 7 in Bacto Marine Broth (Difco 2216) amended with 0.1 % sodium thiosulfate and harvested in stationary phase. *A. fulgidus* (DSM 4304) was grown at 85 °C and pH 7 in MGG-Medium (HUBER et al., 1982) amended with 0.1 % lactate and yeast extract and harvested in late logarithmic phase. *I. hospitalis* (DSM 18386) was grown at 90 °C and pH 5.5 in 1/2 SME-Ignicoccus medium (PAPER et al., 2007) and harvested in stationary phase. *M. prunae* (DSM 10039) was grown at 70 °C and pH 2 in "Allen medium" (ALLEN, 1959) modified by addition of 0.1 % yeast extract (BROCK et al., 1972) and harvested in logarithmic phase. *S. acidocaldarius* (DSM 639) and *S. solfataricus* (DSM 1616) were grown at 75 °C and 80 °C, respectively, and pH 2 in the same medium as *M. prunae* and harvested in stationary phase. *P. furiosus* (DSM 3638) was grown at 95 °C and pH 7 in SME medium supplemented with 0.1 % yeast extract, peptone, and starch (HUBER and STETTER, 2006) and harvested in logarithmic phase. *P. fumarii* (DSM 11204) was grown at 106 °C and pH 6 in 1/2 SME medium amended with 0.1 % $NaNO_3$ (BLÖCHL et al., 1997) and harvested in logarithmic phase. *S. marinus* (DSM 3639) was grown at 85 °C and pH 7 in "Marine-Medium" supplemented with 0.1 % yeast extract and peptone (KELLER et al., 1995) and harvested in logarithmic phase. *T. acidophilum* (DSM 1728) was grown at 55 °C and pH 2.5 in Darland's medium containing 0.1 % yeast extract and 1 % glucose (DARLAND et al., 1970). An extract of *Archaeoglobus profundus* (DSM 5631) harvested in late exponential phase was provided by C. House (Pennsylvania State University).

6.5.3. Literature data

The distribution of quinone types in *Archaea* reported in this study was complemented with literature data compiled from the following sources: COLLINS et al. (1981), THURL

et al. (1985), THURL et al. (1986), COLLINS and TINDALL (1987), TINDALL et al. (1989, 1991), HENSEL et al. (1997), and NAMWONG et al. (2011).

Supplementary Table 6.1 Diagnostic fragment ions in MS^2 mode (related to loss of the headgroup) and midpoint redox potentials (E'_0 at pH 7, ordered by redox potential) of archaeal quinones and methanophenazine as well as bacterial ubiquinone (UQ) and eukaryotal plastoquinone (PQ). NA: not available.

Quinone	Diagnostic ions in MS^2	E'_0 (mV)	Citation (E'_0)
UQ	197.1	+112 ($UQ_{10:10}$)	(SCHNORF, 1966)
SQ	193	NA	-
CQ	179.0, 225.0	+106 ($CQ_{6:0}$)	(SCHÄFER et al., 1993)
PQ	151.1	+80 ($PQ_{9:9}$)	(OKAYAMA, 1976)
BDTQ	249	NA	-
MTK (sat./polyuns.)	219	NA	-
DMK (polyuns.)	173	+36 ($DMK_{8:8}$)	(HOLLÄNDER, 1976)
MK (sat.)	187.1	NA	-
MK (partially unsat.)	187.1	-78 ($MK_{4:1}$)	(WAGNER et al., 1974)
MK (polyuns.)	187.1, 253.1	-67 ($MK_{6:6}$)	(WAGNER et al., 1974)
MMK (sat.)	201.1	NA	-
MMK (polyuns.)	201.1, 267.1	-90 ($MMK_{6:6}$)	(DIETRICH and KLIMMEK, 2002)
MP (partially unsat.)	197.1	-165 ($MP_{5:4}$)	(TIETZE et al., 2003)

Supplementary Table 6.2 Sampling depth and pumped volume of *in situ* pumps inferred chemical zonation as well as density, salinity, and temperature obtained from CTD casts.

Water depth (m)	Pumped volume (l)	Chemical zone	Density (σ_θ)	Salinity (PSU)	Temperature (°C)
40	4.3	Oxic	14.2	17.8	8.5
90	6.1	Suboxic	15.4	18.7	8.5
120	23	Suboxic	15.9	19.8	8.4
150	204	Anoxic	16.4	20.5	8.5
300	10.8	Anoxic	16.8	21.7	8.8
500	11.4	Anoxic	17	22	8.9
700	21.3	Anoxic	17.1	22.2	8.9
900	9	Anoxic	17.2	22.3	9
1200	73.2	Anoxic	17.2	22.3	9

Supplementary Table 6.3 Menaquinone $MK_{6:0}$ and $MK_{6:1}$, and intact polar membrane lipid (IPL) concentrations ($ng\,l^{-1}$) in the Black Sea water column (n.d., not detected). IPL-Cren is the sum of IPLs with monoglycosidic, diglycosidic and hexose-phosphohexose headgroups attached to a crenarchaeol core lipid. Total IPL archaeols include archaeols with glycosidic and phosphatidic headgroups. Total quinones include menaquinones, ubiquinones, vitamin K1, and plastoquinones.

Water depth (m)	$MK_{6:0}$	$MK_{6:1}$	IPL-Cren	Total IPL-archaeols	Total quinones
40	0.18	0.15	7	10.4	4.3
90	0.27	0.24	26	8.8	0.7
120	0.36	0.22	43	8.2	0.6
150	0.06	0.01	6.5	3.3	1
300	0.09	0.02	1.5	79	9.4
500	0.06	0.01	6.2	38	2.6
700	0.02	0.02	2.9	85	2.2
900	0.03	0.01	n.d.	37	2.7
1200	0.01	0.01	0.4	33	0.2

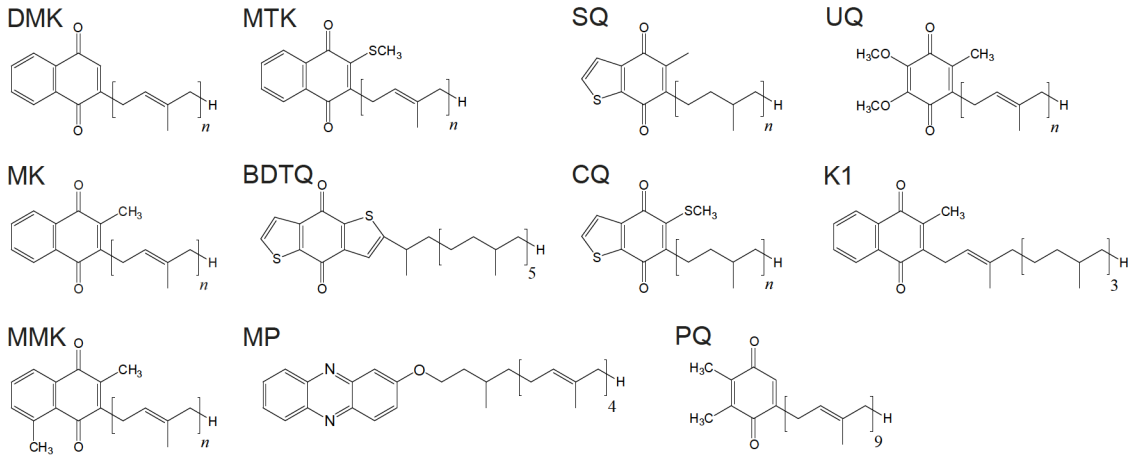

Supplementary Figure 6.1 Structures of respiratory quinone classes detected in cultivated archaea (DMK, MK, MMK, MTK, BDTQ, SQ, CQ) and bacteria (DMK, MK, MMK, MTK, UQ, K1, PQ) as well as methanophenazine, an electron carrier in *Methanosarcinales*. The length and degree of unsaturation of the isoprenoid side chains of quinones may vary from 4 to 14 and completely saturated to fully unsaturated, respectively. DMK: Demethylmenaquinone. MK: Menaquinone (vitamin K2). MMK: Methylmenaquinone. MTK: Methionaquinone. BDTQ: Benzodithiophenoquinone. MP: Methanophenazine. SQ: Sulfolobusquinone. CQ: Caldariellaquinone. PQ: Plastoquinone. UQ: Ubiquinone. K1: Vitamin K1 (synonyms: phylloquinone, $MK_{4:1}$).

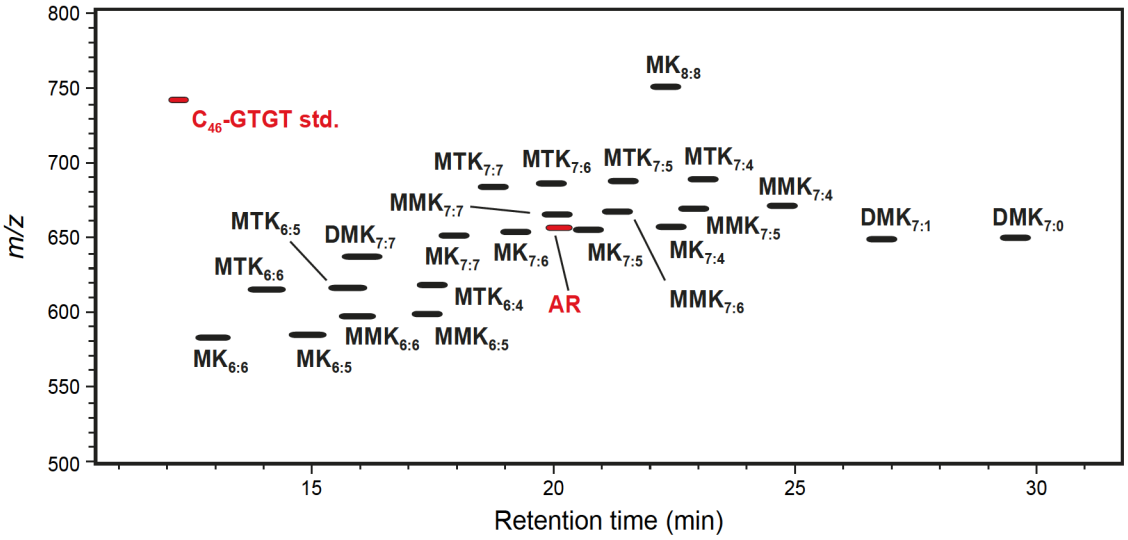

Supplementary Figure 6.2 Reconstructed density map obtained by reversed phase HPLC-MS showing elution of respiratory quinones (black) in an extract of *Thermoplasma acidophilum* relative to the C_{46}-GTGT standard and core archaeol (AR, red).

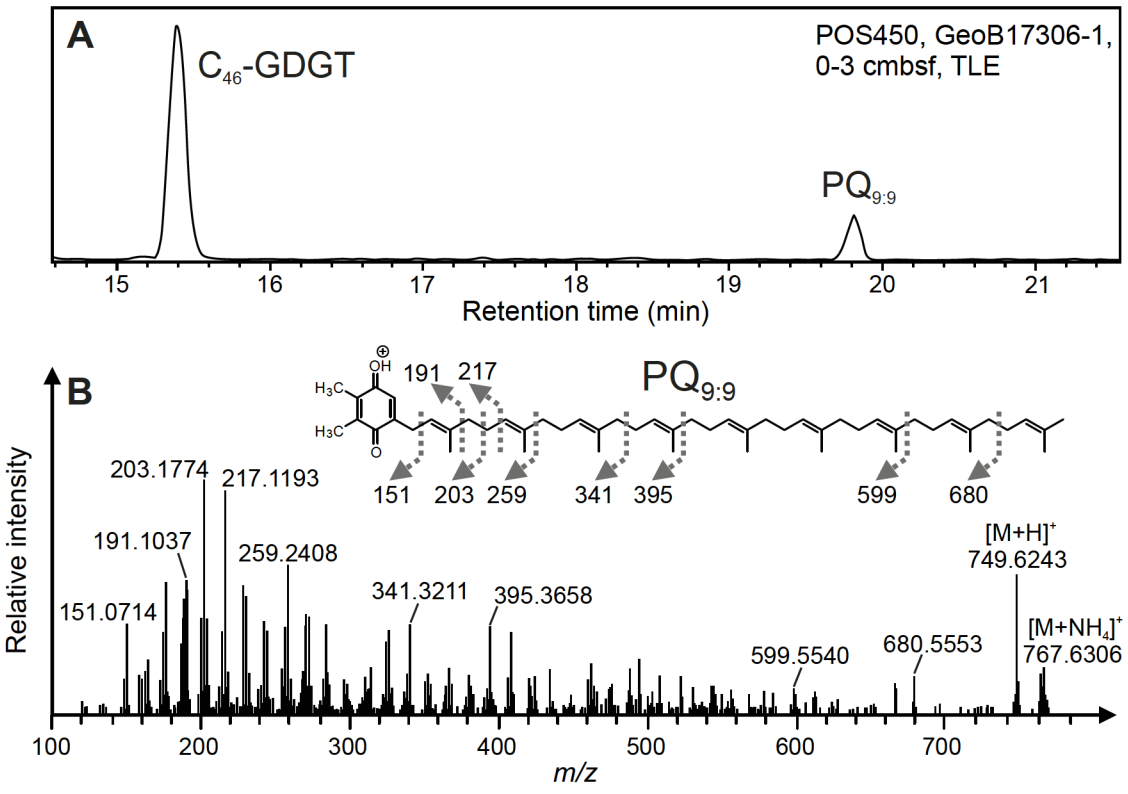

Supplementary Figure 6.3 Extracted ion chromatogram of C_{46}-GTGT and plastoquinone-9 ($PQ_{9:9}$; A) and MS^2 spectrum of $PQ_{9:9}$ obtained from a total lipid extract (TLE) of a marine sediment sample from the western Mediterranean Sea using the reversed phase HPLC-ESI-MS protocol of WÖRMER et al. (2013).

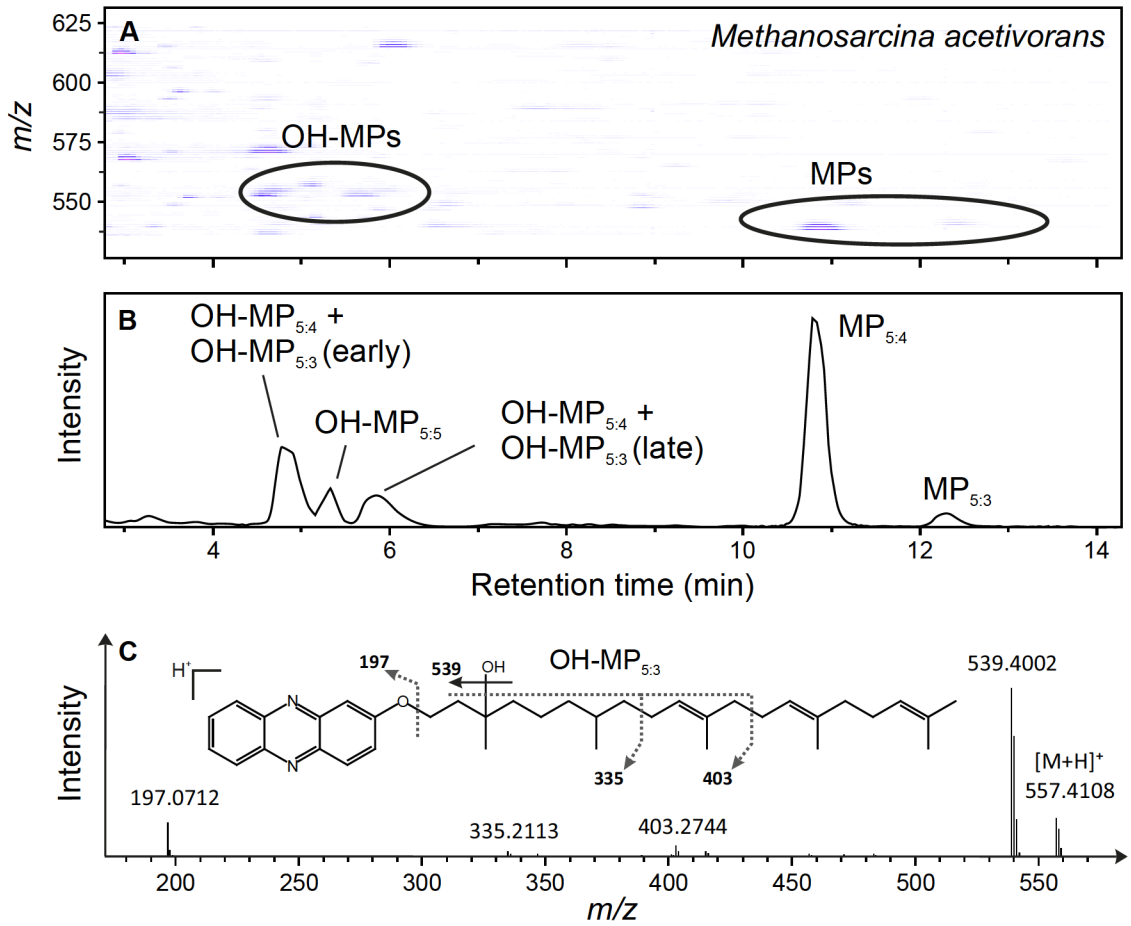

Supplementary Figure 6.4 Density map (A) and extracted ion chromatogram (B) obtained by reversed phase HPLC-MS showing elution of methanophenazines (MPs) and hydroxymethanophenazines (OH-MPs) in an extract of *M. acetivorans*. OH-$MP_{5:4}$ and OH-$MP_{5:3}$ show elution of two isomers. Panel (C) shows the tentative structure (position of double bonds and hydroxyl group not constrained) and MS^2 spectrum of OH-$MP_{5:3}$.

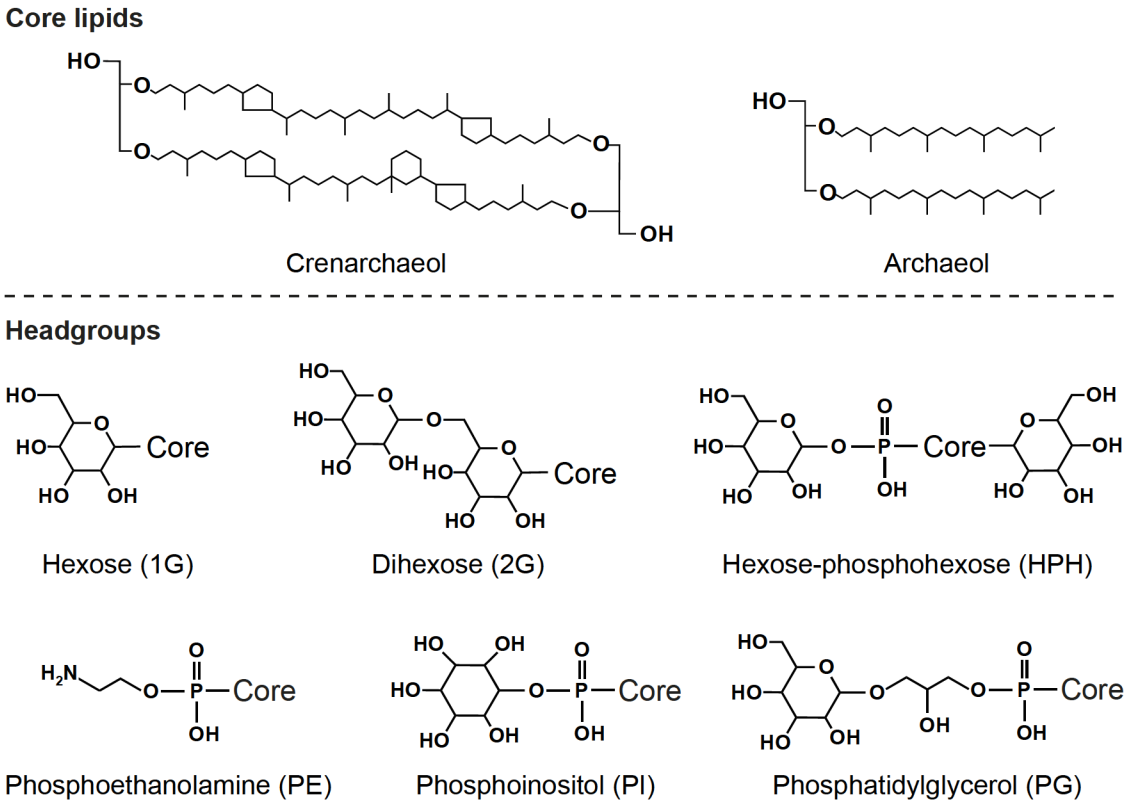

Supplementary Figure 6.5 Structures of archaeal core lipids and polar headgroups used for the calculation of total intact polar crenarchaeal and total intact polar archaeols (Fig. 6.4, Supp. Table 6.2). Intact polar lipids are combinations of a core lipid and one (GDGT, archaeol) or two headgroups (only GDGT).

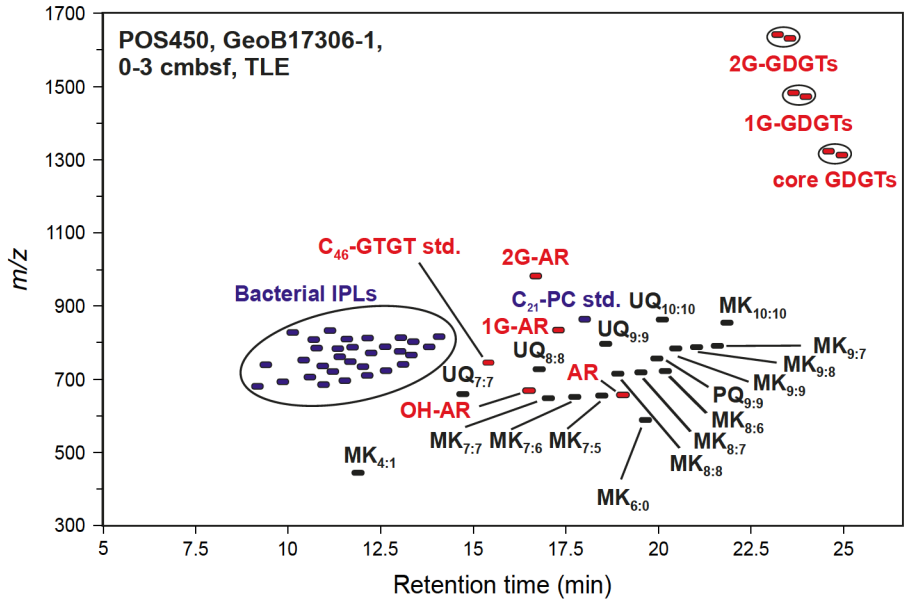

Supplementary Figure 6.6 Reconstructed density map showing elution of archaeal and bacterial respiratory quinones (black) and bacterial (blue) and archaeal (red) intact polar lipids from a marine sediment sample from the western Mediterranean Sea using the reversed phase HPLC-ESI-MS protocol of WÖRMER et al. (2013).

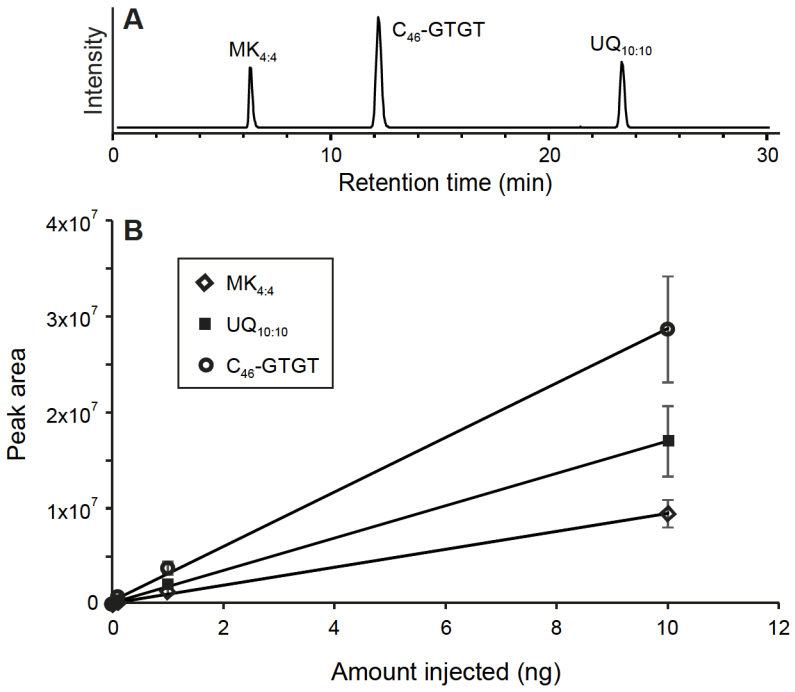

Supplementary Figure 6.7 Base peak chromatogram (**A**) and calibration curve (**B**) of a standard mixtures (0.001 ng, 0.1 ng, 1 ng, 10 ng on column) of C_{46}-GTGT, $MK_{4:4}$ and $UQ_{10:10}$ obtained by reversed phase HPLC-ESI-MS. Coefficient of correlation (r^2) of C_{46}-GTGT, $MK_{4:4}$ and $UQ_{10:10}$ was always >0.99. Error bars represent standard deviation of triplicate analyses.

CHAPTER 7

Sources, distribution and fate of respiratory quinones in the water column and sediments of the Black Sea

Kevin W. Becker[a,+*], **Felix J. Elling**[a,+], Jan M. Schröder[a], Julius S. Lipp[a], Matthias Zabel[b], Kai-Uwe Hinrichs[a]

In preparation for *Geochimica et Cosmochimica Acta*

[+]These authors contributed equally to this work.

[a] Organic Geochemistry Group, MARUM - Center for Marine Environmental Sciences & Department of Geosciences, University of Bremen, 28359 Bremen, Germany
[b] Inorganic Geochemistry Group, MARUM Center for Marine Environmental Sciences & Department of Geosciences, University of Bremen, 28359 Bremen, Germany

*Corresponding author. E-mail: k.becker@uni-bremen.de

Abstract

Isoprenoid quinones are a diverse group of membrane-bound lipids serving as electron carriers in the respiratory chains of almost all organisms. Complementary to the quantitative and phylogenetic information encoded in membrane lipid distributions, quinone compositions reflect specific metabolisms and source organisms. Recent analytical advances enable simultaneous profiling of quinones and membrane lipids in environmental samples. In order to demonstrate the utility of coupled environmental quinone and membrane lipid profiling, we investigated a vertical section of the water column and sediment in the Black Sea, the world's largest anoxic marine basin which is characterized by its pronounced physical, chemical, and microbial stratification. Depth distributions of diagnostic quinones and membrane lipids were correlated with zones of distinct microbial processes: In the oxic photic zone of the water column, high abundances of quinones and membrane lipids were associated with oxygenic photosynthesis and aerobic respiration. Maximum abundances of thaumarchaeal saturated menaquinones and isoprenoid tetraether lipids at the chemocline and the low abundances of other quinone types indicated that archaeal mediated ammonia oxidation was a major respiratory process occurring in the suboxic zone. A distinct peak in abundance of chlorobiumquinone and the characteristic pigment isorenieratene in the deeper anoxic part of the chemocline indicated the occurrence of sulfur-oxidizing anoxygenic photosynthetic green sulfur bacteria. High abundances of specific quinones and membrane lipids in the dark anoxic zone indicated high respiratory activity and biomass of denitrifying, ammonia-oxidizing, sulfur-oxidizing and sulfate-reducing bacteria as well as archaeal-mediated anaerobic oxidation of methane. Sulfate reduction as well as anaerobic oxidation of methane and/or methylotrophic methanogenesis were the major processes identified in the upper sediment based on geochemical data, high abundances of bacterial polyunsaturated menaquinones ester and ether phospholipids as well as *Methanosarcinales*-specific methanophenazines and archaeal diether lipids. The sapropel layer located at 4 m sediment depth was associated with a peak of dissolved ammonium concentration as well as maximum abundances of bacterial and archaeal IPLs and quinones, suggesting intense microbial heterotrophic activity in this organic matter-rich layer. High abundances of biogenic methane in the deeper sediment and the disappearance of methanophenazines near and below the sapropel indicated that methanogenesis in the deep sediment is not driven by *Methanosarcinales* but by other hydrogenotrophic methanogens. Our findings show that the simultaneous analysis of membrane lipids and respiratory quinones permits a reconstruction of the stratification of microbial communities in the water column and sediments of the Black Sea. This approach may therefore be a valuable tool for improving quantitative membrane lipid analyses by providing process-related information from respiratory quinones.

7.1. Introduction

Microbial mediated redox-reactions ultimately drive the global cycling of carbon, nitrogen, sulfur and other biologically active elements (NEWMAN and BANFIELD, 2002; DIETRICH et al., 2006; FALKOWSKI et al., 2008). On a cellular level, these redox reactions are utilized to maintain electron transport and proton gradients across the cytoplasmic membrane, which enable the generation of ATP and thus form the basis of the cellular economy in almost all organisms (MITCHELL, 1961; ANRAKU, 1988; SCHÄFER et al., 1999). An essential component of the electron transport chain are respiratory quinones, which are isoprenoid lipids that shuttle electrons and protons between membrane-bound protein complexes (ANRAKU, 1988; GRAY and ELLIS, 1994). Respiratory quinones are commonly classified based on the structure of a polar cyclic headgroup and can be further distinguished by the length and degree of unsaturation of the head-to-tail linked isoprenoid side chain (COLLINS and JONES, 1981; HIRAISHI, 1999). The distribution of structurally distinct quinones among eukaryotes and prokaryotes is determined both by phylogeny and, due to their distinct redox potentials, also by the operating respiratory pathway (Fig. 7.1; Table 7.1; COLLINS and JONES, 1981; BEKKER et al., 2007; NOWICKA and KRUK, 2010).

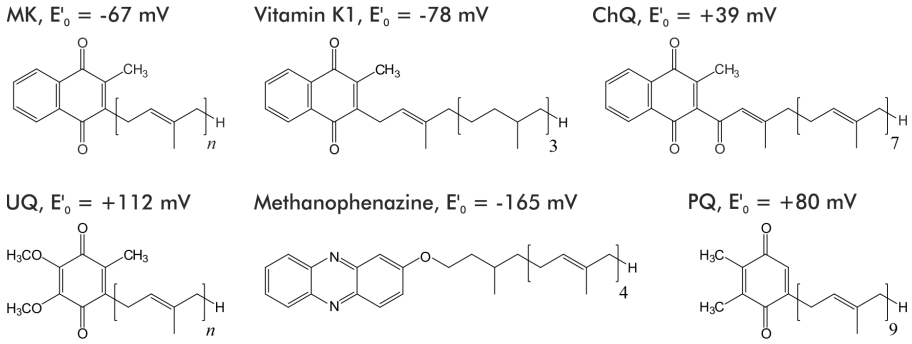

Figure 7.1. Structures and midpoint redox potentials (E_0', at pH 7) of archaeal (MK), bacterial (MK, UQ, PQ, ChQ), and eukaryotal (UQ, PQ, K1) respiratory quinone classes and the *Methanosarcinales*-specific functional quinone analog methanophenazine detected in water column and sediment samples from the southern Black Sea. The length and degree of unsaturation of the isoprenoid side chains of quinones may vary from 4 to 14 and completely saturated to fully unsaturated, respectively, while known methanophenazines comprise exclusively four isoprenoid units. MK: Menaquinone (vitamin K2). UQ: Ubiquinone. PQ: Plastoquinone. K1: Vitamin K1 (synonyms: phylloquinone, MK4:1). Redox potentials compiled from SCHNORF (1966), REDFEARN and POWLS (1968), WAGNER et al. (1974), OKAYAMA (1976), and TIETZE et al. (2003).

The major classes of quinones in bacteria are polyunsaturated ubiquinones (UQs) and menaquinones (MKs), which operate in aerobic and anaerobic metabolisms, respectively. UQs typically contain six ($UQ_{6:6}$) to ten ($UQ_{10:10}$) but in some organisms also up to 14 isoprenoid units and usually one double bond per isoprenoid unit,

hereafter termed fully unsaturated (quinone nomenclature $Q_{m:n}$ indicates headgroup type Q, number of isoprenoid units in the side chain m and number of double bonds n). UQs are involved in electron transport in the mitochondria and other compartments of eukaryotes (NOWICKA and KRUK, 2010). Quinones that are specific for oxygenic photosynthetic eukaryotes and bacteria are vitamin K1 (also known as phylloquinone or $MK_{4:1}$) and plastoquinones (predominantly $PQ_{9:9}$), which occur in photosystems I and II, respectively (Fig. 7.1; AMESZ, 1973; BRETTEL and LEIBL, 2001; NOWICKA and KRUK, 2010).

In contrast to bacteria and eukaryotes, polyunsaturated quinones exclusively occur in two archaeal lineages, the *Thermoplasmatales* and the *Halobacteriales* (Chapter 6; COLLINS et al., 1981; SHIMADA et al., 2001), the latter having acquired quinone biosynthesis genes from bacteria via lateral transfer (NELSON-SATHI et al., 2012). Most archaea produce saturated or partially unsaturated MKs with four to eight isoprenoid units (cf. Chapter 6), while specialized compounds are synthesized by some lineages such as sulfur-containing quinones in *Sulfolobales* (Chapter 6 and references therein). The only organisms that have been suggested not to produce quinones are fermentative bacteria and some representatives of the *Crenarchaeota* and *Euryarchaeota*, including methanogens (cf. Chapter 6). However, methanogenic *Euryarchaeota* of the order *Methanosarcinales* are known to substitute quinones with the functional analog methanophenazine (Fig. 7.1; Chapter 6; ABKEN et al., 1998).

Table 7.1. Diagnostic fragment ions in MS^2 mode (related to loss of the headgroup; from Chapter 6 and Fig. 7.4) and midpoint redox potentials (E_0', at pH 7, ordered by redox potential) of archaeal quinones and methanophenazine as well as bacterial and eukaryotal ubiquinone (UQ), plastoquinone (PQ), and chlorobiumquinone (ChQ). NA: not available.

Quinone	Diagnostic ions in MS^2	E_0' (mV)	Citation (E_0')
UQ	197.1	+112 ($UQ_{10:10}$)	SCHNORF (1966)
PQ	151.1	+80 ($PQ_{9:9}$)	OKAYAMA (1976)
ChQ	201.1	+39 ($ChQ_{7:7}$)	REDFEARN and POWLS (1968)
MK (sat.)	187.1	NA	-
MK (partially unsat.)	187.1	−78 ($MK_{4:1}$)	WAGNER et al. (1974)
MK (polyuns.)	187.1, 253.1	−67 ($MK_{6:6}$)	WAGNER et al. (1974)
MP (partially unsat.)	197.1	−165 ($MP_{5:4}$)	TIETZE et al. (2003)

Given the large structural diversity of respiratory quinones, detailed knowledge of their phylogenetic distribution and their distinct redox-potentials, quinones offer a high

potential as process-specific biomarkers in environmental studies (Chapter 6; HIRAISHI, 1999; URAKAWA et al., 2000; KUNIHIRO et al., 2014). In contrast to the increasing use of intact polar membrane lipid (IPL) analysis in marine environmental samples (e.g., LIPP et al., 2008; SCHUBOTZ et al., 2009; POPENDORF et al., 2011), respiratory quinone analysis has been rarely employed in microbial community profiling (HEDRICK and WHITE, 1986; URAKAWA et al., 2000; URAKAWA et al., 2001; URAKAWA et al., 2005; KUNIHIRO et al., 2014). However, tracing living microbial cells by IPL profiling may prove challenging in some environments (LIPP and HINRICHS, 2009; SCHOUTEN et al., 2010; LIU et al., 2011), particularly due to the largely unconstrained degradation rates of intact lipids (XIE et al., 2013). Environmental IPL-profiling therefore benefits from complementary biomarker approaches (e.g., SCHUBOTZ et al., 2013). Novel high-performance liquid chromatography-mass spectrometry (HPLC-MS) protocols enable simultaneous profiling of quinones and membrane lipids in a single analysis (cf. Chapter 6), thus opening new avenues for complementing the quantitative and phylogenetic information contained in membrane lipid distributions with process-specific quinone distributions.

To demonstrate the utility of coupled environmental quinone and membrane lipid profiling, we studied a sequence of water column and sediment samples in the southern Black Sea (Fig. 7.2). Here, aerobic respiration depletes oxygen in the upper 40 to 200 m of the water column, while a shallow halocline leads to permanent water column stratification and thus prevents oxygenation of deeper waters (SOROKIN, 2002). This oxic-anoxic interface is associated with a multilayered chemocline. The depth of this chemocline is temporally and spatially variable (MURRAY et al., 1989; JØRGENSEN et al., 1991; COOLEN et al., 2007). The oxic zone is separated from the anoxic zone by a 20-40 m thick suboxic transition zone with no detectable sulfide (MURRAY et al., 1989; SOROKIN, 2002). Chemoautotrophic carbon fixation supports high standing stocks of microbial biomass at the chemocline, accounting for 10 to 32 % of photoautotrophic productivity at the surface (KARL and KNAUER, 1991; SOROKIN et al., 1995).

Within the transition zone, microbes mediate a cascade of redox processes that can be traced by the sequence of nitrogen-, sulfur-, and metal species (JANNASCH, 1991; SOROKIN et al., 1995) and associated microbial biomarkers (e.g., SCHUBERT et al., 2006; WAKEHAM et al., 2007; SCHUBOTZ et al., 2009; FUCHSMAN et al., 2011). Quantitatively important processes include ammonium and nitrite cycling by nitrifying archaea and bacteria as well as anaerobic ammonia-oxidizing bacteria (KUYPERS et al., 2003; COOLEN et al., 2007; LAM et al., 2007), sulfide and thiosulfide oxidation e.g., by phototrophic green sulfur bacteria and *Shewanella* spp. (JANNASCH et al., 1991; JØRGENSEN et al., 1991; PERRY et al., 1993), aerobic methane oxidation by *Proteobacteria* (SCHUBERT et al., 2006) as well as bacterial Fe and Mn cycling (e.g.,

NEALSON et al., 1991; FUCHSMAN et al., 2011). In the anoxic zone, sulfate reduction and anaerobic oxidation of methane are major microbial metabolisms (REEBURGH et al., 1991; ALBERT et al., 1995; SCHUBERT et al., 2006; WAKEHAM et al., 2007), which extend into the sediment.

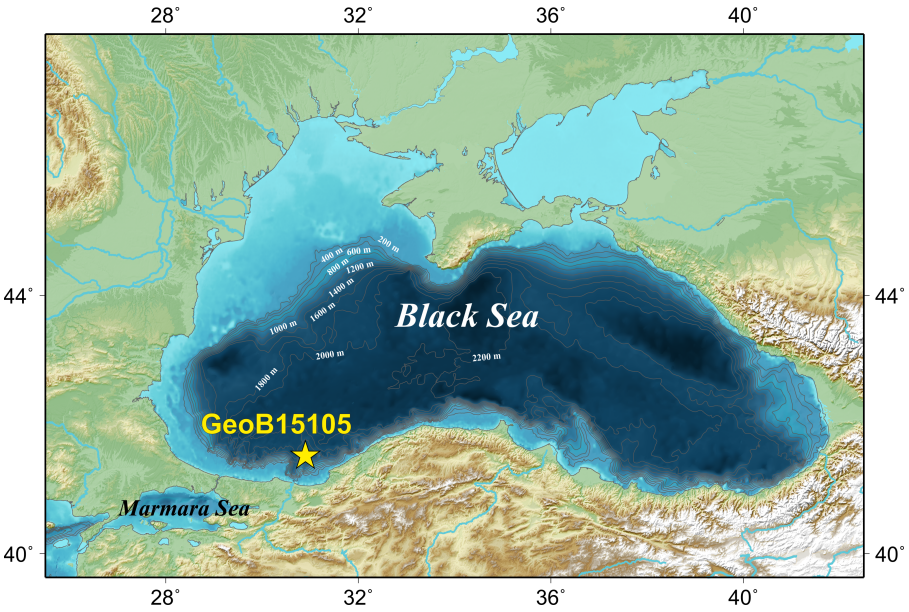

Figure 7.2. Location of the study site at the southern continental slope of the Black Sea (GeoB15105, 41°31.70'N, 30°53.10'E, 1227 m water depth) sampled during R/V Meteor cruise M84/1.

While the depth distribution of the major sedimentary geochemical zones varies spatially, microbial processes form a continuum from the water column to the sediment of the Black Sea (JØRGENSEN et al., 2004; KNAB et al., 2009). Sulfate reduction is the major carbon-remineralizing process in the surface sediments (JØRGENSEN et al., 2001), since other common electron acceptors such as oxygen and nitrate are either depleted at the chemocline (MURRAY and YAKUSHEV, 2006) or settle at the seafloor in reduced form such as iron and manganese (KONOVALOV et al., 2004). The sulfate reduction zone extends up to 4 m into the sediment and partially overlaps with the underlying methanogenic zone (JØRGENSEN et al., 2001, 2004; LELOUP et al., 2007). Anaerobic oxidation of methane occurs both within the surface sediment (REEBURGH et al., 1991; RIEDINGER et al., 2010) as well as within the comparatively broad sulfate methane transition zone (JØRGENSEN et al., 2001).

In this study, we applied novel HPLC-MS protocols to investigate the quinone and lipid distribution in the water column and sediments in the southwestern Black Sea, which allowed the detection of a significantly larger variety of compounds compared to previous techniques (URAKAWA et al., 2000; KUNIHIRO et al., 2014). The depth distributions of diagnostic quinones and membrane lipids in the water column were

correlated with the zonation of microbial processes, such as nitrification and sulfur oxidation. Based on the distribution of quinones in water and sediment samples, we suggest that, while some sedimentary quinones may be derived from the water column, a plethora of compounds is being produced *in situ* and may therefore be used to characterize and quantify the benthic microbial community.

7.2. Materials and Methods

7.2.1. Suspended particulate matter and sediment sampling

Suspended particulate matter and sediment samples were collected in the southern Black Sea in February 2011 at site GeoB15105 (Fig. 7.2; 41°31.70'N, 30°53.10'E, 1227 m water depth) during R/V Meteor cruise M84/1 ('DARCSEAS I'; ZABEL and CRUISE PARTICIPANTS, 2011). Suspended particulate matter was recovered at nine depths (40, 90, 120, 150, 300, 500, 700, 900, 1200 m) by pumping 6 to 204 liters of sea water through two stacked pre-combusted 0.7 µm pore-size glass fiber filters using *in situ* pumps. Recovered filters were immediately wrapped in combusted aluminum foil and stored at −20 °C. Due to the use of 0.7 µm pore-size filters, membrane lipid and quinone concentrations should be regarded as minimum estimates (cf. XIE et al., 2014). Pore water was extracted from sediment cores with Rhizon micro suction samplers (0.1 µm filter width, Rhizosphere Research Products, Wageningen) and split into subsamples for onshore analysis. Sediments were recovered using a multi-corer (GeoB15105-4) and a gravity corer (GeoB15105-2), sampled in a cold room at 4 °C and stored at −20 °C in brown glass bottles until extraction. At the study site, sedimentary units in the sampled upper 8 m comprise laminated coccolith ooze (Unit I, ca. 4 % dry weight TOC) deposited during the last 3 ka as well as an organic-rich sapropel (Unit II, up to 15 % dry wt. TOC) deposited from 7.5 to 3 ka before present (BRUMSACK, 1989; BAHR et al., 2005; KWIECIEN et al., 2008), coeval to the development of water column anoxia in the Black Sea (ARTHUR and DEAN, 1998; ECKERT et al., 2013).

Water column profiles of temperature, fluorescence and depth as well as pressure and dissolved oxygen were measured with a vertical resolution of 1 m using a CTD rosette (GeoB15105-5). Salinity was derived from conductivity, while density was calculated from pressure and temperature measurements as well as salinity.

7.2.2. Water column and pore water chemistry

Water column samples (10 to 20 ml) were directly filtered from the Niskin bottle (0.2 µm syringe micro filter) after the recovery of the CTD-equipped rosette. Pore water samples were taken from closed MUC cores and gravity cores and collected through

rhizon micro suction samplers (5 cm length, 0.2 µm porous polymer). Dissolved sulfate (SO_4^{2-}) was determined by ion chromatography (Metrohm Compact IC, METROSEP A Supp 5 column, conductivity detection after chemical suppression) in samples diluted 1:100 with Milli-Q grade H_2O. Concentrations of dissolved phosphate (PO_4^{3-}) were measured photometrically. One ml of sample was placed in a disposable polystyrene (PS) cuvette (2.5 ml) containing 50 µl ammonium molybdate solution, and amended with 50 µl of an ascorbic acid solution. The extinction of the phosphomolybdenum blue complex was measured after 10 min at a wavelength of 820 nm (Hach Lange DR 5000 photometer). Dissolved ammonium (NH_4^+) was measured using a flow injection, PTFE tape gas separator technique after HALL and ALLER (1992). About 200 to 300 µl of plain sample were injected into a 100 µl loop of a Rheodyne valve and mixed with an alkaline solution (0.01 M NaOH + 0.2 M sodium citrate) to form gaseous NH_3 that passed a PTFE membrane and caused a conductivity signal in a receiving acid solution (0.001 M HCl). The resulting conductivity was determined using a temperature-compensated conductivity meter (Amber Scientific 1056) with a micro flow-through cell (Amber Scientific 529) and recorded on a strip chart recorder. Dissolved hydrogen sulfide (HS^-) was determined in samples fixed with $ZnCl_2$ using the photometric methylene blue method (CLINE, 1969).

7.2.3. Hydrocarbon gases

Concentrations of dissolved methane were determined according to previously reported protocols (KVENVOLDEN and MCDONALD, 1986; D'HONDT et al., 2003). Two to three ml of wet sediment were enclosed in a gas-tight 22-ml glass vial with a Teflon septum and heated for 20 min at 60 °C. After heating, 100 to 500 µl sub-samples were taken from the headspace gas with a gas-tight syringe and analyzed on board by gas chromatography-flame ionization detection (GC-FID). The GC-FID was calibrated on a daily basis using hydrocarbon gas standards (Scotty Specialty Gases). Based on the partial pressure of methane in the headspace gas and the headspace volume, the total amount of released methane was quantified and normalized to the pore-water volume of the extracted sediment sample, using the sample volume and corresponding porosity data of solid phase samples.

The stable carbon isotopic composition of methane ($\delta^{13}CH_4$) was determined from duplicate GC-isotope ratio mass spectrometry (GC-irMS) analyses using a ThermoFinnigan Trace GC Ultra coupled to a DELTA Plus XP mass spectrometer equipped with via a ThermoFinnigan GC Combustion III interface. An aliquot of 200 µl of the headspace gas was injected into the GC using a split ratio of 1:3. The components were separated isothermally at 40 °C for 8 min using a Carboxen-1006 PLOT fused-silica capillary col-

umn (30 m x 0.32 mm ID; Supelco, Inc, USA) at a constant Helium flow of 3 ml min^{-1}. The system was calibrated at the start and end of the run using a reference gas with known carbon isotopic composition. Carbon isotope ratios are reported in the δ-notation as per mil deviation from the Vienna Pee Dee Belemnite standard. Analytical precision was determined by repeated injections of commercially available standards (100 ppm methane, Air Liquide) and was typically better than 1‰.

7.2.4. Quinone and membrane lipid extraction and analysis

Respiratory quinones and membrane lipids were ultrasonically extracted from filters and sediments after addition of an extraction standard (phosphatidylcholine (PC) $C_{21:0}$) following a modified Bligh & Dyer protocol (STURT et al., 2004) with dichloromethane:methanol:buffer (1:2:0.8, v:v:v) using phosphate and trichloroacetic acid (CCl_3CO_2H) buffers (each 2x). After each extraction step, the samples were centrifuged at 800 × *g* for 10 min and the supernatants were collected in a separation funnel. The combined supernatants were then washed three times with de-ionized MilliQ water. After separation into organic phase and water-soluble phase, the organic phase was collected as the total lipid extract (TLE). The TLE was dried under a stream of N_2 and stored at −20 °C until measurement.

Quinones and archaeal IPLs were analyzed by injecting an aliquot of the TLE dissolved in methanol on a Dionex Ultimate 3000 high performance liquid chromatography (HPLC) system connected to a Bruker maXis Ultra-High Resolution quadrupole time-of-flight tandem mass spectrometer (qToF-MS) equipped with an ESI ion source operating in positive mode (Bruker Daltonik, Bremen, Germany). The mass spectrometer was set to a resolving power of 27,000 at m/z 1222 and every analysis was mass-calibrated by loop injections of a calibration standard and correction by lock mass, leading to a mass accuracy of <1-3 ppm. Ion source and other MS parameters were optimized by infusion of standards into the eluent flow from the LC system using a T-piece.

Analyte separation was achieved using reversed phase (RP) HPLC on an ACE3 C_{18} column (2.1 x 150 mm, 3 µm particle size, Advanced Chromatography Technologies, Aberdeen, Scotland) maintained at 45 °C as described previously (ZHU et al., 2013). In brief, analytes were eluted at a flow rate of 0.2 ml min^{-1} isocratically for 10 minutes with 100 % eluent A (methanol:formic acid:14.8 M NH_4^+, 100:0.04:0.10, v:v:v), followed by a linear gradient to 24 % eluent B (2-propanol:formic acid:14.8 M NH_4^+, 100:0.04:0.10, v:v:v) in 5 minutes, followed by a gradient to 65 % B in 55 minutes. The column was then flushed with 90 % B for 10 minutes and re-equilibrated with 100 % A for 10 minutes. Quinones and lipids were identified by retention time, accurate

molecular mass, and MS^2 fragmentation (Table 7.1; cf. Chapter 6; STURT et al., 2004; YOSHINAGA et al., 2011). Integration of peaks was performed on extracted ion chromatograms of ±10 mDa width and included the $[M+H]^+$, $[M+NH_4]^+$, and $[M+Na]^+$ ions. Where applicable, double charged ions were included in the integration.

Additionally, selected samples were analyzed for low-abundance methanophenazines and archaeal lipids under the same chromatographic conditions on a Dionex Ultimate 3000 HPLC system connected to an ABSciEX QTRAP4500 Triple Quadrupole/Ion Trap MS equipped with an ESI ion source operating in positive mode. Target compounds were detected by multiple reaction monitoring of diagnostic MS/MS transitions. Ion source, multiple reaction monitoring transitions and other MS parameters were optimized by direct infusion of commercially available lipid and quinone standards as well as total lipid extracts of *Nitrosopumilus maritimus* and *Methanosarcina acetivorans*.

Bacterial IPLs were analyzed by injecting 1-10 % of the TLE dissolved in dichloromethane:methanol (9:1, v:v) on a Dionex Ultimate 3000 HPLC system connected to a Bruker maXis Ultra-High Resolution qToF-MS equipped with an ESI ion source operating in positive mode as described above. Analyte separation was achieved using normal phase HPLC on an Acquity UPLC BEH Amide column (1.7 µm, 2.1 x 150 mm; Waters Corporation, Eschborn, Germany) maintained at 40 °C as described by WÖRMER et al. (2013). In brief, analytes were eluted at a flow rate of 0.4 ml min^{-1} with 99 % eluent A (acetonitrile:dichloromethane, 75:25, with each 0.01 % formic acid and NH_3) and 1 % eluent B (methanol:water, 50:50, with 0.4 % formic acid and NH_3) for 2.5 min, increasing B to 5 % at 4 min, to 20 % B at 22.5 min and 40 % B at 26.5 min. The column was then flushed with 40 % B for 1 min.

Archaeal IPL and quinone quantification was achieved by injecting a known amount of an internal standard (C_{46}-GTGT) along with the samples. Bacterial IPLs were quantified by comparing their peak areas with the peak area of the extraction standard. The quinone abundances were corrected for the relative response of commercially available menaquinone ($MK_{4:4}$, for MKs, chlorobiumquinone (ChQ), vitamin K1) and ubiquinone ($UQ_{10:10}$, *trans*-isomer, for UQs, PQs) standards (Sigma Aldrich, St. Louis, MO, USA) versus the C_{46}-GTGT standard. Due to a lack of an authentic standard, MP concentrations were not corrected for their relative response and are thus not included in total quinone abundance and distribution patterns as well as calculations of diversity indices. The detection limit for quinones, intact polar and neutral lipids as detected for authentic standards using the qToF-MS was approximately 1 pg, depending on compound class and considering a signal-to-noise ratio of greater than 3.

Archaeal lipid abundances were corrected for response factors of commercially available and purified standards. Purified standards were obtained from extracts of *Archaeoglobus fulgidus* as described in ELLING et al. (2014). The abundances of mono-

(1G) and diglycosidic (2G) glycerol dibiphytanyl glycerol tetraethers (GDGTs) and hydroxylated GDGTs were corrected for the response of purified acyclic 1G- and 2G-GDGT standards, respectively. Due to the lack of an identical standard, the abundances of hexose phosphohexose (HPH) GDGTs were corrected for the response of a commercially available phosphatidylglycerol-hexose GDGT standard (Matreya LLC, Pleasant Gap, PA, USA) as described in ELLING et al. (2014). The abundances of mono- and diglycosidic archaeol were corrected for the respective purified standard, while phosphatidylglycerol (PG), phosphatidylinositol (PI) and phosphatidylethanolamine (PE) archaeol abundances were corrected for the response of a commercial phosphatidylethanolamine archaeol standard (Avanti Polar Lipids Inc., Alabaster, AL, USA).

The abundances of isorenieratene were corrected by the relative response of a commercial β-carotene standard (Sigma Aldrich). Similarly, the abundances of cholesterol and alkenones were corrected by the relative response of a commercial cholesterol standard (Sigma Aldrich) and synthetic $C_{37:2}$ and $C_{37:3}$ alkenone standards (RECHKA and MAXWELL, 1988). The abundances of diacylglycerol (DAG) and dietherglycerol (DEG) lipids with phosphatidylglycerol (PG), PE, monomethyl PE (PME) and dimethyl PE (PDME), were corrected by the relative responses of commercial DAG-$C_{16:0/16:0}$ standards with the respective headgroup (Avanti). The abundances of intact polar acyletherglycerol (AEG) lipids were corrected for the response of the respective DAG standard. The abundances of diphosphatidylglycerol (DPG), PC-DEG, 1G- and 2G-DAG lipids were corrected by the relative responses of DPG-$C_{18:1}$, PC-DEG-$C_{16:0/16:0}$ standards, 1G-DAG-$C_{16:0/16:0\text{-cyclopropyl}}$ (Avanti) and 2G-DAG-$C_{18:0/18:0}$ (Matreya) standards, respectively. Abundances of monoglycosidic Ceramides (1G-Cer) and hydroxylated PG (PG-OH)-Cer were corrected for the relative response of a 1G-Cer-$C_{18:1/18:0}$ standard (Avanti). Due to a lack of appropriate standards, ornithine and betaine lipids as well as DAG lipids with PI headgroups were not corrected for their relative response.

Microbial (MD_q) and bioenergetic divergence indices (BD_q) were calculated after IWASAKI and HIRAISHI (1998):

$$MD_q = \left(\sum_{k=1}^{p} \sqrt{x_k} \right)^z \qquad \text{(Eq. 1)}$$

where x_k indicates the abundance of quinone k relative to total quinones.

$$BD_q = \left(\sqrt{UQ} + \sqrt{PQ + K1} + \sqrt{polyuns\ MK} + \sqrt{sat + monouns\ MK} + \sqrt{ChQ} \right)^2 \qquad \text{(Eq. 2)}$$

where UQ, PQ, vitamin K1, polyunsaturated (polyuns) MK, saturated (sat) MK, mono-

unsaturated (monouns) MK and ChQ indicate the relative abundance of UQs, PQs, vitamin K1, polyuns MKs, sat MKs, monouns MKs and ChQ of total quinones as 1, respectively.

7.3. Results

7.3.1. Water column and sediment chemistry

Geochemical data of the Black Sea water column revealed a strong vertical stratification (Fig. 7.3). The salinity increased from 17.7 at the surface to 22.3 in deep waters (Fig. 7.3A). The steepest increase occurred between 80 and 150 meters below sea level (mbsl). The temperature profile behaved similarly and ranged between 8.5 and 9 °C (Fig. 7.3A). A minimum in fluorescence was detected at 70 mbsl (Fig. 7.3B). Dissolved oxygen concentrations decreased in a narrow depth interval between 70 and 150 mbsl from more than 250 $\mu mol\,kg^{-1}$ to below detection (Fig. 7.3C). Hydrogen sulfide was first detected below a depth of 100 mbsl and slightly increased in concentration to 11.5 $\mu mol\,l^{-1}$ at ca. 1100 mbsl (Fig. 7.3C). In the sample from 1205 mbsl, HS^- concentration showed a strong increase to 38.6 $\mu mol\,l^{-1}$. Both, dissolved phosphate (PO_4^{3-}) and ammonium (NH_4^+) were only detected below 150 mbsl. While PO_4^{3-} showed a distinct peak at this depth, NH_4^+ increased towards the seafloor. Phosphate concentrations followed this trend between 200 and 1200 m (Fig. 7.3D). The suboxic zone is located at approximately 70 to 150 m water depth at the boundary between the oxic surface and anoxic deep layers. In this zone O_2 and HS^- co-occur and the concentrations of both are low. Thus, we defined the zonation of the water column at site GeoB15105 as follows: oxic zone from 0 to 70 mbsl, suboxic zone (chemocline) from 70 to 150 mbsl, and anoxic zone from 150 mbsl to the seafloor.

The pore water profiles of dissolved PO_4^{3-} and NH_4^+ followed similar trends with increasing concentrations within the first 2 m of the sediment (Fig. 7.3E). Ammonium concentrations were ca. eight to ten times higher than phosphate concentrations. While NH_4^+ concentrations stayed fairly constant below 200 cm below seafloor (cmbsf), PO_4^{3-} concentrations slightly decreased towards the deepest sample. Dissolved sulfate decreased with sediment depth, reaching minimum values at 400 cmbsf. Hydrogen sulfide concentrations showed a maximum at approximately 100 cmbsf. Below 400 cmbsf, concentrations were close to zero (Fig. 7.3F). Methane concentrations were low (<75 µmol) in the top 30 cm of the sediment, but increased to almost 15.4 mM at 623 cmbsf. The $\delta^{13}C_{CH_4}$ values significantly decreased from −53‰ to −88.5‰ within the top 127 cmbsf. Below this depth, $\delta^{13}C_{CH_4}$ values increased to −69‰ in the deepest investigated sample (Fig. 7.3G).

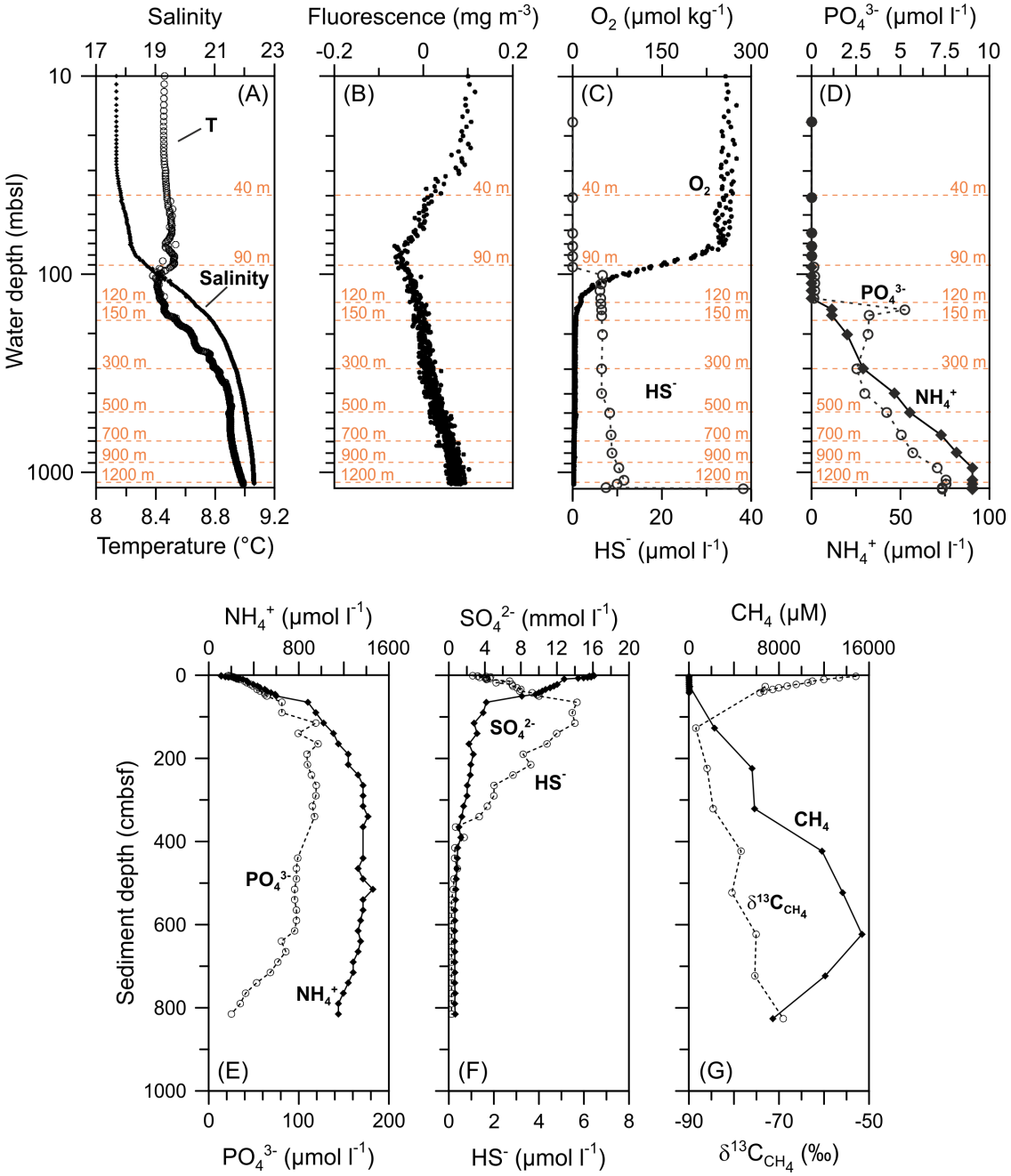

Figure 7.3. Chemistry for the Black Sea water column and pore waters of the sediment. For the water column salinity and temperature (A), fluorescence (B), dissolved oxygen and hydrogen sulfide (C), and phosphate and ammonium (D) are shown. Additionally, sampling depth for lipid and quinone analysis are indicated by horizontal dashed lines. The depth is shown on a logarithmic scale (10 to 1200 mbsl) to emphasize the suboxic zone. For the pore waters phosphate and ammonium (E), sulfate and hydrogen sulfide (F), and methane and δ^{13}C of methane (G) are shown.

7.3.2. Detection of novel quinones

Quinones detected in the Black Sea suspended particulate matter and sediment samples comprised vitamin K1, $PQ_{9:9}$, $ChQ_{7:7}$, polyunsaturated UQs and MKs with variable chain lengths and degrees of unsaturation, fully saturated and monounsaturated MK_6 as well as the functional quinone analogs $MP_{5:4}$ and $MP_{5:3}$ (Fig. 7.5A). $ChQ_{7:7}$ was detected here for the first time in environmental samples. The structure of $ChQ_{7:7}$ was confirmed by comparing MS^2 spectra of $ChQ_{7:7}$ in the samples (Fig. 7.4) with literature data (POWLS et al., 1968).

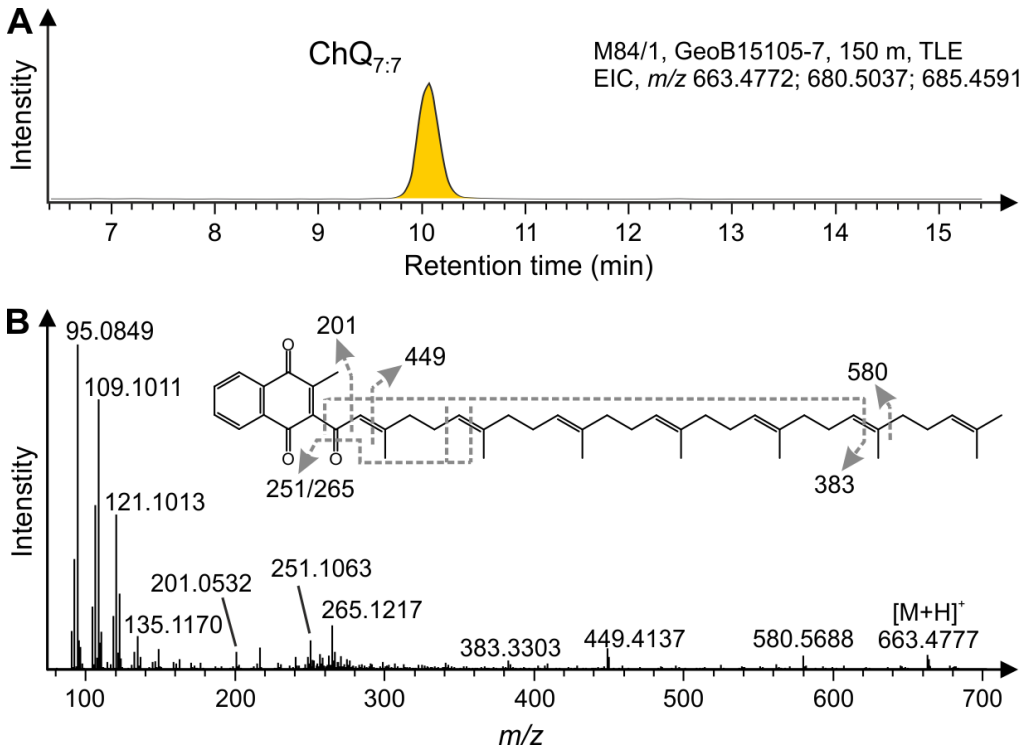

Figure 7.4. (A) Extracted ion chromatogram (EIC), obtained by RP-HPLC-ESI-MS, showing elution of chlorobiumquinone ($ChQ_{7:7}$) in a Black Sea suspended particulate matter sample from 150 m water depth. (B) MS^2 spectrum and structure of $ChQ_{7:7}$ ($[M+H]^+$ ion of m/z 663.5) as well as major product ions in the range m/z 50-700.

We additionally tentatively identified several novel UQ and MK isomers based on accurate molecular mass in full scan (MS^1) mode and characteristic fragmentation in MS^2 mode (Fig. 7.5). The quinones $UQ_{7:7}$ to $UQ_{10:10}$ each showed one early ($UQ_{m:n}$(a)) and one late ($UQ_{m:n}$(b)) eluting isomer and the two associated compounds for each UQ revealed highly similar MS^2 fragmentation (Fig. 7.3B). The major product ion at m/z 197.1 represented the UQ head group. Minor fragments resulted from fragmentation of the isoprenoid side chain. Up to four isomers ($MK_{m:n}$(a-d)) were detected In the extracted ion chromatograms of fully unsaturated MKs. In this study, these isomers are numbered consecutively from 'a' to 'd' from early to late eluting (Fig. 7.5). As for

UQ isomers, MK isomers showed highly similar fragmentation patterns characterized by dominant product ions at m/z 187.1 (head group) and fragments of the isoprenoid side chain (Fig. 7.5C). In total, 43 different quinone structures were identified in the water column and sediment samples. Due to the lack of authentic standards for MPs, these compounds could not be corrected for their relative response and are thus not included in total quinone abundance and distribution patterns as well as MD_q and BD_q calculations.

7.3.3. Relative abundances of quinone groups in the Black Sea water column and sediments

Total quinone concentrations in the water column ranged between 0.21 and 9.44 ng l^{-1} (Fig. 7.6). The highest concentrations in the water column were measured at 40 mbsl within the oxic zone and at 300 mbsl within the anoxic part of the water column. From the oxic zone to the chemocline, concentrations decreased seven-fold. The lowest concentrations occurred in the deepest water column sample at 1200 mbsl. In the sediments, concentrations were highly variable and ranged from 1.7 to more than 1000 ng g^{-1} sediment dry weight (sed. dw.). The highest concentrations were measured in the surface sediment and the sapropel layer. Below the sapropel (lithological Unit II), concentrations were lowest and showed little variability.

The relative distribution of quinone groups showed large differences in the different redox zones of the Black Sea water column (Fig. 7.6). At 40 mbsl (oxic zone), UQs and PQs were the major components, with UQs contributing more than 50 % and PQs more than 30 % to the total quinone pool, respectively. Archaeal menaquinones ($MK_{6:0}$ and $MK_{6:1}$) and vitamin K1 accounted for ca. 8 % each in the same sample. At the chemocline, archaeal menaquinones were the major contributors, whereas UQs were minor compounds with 2.6 % and 8 % relative abundance in 90 and 120 mbsl, respectively. At the lower boundary of the chemocline (150 mbsl), UQs were again the dominant compounds (46 % relative abundance). Polyunsaturated MKs and $ChQ_{7:7}$ were also detected in significant amounts in this sample, each contributing 22 % to the total quinone pool. In the deeper anoxic water column samples (300-1200 mbsl), polyunsaturated MKs and UQs occurred in similar proportions and account for more than 80 % of total quinones in the samples, whereas saturated and monounsaturated MKs as well as PQs were only minor components. Vitamin K1 was detected in trace amounts in the same samples. $ChQ_{7:7}$ occurred in trace amounts at 300 and 500 mbsl, but was absent in the deeper water column.

In the top 400 cmbsf (lithological Unit I), UQs and PQs were the dominant quinone types, contributing in sum to more than 80 % of total quinones (Fig. 7.6A). Here,

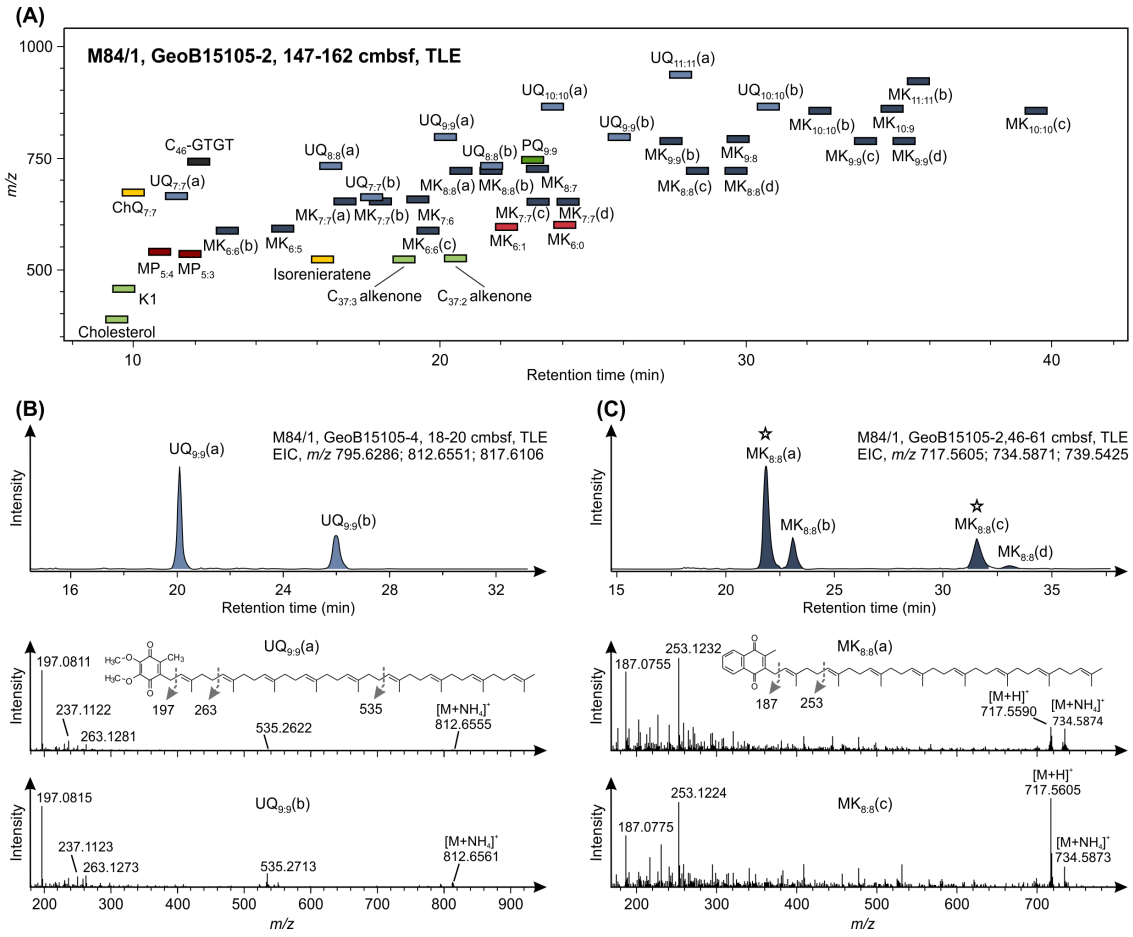

Figure 7.5. (A) Reconstructed RP-UHPLC-ESI-MS density map showing elution order and *m/z* of all identified quinones, methanophenazines and the C_{46}-GTGT standard in sample M84/1, GeoB15105-2, 147-162 cmbsf. Colors indicate different quinone structures associated with distinct microbial metabolisms: green = photosynthetic quinones vitamin K1 (light green) and PQ (dark green), red = archaeal quinones (saturated and monounsaturated MKs) and *Methanosarcinales*-specific functional quinone analog MPs (dark red), light blue = aerobic bacterial quinones (UQs), dark blue = anaerobic bacterial quinones (polyunsaturated MKs) and yellow = the green sulfur bacterial ChQ. Quinones labeled with characters, e.g., $UQ_{9:9}$(a) and (b) or $MK_{8:8}$(a), (b), (c) and (d), have the same molecular mass. Elution of eukaryotic apolar lipids cholesterol and C_{37} alkenones as well as isorenieratene, a biomarker pigment specific for green sulfur bacteria. (B) EIC of $UQ_{9:9}$ in sample M84/1, GeoB15105-4, 18-20 cmbsf illustrating an early and late eluting isomer ($UQ_{9:9}$(a) and $UQ_{9:9}$(b), respectively), and their corresponding MS^2 spectra. Both compounds revealed highly similar fragmentation patterns. (C) EIC of $MK_{8:8}$ in sample M84/1, GeoB15105-2 46-61 cmbsf showing four isomers ($MK_{8:8}$(a-d)). MS^2 spectra of two representatives ($MK_{8:8}$(a) and (c), indicated by star in the EIC) revealed highly similar product ions. Structures of $UQ_{9:9}$ and $MK_{8:8}$ and the formation of major product ions are also shown. MK, menaquinone; UQ, ubiquinone; K1, vitamin K1 (synonyms: phylloquinone, $MK_{4:1}$); PQ, plastoquinone; ChQ, chlorobiumquinone; MP, methanophenazine; GTGT, glycerol trialkyl glycerol tetraether.

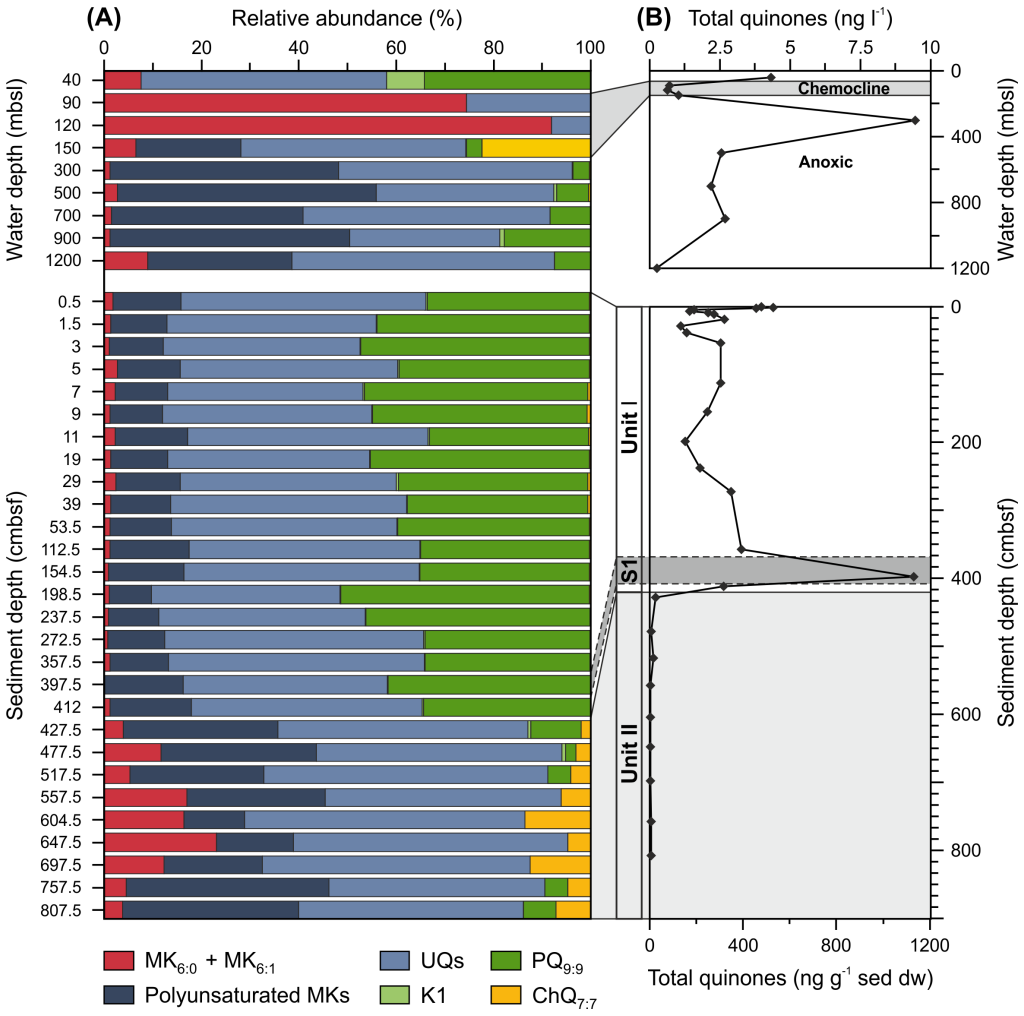

Figure 7.6. Relative abundances of major quinones (A) and absolute quinone abundance (B) in the water column and sediments of the southern Black Sea (cruise M84/1, station GeoB15105). Shaded area in the water column profile corresponds to the chemocline. In the sediment, the marine (Unit I, white) and lacustrine (Unit II, light grey) units, as well as the sapropel (S1, dark grey) are denoted.

polyunsaturated MKs were also detected in significant amounts with relative abundances between 9 % and 17 %, whereas $MK_{6:0}$ and $MK_{6:1}$ were only minor components. Similarly, vitamin K1 and $ChQ_{7:7}$ were minor compounds in Unit I sediments. Below 400 cmbsf (lithological Unit II), the quinone distribution showed a different pattern: UQs were still the dominant quinone group, but PQs were almost absent (Fig. 7.6). $MK_{6:0}$ and $MK_{6:1}$ increased in relative abundance with a maximum at 647.5 cmbsf, accounting for 23 % of total quinones. The abundance of polyunsaturated MKs also increased and $ChQ_{7:7}$ contributed significantly to the total quinone pool with relative abundances of up to 14 % in the deeper sediment (cmbsf).

7.3.4. Relative abundances of quinone isomers

The distribution of the 'regular' menaquinones and ubiquinones compared to the later eluting isomers showed large differences between the oxic and anoxic water column and the sediments (Fig. 7.7). Based on the retention time of the commercially available standard ($UQ_{10:10}$), UQs labeled with '(a)' were referred to as regular compounds and the later eluting UQs (labeled with '(b)') were defined as isomers. Similarly, based on the retention time difference of the $MK_{4:4}$ standard relative to the compounds with longer isoprenoid side chains, MKs labeled with '(b)' were defined as regular MKs and other quinones with the same molecular mass were assigned as isomers (a, c, d; Fig. 7.7).

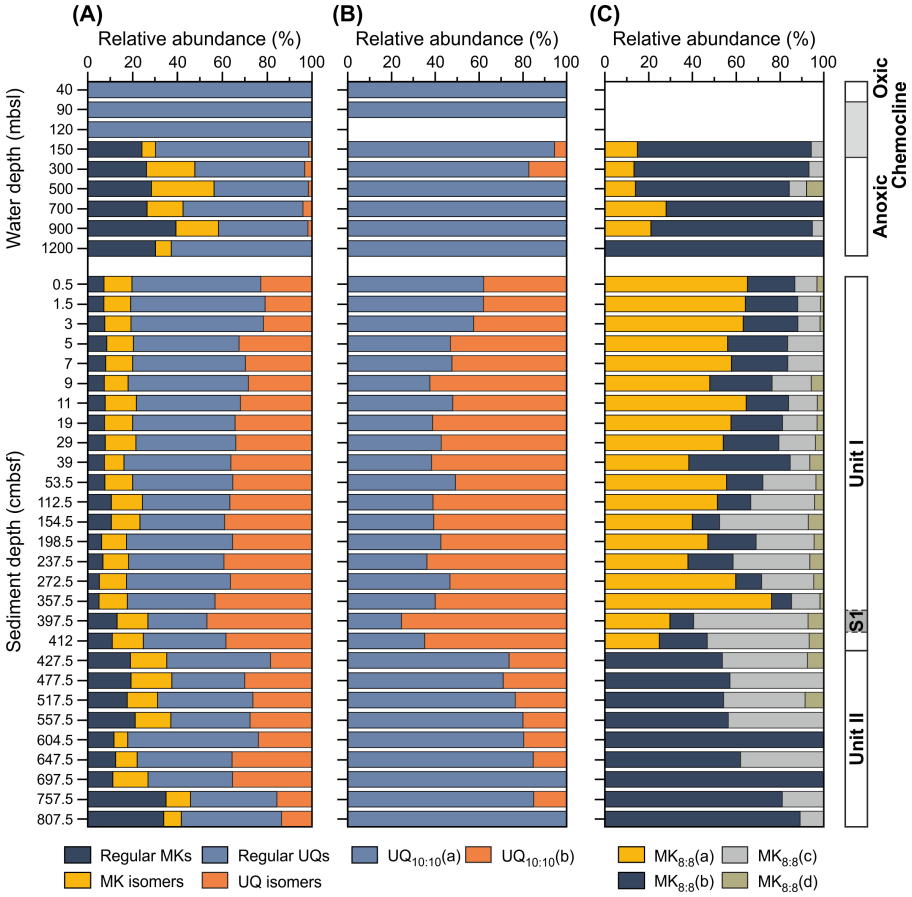

Figure 7.7. Relative abundances of summed menaquinone and ubiquinone isomers (A), isomers of $UQ_{10:10}$ (B), and isomers of $MK_{8:8}$ (C) in the water column and sediments of the southern Black Sea (cruise M84/1, station GeoB15105).

The samples from the oxic zone and the chemocline contained only regular UQs, whereas regular UQs and MKs as well as their isomers occurred in the anoxic zone (Fig. 7.7a). While UQ isomers were only minor constituents compared to the regular compounds, MK isomers were almost as abundant as the corresponding regular MKs in the water column. In the sediments, this pattern shifted towards higher relative

abundances of the UQ and MK isomers compared to the respective regular compounds, and the distribution pattern of total isomers showed little variability (Fig. 7.7a). However, analysis of the detailed distribution of isomers of individual quinones revealed major changes in the water column and sediment samples (Fig. 7.7b). For example, the late eluting $UQ_{10:10}$(b) only occurred in two water column samples (150 and 300 mbsl) and showed a low relative abundance compared to the early eluting $UQ_{10:10}$(a) (Fig. 7.7b), whereas $UQ_{10:10}$(b) was of greater abundance in the sediment, especially in lithological Unit I.

Differences in the distribution of isomers was even more pronounced for the four $MK_{8:8}$ isomers (Fig. 7.7c). In the samples from the anoxic water column, the most abundant $MK_{8:8}$ isomer was $MK_{8:8}$ (b). Similar to the distribution of $UQ_{10:10}$, the other MK isomers became dominant over the regular compound in lithological Unit I. Here, $MK_{8:8}$(a) was the most abundant isomer with up to 60 % relative abundance. In Unit II, $MK_{8:8}$(a) was not detected and $MK_{8:8}$(b) was the dominant isomer. With increasing sediment depth, the relative abundance of $MK_{8:8}$(c) increased to a maximum in the sapropel. $MK_{8:8}$(d) was a minor compound in all samples with relative abundances lower than 10 % of total $MK_{8:8}$.

7.3.5. Absolute abundances of individual quinones

Concentration profiles of the quinones associated with oxygenic photosynthesis, i.e., vitamin K1 and $PQ_{9:9}$, showed a distinct maximum in the oxic zone with concentrations of 0.3 and 1.5 ng l^{-1}, respectively, and a decrease to below the detection limit in the chemocline (Fig. 7.8A, B). In the anoxic part of the water column, both compounds showed more than five-fold lower concentrations compared to the oxic zone. $ChQ_{7:7}$ was not detected at shallower water depths and showed concentration maximum at 150 mbsl (0.23 ng l^{-1}), below which concentrations were one order of magnitude lower (<0.03 ng l^{-1}; Fig. 7.8C). $UQ_{7:7}$ (a) showed a similar depth trend (Fig. 7.8D), while concentration maxima for other UQs were observed in the anoxic water column mainly at 300 mbsl (Fig. 7.8E-J).

The concentration of $MK_{6:0}$ increased from oxic waters (0.18 ng l^{-1}) to the suboxic waters of the chemocline at 120 m (0.36 ng l-1; Fig. 7.8K). Concentrations of $MK_{6:1}$ were similar in the oxic waters (0.14 ng l^{-1}) but showed a shallower maximum at the chemocline at 90 m (0.24 ng l^{-1}; Fig. 7.8L). The concentrations of both $MK_{6:0}$ and $MK_{6:1}$ were one order of magnitude lower in the anoxic part of the water column below 150 m (0.01 ng l^{-1}) as compared to the oxic and suboxic zones. Concentrations of polyunsaturated MKs with different length and degree of unsaturation of the isoprenoid side chain varied between 10 pg l^{-1} and ca. 1 ng l^{-1} (Fig. 7.8M-Ai). All MKs

containing six isoprenoid units, including partially saturated compounds, showed a distinct maximum in the anoxic zone at 300 mbsl. The only other quinone that showed a similar concentration profile was $MK_{10:8}$. Many other MKs showed two concentration maxima, one at 300 mbsl and a deeper one at 700 mbsl. For example, $MK_{7:7}$ isomers, $MK_{8:8}$ isomers (except for $MK_{8:8}$(d)), $MK_{8:7}$ and $MK_{8:6}$, $MK_{9:9}$(b), $MK_{9:8}$, $MK_{10:10}$(a) and $MK_{10:9}$. $MK_{9:9}$(c) and $MK_{10:10}$(b) were the only MKs that showed a single maximum at 700 mbsl. $MK_{7:5}$ and $MK_{11:11}$(b) showed a deeper concentration maximum at 900 mbsl.

In the sediment, depth profiles of individual quinones were more uniform compared to the water column (Fig. 7.9) and mainly tracked total quinone concentrations (see Fig. 7.6B). Most quinones showed a pronounced concentration maximum in the sapropel layer at 397.5 cmbsf, with the exceptions of $ChQ_{7:7}$, $MK_{6:0}$, $MK_{6:1}$, $UQ_{11:11}$(a) and (b) as well as a few fully unsaturated and partially saturated MKs. Vitamin K1, $PQ_{9:9}$, $ChQ_{7:7}$, $MK_{6:0}$, most fully unsaturated MKs and all regular UQs additionally showed high concentrations in the surface sediments, which rapidly decreased within the first 20 to 30 cm sediment depth. For the late eluting UQ isomers as well as several fully unsaturated MKs, elevated concentrations in surface sediments were not observed. In Unit II, concentrations of individual quinones were more than one order of magnitude lower that in Unit I. Highest concentrations in the sediments were observed for $PQ_{9:9}$ with values of up to 470 $ng\,l^{-1}$ sed. dw. in the sapropel layer. The concentrations of vitamin K1, $ChQ_{7:7}$, and $MK_{6:1}$ and $MK_{6:0}$ were approximately two orders of magnitude lower as compared to $PQ_{9:9}$. Within the UQs, compounds with seven to ten isoprenoid units revealed similar concentrations, which were about ten-fold higher than concentrations for vitamin K1, $ChQ_{7:7}$, and $MK_{6:0}$ and $MK_{6:1}$ as well as $UQ_{11:11}$. The concentrations of the different polyunsaturated MKs showed large variability. While concentrations of partially saturated MKs were mainly below 1 $ng\,g^{-1}$ sed. dw., the concentrations of some fully unsaturated $MK_{6:6}$, $MK_{7:7}$ and $MK_{8:8}$ isomers were at least one order of magnitude higher. Highest concentrations within the polyunsaturated MKs were observed for $MK_{6:6}$(b), $MK_{7:7}$(c), $MK_{8:8}$(a) and $MK_{8:8}$(c).

7.3.6. Microbial diversity and bioenergetic divergence (MD_q and BD_q)

Microbial diversity (MD_q) and bioenergetic divergence (BD_q) indices were calculated from quinone abundances using equations (1) and (2) and grouped according to the water column redox zones and the lithological units (Fig. 7.10). Note that MD_q represents overall quinone diversity based on relative abundances of all individual quinones, while BD_q describes headgroup type richness, i.e., functional diversity.

Samples from the same water column zones and sedimentary units showed similar

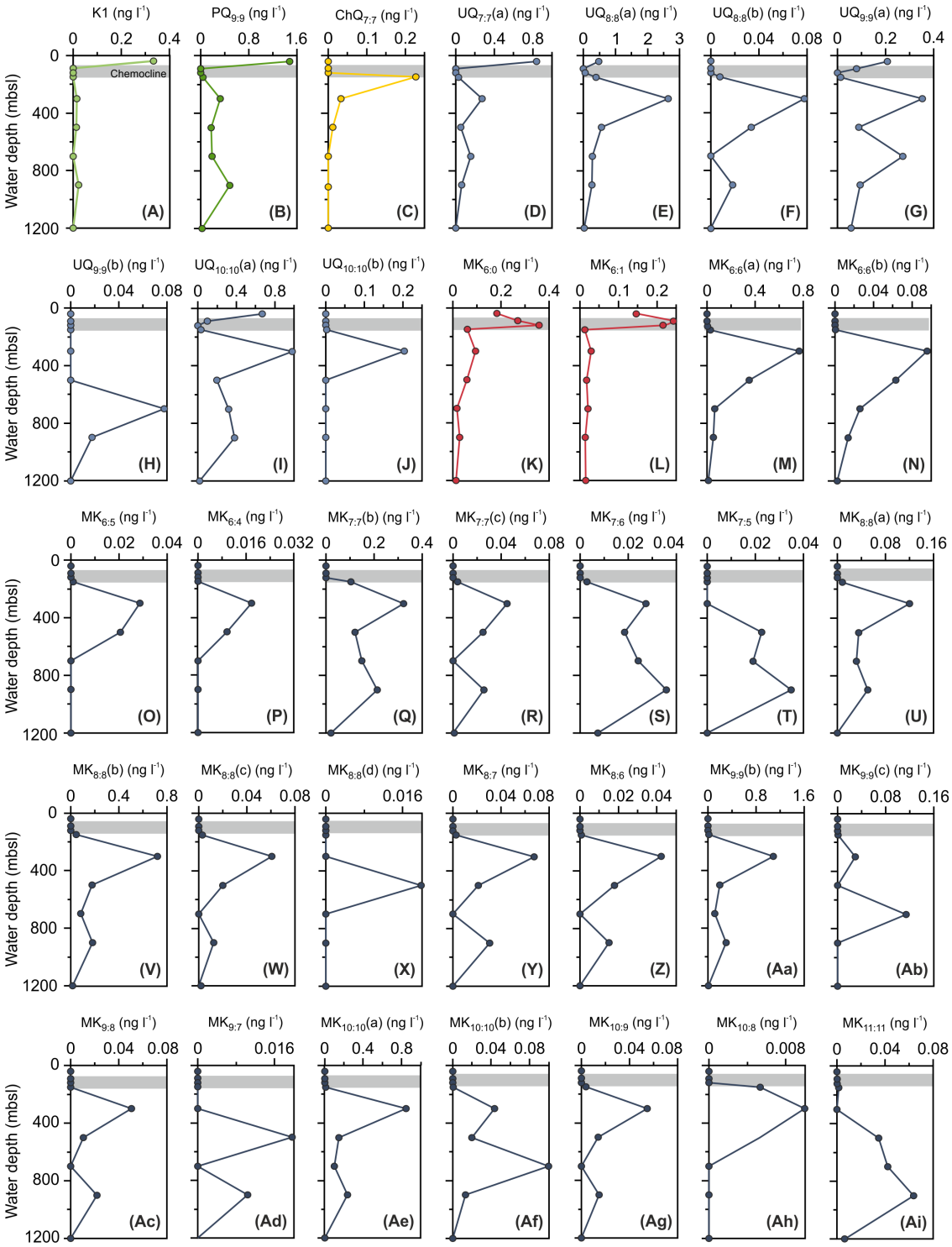

Figure 7.8. Depth profiles of all quinones detected in the Black Sea water column. Shaded areas correspond to the chemocline. Colors indicate different quinone structures associated with distinct microbial metabolisms: green = photosynthetic quinones vitamin K1 (light green) and PQ (dark green), red = archaeal quinones (saturated and monounsaturated MKs, light red), light blue = aerobic bacterial quinones (UQs), dark blue = anaerobic bacterial quinones (polyunsaturated MKs) and yellow = the green sulfur bacterial ChQ. MK, menaquinone; UQ, ubiquinone; K1, vitamin K1; PQ, plastoquinone; ChQ, Chlorobiumquinone.

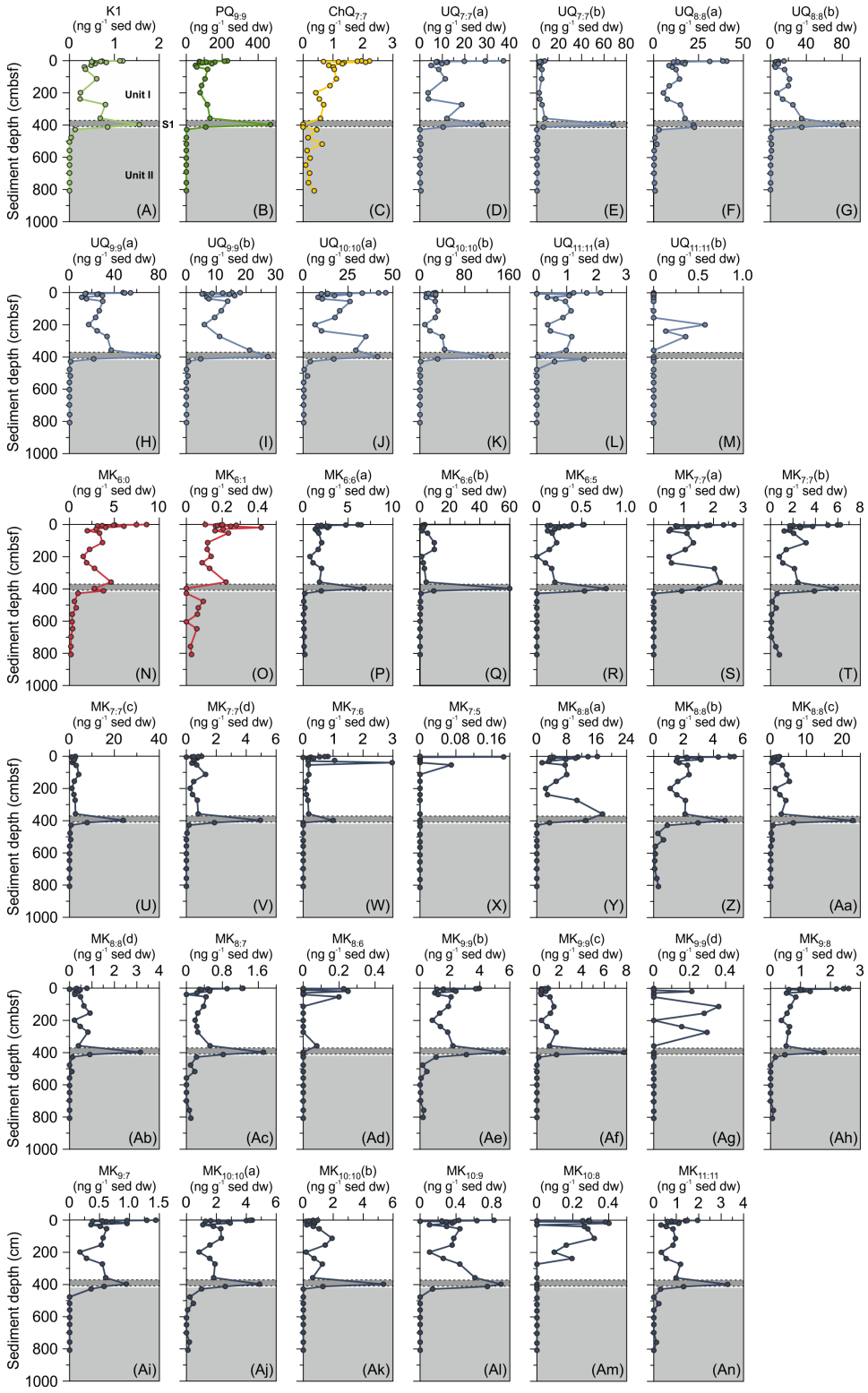

Figure 7.9. Depth profiles of all quinones detected in Black Sea sediments. Marine (Unit I, light grey) and lacustrine (Unit II, intermediate grey) lithological units as well as the sapropel (S1, dark grey) are denoted. Colors indicate different quinone structures associated with distinct microbial metabolisms: green = photosynthetic quinones vitamin K1 (light green) and PQ (dark green), red = archaeal quinones (saturated and monounsaturated MKs), light blue = aerobic bacterial quinones (UQs), dark blue = anaerobic bacterial quinones (polyunsaturated MKs), and yellow = green sulfur bacterial ChQ. MK, menaquinone; UQ, ubiquinone; K1, vitamin K1; PQ, plastoquinone; ChQ, Chlorobiumquinone.

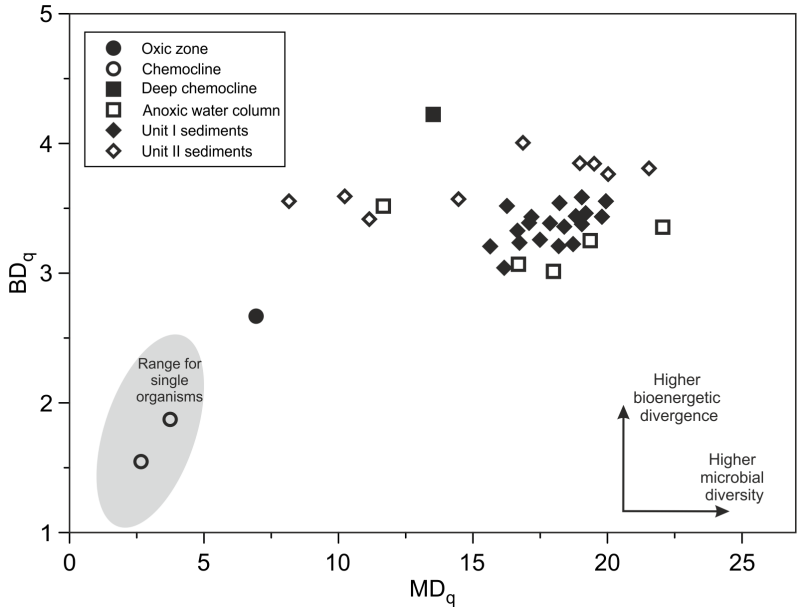

Figure 7.10. Cross plot of microbial divergence (MD_q) and bioenergetic divergence (BD_q) indices after IWASAKI and HIRAISHI (1998) for water column and sediment samples from the southern Black Sea (M84/1, GeoB15105). The range for single organisms is indicated by the grey area (based on the distribution of quinones in 24 archaeal strains shown in Chapter 6.

BD_q values, whereas MD_q values were divergent. The lowest BD_q and MD_q indices were observed in samples from the chemocline at 90 and 120 mbsl, with MD_q values below 5 and BD_q values below 2. Low MD_q and BD_q values distinguish the sample from the oxic (photic) zone from the rest of the obtained dataset. The deep chemocline sample (150 mbsl) showed the highest BD_q values of all samples (4.2), while MD_q values were intermediate with 13.5. The samples from the anoxic zone showed BD_q values between 3 and 3.5, whereas the MD_q values were in a broad range from 11.6 to 22. All samples from Unit I showed relatively high values but little variability for both indices (15.6-20 MD_q, 3-3.6 BD_q). A similar pattern was observed for the samples from sediment Unit II, albeit with a higher BD_q index (3.4-4) for most samples.

7.3.7. Methanophenazines

Methanophenazines were absent in the oxic part of the water column and the chemocline but were detected in the anoxic part of the water column, except at 1200 mbsl (Fig. 7.11). Highest concentrations occurred at 300, 500 and 900 mbsl with values between 13 and 17 $pg\,l^{-1}$. The concentrations of methanophenazine decreased strongly with depth from 9 cmbsf (311 $pg\,g^{-1}$ sed. dw.) towards 400 cmbsf (below detection limit).

7.3.8. Relative abundances of IPLs

For examining their distribution in the water column and sediments, IPLs (see Fig. 7.12 for chemical structures) were grouped by headgroup and core lipid type irrespective of side chain structure into intact polar archaeols (IP-AR), GDGTs (IP-GDGTs), glycosidic (G-) and phosphatidic (P-) DAG, AEG, and DEG, as well as DPG, 1G-Cer, PG-(OH)-Cer, Ornithines (OL), and Betaines (BL).

The profiles of total quinones (Fig. 7.6) and total IPLs (Fig. 7.13) were similar in the water column and within the sediment. In the water column, IPL concentrations decreased from the oxic zone to the chemocline and showed maxima at 300 and 900 mbsl similar to quinone concentrations (Fig. 7.13). In comparison to quinone concentrations, IPL concentrations in the surface sediments showed a steeper decrease towards deeper sediments and a less distinct maximum in the sapropel layer. Overall, IPL concentrations were approximately one order of magnitude higher than quinone concentrations in both the sediment and the water column.

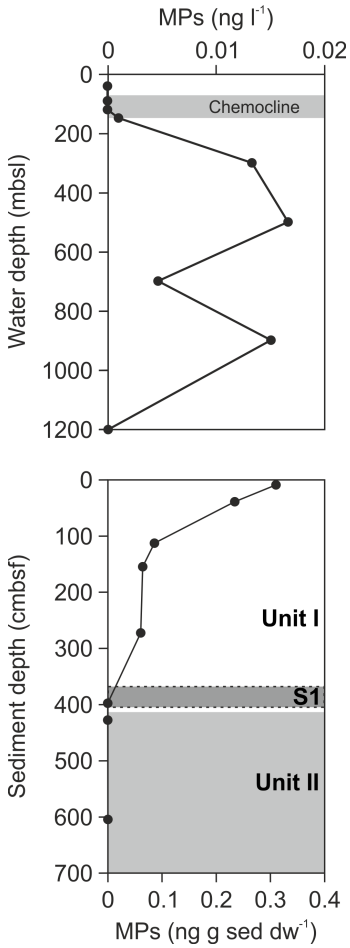

Figure 7.11. Profile of total methanophenazines ($MP_{5:4}$ and $MP_{5:3}$) in the water column and sediments of the southern Black Sea (cruise M84/1, station GeoB15105).

Similar to the distribution of major quinone groups, specific IPL classes were associated with distinct geochemical zones. In the oxic zone, G-DAGs were the dominant IPLs, contributing almost 80 % to the total IPL pool. Minor IPL groups were P-DAG and BL, which were detected in similar amounts throughout the water column. Small amounts of IP-GDGTs and IP-ARs as well as P-AEG and P-DEG were also detected in the oxic zone. In the upper chemocline P-DAGs and IP-GDGTs increased in relative abundance. Here, archaeal IPLs accounted for about 10 % of total IPLs, which was the highest relative abundance of these compounds in the water column. Relative abundances of G-DAGs at the chemocline and in the anoxic zone were lower than in the oxic zone but still accounted for up to 30 % of the IPLs. 1G-Cer and DPG first appeared within the chemocline (120 mbsl) and were detected throughout the anoxic water column. In the deepest part of the chemocline

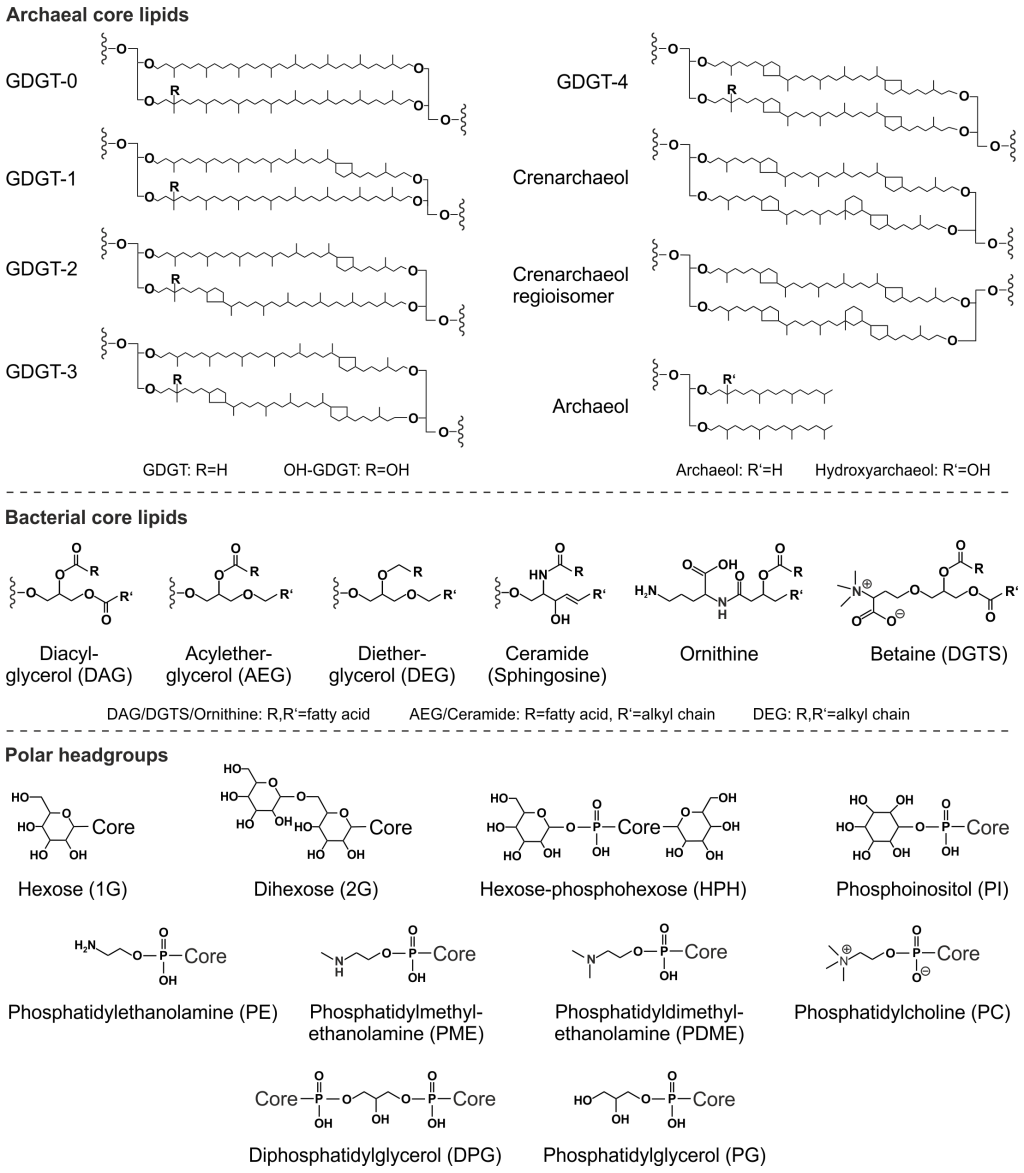

Figure 7.12. Structures of archaeal and bacterial core lipids and associated polar headgroups detected in Black Sea water column and sediment samples.

(150 mbsl), P-AEG and especially P-DEG increased in relative abundance, the latter accounting for more than 25 % of total IPLs. The combined relative abundance of these two groups was about 40 % throughout the anoxic zone. In contrast, concentrations of P-DAG decreased from the chemocline to the deep anoxic zone. Ornithine lipids (OL) and PG-(OH)-Cer were detected in low abundance only in the anoxic zone, where archaeal IPLs showed very low relative abundances.

The IPL composition of the sediments differed strongly from that of the water column (Fig. 7.13). P-DEG was the dominant IPL group with almost 40 % relative abundance in surface sediments. Other major groups in surface sediments were BL, IP-GDGTs and P-DAG. G-DAG were detected only in trace amounts and disappeared below the surface.

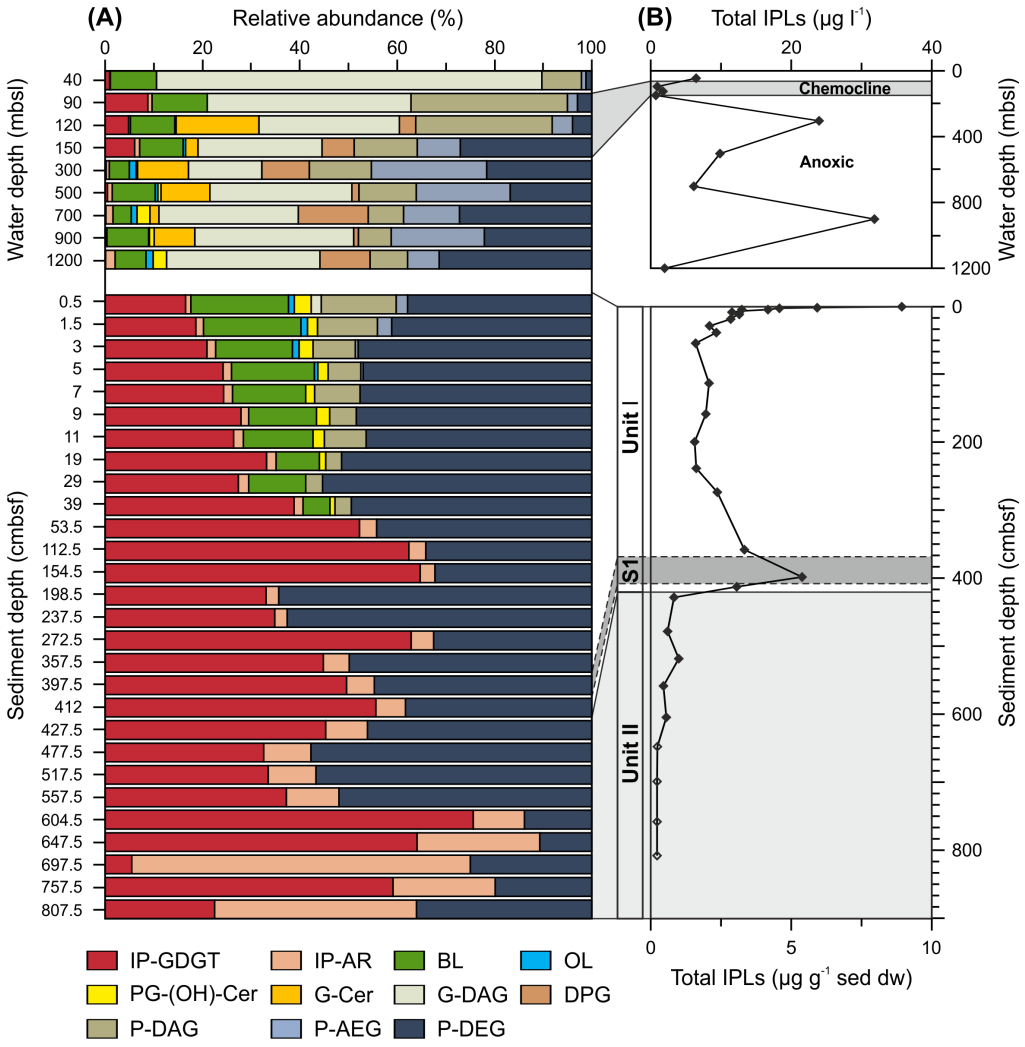

Figure 7.13. Relative abundances of IPL groups (A) and absolute IPL abundance (B) in the water column and sediments of the southern Black Sea (cruise M84/1, station GeoB15105). Shaded area in the water column profile corresponds to the chemocline. In the sediment, the marine (Unit I, white) and lacustrine (Unit II, light grey) units, as well as the sapropel (S1, dark grey) are denoted. IPL data from SCHRÖDER (2015) except for water column samples from 150 m, 300 m, 500 m, and 900 m water depth.

DPG and 1G-Cer were not detected in the sediments and OL, P-AEG PG-(OH)-Cer and IP-ARs only occurred in very low relative abundance (<3.5 %). Within the upper 39 cmbsf, acyl side chain containing IPLs steadily decreased in relative abundance with depth, whereas relative abundances of ether-based lipids such as IP-GDGTs and P-DEG increased. Only IP-GDGTs, P-DEG and IP-AR were detected below 39 cmbsf in lithological Unit I, where either IP-GDGTs or P-DEG dominated the total IPL pool. The relative abundance of IP-ARs was low (∼5 %) but progressively increased with depth in sediment Unit I. IPL distributions in the upper part of Unit II (427.5-557.5 cmbsf) closely resembled the distribution of the lower part of Unit I. However, below 557.5 cmbsf, archaeal IPLs clearly dominated over bacterial P-DEG, although P-DEG

still accounted for about 25 to 36 % of total IPLs. IP-ARs showed highest relative abundances of all samples below 557.5 cmbsf and were the dominant IPL group at 697.5 and 807.5 cmbsf.

7.3.9. Absolute abundances of IPLs and apolar lipids relative to quinones

The concentrations of the different IPL groups showed significant variations in the water column and, in part, within the sediment (Fig. 7.14). Depth-dependent concentrations of G-DAG, BL and P-DAG (Fig. 7.14A-C) strongly resembled each other. They showed a decrease from the oxic water column to the chemocline and a maximum at 900 mbsl (G-DAG and BL; Fig. 7.14A, B) and at 300 mbsl (P-DAG; Fig. 7.14C). The G-DAG depth profile was similar to the profiles of $PQ_{9:9}$ and vitamin K1, whereas the P-DAG profile was more similar to those of $UQ_{8:8}$(a), $UQ_{9:9}$(a) and $UQ_{10:10}$(a) (Figs. 7.9 and 7.14), although the distribution in the anoxic waters also matched some MK profiles. P-AEG, PE-DEG and 1G-Cer followed largely the same trend as P-DAG in the anoxic water column and concentrations were in a similar range. However, they were absent in the oxic zone and the chemocline (Fig. 7.14D, E, and H). DPG, OL, and PG-(OH)-Cer were minor components or absent within the chemocline and the oxic zone (Fig. 7.14F, G and I).

The concentrations of both DPG and OL peaked in the anoxic water column at 300 mbsl, which coincided with peaks in abundance in most other IPL groups, whereas the secondary maximum occurred slightly shallower at 700 mbsl instead of 900 mbsl observed e.g., for G-DAG, BL or P-DEG (Fig. 7.14F and G). The concentration of PG-(OH)-Cer only peaked at 700 mbsl in the anoxic zone (Fig. 7.14I). The concentration profiles of archaeal IP-GDGTs and IP-ARs were distinct from each other and bacterial IPLs in the water column: IP-GDGT concentrations increased from the oxic zone to the chemocline (Fig. 7.14J), while they were low throughout the anoxic water column. This distinct maximum in the chemocline was not observed in the depth profile of IP-AR. Within the chemocline and in the upper oxic water column, concentrations of IP-AR were low, whereas IP-AR concentrations were at least three times higher in the anoxic zone (Fig. 7.14K). The depth profile of IP-GDGTs followed a similar trend as compared to $MK_{6:0}$ and $MK_{6:1}$ (Figs. 7.1 and 7.14), and IP-ARs largely followed the trend of MPs (Figs. 7.11 and 7.14). In the water column, the apolar lipid isorenieratene showed a distinct maximum at 150 mbsl and was absent in the rest of the water column except for minor abundances at 300 mbsl (Fig. 7.14), and thus reflected the depth profile of $ChQ_{7:7}$ (Fig. 7.8). The concentrations of cholesterol as well as summed $C_{37:2}$ and $C_{37:3}$ alkenones were highest in the oxic zone, decreased strongly with water depth within the chemocline and remained low throughout the anoxic water column.

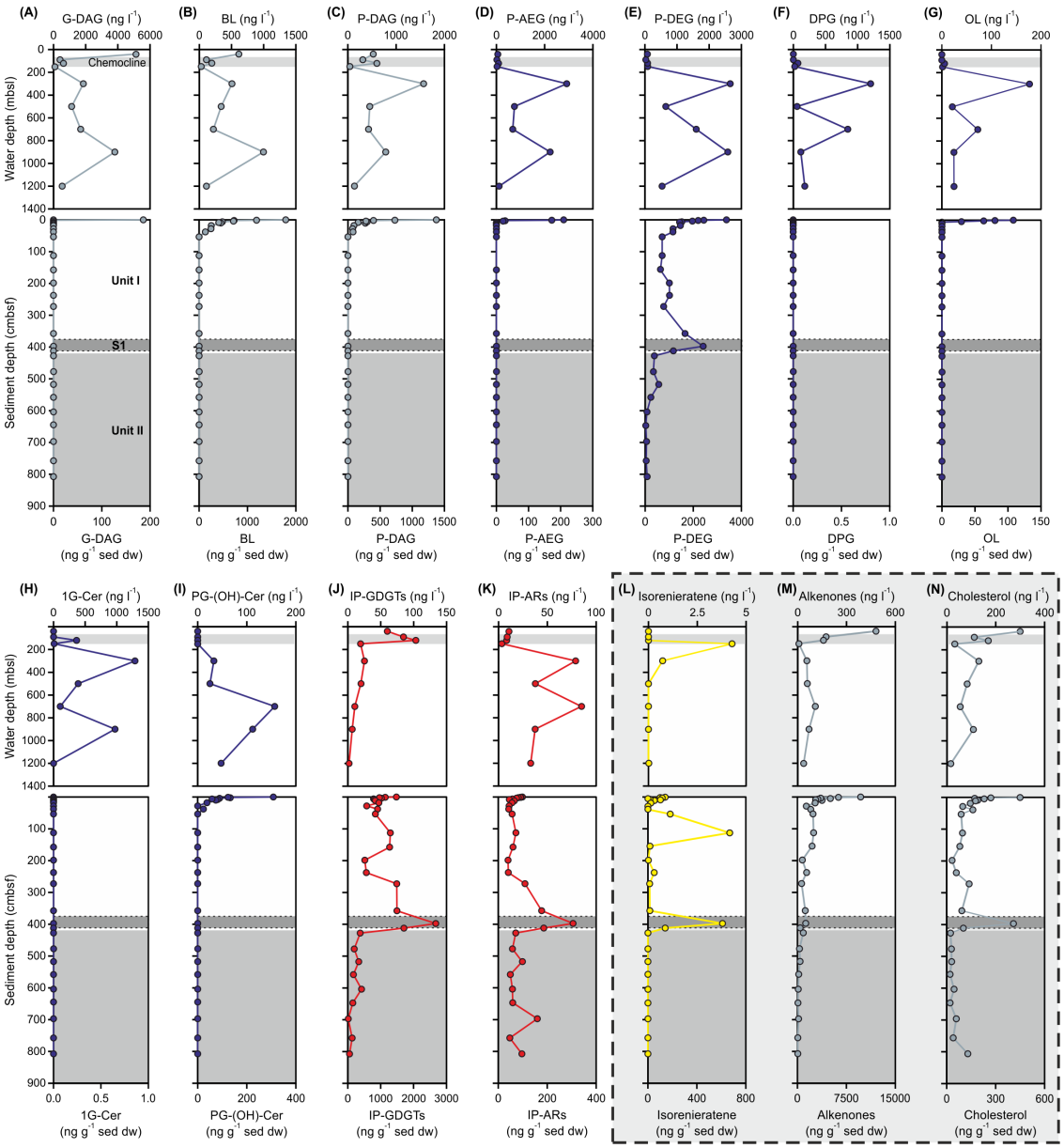

Figure 7.14. Depth profiles of IPL groups, isorenieratene, alkenones, and cholesterol detected in the water column and sediments of the Black Sea. IPL data from SCHRÖDER (2015) except for water column samples from 150 m, 300 m, 500 m, and 900 m water depth. Shaded areas in water column profiles correspond to the chemocline. Marine (Unit I, light grey) and lacustrine (Unit II, intermediate grey) lithological units as well as the sapropel (S1, dark grey) are denoted for sediment profiles. Color code: blue green, bacterial and/or eukaryotic lipids present in oxic waters; blue, bacterial and/or eukaryotic lipids only present in chemocline and anoxic waters; red, archaeal lipids. Abbreviations: G, glycosidic headgroup-bearing; P, phosphatidic headgroup-bearing; DPG, diphosphatidyl glycerol; BL, betaine lipids; OL, ornithine lipid; PG-(OH), hydroxy-phosphatidylglycerol; DAG, diacyl glycerol; AEG, acyl ether glycerol; DEG, diether glycerol; Cer, ceramide; IP, intact polar; GDGT, glycerol dibiphytanyl glycerol tetraether; AR, archaeol.

In the sediment, the majority of IPL species were only detected in the surface (Fig. 7.14). For example, the concentrations of BL, P-DAG, P-AEG, OL and PG-(OH)-Cer decreased exponentially with depth within the upper 50 cmbsf (Fig. 7.14B-D, G, I). In contrast, the concentrations of P-DEG, IP-GDGTs and IP-ARs were relatively high within the sediment showing a slight decrease within the first 50 cmbsf and a pronounced peak within the sapropel layer (Fig. 7.14E, J, and K), which was similar to most quinone profiles (cf. Fig. 7.9) and invariably low concentrations in Unit II. Isorenieratene showed two concentration maxima, at 112.5 cmbsf and in the sapropel, but was otherwise low in concentration or absent (Fig. 7.14L). In contrast to the water column, IP-AR and MP concentrations were decoupled in the sediments (cf. Figs. 7.11 and 7.14K). The concentrations of alkenones were highest at the sediment surface, decreased strongly within the upper 30 cmbsf and remained low throughout the rest of Unit I and Unit II. The concentration profile of cholesterol was similar but showed a peak in the sapropel layer.

7.4. Discussion

7.4.1. Structural elucidation of isomers

The almost identical MS^2 spectra of the various chromatographically resolved isomers of UQs and MKs suggest that they have highly similar structures, respectively, whose exact structural differences cannot be determined using the applied methods. However, isomers of MKs have already been reported. For example, two $MK_{9:8}$ peaks have been resolved by thin layer chromatography in the actinomycete *Mycobacterium phlei* and identified by NMR as *cis*- and *trans*-isomers, respectively (DUNPHY et al., 1968). Similarly, *cis*- and *trans*-isomers of $MMK_{7:7}$ (methylated menaquinone) have been identified in the archaeon *Thermoplasma acidophilum* (SHIMADA et al., 2001). To the best of our knowledge, these are the only published descriptions of naturally occurring respiratory quinone isomers. For both $MK_{9:8}$ and $MMK_{7:7}$, the double bond of the isoprene unit that was nearest to the menaquinone headgroup was suggested to be a *cis* configuration (DUNPHY et al., 1968; SHIMADA et al., 2001). Based on comparison with the retention time of the commercially available $UQ_{10:10}$ (*trans*) standard, the early eluting UQ isomers (a-series) in our samples represent *trans*-isomers (cf. Fig. 7.5). Thus, the late eluting isomers (b-series) potentially represent *cis*-isomers. The same might apply for the MK isomers, but here a maximum of four chromatographically separated isomers were detected. It seems unlikely that the four isomers represent compounds with *cis* configurations at different double bond positions or multiple *cis* configurations, since similar retention time patterns may be expected. Assuming the same retention time difference for *cis* and *trans*-isomers as for UQs, one early and

one late eluting MK could represent a couple with *cis*- and *trans*-configuration, e.g., $MK_{8:8}$(a or b) and $MK_{8:8}$(c or d). Furthermore, the isomers may not represent variable double bond positions, since MK isomers were only detected for fully unsaturated (i.e., one saturation per isoprene unit) quinones. The structural differences of the MK and UQ isomers remain unconstrained and further investigation is needed to unambiguously identify their structure, for example by NMR.

7.4.2. Microbial stratification in the Black Sea water column and biomarker potential of respiratory quinones

Combined respiratory quinone and membrane lipid profiling resolved the stratification of microbial communities and metabolisms along the redox gradients of the southern Black Sea. Quinones, apolar lipids and intact polar lipids of similar biological origin were significantly correlated (Fig. 7.15), which supports the utility of respiratory quinones as biomarkers for microbial community composition and associated respiratory processes.

The derived depth zonation and the potential sources of quinones and membrane lipids in the southern Black Sea are summarized in Table 7.2. Microbial communities and metabolisms were separated into 1) the oxic (photic) zone supporting oxygenic photosynthesis, 2) the suboxic zone dominated by thaumarchaeal ammonia oxidation, 3) the anoxic photic zone inhabited by sulfur-oxidizing photosynthetic bacteria, and 4) (dark) anoxic zone which supports a diversity of bacterial and archaeal metabolisms such as methane oxidation, anammox and sulfate reduction.

The diversity of respiratory quinones in a sample (MD_q), as well as the BD_q, which reflects the mode of respiration that dominates in a sample, showed large variations between different geochemical zones (Fig. 7.10), while samples from the same zone grouped in a close proximity in the MD_q versus BD_q coordinate system. The highest quinone diversities were observed in the anoxic water column as well as in the sediments. As most organisms contain only one to two abundant quinones (COLLINS and JONES, 1981; NOWICKA and KRUK, 2010), high quinone diversity translates to high microbial diversity in the anoxic zone. In contrast, low BD_q and MD_q values within the range for single organisms in the samples from the chemocline suggest that a single metabolism dominates respiratory activity in the suboxic zone. The oxic photic zone exhibited intermediate MD_q and BD_q values, which likely results from the predominance of oxygenic photosynthesis and a low diversity of aerobic respiration pathways. Highest bioenergetic divergence occurred within the photic anoxic zone, suggesting a high diversity of anaerobic metabolisms. The MD_q and BD_q values reported here are much higher as those previously reported for sewage sludge

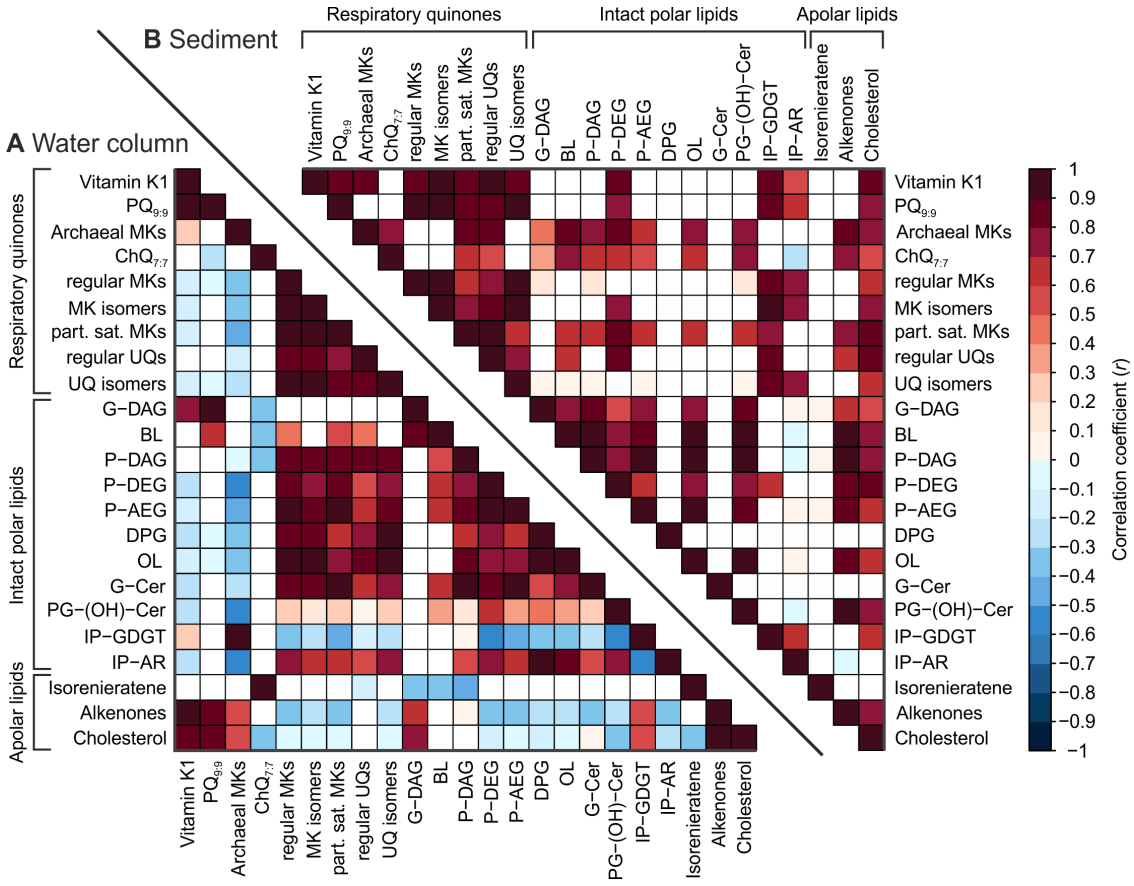

Figure 7.15. Linear correlation coefficients (p <0.05) calculated from concentrations of respiratory quinones as well as apolar and intact polar lipids in the Black Sea water column (A) and sediments (B). Lipid nomenclature as described in Fig. 7.14.

(IWASAKI and HIRAISHI, 1998; HIRAISHI, 1999) as well as shallow (URAKAWA et al., 2001) and deep marine sediments (CARDACE et al., 2006), and may be related to the larger diversity of quinones and isomers detectable by the improved analytical methods utilized in this study.

7.4.2.1. Oxic water column (0-90 mbsl): Oxygenic photosynthesis and bacterial aerobic respiration

The major quinone types in the oxic water column are associated with aerobic autotrophy and heterotrophy (UQs) as well as oxygenic photosynthesis (UQs, vitamin K1 and $PQ_{9:9}$; HIRAISHI, 1999). Sources for $UQ_{9:9}$, $UQ_{10:10}$, vitamin K1 and $PQ_{9:9}$ are both cyanobacteria and eukaryotic algae (Table 7.2; AMESZ, 1973; COLLINS and JONES, 1981; BRETTEL and LEIBL, 2001; NOWICKA and KRUK, 2010), while UQs with side chain lengths of 7 to 10 are additionally produced by α-, β-, and γ-*Proteobacteria* (Table 7.2; HIRAISHI, 1999; NOWICKA and KRUK, 2010). Only the *trans*-isomers (a-series) were

Table 7.2. Geochemical zonation, source organisms of quinones and intact polar lipids as well as associated biogeochemical processes in the water column of the southern Black Sea. Quinone and lipid data compiled from SHIVELY and BENSON (1967), GOLDFINE and HAGEN (1968), HOOPER et al. (1972), MAKULA and FINNERTY (1975), MAKULA (1978), COLLINS and JONES (1981), KNUDSEN et al. (1982), DISPIRITO et al. (1983), ALEEM and SEWELL (1984), COLLINS and GREEN (1985), SITTIG and SCHLESNER (1993), HARWOOD (1998), BRINKHOFF et al. (1999), HIRAISHI and KATO (1999), RÜTTERS et al. (2001), STURT et al. (2004), KOGA and MORII (2005), OVERMANN (2006), HÖLZL and DÖRMANN (2007), SØRENSEN et al. (2008), SCHUBOTZ et al. (2009), NOWICKA and KRUK (2010), PITCHER et al. (2011a), MOORE et al. (2013), SEIDEL et al. (2013), ALI et al. (2015), and KULICHEVSKAYA et al. (2015); *not detected.

Zone	Quinone type	Lipid class	(Putative) source organism	Biogeochemical process
Oxic (0-90 m)	Vitamin K1, $PQ_{9:9}$, $UQ_{7:7}$, $UQ_{9:9}$, $UQ_{10:10}$	G-DAG, BL, P-DAG, Alkenones, Cholesterol	*Cyanobacteria*, eukaryotic algae	Oxygenic photosynthesis
	$UQ_{7:7}$, $UQ_{8:8}$, $UQ_{9:9}$, $UQ_{10:10}$	G-DAG, P-DAG, P-AEG, P-DEG	Diverse *Proteobacteria*	Bacterial autotrophy & heterotrophy
Suboxic (90-120 m)	$MK_{6:0}$, $MK_{6:1}$	IP-GDGTs, IP-ARs	*Thaumarchaeota*	Ammonia oxidation
	$UQ_{8:8}$, $UQ_{10:10}$	G-DAG, P-DAG, DPG	*α-Proteobacteria* (e.g., *Nitrobacter*, type II methanotrophs)	Nitrite, iron & aerobic methane oxidation
	$UQ_{8:8}$	P-DAG, DPG	*β-Proteobacteria* (e.g., *Nitrosomonas*, *Thiobacillus*)	Ammonia, iron & sulfur oxidation
	$UQ_{8:8}$, $UQ_{9:9}$	P-DAG, DPG	*γ-Proteobacteria* (e.g., (*Marinobacter*, *Thiomicrospira*, *Nitrosococcus*, *Nitrococcus*, type I methanotrophs)	Ammonia, sulfur, iron, nitrite & aerobic methane oxidation
Photic anoxic (120-150 m)	ChQ, $MK_{7:7}$	G-DAG, P-DAG, DPG, Isorenieratene	Green sulfur bacteria (*Chlorobiaceae*)	Anoxygenic photosynthesis
Dark anoxic (150-1200 m)	$MK_{6:6}$	P-DAG, P-AEG, P-DEG, OL	*δ-* (*Desulfomonas*, *Desulfovibrio*), *ϵ-Proteobacteria* (e.g., *Sulfurimonas*)	Sulfate reduction, Sulfur oxidation
	$MK_{7:7}$	P-DAG, P-AEG, P-DEG	*δ-Proteobacteria* (*Desulfobacter*, *Desulfococcus*, *Desulfosarcina*)	Sulfate reduction
	$MK_{6:6}$	P-DAG, OL, BL, (PC- & PE-ladderanes*)	*Planctomycetes*	Anaerobic ammonium oxidation
	$MK_{7:7}$, $MK_{8:8}$	IP-GDGTs, IP-ARs	Planktonic *Euryarchaeota* and *Crenarchaeota*	Unknown
	$MK_{8:8}$	P-DAG, P-AEG, P-DEG	*δ-Proteobacteria* (*Desulfuromonas*)	Sulfate reduction
	$MK_{7:7}$, $MK_{9:9}$	G-DAG, P-DAG, BL	*Firmicutes* (e.g., *Desulfotomaculum*)	E.g., sulfate reduction
	$MK_{8:8}$, $MK_{8:7}$, $MK_{8:6}$, $MK_{9:9}$, $MK_{9:8}$, $MK_{9:7}$, $MK_{10:9}$, $MK_{10:10}$, $MK_{11:11}$	G-DAG, P-DAG	*Actinobacteria*	E.g., nitrate reduction
	$MP_{5:4}$, $MP_{5:3}$	IP-ARs	*Methanosarcinales*, anaerobic methane oxidizing archaea (ANME)	*Methanogenesis*, anaerobic oxidation of methane
	Regular UQs	-	Unknown anaerobic source or fossil detritus	-
	UQ isomers	-	Unknown anaerobic source	-
	Vitamin K1, $PQ_{9:9}$	-	Unknown anaerobic source or fossil detritus	-

detected in the oxic zone, indicating that aerobic organisms predominantly synthesize UQs with this specific stereochemical configuration.

The major IPLs in the oxic zone, G-DAGs, are widely distributed among cyanobacteria and phototrophic eukaryotes (BENNING et al., 1995; SANINA et al., 2004; HÖLZL and DÖRMANN, 2007) but are also produced by heterotrophic bacteria (GOLDFINE, 1984; DOWHAN, 1997; POPENDORF et al., 2011). The abundances of the apolar lipids cholesterol, produced by all eukaryotes, and alkenones, originating from eukaryotic algae, co-vary with the abundances of the algal respiratory quinones $PQ_{9:9}$ and vitamin K1 as well as G-DAG (Figs. 7.8, 7.14 and 7.15). This indicates that algae are the major source of these lipids in the oxic zone of the Black Sea (Table 7.2). In addition to G-DAGs, algae synthesize P-DAG lipids (SANINA et al., 2004; SUZUMURA, 2005), and, as a response to phosphorous limitation, also BLs (e.g., VAN MOOY et al., 2009). However, BL and P-DAG abundances are not correlated to those of algal biomarkers (Figs. 7.8, 7.14 and 7.15), indicating that they may originate primarily from bacterial sources as previously suggested for other oceanic provinces (cf. BENNING et al., 1995; LIN et al., 2006; SCHUBOTZ et al., 2009; VAN MOOY and FREDRICKS, 2010).

The detection of $MK_{6:0}$ and $MK_{6:1}$ further indicates thaumarchaeal respiratory activity at this depth (cf. Chapter 6), although the concentrations of these quinones and the contribution to the overall respiratory quinone pool were comparatively small (Fig. 7.6). Similarly, low abundances of thaumarchaeal biomass in the oxic zone are implicated by minor abundances of intact polar GDGTs (Figs. 7.8 and 7.14), which are thought to be predominantly sourced by planktonic *Thaumarchaeota* (e.g., Chapter 5; PITCHER et al., 2011a), but have recently been suggested to be also produced by Marine Group II *Euryarchaeota* (LINCOLN et al., 2014a).

7.4.2.2. Suboxic zone (90 and 120 mbsl): Archaeal ammonia-oxidation, bacterial sulfur-, methane- and nitrite-oxidation

The quinone composition in the suboxic zone is substantially different from that observed in the oxic zone. The predominance of thaumarchaeal quinones (>70 % of total quinones, (Fig. 7.8) and the decrease in dissolved ammonium concentration (Fig. 7.3) indicate that archaeal ammonia-oxidation is the major respiratory process in these layers as suggested in an earlier study (cf. Chapter 6). Moreover, the depth profiles of both intact polar GDGTs and the thaumarchaeal quinones $MK_{6:0}$ and $MK_{6:1}$ showed a distinct concentration maximum in the suboxic zone (Figs. 7.8 and 7.14) in agreement with similar observations based on the abundances of thaumarchaeal 16S rRNA and *amoA* indicating maximum thaumarchaeotal abundance in the chemocline (ammonia monooxygenase subunit A) gene biomarkers (COOLEN et al., 2007; LAM et al., 2007).

The absence of quinones involved in photosynthesis indicates that cyanobacteria and eukaryotic algae do not inhabit the suboxic zone or are metabolically not active.

The UQs detected in the suboxic zone likely originate from aerobic ammonia-, iron-, and sulfur-oxidizing α-, β- and γ-*Proteobacteria* as well as aerobic nitrite- and methane-oxidizing α- and γ-*Proteobacteria* (Table 7.2; COLLINS and GREEN, 1985; HIRAISHI, 1999). The occurrence of these biogeochemical processes in the Black Sea chemocline has also been attested by previous geochemical as well as gene and lipid biomarker surveys (e.g., DURISCH-KAISER et al., 2005; KONOVALOV et al., 2005; SCHUBERT et al., 2006; WAKEHAM et al., 2007). *Proteobacteria* are probably the producers of the abundant P-DAGs as well as G-DAGs and DPGs (BARRIDGE and SHIVELY, 1968; SHORT et al., 1969; MAKULA, 1978; GOLDFINE, 1984; FANG et al., 2000) detected in the suboxic zone and thus represent a major part of the microbial biomass in this part of the Black Sea water column.

The concentrations of both IPLs and quinones are comparatively low in the samples from the chemocline (Figs. 7.8 and 7.14), suggesting low microbial biomass and respiratory activity. This is in contrast to other studies where high microbial activity was proposed to occur at the chemocline (e.g., WAKEHAM et al., 2007) but in line with decreased microbial cell densities compared to the oxic and anoxic zones as inferred from fluorescence *in situ* hybridization counts (e.g., PIMENOV and NERETIN, 2006). Since IPLs are tracers for microbial biomass while quinone concentrations are related to biomass and respiratory activity, our results suggest that microbial biomass in the chemocline is dominated by diverse bacteria, whereas respiratory activity is dominated by ammonia-oxidizing *Thaumarchaeota*.

7.4.2.3. Photic anoxic zone (120-150 mbsl): Bacterial anoxygenic photosynthesis

Penetration of H_2S-containing water into the photic zone (Fig. 7.3) may result in bacterial anoxygenic photosynthesis. Indeed, $ChQ_{7:7}$ and the carotenoid isorenieratene (REPETA and SIMPSON, 1991), which are both diagnostic for anaerobic phototrophic green sulfur bacteria of the family *Chlorobiaceae* (FRYDMAN and RAPOPORT, 1963; OVERMANN, 2006), showed distinct concentration maxima in anoxic, sulfidic waters at 150 mbsl (Figs. 7.6 and 7.8). This habitat depth is close to the maximum depth for phototrophic growth suggested for the Black Sea based on the optical transparency of seawater (REPETA, 1993). $MK_{7:7}$, which is a major quinone in the chlorosomes of *Chlorobiaceae* (FRYDMAN and RAPOPORT, 1963; FRIGAARD et al., 1997), is the only MK that significantly increased in concentration at this depth (b-isomer, Fig. 7.8), further suggesting a major contribution of these organisms to respiratory activity at the deep chemocline. The abundance of a single *Chlorobium* phylotype at the deep chemocline

at depths of up to 145 mbsl has been reported to be a widespread feature of the Black Sea and attributed to extremely low-light adaptation of this particular phylotype (OVERMANN et al., 1992; MANSKE et al., 2005; MARSCHALL et al., 2010). The major polar lipids of *Chlorobiaceae* are G-DAG, P-DAG and DPG (OVERMANN, 2006), which were also abundant at this depth (Figs. 7.13 and 7.14). The peak of $ChQ_{7:7}$ at the deep chemocline, the distinctive co-variation with isorenieratene as well as $MK_{7:7}$ and the abundance of characteristic IPLs support the use of $ChQ_{7:7}$ as a biomarker for anaerobic photosynthesis in the environment, which we demonstrate for the first time in the present paper.

7.4.2.4. Anoxic zone (150 – 1200 mbsl): Sulfate and nitrate reduction, anammox, and sulfur oxidation

The first appearance of polyunsaturated MKs in the anoxic zone (including the deep chemocline at 150 mbsl) reflects a shift of aerobic and micro-aerobic archaeal and bacterial respiration to mainly bacterial, MK-dependent, anaerobic respiration (Figs. 7.6 and 7.8). Likely sources of polyunsaturated MKs in the anoxic zone are diverse sulfate-reducing *δ-Proteobacteria*, such as *Desulfobacter*, *Desulfococcus*, and *Desulfosarcina* spp., which produce predominantly $MK_{7:7}$. Furthermore, *Desulfovibrio* and *Desulfuromonas* synthesize $MK_{6:6}$, and $MK_{8:8}$, respectively, as major quinones (Table 7.2; COLLINS and JONES, 1981). Sulfur oxidizing *ϵ-Proteobacteria* of the genus *Sulfurimonas* might represent an additional source of $MK_{6:6}$ in the Black Sea (FUCHSMAN et al., 2011). Potential sources for $MK_{7:7}$ and $MK_{9:9}$ are sulfate-reducing *Firmicutes* related to the genus *Desulfotomaculum* (e.g., COLLINS and JONES, 1981). Several of these bacterial clades have been suggested to be responsible to a large extent of dark carbon fixation below the chemocline (PIMENOV and NERETIN, 2006). The occurrence of quinones of sulfate reducing bacteria in the anoxic zone is also consistent with the IPL distribution, which is similar to that reported by SCHUBOTZ et al. (2009). Bacterial intact polar ether lipids (AEGs and DEGs) which are almost exclusively associated with anaerobic bacteria (e.g., KIM et al., 1970) and particularly sulfate reducers (Table 7.2; RÜTTERS et al., 2001; STURT et al., 2004), were detected throughout the anoxic water column (Figs. 7.13 and 7.14). Since sulfate reducing and sulfur oxidizing *Proteobacteria* contain a mix of DAG, AEG and DEG core lipids, they are likely also a major source for P-DAGs (e.g., RÜTTERS et al., 2001). Moreover, ornithine lipids were detected in minor abundances in the anoxic zone and might originate from sulfate reducing bacteria such as *Desulfovibrio* spp. (MAKULA and FINNERTY, 1975; SCHUBOTZ et al., 2009; SEIDEL et al., 2013). The association of these IPLs with specific quinones is supported by the correlation of P-DAG and OL abundances with those of $MK_{6:6}$(a+b),

$MK_{8:8}$(a+b) and $MK_{9:9}$(b) (Figs. 7.8, 7.14 and 7.15) and concentration maxima of these compounds in the upper anoxic zone (300 mbsl). An activity and abundance maximum of sulfate reducers and sulfur oxidizers in the upper anoxic zone is consistent with the observations that these bacteria first appear beneath the chemocline (DURISCH-KAISER et al., 2005; LIN et al., 2006; WAKEHAM et al., 2007; FUCHSMAN et al., 2011) and that sulfur oxidation and sulfate reduction rates are highest in the upper anoxic zone of the Black Sea (JØRGENSEN et al., 1991; ALBERT et al., 1995).

Other sources of $MK_{6:6}$ might be *Planctomycetes* (WARD et al., 2006; KULICHEVSKAYA et al., 2007, 2008; KULICHEVSKAYA et al., 2015). Bacteria affiliated with a deeply-branching monophyletic lineage of this phylum perform the reduction of NO_2^- to N_2 by NH_4^+, i.e., anaerobic ammonium oxidation (anammox). Based on the analysis of 16S ribosomal RNA gene markers and the anammox specific ladderane lipids, anammox bacteria have been shown to be mainly present within the suboxic zone (e.g., KUYPERS et al., 2003; WAKEHAM et al., 2007). Moreover, COOLEN et al. (2007) and LAM et al. (2007) proposed the co-occurrence and coupling of bacterial anammox and archaeal ammonia-oxidation within the chemocline of the central Black Sea. The quinone profiles at our study site in the southern Black Sea indicate a vertical separation of the depth habitats of ammonia-oxidizing *Thaumarchaeota* and anammox bacteria, with *Thaumarchaeota* being confined to the suboxic zone and anammox bacteria residing within the upper anoxic zone (cf. Table 7.2), although geochemical coupling of these processes cannot be excluded. High sulfide concentrations appear to inhibit growth of anammox bacteria (JENSEN et al., 2008) and thus anammox bacteria are likely restricted to the upper part of the anoxic zone. IPLs detected in the anoxic zone, such as P-DAG, OL and BL, might in part be sourced from anammox bacteria (MOORE et al., 2013; KULICHEVSKAYA et al., 2015), but their diagnostic intact polar ladderane lipids were not detected, probably because of their typically low abundance (JAESCHKE et al., 2009).

Fully unsaturated and partially saturated MKs with chains lengths of 8 to 11 have been commonly associated with bacteria of the phylum *Actinobacteria* (Table 7.2; COLLINS and JONES, 1981; URAKAWA et al., 2005). In particular, *Actinobacteria* have been implicated in denitrification, i.e., the heterotrophic reduction of NO_3^- to N_2, within the anoxic zone of the Black Sea (FUCHSMAN et al., 2011). Quinones with 9 to 11 isoprenoid units are abundant in the anoxic zone of the Black Sea, especially in the deeper part (Fig. 7.8), and thus indicate a significant contribution of *Actinobacteria* to the metabolic activity, possibly denitrification, in the deep anoxic Black Sea. Furthermore, *Actinobacteria* might be a source of the abundant P-DAGs and G-DAGs observed in the deeper part of the Black Sea water column (Fig. 7.14).

Late eluting UQ isomers (b-series) occurred only in the anoxic water column and

were absent from the oxic and suboxic zones, suggesting production of these compounds by unknown anaerobic bacteria (Fig. 7.8). Alternatively, lateral intrusions of modified Bosporus water represent a significant mechanism providing dissolved oxygen to the suboxic and upper anoxic zones of the Black Sea (LEWIS and LANDING, 1991; TEBO, 1991) and might explain the occurrence of UQs in the anoxic water column. These lateral injections of oxygen-enriched waters have been further suggested to cause stabilization of the suboxic zone, balance its redox budget and enable extensive autocatalytic and microbial Mn(II) oxidation by dissolved oxygen in the western and southwestern Black Sea close to our study site (TEBO, 1991; OGUZ et al., 2001; KONOVALOV et al., 2003; SCHIPPERS et al., 2005).

Alternatively, the detection of quinones typically associated with aerobic processes, $PQ_{9:9}$ and UQs, in the anoxic water column might be indicative of an allochthonous origin by vertical transport from the oxic zone or lateral transport from the upper continental slope. Sediment trap investigations demonstrated that terrestrial organic matter accumulated during periods of low organic carbon flux associated with high freshwater runoff particularly in the late winter and late spring, and/or by an influx of particles resuspended by storms from the basin margins (HONJO et al., 1987; HAY et al., 1990). Therefore, the high lipid and quinone concentrations in the anoxic zone compared to the oxic and suboxic zones (Figs. 7.6 and 7.8) might result from lateral transport of fossil biomass but may also be explained by high productivity *in situ* that is stimulated or sustained by lateral input of fresh organic matter and electron acceptors used by anaerobic microbes, e.g., sulfate reducing bacteria.

1G-Cer contribute up to 15 % of the total IPLs in the suboxic and anoxic zones (Fig. 7.13). However, the sources of these lipids, which are typically associated with eukaryotes, below the oxic zone remain unconstrained. SCHUBOTZ et al. (2009) suggested an unknown anaerobic bacterial origin for these lipids based on a bacteria-like fatty acid composition of 1G-Cer in the anoxic zone contrary to a eukaryotic fatty acid composition observed in the photic zone. The fact that 1G-Cer abundances in our dataset are not correlated with eukaryotic biomarkers such as $PQ_{9:9}$, vitamin K1, alkenones and cholesterol but with UQs and MKs (Fig. 7.15) strongly suggest a bacterial origin of these compounds below the oxic zone and thus support the hypothesis of SCHUBOTZ et al. (2009).

MPs are characteristic biomarkers for members of the archaeal order *Methanosarcinales* (cf. Chapter 6), which comprise the metabolically most versatile methanogens utilizing $CO_2 + H_2$, acetate, and methylated compounds as substrates (KENDALL and BOONE, 2006). Methanogens are likely outcompeted for acetate and H_2 by sulfate reducing bacteria in the anoxic zone of the Black Sea due to thermodynamic constraints (e.g., ABRAM and NEDWELL, 1978; OREMLAND and POLCIN, 1982; LIN et

al., 2012). Thus, utilization of non-competitive methylated substrates (OREMLAND and POLCIN, 1982; OREMLAND et al., 1982) is a likely methanogenic pathway of the *Methanosarcinales* in the Black Sea. Although water column methane concentrations were not measured at our study site, methane is present in significant amounts in the anoxic zone at other sites in the Black Sea (e.g., REEBURGH et al., 1991; WAKEHAM et al., 2007). It was suggested that most of the methane present in the Black Sea water column derives from the sediments (REEBURGH et al., 1991), but the presence of MP indicates that methylotrophic methanogenesis may also occur within the anoxic water column. However, anaerobic methane oxidizing ANME-2 archaea that are phylogenetically closely related to the *Methanosarcinales* have been detected in the anoxic water column of the Black Sea (VETRIANI et al., 2003; SCHUBERT et al., 2006; WAKEHAM et al., 2007). While the presence of MP in ANME-2 has not been constrained due to a lack of cultured representatives, these methanotrophic archaea might represent an additional source of MP. Intact polar ARs showed a similar profile as MPs and these compounds are thus likely sourced from the same euryarchaeal sources, *Methanosarcinales* (KOGA and MORII, 2005) and ANME (ROSSEL et al., 2008), but may also be produced by other uncultivated anaerobic planktonic euryarchaeotal groups present in the anoxic zone of the Black Sea (VETRIANI et al., 2003).

Other quinones specific for archaea, i.e., fully saturated menaquinones or menaquinone derivatives (cf. Chapter 6), were not detected in the anoxic zone of the Black Sea. This indicates that either most anaerobic planktonic *Cren-* and *Euryarchaeota* do not produce quinones or that these archaea synthesize bacterial-like polyunsaturated quinones similar to those found in extremely halophilic archaea of the order *Halobacteriales* (COLLINS et al., 1981) and thermophilic archaea of the order *Thermoplasmatales* (cf. Chapter 6), the latter being phylogenetically related to uncultivated planktonic Marine Group II *Euryarchaeota* also found in the Black Sea (e.g., DELONG, 1998; VETRIANI et al., 2003).

7.4.3. Respiratory quinones and IPLs in the Black Sea sediments

In contrast to the water column, where positive and negative correlations between the investigated quinones and lipids were observed, quinones and lipids in the sediments were exclusively positively correlated (Fig. 7.15). Moreover, quinones as well as IPLs were correlated to the abundance of cholesterol (Fig. 7.15), which might be used as a tracer of fossil biomass. This suggests that the lipid biomarker concentrations follow total organic carbon content and thus, that most compounds originate either from fossil detritus or that the microbial abundance and activity *in situ* is strongly dependent on organic matter availability.

Whereas archaeal IPLs only represent minor components in all water column samples, the bacterial to archaeal IPL ratio is much more balanced in the sediments (Fig. 7.13). This signal is not reflected in the quinone composition, (Fig. 7.6). Both saturated and polyunsaturated menaquinones, which are potentially produced by archaea (cf. Chapter 6) showed low relative abundances in the sediments, suggesting that the sedimentary archaea do not produce significant amounts of quinones.

In the upper 2-4 mbsf, the mineralization of the organic matter is mainly driven by sulfate reduction as sulfate constitutes the major electron acceptor in Black Sea sediments (JØRGENSEN et al., 2001). Due to the lack of electron acceptors, fermenters, methanogens and acetogens are likely the only microbes that are active in the sulfate-depleted (methanogenic) zone. Since, acetogenesis, especially with H_2 as the electron donor, is thermodynamically less favorable than methanogenesis (e.g., LIN et al., 2012), homoacetogens are typically outcompeted by methanogens in many habitats (LIU and WHITMAN, 2008). Since most fermenters have lost the ability to produce quinones (COLLINS and JONES, 1981; NOWICKA and KRUK, 2010) and hydrogenotrophic methanogens do not contain quinones or functional quinone analogs (cf. Chapter 6; THAUER et al., 2008), the quinone abundance and diversity is expected to be low in the methanogenic zone.

7.4.3.1. Evidence for preservation of quinones in Unit I sediments

The range of quinone types detected in the sediment was similar to the anoxic water column, but the relative abundances of quinones were significantly different (Fig. 7.6). $PQ_{9:9}$ was the most abundant quinone, similar to the oxic zone of the water column. Since $PQ_{9:9}$ is not known to be produced by non-photosynthetic and anaerobic microorganisms, the high relative abundance of this quinone indicates that a large fraction of the quinone pool may originate from allochthonous, photic zone-derived organic matter. Moreover, the depth profile of the eukaryotic apolar lipid cholesterol was similar to that of $PQ_{9:9}$ (Figs. 7.9, 7.14 and 7.15) further supporting a fossil origin of $PQ_{9:9}$. The concentration of vitamin K1 was very low in the sediments although the depth profile was similar to cholesterol and $PQ_{9:9}$ (Figs. 7.6 and 7.9), indicating different degradation kinetics of the two quinone types that might be related for example to the different headgroup types or the length of the isoprenoid chain. Similarly, URAKAWA et al. (2000) and URAKAWA et al. (2005) detected significant amounts of $PQ_{9:9}$ and vitamin K1 in shallow marine sediments and suggested that these quinones originate from phytoplankton detritus. The same likely applies for the *Chlorobiaceae*-specific $ChQ_{7:7}$ at our study site. $ChQ_{7:7}$ and isorenieratene do not follow the same trend in the sediments despite originating from the same biological source (Fig. 7.9). This observa-

tion indicates rapid degradation of $ChQ_{7:7}$ as further exemplified by its strong decrease in abundance within the uppermost sediment (Fig. 7.14), whereas isorenieratene is well preserved in the sedimentary record of the Black Sea (Fig. 7.14; cf. REPETA, 1993). Maxima in sedimentary isorenieratene concentrations were interpreted to represent periods of a shallow chemocline position, whereas absence of isorenieratene was assumed to indicate chemocline depths below the euphotic zone (REPETA, 1993; SINNINGHE DAMSTÉ et al., 1993). Thus, the two peaks observed at approximately 100 cmbsf and in the sapropel layer (ca. 400 cmbsf) at our study site reflect periods of a shallow chemocline with abundant green sulfur bacteria in the Black Sea water column (Fig. 7.14).

The distribution of UQ and MK isomers differed significantly between the water column and the sediments (see Fig. 7.7) and suggests either different communities inhabiting the two environments and/or different adaptation mechanisms, while significant transport of UQ and MK isomers from the water column to the sediments seems unlikely to explain the strongly diverging quinone composition on the sediment (Figs. 7.7 and 7.9). Modification of quinone stereochemistry may strongly affect the physicochemical properties of these compounds similar to the influence of fatty acid *cis*/*trans* isomerism on membrane fluidity in bacteria (GUCKERT et al., 1986; HEIPIEPER et al., 1992; LOFFELD and KEWELOH, 1996), and may thus represent an adaptation mechanism characteristic for benthic bacteria. In contrast, the *cis*/*trans* ratio of fatty acids has also been used as an index for early diagenesis based on the assumption that *cis*-isomers are preferentially degraded and clay-catalyzed conversion of the *cis* isomers to the *trans* isomers occurs abiotically in the sediments (VAN VLEET and QUINN, 1979). Analogously, quinone isomers may represent either life signals of the benthic microbial community or transformation products of allochthonous lipids.

7.4.3.2. Evidence for benthic bacterial activity

The co-occurrence of polyunsaturated MKs and P-DEG lipids that we observed throughout the sediment suggests the presence of indigenous sulfate reducing bacteria (COLLINS and JONES, 1981; RÜTTERS et al., 2001; STURT et al., 2004). Based on gene analysis, (LELOUP et al., 2007) showed that sulfate-reducing microorganisms including *Deltaproteobacteria*, *Desulfobacteraceae* and *Desulfovibrionales* were predominant in the sulfate reduction zone but also occurred in the methanogenic zone of the northwestern Black Sea. ALBERT et al. (1995) observed that modeled acetate, lactate, and formate turnover times in central Black Sea surface sediments were generally less than one day, suggesting that sulfate reduction may be limited by the supply of these substrates through fermentation. Moreover, some sulfate reducing bacteria,

such as some *Desulfovibrio* and *Desulfobacter* species may also switch to fermentative metabolisms and perform for example disproportionation of thiosulfate (e.g., KRUMHOLZ et al., 1997; RABUS et al., 2006). Occurrence of this process in marine sediments has been confirmed by radiotracer experiments and recognized as an important component of the sulfur cycle (JØRGENSEN, 1990; JØRGENSEN et al., 1991). Thus, the sulfate reducers inhabiting deep, sulfate-depleted sediments in the Black Sea potentially switch to fermentation as an alternative form of energy conservation, which may explain the abundance of MKs and DEG IPLs in the sulfate-depleted sediments (cf. Fig. 7.13). An additional explanation for the high abundances of MKs and DEG IPLs is the formation of endospores and/or persistence of dormant microbial populations under unfavorable, e.g., sulfate-limited conditions as previously suggested by (LELOUP et al., 2007). These hypotheses are not necessarily exclusive. All bacterial IPLs except for P-DEGs abundant in the surficial sediments were not detected below 40 cmbsf, where sulfate became depleted (Fig. 7.3). This switch to ether-based lipids would be consistent with the notion that ether-lipids are more stable and less permeable to ions as compared to ester-based analogs, resulting in reduced maintenance energy (VALENTINE, 2007).

7.4.3.3. Evidence for benthic archaeal activity

MPs were present within the top 400 cmbsf, which indicates the presence of *Methanosarcinales* and/or ANME-2 at these depths (Fig. 7.9). Similar to the anoxic water column, these archaea either produce methane via methylotrophic methanogenesis (*Methanosarcinales*), due to competition for acetate and hydrogen with sulfate-reducers in the presence of abundant sulfate (OREMLAND and POLCIN, 1982), or are associated with the anaerobic oxidation of methane (ANME-2, e.g., HINRICHS et al., 1999; ORPHAN et al., 2001). The oxidation of methane has been demonstrated to occur in Black Sea sediments (e.g., REEBURGH et al., 1991; JØRGENSEN et al., 2001) and sulfate and methane profiles revealed patterns typical for the anaerobic oxidation of methane at our study site (Fig. 7.3; cf. BARKER and FRITZ, 1981; WHITICAR, 1999; YOSHINAGA et al., 2014). Thus, it is probable that the MPs observed in the sulfate reduction zone originate at least partly from ANME-2. Analysis of the stable carbon isotopic composition of MPs or the analysis of ANME-2 enrichment cultures for the occurrence of MPs will be helpful for testing their potential for MP synthesis.

Since methanogenesis has been shown to predominantly occur in the limnic sediments (Unit II) below the sulfate-reduction zone (JØRGENSEN et al., 2004), and MPs were not detected at these depths, *Methanosarcinales* are likely not abundant below the sulfate-reduction zone. Instead, CO_2-reduction by hydrogenotrophic methanogens,

e.g., *Methanobacteriales* or *Methanococcales* which do not produce quinones, is more likely to occur in the deep sediments. The $\delta^{13}C_{CH_4}$ values of approximately −75‰ observed in the methanogenic zone are also consistent with the range of values characteristically associated with CH_4 produced via CO_2-reduction (WHITICAR et al., 1986) assuming $\delta^{13}C_{CO_2}$ of ca. −20‰ for the Black Sea sediments (e.g., KNAB et al., 2009). The strongly depleted $\delta^{13}C_{CH_4}$ values observed below the sulfate-methane transition zone (ca. 100-200 cmbsf; Fig. 7.3) likely result from carbon isotope equilibration between methane and CO_2 during anaerobic oxidation of methane under low sulfate concentrations (<0.5 mM, cf. YOSHINAGA et al., 2014).

In contrast to the water column, IP-ARs do not follow the same trend as MPs (Figs. 7.11 and 7.14, which implies additional benthic archaeal sources for IP-ARs. Sources of IP-ARs in the sulfate-depleted zone might be hydrogenotrophic methanogens such as *Methanobacteriales* and *Methanococcales* (KOGA et al., 1993; KOGA and MORII, 2005) or benthic heterotrophic archaea as suggested by BIDDLE et al. (2006) for deeply buried sediments at the Peru margin.

The abundances of thaumarchaeal quinones ($MK_{6:0}$ and $MK_{6:1}$) and intact GDGTs appear to be decoupled in the sediments, whereas they showed a strong positive correlation in the water column (Fig. 7.15). Thus, the two compound groups might also have different sources in the sediments as discussed for MPs and IP-ARs. Intact GDGTs have been detected in a variety of sedimentary systems as major IPLs (e.g., LIPP et al., 2008; LIPP and HINRICHS, 2009; LIU et al., 2011), which is consistent with our data (Fig. 7.13).

Intact GDGTs, particularly 2G-GDGTs, have been associated with ANME-1 archaea at cold methane seeps (ROSSEL et al., 2008). Additionally, some methanogens, such as members of the order *Methanobacteriales*, are able to synthesize acyclic GDGTs (KOGA and MORII, 2005). Similarly to IP-ARs, the isotopic signature of intact GDGTs from deeply buried sediments provided evidence for a heterotrophic benthic archaeal source (BIDDLE et al., 2006). Additionally, archaeal 16S rRNA surveys have revealed various lineages of uncultured archaea, such as the Miscellaneous Crenarchaeotal Group (MCG), that occur ubiquitously in subsurface habitats (e.g., BIDDLE et al., 2006; SØRENSEN and TESKE, 2006). The lipid composition of these benthic archaeal lineages remains unconstrained due to a paucity of cultivated representatives. However, GDGT production by these lineages is plausible due to their close phylogenetic relatedness to cultivated, GDGT-producing thermophiles (cf. PEARSON and INGALLS, 2013; SCHOUTEN et al., 2013). However, intact GDGTs in sediments might also partly be derived from benthic *Thaumarchaeota*. Although only aerobic growth has been reported for cultured *Thaumarchaeota* (e.g., KÖNNEKE et al., 2005; STAHL and DE LA TORRE, 2012), several studies reported that thaumarchaeal phylotypes are present in

anoxic subsurface sediments (INAGAKI et al., 2006; ROUSSEL et al., 2009; JORGENSEN et al., 2012). JORGENSEN et al. (2012) suggested that sediment-specific thaumarchaeal lineages might oxidize ammonia with alternative so far unknown electron acceptors or produce oxygen intracellularly, similar to the methane oxidizing bacterium *Candidatus* Methylomirabilis oxyfera (ETTWIG et al., 2010). The decoupling of the abundances of thaumarchaeal MKs and IP-GDGTs and the contrasting correlations of IP-AR and IP-GDGT as well as polyunsaturated quinones in the sediment (Fig. 7.15) suggests, however, that the benthic archaea synthesize either bacterial-like quinones or are devoid of quinones.

Production of CO_2 as well as ammonium and phosphate by a consortium of fermentative and methanogenic microbes typically occurs during the remineralization of sedimentary organic matter (e.g., MEGONIGAL et al., 2003; BURDIGE, 2006; BURDIGE and KOMADA, 2013). We observed highest concentrations of PO_4^{3-} and NH_4^+ in the pore waters at ca. 400 cmbsf near the organic-rich sapropel layer, whereas concentrations above and below this depth showed a decreasing trend, indicating their production at the sapropel (Fig. 7.3). This provides strong evidence for microbial activity within deep sediments of the Black Sea. PARKES et al. (2000) and COOLEN et al. (2002) reported high bacterial cell numbers and enhanced hydrolytic enzyme activity in a Mediterranean sapropel suggestive of high microbial activity in these organic-rich layers. COOLEN et al. (2002) further found particularly green non-sulfur bacteria (*Chloroflexus*-like organisms) to be active within the sapropels. *Chloroflexi* synthesize exclusively polyunsaturated MKs (IMHOFF and BIAS-IMHOFF, 1995; ZHI et al., 2014), which may explain the high abundance of these quinones in the sapropel.

7.4.3.4. Microbial activity versus preservation of paleo-signals in Unit II sediments

Absolute concentrations of IPLs and quinones were low in Unit II, indicating much less biomass than in the overlying sediments. These sediments were deposited during the last glacial when the Black Sea was a freshwater lake (ROSS et al., 1970; DEGENS and ROSS, 1972). The total organic carbon content in these layers is comparably low (JØRGENSEN et al., 2004) due to well oxygenated conditions during the time of deposition (ROSS et al., 1970; DEGENS and ROSS, 1972), potentially explaining the absence of the photosynthetic quinones, especially $PQ_{9:9}$. Since the organic carbon in the deep limnic deposits mostly consists of terrestrial recalcitrant material (CALVERT et al., 1987), it is likely less available to microbes as a carbon and energy source, which might explain the low abundance of IPLs and quinones in Unit II sediments.

We further observed high relative abundances of $ChQ_{7:7}$ in Unit II sediments (Fig. 7.6), which can hardly be explained by the benthic production of this quinone

specific for photosynthetic green sulfur bacteria. It was suggested that the water column was fully oxygenated during the lacustrine phase (e.g., DEUSER, 1972) and thus a fossil source from *Chlorobiaceae*, which is the only known source for $ChQ_{7:7}$, is unlikely. Additionally, isorenieratene was not detected in the samples from Unit II and the preservation potential of this compound seems to be much higher as observed for Unit II. The occurrence of $ChQ_{7:7}$ in Unit II sediments thus suggests that there is either a so far unconstrained benthic source or a specific preservation mechanism for this compound.

Apart from microbial life *in situ*, fossilization of IPLs might significantly contribute to the observed signal. Although it is generally assumed that IPLs are degraded quickly after cell death (WHITE et al., 1979; HARVEY et al., 1986), more recent studies revealed evidence that the turnover times of IPLs outside living cells are dependent on their structural properties (LOGEMANN et al., 2011). Whereas intact lipids that contain ester-bound moieties are rapidly degraded by microbes independent of the polar head group, significant proportions of ether-lipids, such as archaeal and bacterial diether and archaeal tetraether lipids, may not be degraded during early diagenesis and may thus contribute to the recalcitrant organic matter in deeply buried sediments (SCHOUTEN et al., 2010; LOGEMANN et al., 2011; XIE et al., 2013). The turnover times for respiratory quinones have not been studied yet, but incubation experiments by HEDRICK and WHITE (1986) indicate rapid changes of the quinone distribution within a few days when anoxic sediments were incubated under aerobic conditions and vice versa. However, particularly the high relatively high abundances of $PQ_{9:9}$ observed in Unit I sediments may attest a recalcitrant character at least to some quinone types. Thus, the quinone and IPL signals in Black Sea sediments likely reflect mixed allochthonous and autochthonous sources.

7.5. Conclusions

Our comprehensive analysis of respiratory quinone and membrane lipid distributions in the Black Sea water column demonstrates that this combined approach is capable of resolving the stratification of microbial abundances, community composition and metabolisms along the redox gradients of the southern Black Sea, which are summarized in Fig. 7.16.

The oxic, photic zone of the Black Sea water column was dominated by high abundances of quinones (UQs, vitamin K1, $PQ_{9:9}$) and IPLs (G-DAG, BL, P-DAG) associated with oxygenic photosynthesis and aerobic respiration. In contrast, low concentrations of IPLs and respiratory quinones indicated comparatively low biomass and metabolic activity in the suboxic zone at the upper chemocline. Here, high relative

abundances of thaumarchaeal menaquinones ($MK_{6:0}$ and $MK_{6:1}$) and low relative abundances of thaumarchaeal IPLs (IP-GDGTs) indicated that respiratory activity but not biomass was dominated by thaumarchaeal ammonia-oxidizers. In contrast, low respiratory activity but high contributions to the total microbial biomass were likely associated with aerobic proteobacterial methane-, iron-, and nitrite-oxidizers (UQs, P-DAGs, G-DAGs).

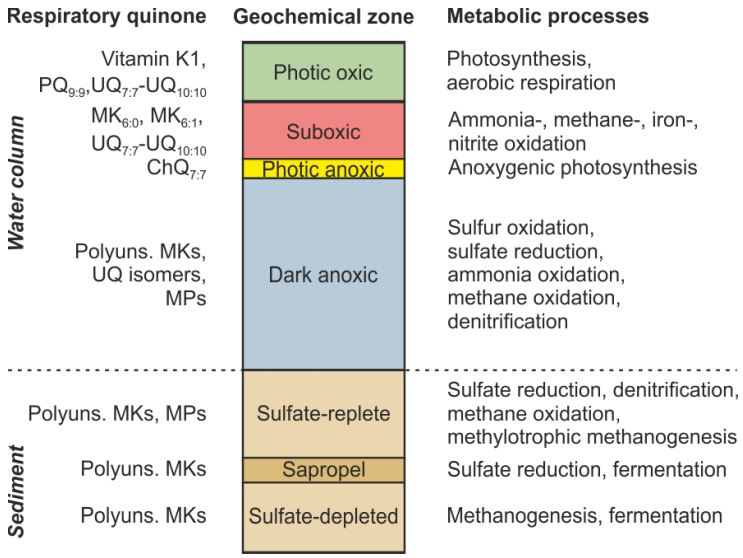

Figure 7.16. Schematic representation of the distribution of respiratory quinones and associated metabolic processes.in the different geochemical zones of the Black Sea.

A pronounced maximum in $ChQ_{7:7}$ and the pigment isorenieratene indicated metabolically active, extremely low-light-adapted *Chlorobiaceae* performing anoxygenic photosynthesis in the lower anoxic chemocline.

High abundances of MKs, distinct UQ isomers and bacterial ether (AEG, DEG) and ester (DAG) IPLs indicated high respiratory activity and biomass in the dark anoxic zone below the chemocline associated with a high diversity of bacterial metabolisms such as sulfate reduction, anammox and denitrification by β-, and ϵ-*Proteobacteria*, *Firmicutes*, *Planctomycetes*, and *Actinobacteria*. Presence of methanogens affiliated with the *Methanosarcinales* and/or methanotrophic archaea of the ANME-2 clade was indicated by characteristic MPs and high abundances of IP-ARs.

Sulfate reduction and sulfate-dependent anaerobic oxidation of methane were the major processes identified in the upper sediment based on sulfate and methane concentration and $\delta^{13}C_{CH_4}$ profiles, high abundances of bacterial MKs as well as ester and ether lipids and archaeal MPs and IP-ARs. Alternatively, MPs and IP-ARs might also be sourced by *Methanosarcinales* performing methylotrophic methanogenesis in the presence of sulfate. The sapropel layer located at 4 mbsf was associated with a peak of dissolved ammonium concentration as well as maximum abundances of bacterial and

archaeal IPLs and quinones, suggesting intense microbial heterotrophic activity in this organic-matter rich layer. The detection of high abundances of biogenic methane in the deeper sediment and the disappearance of MPs near and below the sapropel indicated that methanogenesis in the deep sediment was not driven by *Methanosarcinales* but by hydrogenotrophic methanogens, e.g., *Methanobacteriales* and *Methanococcales*.

In conclusion, combined membrane lipid and respiratory quinone profiling provides a useful tool to trace abundances and metabolic processes of microbial communities involved in the cycling of carbon, nitrogen, and sulfur in the stratified Black Sea. Thus, it appears as a promising technique for enhancing the quantitative aspect of membrane lipid analyses with process-related information from respiratory quinones.

Acknowledgements

We are grateful to the crew, chief scientist M. Zabel, and the scientific shipboard party of R/V Meteor cruise M84/1 (DARCSEAS I). L. Wörmer, N.I. Goldenstein, C. Zhu, T. Meador, S. Pape, and T. Goldhammer are thanked for supporting sampling and instrumental analyses. We thank F. Schmidt for support with statistical analyses. We thank Dr. Ian Bull (University of Bristol) for providing alkenone standards. This study was funded by the European Research Council under the European Union's Seventh Framework Programme–'Ideas' Specific Programme, ERC grant agreement No. 247153 (Advanced Grant DARCLIFE; PI: K.-U.H.) and by the Deutsche Forschungsgemeinschaft through the Gottfried Wilhelm Leibniz Prize awarded to K.-U.H. (Hi 616-14-1) and instrument grant Inst 144/300-1 (HPLC-qToF system).

CHAPTER 8

Conclusions and Outlook

Thaumarchaeal GDGT membrane lipids are used as biomarkers for the distribution and metabolisms of archaeal communities in the environment as well as for the reconstruction of paleoenvironmental conditions (cf. BROCKS and PEARSON, 2005; SCHOUTEN et al., 2013). The interpretation of lipid signatures in environmental samples relies on an accurate knowledge of the distribution of lipid biomarkers among cultivated organisms, the environmental factors influencing their abundance as well as their geological fate in the environment (cf. BROCKS and PEARSON, 2005; BROCKS and BANFIELD, 2009). However, the interpretation of GDGTs as biomarkers of living *Thaumarchaeota* is restricted by the paucity of direct observations in culture experiments and the limited availability of cultured thaumarchaeal representatives. The aim of this thesis was to constrain the influences of physiological and environmental parameters on lipid composition in thaumarchaeal pure cultures in order to enhance our ability to reliably reconstruct past environments based on the geologic record and to improve interpretations of intact polar GDGT distributions used for tracing thaumarchaeal abundance and activity in the marine water column (**Part I**). Utilization of recently developed analytical protocols that enable simultaneous quantification of the relative abundances of archaeal IPLs and their core lipid compositions facilitated a re-appraisal of the complexity of the thaumarchaeal lipidome and allowed identification of novel biomarkers (**Parts I and II**).

Influence of physiological and environmental factors on membrane lipid composition in *Thaumarchaeota*

In this thesis, the influences of growth phase, temperature, salinity, and pH on lipid composition were investigated in batch culture experiments with a pure culture of the marine planktonic thaumarchaeon *Nitrosopumilus maritimus*. Two novel planktonic thaumarchaeal strains phylogenetically closely related to *N. maritimus*, strain NAOA2 and strain NAOA6, were isolated from the South Atlantic Ocean, which represent the first thaumarchaeal pure cultures obtained from the open ocean.

In **Chapter 3**, I demonstrated that the lipid composition of *N. maritimus* changes markedly with growth phase. The results indicate that high abundances of 1G-GDGTs relative to HPH-GDGTs in the water column do not necessarily indicate 'fossil' intact polar lipids originating from unviable biomass. Instead, HPH-GDGT abundance seems to be linked to growing and metabolically active cells rather than to the abundance of viable cells. I therefore propose that a high ratio of 1G- to HPH-GDGTs indicates thaumarchaeal communities at steady state, i.e., scarcity of suitable electron donors, while relatively high HPH-GDGT proportions indicate metabolically active thaumarchaeal assemblages. As demonstrated in **Chapter 5**, HPH-GDGTs are also not abundant in most marine planktonic thaumarchaeal strains. Consequently, lipids such as 2G- and 2G-OH-GDGTs, i.e., compounds whose relative proportions do not change significantly during growth and are abundant in all cultivated marine planktonic *Thaumarchaeota*, have the greatest potential for quantification of viable thaumarchaeal biomass in aquatic samples. Furthermore, I show that distinct TEX_{86} values of the different intact polar GDGT classes observed in the marine water column are biosynthetic signatures of *Thaumarchaeota*. A strong increase of TEX_{86}-temperatures of specific IPLs and total GDGTs between growth phase and stationary phase indicates that metabolic state has a profound effect on GDGT cyclization and thus TEX_{86}-derived temperatures. Moreover, the relative contributions of individual IPLs as potential sources of individual core GDGTs change during growth, and the four core GDGTs included in the TEX_{86} are generally sourced in different proportions from the principal IPL precursors. Consequently, diagenetic processes may distinctly affect the individual core GDGTs during their hydrolytic release from polar precursors.

In **Chapter 4**, I demonstrate that marine planktonic *Thaumarchaeota* respond sensitively to changing growth temperatures by adjusting their membrane lipid composition, in particular the content of crenarchaeol. In contrast to previous hypotheses suggesting that crenarchaeol increases membrane fluidity and might therefore represent an adaptation to cold environments, crenarchaeol appears to be involved in maintaining membrane functioning at elevated temperatures. Significantly different IPL composi-

tions in the three marine thaumarchaeal isolates *N. maritimus*, strain NAOA2, and strain NAOA6 imply that the IPL composition of environmental samples might be driven not only by physiological and environmental factors but also by thaumarchaeal diversity. In the three studied thaumarchaeal strains, changes of TEX_{86} signatures with temperature result primarily from changes in the relative abundances of the major IPL classes 1G-, HPH- and 2G-GDGTs, each of which are affiliated with distinct core GDGT compositions. The disparate relationships of TEX_{86} and growth temperature that we observed among the three closely related thaumarchaeal strains suggests that changes in community composition may exert a strong control on TEX_{86}. Therefore, environmental TEX_{86} signals may represent a mixture of temperature adaptation, nutrient conditions and community dynamics, which might account for the subsurface decoupling of TEX_{86} and in situ temperature observed in marine water column profiles. In contrast, salinity does not appear to influence lipid composition and TEX_{86} in marine *Thaumarchaeota* while pH exerts a minor influence on these parameters. Collectively, these results suggest that a complex interplay of physiological and environmental processes influences the formation of the TEX_{86} signal, thus questioning the paleogeographical and temporal applicability of the TEX_{86} paleothermometer.

Novel chemotaxonomic biomarkers for distinct archaeal clades

In order to identify diagnostic biomarkers for specific archaeal clades, the lipidomes of 11 thaumarchaeal pure and enrichment cultures from soil, geothermal habitats, and the surface ocean were analyzed (**Chapter 5**). The relative abundances of core lipids in cultivated *Thaumarchaeota* appear to be determined by phylogeny, while the IPL composition is reflective of the habitat or growth conditions. While all thaumarchaeal strains synthesize crenarchaeol as a major core lipid, OH-GDGTs are only found in Group I.1a as well as the sister group SAGMCG-1. High abundances of GDGT-4, GDDs, and the crenarchaeol regioisomer are characteristic for group I.1b *Thaumarchaeota*, while the apolar lipid methoxy archaeol is particularly abundant in SAGMCG-1. Thermophilic *Thaumarchaeota* of the HWCG-III cluster are distinct from the other thaumarchaeal groups by synthesizing large amounts of GTGTs. The described core lipid and IPL profiles in cultivated *Thaumarchaeota* may help to interpret the IPL signatures observed in environmental samples and may be used to identify specific thaumarchaeal clades.

The complementary analysis of 21 euryarchaeal and crenarchaeal species shows that the novel apolar lipid methoxy archaeol is found exclusively in *Thaumarchaeota*. The characteristic distribution of methoxy archaeol and intact polar GDGTs along a depth

profile through the OMZ in the equatorial North Pacific Ocean further suggests that methoxy archaeol may be used as a biomarker for *Thaumarchaeota* in the environment.

Two abundant compounds in the lipidome of *N. maritimus* were identified as respiratory quinones, which are membrane-bound lipids functioning as electron carriers in the respiratory chains of almost all organisms (**Chapters 5 and 6**). Analysis of 11 thaumarchaeal as well as 21 eury- and crenarchaeal species revealed that the menaquinones $MK_{6:0}$ and $MK_{6:1}$ are the sole respiratory quinones in *Thaumarchaeota* and that the structural variations of quinones and their distribution among the Archaea bear significant chemotaxonomic information and high biomarker potential for classification and quantification of distinct archaeal orders in the environment. In **Chapter 7**, we demonstrate that combined membrane lipid and respiratory quinone profiling can be used to trace abundances and metabolic processes of archaeal, bacterial, and eukaryotal clades involved in the cycling of carbon, nitrogen, and sulfur and thus resolve the microbial stratification in the chemocline, anoxic waters and sediments of the Black Sea. Therefore, the simultaneous analysis of membrane lipids and respiratory quinones appears as a promising technique for enhancing the quantitative aspect of membrane lipid analyses with process-related information from respiratory quinones.

Outlook

While results from batch culture experiments might not be directly transferable to the environment, the absence of a universal TEX_{86}–temperature relationship in cultivated *Thaumarchaeota* and the influences of growth phase and pH on TEX_{86} in *N. maritimus* suggest that current global calibration models for the TEX_{86} paleothermometer might not be universally applicable. Therefore, the comprehensive investigation of TEX_{86}–temperature relationships in yet to be cultivated *Thaumarchaeota* from a wide range of environments, e.g., from the deep marine water column, are needed to develop a mechanistic understanding of the influence of community composition on TEX_{86} signals and to reliably interpret the geologic GDGT record. The results presented here further imply that specifically adapted archaeal communities may be recognizable by distinct GDGT distributions. Knowledge of the ecological significance of distinct GDGT signatures may then be used to develop alternative calibration models using modern analogue environments as suggested by (TIERNEY and TINGLEY, 2014). Additional parameters that have not been assessed here are the influence of growth rate, i.e., the dependency on the rate of electron donor supply, and the influence of dissolved oxygen concentration on lipid composition in *Thaumarchaeota*. These parameters might be especially important in environments with extremely limited ammonia availability such as the deep ocean as well as in oceanic oxygen minimum zones, respectively.

The novel biomarkers diagnostic for *Thaumarchaeota* described here – methoxy archaeol, $MK_{6:0}$ and $MK_{6:1}$ menaquinones – appear to be well suited for tracing the presence and activity of planktonic *Thaumarchaeota* independently from GDGTs. Thus, these biomarkers offer a high potential for distinguishing thaumarchaeal and euryarchaeal sources of GDGTs in the environment, the latter having recently been implicated as a major source of GDGTs in the ocean (LINCOLN et al., 2014a).

The combined study of membrane lipids and respiratory quinones in the marine water column and sediments from a range of environments harboring different microbial communities may facilitate the assignment of specific metabolisms to microbial 'orphan lipids' and thus, the identification of possible source organisms. However, the effects of physiological and environmental parameters on quinone composition in archaea and bacteria as well as the role of quinone in membrane lipid adaptation remain largely unconstrained, but may be determined using pure culture- or mesocosm experiments. Moreover, the fate of respiratory quinones in the marine water column and sediments, i.e., their diagenetic stability, needs to be constrained in order to confirm their utility as biomarkers for living cells.

CHAPTER 9

Contributions as Co-Author

9.1. Identification of isoprenoid glycosidic glycerol dibiphytanol diethers and indications for their biosynthetic origin

Travis B. Meador[a,*], Chun Zhu[a], **Felix J. Elling**[a], Martin Könneke[a] and Kai-Uwe Hinrichs[a]

Published in *Organic Geochemistry*
2014
Vol. 69, pages 70-75. doi: 10.1016/j.orggeochem.2014.02.005

[a] Organic Geochemistry Group, MARUM - Center for Marine Environmental Sciences & Department of Geosciences, University of Bremen, 28359 Bremen, Germany

[*] Corresponding author. E-mail: travis.meador@uni-bremen.de

Abstract A series of archaeal lipid biomarkers, the isoprenoid glycerol dibiphytanol diethers (GDDs), was recently described and proposed to represent either biosynthetic intermediates or diagenetic products of the relatively more abundant glycerol dibiphytanyl glycerol tetraether (GDGT) lipids (Liu, X.-L., Lipp, J.S., Schröder, J.M., Summons, R.E., Hinrichs, K.-U., 2012. Isoprenoid glycerol dialkanol diethers: a series of novel lipids in marine sediments. Organic Geochemistry 43, 50–55). Here we report a novel series of polar lipids comprising a glycosidic head group and GDD core lipids with varying cycloalkyl distributions (1G-GDDs), which were found in estuarine and hot spring sediments, as well as in a pure culture of the mesophilic thaumarchaeon *Nitrosopumilus maritimus*. 1G-GDDs represented up to 4% of the corresponding monoglycosidic GDGTs (1G-GDGTs). The distinct cycloalkyl distribution patterns of these intact polar lipids (IPLs) and detection of 1G-GDDs in an archaeal culture suggest a biosynthetic source of 1G-GDDs rather than formation exclusively via diagenetic removal of a glycerol moiety from 1G-GDGTs.

9.2. Membrane lipids from marine planktonic archaea: taxonomic signatures and adaptive patterns

Chun Zhu[a,b,*], Stuart G. Wakeham[c], **Felix J. Elling**[a], Gesine Mollenhauer[a,d], Andreas Basse[a,d], Gerard J. M. Versteegh[a], Martin Könneke[a] and Kai-Uwe Hinrichs[a]

In preparation

[a] MARUM - Center for Marine Environmental Sciences & Department of Geosciences, University of Bremen, 28359 Bremen, Germany
[b] School of Earth and Ocean Sciences, Cardiff University, Cardiff, CF10 3AT, U.K.
[c] Skidaway Institute of Oceanography, 10 Ocean Science Circle, Savannah, GA 31411
[d] Alfred-Wegener-Institute for Polar and Marine Research (AWI), Bremerhaven, Germany

[*] Corresponding author. E-mail: zhuc3@cardiff.ac.uk

Abstract Archaea colonize the entire ocean and mediate globally relevant biogeochemical processes. Their membrane lipids have provided unique insights into present and past archaeal ecology. However, studies of archaeal lipid patterns in marine suspended particulate matter (SPM) and sediments mainly focused on fully saturated glycerol dibiphytanyl glycerol tetraethers (GDGTs), which do not capture the considerable diversity of planktonic archaea. Moreover, GDGTs are primarily considered to be planktonic thaumarchaeotal products while diagnostic biomarkers for planktonic Euryarchaeota have not been established. Likewise, adaptation of archaeal lipids to conditions in sub- and aphotic zones remains unconstrained. Here, we comprehensively analyze the archaeal lipidome in 168 SPM samples ranging from surface to abyssal depths in diverse oceanic regimes. We find numerous unsaturated archaeal ether lipids that extend the known inventory of planktonic archaeal lipids. Based on characteristic distributions, we tentatively assign tetra-unsaturated archaeol to the euphotic euryarchaeotal ecotype encoding proteorhodopsins, and tri- to octa-unsaturated GDGTs to anaerobic and/or microaerophilic planktonic Euryarchaeota. Lipid patterns further distinguish archaeal groups residing in surface (< 100 m) versus deep (≥ 100 m) oxygenated waters. The deep water group overall produces more saturated diglycosidic lipids than its surface counterpart. Adaptation of major membrane lipids

to habitat temperature also differentiates these two archaeal groups is expressed in distinct thermal regulations on the degrees of cyclization and hydroxylation of saturated diglycosidic lipids. The chemotaxonomic and adaptive signatures identified in this study extend the foundation for applications of archaeal lipids in microbial ecology and paleoceanography.

9.3. Hydroxylated isoprenoidal GDGTs in China coastal seas and their potential as paleotemperature proxy in mid-to-low latitude marginal seas

Xiaoxia Lü[a,b,c,*], Xiaolei Liu[a], **Felix J. Elling**[a], Huan Yang[b], Shucheng Xie[b], Jinming Song[d], Xuegang Li[d], Huamao Yuan[d], Ning Li[d] and Kai-Uwe Hinrichs[a]

Submitted to *Organic Geochemistry*

[a] Organic Geochemistry Group, MARUM - Center for Marine Environmental Sciences & Department of Geosciences, University of Bremen, 28359 Bremen, Germany
[b] State Key Laboratory of Biogeology and Environmental Geology, China University of Geosciences (Wuhan), 430074, Wuhan, China
[c] Faculty of Earth Resource, China University of Geosciences (Wuhan), 430074, Wuhan, China
[d] Institute of Oceanology, Chinese Academy of Sciences, 266071, Qingdao, China

[*] Corresponding author. E-mail: luxiaox@163.com

Abstract Hydroxylated isoprenoidal GDGTs (OH-GDGTs), with one or two hydroxyl groups in the biphytane chains, major compounds of planktonic thaumarchaeota, occur widely in marine and lacustrine sediments. In order to examine the potential of OH-GDGTs as recorders of local variations of sea surface temperature (SST), we collected 70 surface sediments from the China coastal seas (CCS), including 16 samples from the Yangtze Estuary, to determine their tetraether lipid compositions. The proportion of OH-GDGTs of total isoprenoidal GDGTs increases with latitude from 1.8% to 12.8% and is highly correlated to SST as indicated by redundancy analysis. The variation of OH-GDGT composition is best captured by the ring index (RI-OH), which is significantly correlated with both summer and autumn SST and is associated with minimum residual SST relative to remote sensing data. The large input of terrigenous organic matter in the Yangtze Estuary appears to have no significant influence on the OH-GDGT-based proxy. Our analyses suggest the RI-OH could serve as a useful proxy for recording warm seasonal SST in the China coastal seas.

9.4. Multiple evidences for methylotrophic methanogenesis as the dominant methanogenic pathway in deep-sea hypersaline sediments

Guang-Chao Zhuang[a,b,+], **Felix J. Elling**[a,+,*], Lisa M. Nigro[c], Vladimir Samarkin[d], Samantha B. Joye[d], Andreas Teske[c] and Kai-Uwe Hinrichs[a]

In preparation for *Geochimica et Cosmochimica Acta*

[+]These authors contributed equally to this work

[a] Organic Geochemistry Group, MARUM - Center for Marine Environmental Sciences & Department of Geosciences, University of Bremen, 28359 Bremen, Germany
[b] Key Laboratory of Marine Chemistry Theory and Technology, Ministry of Education, College of Chemistry and Chemical Engineering, Ocean University of China, 266100 Qingdao, China
[c] Department of Marine Sciences, University of North Carolina at Chapel Hill, Chapel Hill, 27599 NC, USA
[d] Department of Marine Sciences, University of Georgia, 30602 Athens, GA, USA

[*] Corresponding author. E-mail: felling@marum.de

Abstract Among Earth's most extreme habitats, dark, deep and anoxic brines host unique microbial ecosystems that remain largely unexplored. As the terminal step of organic matter degradation, methanogenesis is a potentially significant but poorly constrained process supporting carbon cycling in deep-sea hypersaline environments. Here we integrated biogeochemical and phylogenetic analyses as well as incubation experiments to unravel the origin of methane in hypersaline sediments of Orca Basin in the northern Gulf of Mexico. Significant concentrations of methane (up to 3.4 mM) coexisted with high concentrations of sulfate (16-43 mM) in two sediment cores retrieved from the southern and northern sections of Orca Basin. Strong ^{13}C-depletion ($\delta^{13}CH_4$: −76.7 to −89.1‰) as well as high methane to ethane ratios (600-3000) pointed to a biological source of methane. While low concentrations of competitive substrates limited the significance of hydrogenotrophic and acetoclastic methanogenesis, the high abundance of non-competitive methylated substrates and their precursors

(e.g., methanol, trimethylamine, dimethylsulfide, dimethylsulfoniopropionate) suggested that methane could be generated through methylotrophic methanogenesis in the hypersaline sediment of Orca Basin. The carbon isotope systematics of methylated substrates and methane supported methylotrophic methanogenesis as the dominant source of methane in Orca Basin sediments. Thermodynamic calculations demonstrated that hydrogenotrophic and acetoclastic methanogenesis were unlikely to occur under *in situ* conditions, while methylotrophic methanogenesis from methylated substrates was highly favorable. Stable isotope tracer and radiotracer experiments with ^{13}C bicarbonate, acetate and methanol as well as ^{14}C-labeled methylamine indicated that methylotrophic methanogenesis was the predominant methanogenic pathway in Orca Basin sediment. Based on 16S rRNA gene sequences, halophilic methylotrophic methanogens related to the genus *Methanohalophilus* dominated the benthic archaeal community in the northern basin but also occurred in the southern basin. High abundances of methanogen lipid biomarkers such as intact polar and polyunsaturated hydroxyarchaeols were detected in sediments from the northern basin but were of lower abundance in sediments from the southern basin. Strong ^{13}C-depletion of saturated and monounsaturated hydroxyarchaeol were consistent with methylotrophic methanogenesis as the major methanogenic pathway. Collectively, the availability of methylated substrates, thermodynamic calculations, experimentally determined methanogenic activity as well as lipid and gene biomarkers strongly suggested the occurrence and predominance of methylotrophic methanogenesis in Orca Basin sediment. Our findings elucidate the significance of methylotrophic methanogenesis for methane production in the presence of sulfate in deep marine hypersaline environments.

9.5. The contribution of biogas residues to soil organic matter formation and CO_2 emissions in an arable soil

Halil Coban[a,b,*], Anja Miltner[b], **Felix J. Elling**[c], Kai-Uwe Hinrichs[c] and Matthias Kästner[b]

Published in *Soil Biology and Biochemistry*
2015
Vol. 86, pages 108-115. doi: 10.1016/j.soilbio.2015.03.023

[a] UFZ-Helmholtz Centre for Environmental Research, Department of Bioenergy, Permoserstr. 15, 04318 Leipzig, Germany
[b] UFZ-Helmholtz Centre for Environmental Research, Department of Environmental Biotechnology, Permoserstr. 15, 04318 Leipzig, Germany
[c] Organic Geochemistry Group, MARUM - Center for Marine Environmental Sciences & Department of Geosciences, University of Bremen, 28359 Bremen, Germany

[*] Corresponding author. E-mail: halil.coban@ufz.de

Abstract The biogas production process generates as side-products biogas residues containing microbial biomass which could contribute to soil organic matter formation or induce CO_2 emissions when applied to arable soil as fertilizer. Using an isotope labelling approach, we labelled the microbial biomass in biogas residues, mainly G^+ bacteria and methanogenic archaea via $KH^{13}CO_3$, and traced the fate of microbial biomass carbon in soil with an incubation experiment lasting 378 days. Within the first seven days, 40% of the carbon was rapidly mineralized and after that point mineralization continued, reaching 65% by the end of the experiment. Carbon mineralization data with 93% recovery could be fitted to a two-pool degradation model which estimated proportions and degradation rate constants of readily and slowly degrading pools. About 49% of the carbon was in the slowly degrading pool with a half-life of 1.9 years, suggesting mid-term contribution to living and non-living soil organic matter formation. Biogas residues caused a priming effect at the beginning, thus their intensive application should be avoided.

9.6. Heterotrophic bacteria from a lake without phosphate

Mengyin Yao[a], **Felix J. Elling**[b], CarriAyne Jones[c], Sulung Nomosatryo[d], Christopher P. Long[e], Sean A. Crowe[f], Maciek R. Antoniewicz[e], Kai-Uwe Hinrichs[b], Julia A. Maresca[a,*]

Submitted to *Environmental Microbiology*

[a] Department of Civil and Environmental Engineering, University of Delaware, Newark, DE 19716
[b] Organic Geochemistry Group, MARUM-Center for Marine Environmental Sciences, University of Bremen, 28334 Bremen, Germany
[c] Department of Microbiology and Immunology, University of British Columbia, Vancouver, BC, Canada V6T 1Z3
[d] Research Center for Limnology, Indonesian Institute of Sciences, Cibinong, West Java, Indonesia 16911
[e] Department of Chemical and Biomolecular Engineering, University of Delaware, Newark DE 19716
[f] Department of Microbiology and Immunology, Department of Earth, Ocean, and Atmosphere Sciences, University of British Columbia, Vancouver, BC, Canada V6T 1Z4

[*] Corresponding author. E-mail: jmaresca@udel.edu

Abstract Phosphorus-starved heterotrophic bacteria were isolated from Lake Matano, Indonesia, a lake whose phosphate concentration is below the detection limit of standard techniques. Here, we de-scribe the isolation of 8 strains of heterotrophic bacteria capable of growth on vanishingly low amounts of phosphate. These isolates are closely related to soil bacteria and are capable of growth on a variety of soluble and insoluble sources of phosphorus. When transferred to medium without phosphate, the isolates reduce their growth rates, reduce the RNA content, and replace 86-100% of their membrane lipids with phosphorus-free lipids. Similar changes in lipid composition have been observed in marine photoautotrophs and soil heterotrophs, and similar flexibility in phosphorus sources has been demonstrated in marine and soil-dwelling heterotrophs. Our results demonstrate that the strategies used in marine and soil environments are also employed in ultra-oligotrophic freshwater systems, but are taken further than their normal ranges.

9.7. Identification, formation and distribution of fatty acid-substituted glycerol dialkyl glycerol tetraethers in marine sediments

Kevin W. Becker[a,*], **Felix J. Elling**[a], Julius S. Lipp[a], Jan M. Schröder[a], Thomas W. Evans[a], Marcus Elvert[a], Martin Könneke[a] and Kai-Uwe Hinrichs[a]

In preparation for *Organic Geochemistry*

[a] Organic Geochemistry Group, MARUM - Center for Marine Environmental Sciences & Department of Geosciences, University of Bremen, 28359 Bremen, Germany

[*] Corresponding author. E-mail: k.becker@uni-bremen.de

Abstract Archaeal isoprenoid glycerol dialkyl glycerol tetraethers (*i*GDGTs) are abundant components of marine sedimentary organic matter and are used in paleoenvironmental reconstructions. During diagenesis, a significant fraction of free *i*GDGTs can be incorporated into macromolecules. However, the diagenetic reaction mechanisms involving *i*GDGTs remain unresolved. We identified a potential macromolecule precursor, fatty acid-substituted *i*GDGTs (FA-*i*GDGTs), in a globally distributed set of sediment samples and the archaeal culture *Nitrosopumilus maritimus* by high performance liquid chromatography-tandem mass spectrometry (HPLC-MS^2). Instead of a biosynthetic origin, a diagenetic origin of these compounds is proposed. First, a stable isotope probing experiment with *N. maritimus* did not reveal label uptake into the fatty acids and second, FA-*i*GDGTs in environmental samples appear to be in chemical equilibrium with *i*GDGTs. Moreover, the fatty acids connected to FA-*i*GDGTs are similar to the free fatty acids found in the investigated sediments. FA-*i*GDGTs are likely produced by esterification of free fatty acids and *i*GDGTs in sediments during early diagenesis and their formation seems to be dependent on reactant availability, hydrolytic conditions and water activity.

References

Abken, H. J., M. Tietze, J. Brodersen, S. Bäumer, U. Beifuss, and U. Deppenmeier (1998). Isolation and characterization of methanophenazine and function of phenazines in membrane-bound electron transport of *Methanosarcina mazei* Gö1. *Journal of Bacteriology* **180** (8), 2027–2032.

Abram, J. W. and D. B. Nedwell (1978). Inhibition of methanogenesis by sulphate reducing bacteria competing for transferred hydrogen. *Archives of Microbiology* **117** (1), 89–92. doi: 10.1007/BF00689356.

Adkins, J. F., K. McIntyre, and D. P. Schrag (2002). The salinity, temperature, and δ^{18}O of the glacial deep ocean. *Science* **298**, 1769–1773. doi: 10.1126/science.1076252.

Albers, S.-V. and B. H. Meyer (2011). The archaeal cell envelope. *Nature Reviews Microbiology* **9** (6), 414–426. doi: 10.1038/nrmicro2576.

Albert, D. B., C. Taylor, and C. S. Martens (1995). Sulfate reduction rates and low molecular weight fatty acid concentations in the water column and surficial sediments of the Black Sea. *Deep-Sea Research I* **42** (7), 1239–1260. doi: 10.1016/0967-0637(95)00042-5.

Aleem, M. I. H. and D. L. Sewell (1984). Oxidoreductase systems in *Nitrobacter agilis*. In: *Microbial Chemoautotrophy*. Ed. by W. R. Strohl and O. H. Tuovinen. Columbus, OH: Ohio State University Press, pp. 185–210.

Ali, M., M. Oshiki, T. Awata, K. Isobe, Z. Kimura, H. Yoshikawa, D. Hira, T. Kindaichi, H. Satoh, T. Fujii, and S. Okabe (2015). Physiological characterization of anaerobic ammonium oxidizing bacterium '*Candidatus* Jettenia caeni'. *Environmental Microbiology*. doi: 10.1111/1462-2920.12674.

Allen, M. B. (1959). Studies with Cyanidium caldarium, an anomalously pigmented chlorophyte. *Archiv für Mikrobiologie* **32** (3), 270–277. doi: 10.1007/BF00409348.

Alm, E. W., D. B. Oerther, N. Larsen, D. A. Stahl, and L. Raskin (1996). The Oligonucleotide Probe Database. *Applied and Environmental Microbiology* **62** (10), 3557–3559.

Alonso-Sáez, L., A. S. Waller, D. R. Mende, K. Bakker, H. Farnelid, P. L. Yager, C. Lovejoy, J.-É. Tremblay, M. Potvin, F. Heinrich, M. Estrada, L. Riemann, P. Bork, C. Pedrós-Alió, and S. Bertilsson (2012). Role for urea in nitrification by polar marine Archaea. *Proceedings of the National Academy of Sciences of the United States of America* **109** (44), 17989–17994. doi: 10.1073/pnas.1201914109.

Aluwihare, L. I., D. J. Repeta, and R. F. Chen (2002). Chemical composition and cycling of dissolved organic matter in the Mid-Atlantic Bight. *Deep Sea Research Part II: Topical Studies in Oceanography* **49** (20), 4421–4437. doi: 10.1016/S0967-0645(02)00124-8.

Amesz, J. (1973). The function of plastoquinone in photosynthetic electron transport. *Biochimica et Biophysica Acta* **301**, 35–51.

Anraku, Y. (1988). Bacterial electron transport chains. *Annual Review of Biochemistry* **57** (1), 101–132. doi: 10.1146/annurev.biochem.57.1.101.

Antonov, J. I., D. Seidov, T. P. Boyer, R. A. Locarnini, A. V. Mishonov, H. E. Garcia, O. K. Baranova, M. M. Zweng, and D. R. Johnson (2010). *World Ocean Atlas 2009, Volume 2: Salinity*. Ed. by S. Levitus. NOAA Atlas. Vol. 2. Washington, D.C.: U.S. Government Printing Office, 184 pp.

Arrigo, K. R. (2005). Marine microorganisms and global nutrient cycles. *Nature* **437** (7057), 349–355. doi: 10.1038/nature04159.

Arthur, M. A. and W. E. Dean (1998). Organic-matter production and preservation and evolution of anoxia in the Holocene Black Sea. *Paleoceanography* **13** (4), 395–411. doi: 10.1029/98PA01161.

AUGUET, J.-C. and E. O. CASAMAYOR (2008). A hotspot for cold crenarchaeota in the neuston of high mountain lakes. *Environmental Microbiology* **10**, 1080–1086. DOI: 10.1111/j.1462-2920.2007.01498.x.

AUGUET, J.-C. and E. O. CASAMAYOR (2013). Partitioning of *Thaumarchaeota* populations along environmental gradients in high mountain lakes. *FEMS Microbiology Ecology* **84** (1), 154–164. DOI: 10.1111/1574-6941.12047.

AUGUET, J.-C., A. BARBERAN, and E. O. CASAMAYOR (2010). Global ecological patterns in uncultured Archaea. *The ISME Journal* **4** (2), 182–190. DOI: 10.1038/ismej.2009.109.

AUGUET, J.-C., X. TRIADÓ-MARGARIT, N. NOMOKONOVA, L. CAMARERO, and E. O. CASAMAYOR (2012). Vertical segregation and phylogenetic characterization of ammonia-oxidizing Archaea in a deep oligotrophic lake. *The ISME Journal* **6** (9), 1786–1797. DOI: 10.1038/ismej.2012.33.

BAHR, A., F. LAMY, H. ARZ, H. KUHLMANN, and G. WEFER (2005). Late glacial to Holocene climate and sedimentation history in the NW Black Sea. *Marine Geology* **214**, 309–322. DOI: 10.1016/j.margeo.2004.11.013.

BAKER-AUSTIN, C. and M. DOPSON (2007). Life in acid: pH homeostasis in acidophiles. *Trends in Microbiology* **15** (4), 165–171. DOI: 10.1016/j.tim.2007.02.005.

BANO, N., S. RUFFIN, B. RANSOM, and J. T. HOLLIBAUGH (2004). Phylogenetic composition of Arctic Ocean archaeal assemblages and comparison with Antarctic assemblages. *Applied and Environmental Microbiology* **70** (2), 781–789. DOI: 10.1128/AEM.70.2.781-789.2004.

BARKER, J. F. and P. FRITZ (1981). Carbon isotope fractionation during microbial methane oxidation. *Nature* **293** (5830), 289–291. DOI: 10.1038/293289a0.

BARRIDGE, J. K. and J. M. SHIVELY (1968). Phospholipids of the Thiobacilli. *Journal of Bacteriology* **95** (6), 2182–2185.

BASSE, A., C. ZHU, G. J. VERSTEEGH, G. FISCHER, K.-U. HINRICHS, and G. MOLLENHAUER (2014). Distribution of intact and core tetraether lipids in water column profiles of suspended particulate matter off Cape Blanc, NW Africa. *Organic Geochemistry* **72**, 1–13. DOI: 10.1016/j.orggeochem.2014.04.007.

BAY, D. C., S. C. BOOTH, and R. J. TURNER (2015). Respiration and ecological niche influence bacterial membrane lipid compositions. *Environmental Microbiology* **17** (5), 1777–1793. DOI: 10.1111/1462-2920.12637.

BECKER, K. W., J. S. LIPP, C. ZHU, X.-L. LIU, and K.-U. HINRICHS (2013). An improved method for the analysis of archaeal and bacterial ether core lipids. *Organic Geochemistry* **61**, 34–44. DOI: 10.1016/j.orggeochem.2013.05.007.

BEKKER, M., G. KRAMER, A. F. HARTOG, M. J. WAGNER, C. G. DE KOSTER, K. J. HELLINGWERF, and M. J. T. DE MATTOS (2007). Changes in the redox state and composition of the quinone pool of *Escherichia coli* during aerobic batch-culture growth. *Microbiology* **153**, 1974–1980. DOI: 10.1099/mic.0.2007/006098-0.

BELMAR, L., V. MOLINA, and O. ULLOA (2011). Abundance and phylogenetic identity of archaeoplankton in the permanent oxygen minimum zone of the eastern tropical South Pacific. *FEMS Microbiology Ecology* **78** (2), 314–326. DOI: 10.1111/j.1574-6941.2011.01159.x.

BEMAN, J. M., B. N. POPP, and C. a. FRANCIS (2008). Molecular and biogeochemical evidence for ammonia oxidation by marine Crenarchaeota in the Gulf of California. *The ISME Journal* **2** (4), 453–453. DOI: 10.1038/ismej.2008.33.

BENNING, C., Z. H. HUANG, and D. A. GAGE (1995). Accumulation of a novel glycolipid and a betaine lipid in cells of *Rhodobacter sphaeroides* grown under phosphate limitation. *Archives of Biochemistry and Biophysics* **317** (1), 103–111. DOI: 10.1006/abbi.1995.1141.

BENTLEY, R. and R. MEGANATHAN (1982). Biosynthesis of vitamin K (menaquinone) in Bacteria. *Microbiological Reviews* **46** (3), 241–280.

BERG, C., V. VANDIEKEN, B. THAMDRUP, and K. JÜRGENS (2014). Significance of archaeal nitrification in hypoxic waters of the Baltic Sea. *The ISME Journal*, 1–14. DOI: 10.1038/ismej.2014.218.

BIDDLE, J. F., J. S. LIPP, M. A. LEVER, K. G. LLOYD, K. B. SØRENSEN, R. ANDERSON, H. F. FREDRICKS, M. ELVERT, T. J. KELLY, D. P. SCHRAG, M. L. SOGIN, J. E. BRENCHLEY, A. TESKE, C. H. HOUSE, and K.-U. HINRICHS (2006). Heterotrophic Archaea dominate sedimentary subsurface ecosystems off Peru. *Proceedings of the National Academy of Sciences of the United States of America* **103** (10), 3846–3851. DOI: 10.1073/pnas.0600035103.

BILLER, S. J., A. C. MOSIER, G. F. WELLS, and C. A. FRANCIS (2012). Global biodiversity of aquatic ammonia-oxidizing archaea is partitioned by habitat. *Frontiers in Microbiology* **3**, 252. DOI: 10.3389/fmicb.2012.00252.

BINTRIM, S. B., T. J. DONOHUE, J. HANDELSMAN, G. P. ROBERTS, and R. M. GOODMAN (1997). Molecular phylogeny of Archaea from soil. *Proceedings of the National Academy of Sciences of the United States of America* **94** (1), 277–282. DOI: 10.1073/pnas.94.1.277.

BLAINEY, P. C., A. C. MOSIER, A. POTANINA, C. A. FRANCIS, and S. R. QUAKE (2011). Genome of a low-salinity ammonia-oxidizing archaeon determined by single-cell and metagenomic analysis. *PloS One* **6** (2), e16626. DOI: 10.1371/journal.pone.0016626.

BLÖCHL, E., R. RACHEL, S. BURGGRAF, D. HAFENBRADL, H. W. JANNASCH, and K. O. STETTER (1997). *Pyrolobus fumarii*, gen. and sp. nov., represents a novel group of archaea, extending the upper temperature limit for life to 113°*C*. *Extremophiles* **1** (1), 14–21. DOI: 10.1007/s007920050010.

BOLLMANN, A., E. FRENCH, and H. J. LAANBROEK (2011). Isolation, cultivation, and characterization of ammonia-oxidizing bacteria and archaea adapted to low ammonium concentrations. *Methods in Enzymology* **486** (11), 55–88. DOI: 10.1016/B978-0-12-381294-0.00003-1.

BOUCHER, Y., C. J. DOUADY, R. T. PAPKE, D. A. WALSH, M. E. R. BOUDREAU, C. L. NESBØ, R. J. CASE, and W. F. DOOLITTLE (2003). Lateral gene transfer and the origins of prokaryotic groups. *Annual Review of Genetics* **37**, 283–328. DOI: 10.1146/annurev.genet.37.050503.084247.

BOUCHER, Y., H. HUBER, L. HARIDON, K. O. STETTER, and W. F. DOOLITTLE (2001). Bacterial Origin for the Isoprenoid Biosynthesis Enzyme HMG-CoA Reductase of the Archaeal Orders Thermoplasmatales and Archaeoglobales. *Molecular Biology and Evolution* **18** (7), 1378–1388.

BOUSKILL, N. J., D. EVEILLARD, D. CHIEN, A. JAYAKUMAR, and B. B. WARD (2012). Environmental factors determining ammonia-oxidizing organism distribution and diversity in marine environments. *Environmental Microbiology* **14** (3), 714–729. DOI: 10.1111/j.1462-2920.2011.02623.x.

BOYD, E. S., T. L. HAMILTON, J. WANG, L. HE, and C. L. ZHANG (2013). The role of tetraether lipid composition in the adaptation of thermophilic archaea to acidity. *Frontiers in Microbiology* **4**, 62. DOI: 10.3389/fmicb.2013.00062.

BOYD, E. S., A. PEARSON, Y. PI, W.-J. LI, Y. G. ZHANG, L. HE, C. L. ZHANG, and G. G. GEESEY (2011). Temperature and pH controls on glycerol dibiphytanyl glycerol tetraether lipid composition in the hyperthermophilic crenarchaeon *Acidilobus sulfurireducens*. *Extremophiles* **15** (1), 59–65. DOI: 10.1007/s00792-010-0339-y.

BRANDES, J. A., A. H. DEVOL, and C. DEUTSCH (2007). New developments in the marine nitrogen cycle. *Chemical Reviews* **107** (2), 577–589. DOI: 10.1021/cr050377t.

BRASSELL, S. C. (2014). Climatic influences on the Paleogene evolution of alkenones. *Paleoceanography* **29**, 255–272. DOI: 10.1002/2013PA002576.

BRETTEL, K. and W. LEIBL (2001). Electron transfer in photosystem I. *Biochimica et Biophysica Acta* **1507**, 100–114.

BRINKHOFF, T., G. MUYZER, C. O. WIRSEN, and J. KUEVER (1999). *Thiomicrospira chilensis* sp. nov., a mesophilic obligately chemolithoautotrophic sulfuroxidizing bacterium isolated from a *Thioploca mat*. *International Journal of Systematic Bacteriology* **49 Pt 2** (1 999), 875–879. DOI: 10.1099/00207713-49-2-875.

BROCHIER-ARMANET, C., B. BOUSSAU, S. GRIBALDO, and P. FORTERRE (2008). Mesophilic Crenarchaeota: proposal for a third archaeal phylum, the Thaumarchaeota. *Nature Reviews Microbiology* **6** (3), 245–252. DOI: 10.1038/nrmicro1852.

BROCHIER-ARMANET, C., P. FORTERRE, and S. GRIBALDO (2011). Phylogeny and evolution of the Archaea: one hundred genomes later. *Current Opinion in Microbiology* **14** (3), 274–281. DOI: 10.1016/j.mib.2011.04.015.

BROCHIER-ARMANET, C., S. GRIBALDO, and P. FORTERRE (2012). Spotlight on the Thaumarchaeota. *The ISME Journal* **6** (2), 227–30. DOI: 10.1038/ismej.2011.145.

BROCK, T. D., K. M. BROCK, R. T. BELLY, and R. L. WEISS (1972). *Sulfolobus*: A new genus of sulfur-oxidizing bacteria living at low pH and high temperature. *Archiv für Mikrobiologie* **84** (1), 54–68. DOI: 10.1007/BF00408082.

BROCKS, J. J. and A. PEARSON (2005). Building the Biomarker Tree of Life. *Reviews in Mineralogy and Geochemistry* **59**, 233–258. DOI: 10.2138/rmg.2005.59.10.

BROCKS, J. J. and J. BANFIELD (2009). Unravelling ancient microbial history with community proteogenomics and lipid geochemistry. *Nature Reviews Microbiology* **7**, 601–609. DOI: 10.1038/nrmicro2167.

BROWN, J. R. and W. F. DOOLITTLE (1997). *Archaea* and the prokaryote-to-eukaryote transition. *Microbiology and Molecular Biology Reviews* **61** (4), 456–502.

BRUMSACK, H. J. (1989). Geochemistry of Recent TOC-rich sediment from the Gulf of California and the Black Sea. *Geologische Rundschau* **78**, 851–882.

BURDIGE, D. J. (2006). *Geochemistry of Marine Sediments*. Princeton, USA: Princeton University Press, p. 624.

BURDIGE, D. J. and T. KOMADA (2013). Using ammonium pore water profiles to assess stoichiometry of deep remineralization processes in methanogenic continental margin sediments. *Geochemistry, Geophysics, Geosystems* **14** (5), 1626–1643. DOI: 10.1002/ggge.20117.

CABELLO, P., M. D. ROLDÁN, and C. MORENO-VIVIÁN (2004). Nitrate reduction and the nitrogen cycle in archaea. *Microbiology* **150** (11), 3527–3546. DOI: 10.1099/mic.0.27303-0.

CAFFREY, J. M., N. BANO, K. KALANETRA, and J. T. HOLLIBAUGH (2007). Ammonia oxidation and ammonia-oxidizing bacteria and archaea from estuaries with differing histories of hypoxia. *The ISME Journal* **1** (7), 660–662. DOI: 10.1038/ismej.2007.79.

CALVERT, S. E., J. S. VOGEL, and J. R. SOUTHON (1987). Carbon accumulation rates and the origin of the Holocene sapropel in the Black Sea. *Geology* **15** (10), 918–921.

CANFIELD, D. E., F. J. STEWART, B. THAMDRUP, L. DE BRABANDERE, T. DALSGAARD, E. F. DELONG, N. P. REVSBECH, and O. ULLOA (2010). A cryptic sulfur cycle in oxygen-minimum-zone waters off the Chilean coast. *Science* **330** (6009), 1375–1378. DOI: 10.1126/science.1196889.

CAO, H., J.-C. AUGUET, and J.-D. GU (2013). Global ecological pattern of ammonia-oxidizing archaea. *PloS One* **8** (2), e52853. DOI: 10.1371/journal.pone.0052853.

CAPONE, D. G. and D. A. HUTCHINS (2013). Microbial biogeochemistry of coastal upwelling regimes in a changing ocean. *Nature Geoscience* **6** (9), 711–717. DOI: 10.1038/ngeo1916.

CARDACE, D., J. D. MORRIS, A. D. PEACOCK, and D. C. WHITE (2006). Habitability of subseafloor sediments at the Costa Rica convergent margin. In: *Proceedings of the Ocean Drilling Program, Scientific Results Volume 205*. Ed. by J. D. Morris, H. W. Villinger, and A. Klaus. College Station, TX, USA: Ocean Drilling Program.

CARINI, P., A. E. WHITE, E. O. CAMPBELL, and S. J. GIOVANNONI (2014). Methane production by phosphate-starved SAR11 chemoheterotrophic marine bacteria. *Nature Communications* **5**, 4346. DOI: 10.1038/ncomms5346.

CARRILLO HERNANDEZ, T. d. J. (2004). "Caractérisation moléculaire et isotopique de biomarqueurs de milieux de dépôt anciens très immatures: (Jurassique supérieur de la plate-forme russe)". PhD Thesis. University of Strasbourg.

CAVALIER-SMITH, T. (2014). The Neomuran Revolution and Phagotrophic Origin of Eukaryotes and Cilia in the Light of Intracellular Coevolution and a Revised Tree of Life. *Cold Spring Harbor Perspectives in Biology* **6** (9), a016006. DOI: 10.1101/cshperspect.a016006.

CHONG, P. L.-G. (2010). Archaebacterial bipolar tetraether lipids: Physico-chemical and membrane properties. *Chemistry and Physics of Lipids* **163** (3), 253–265. DOI: 10.1016/j.chemphyslip.2009.12.006.

CHONG, P. L.-G., M. SULC, and R. WINTER (2010). Compressibilities and volume fluctuations of archaeal tetraether liposomes. *Biophysical Journal* **99** (10), 3319–3326. DOI: 10.1016/j.bpj.2010.09.061.

CHURCH, M. J., B. WAI, D. M. KARL, and E. F. DELONG (2010). Abundances of crenarchaeal *amoA* genes and transcripts in the Pacific Ocean. *Environmental Microbiology* **12** (3), 679–688. DOI: 10.1111/j.1462-2920.2009.02108.x.

CIOBANU, M.-C., G. BURGAUD, A. DUFRESNE, A. BREUKER, V. RÉDOU, S. BEN MAAMAR, F. GABOYER, O. VANDENABEELE-TRAMBOUZE, J. S. LIPP, A. SCHIPPERS, P. VANDENKOORNHUYSE, G. BARBIER, M. JEBBAR, A. GODFROY, and K. ALAIN (2014). Microorganisms persist at record depths in the subseafloor of the Canterbury Basin. *The ISME Journal* **8** (7), 1370–1380. DOI: 10.1038/ismej.2013.250.

CLINE, J. D. (1969). Spectrophotometric determination of hydrogen sulfide in natural waters. *Limnology and Oceanography* **14** (3), 454–458.

COATES, C. S., J. ZIEGLER, K. MANZ, J. GOOD, B. KANG, S. MILIKISIYANTS, R. CHATTERJEE, S. HAO, J. H. GOLBECK, and K. V. LAKSHMI (2013). The structure and function of quinones in biological solar energy transduction: a cyclic voltammetry, EPR, and hyperfine sub-level correlation (HYSCORE) spectroscopy study of model naphthoquinones. *The Journal of Physical Chemistry. B* **117** (24), 7210–7220. DOI: 10.1021/jp401024p.

COFFINET, S., A. HUGUET, D. WILLIAMSON, L. BERGONZINI, C. ANQUETIL, A. MAJULE, and S. DERENNE (2015). Occurrence and distribution of glycerol dialkanol diethers and glycerol dialkyl glycerol tetraethers in a peat core from SW Tanzania. *Organic Geochemistry* **83-84**, 170–177. DOI: 10.1016/j.orggeochem.2015.03.013.

COLLINS, M. D. and P. N. GREEN (1985). Isolation and characterization of a novel coenzyme Q from some methane-oxidizing bacteria. *Biochemical and Biophysical Research Communications* **133** (3), 1125–1131. DOI: 10.1016/0006-291X(85)91253-7.

COLLINS, M. D. (1985). Isoprenoid quinone analyses in bacterial classification and identification. In: *Chemical Methods in Bacterial Systematics*. Ed. by M. Goodfellow and D. E. Minnikin.

COLLINS, M. D. and B. J. TINDALL (1987). Occurrence of menaquinones and some novel methylated menaquinones in the alkaliphilic, extremely halophilic archaebacterium *Natronobacterium gregoryi*. *FEMS Microbiology Letters* **43** (3), 307–312. DOI: 10.1016/0378-1097(87)90417-4.

COLLINS, M. D., H. N. M. ROSS, B. J. TINDALL, and W. D. GRANT (1981). Distribution of isoprenoid quinones in halophilic bacteria. *Journal of Applied Bacteriology* **50** (3), 559–565. DOI: 10.1111/j.1365-2672.1981.tb04258.x.

COLLINS, M. D. and D. JONES (1981). Distribution of isoprenoid quinone structural types in bacteria and their taxonomic implications. *Microbiological Reviews* **45** (2), 316–354.

COMITA, P. B. and R. B. GAGOSIAN (1983). Membrane lipid from deep-sea hydrothermal vent methanogen: a new macrocyclic glycerol diether. *Science* **222** (4630), 1329–1331. DOI: 10.1126/science.222.4630.1329.

COOLEN, M. J. L., B. ABBAS, J. VAN BLEIJSWIJK, E. C. HOPMANS, M. M. M. KUYPERS, S. G. WAKEHAM, and J. S. SINNINGHE DAMSTÉ (2007). Putative ammonia-oxidizing Crenarchaeota in suboxic waters of the Black Sea: a basin-wide ecological study using 16S ribosomal and functional genes and membrane lipids. *Environmental Microbiology* **9** (4), 1001–1016. DOI: 10.1111/j.1462-2920.2006.01227.x.

COOLEN, M. J. L., H. CYPIONKA, A. M. SASS, H. SASS, and J. OVERMANN (2002). Ongoing modification of Mediterranean Pleistocene sapropels mediated by prokaryotes. *Science* **296** (5577), 2407–2410. DOI: 10.1126/science.1071893.

DANNENMULLER, O., K. ARAKAWA, T. EGUCHI, K. KAKINUMA, S. BLANC, A.-M. ALBRECHT, M. SCHMUTZ, Y. NAKATANI, and G. OURISSON (2000). Membrane properties of archaeal macrocyclic diether phospholipids. *Chemistry* **6** (4), 645–654. DOI: 10.1002/(SICI)1521-3765(20000218)6:4<645::AID-CHEM645>3.0.CO;2-A.

DARLAND, G., T. D. BROCK, W. SAMSONOFF, and S. F. CONTI (1970). A thermophilic, acidophilic mycoplasma isolated from a coal refuse pile. *Science* **170** (3965), 1416–1418.

DAUGHTON, C. G., A. M. COOK, and M. ALEXANDER (1979). Biodegradation of phosphonate toxicants yields methane or ethane on cleavage of the C-P bond. *FEMS Microbiology Letters* **5** (2), 91–93. DOI: 10.1016/0378-1097(79)90191-5.

DAWSON, K. S., K. H. FREEMAN, and J. L. MACALADY (2012). Molecular characterization of core lipids from halophilic archaea grown under different salinity conditions. *Organic Geochemistry* **48**, 1–8. DOI: 10.1016/j.orggeochem.2012.04.003.

DE LA TORRE, J. R., C. B. WALKER, A. E. INGALLS, M. KÖNNEKE, and D. A. STAHL (2008). Cultivation of a thermophilic ammonia oxidizing archaeon synthesizing crenarchaeol. *Environmental Microbiology* **10** (3), 810–818. DOI: 10.1111/j.1462-2920.2007.01506.x.

DE ROSA, M. and A. GAMBACORTA (1988). The lipids of archaebacteria. *Progress in Lipid Research* **27** (3), 153–175. DOI: 10.1016/0163-7827(88)90011-2.

DE ROSA, M., S. DE ROSA, A. GAMBACORTA, L. MINALE, R. H. THOMSON, and R. D. WORTHINGTON (1977). Caldariellaquinone, a unique benzo[*b*]thiophen-4,7-quinone from *Caldariella acidophila*, an extremely thermophilic and acidophilic bacterium. *Journal of the Chemical Society, Perkin Transactions 1* **6**, 653–657. DOI: 10.1039/p19770000653.

DE ROSA, M., E. ESPOSITO, A. GAMBACORTA, B. NICOLAUS, and J. D. BU'LOCK (1980). Effects of temperature on ether lipid composition of *Caldariella acidophila*. *Phytochemistry* **19** (5), 827–831. DOI: 10.1016/0031-9422(80)85120-X.

DE ROSA, M., A. GAMBACORTA, W. D. GRANT, V. LANZOTTI, and B. NICOLAUS (1988). Polar Lipids and Glycine Betaine from Haloalkaliphilic Archaebacteria. *Microbiology* **134** (1), 205–211. DOI: 10.1099/00221287-134-1-205.

DE ROSA, M., A. GAMBACORTA, B. NICOLAUS, B. CHAPPE, and P. ALBRECHT (1983). Isoprenoid ethers; backbone of complex lipids of the archaebacterium *Sulfolobus solfataricus*. *Biochimica et Biophysica Acta* **753** (2), 249–256. DOI: 10.1016/0005-2760(83)90014-0.

DEGENS, E. T. and D. A. ROSS (1972). Chronology of the Black Sea over the last 25,000 years. *Chemical Geology* **10**, 1–16. DOI: 10.1016/0009-2541(72)90073-3.

DELONG, E. F. (1992). Archaea in coastal marine environments. *Proceedings of the National Academy of Sciences of the United States of America* **89** (12), 5685–5689. DOI: 10.1073/pnas.89.12.5685.

DELONG, E. F. (1998). Everything in moderation: Archaea as 'non-extremophiles'. *Current Opinion in Genetics & Development* **8** (6), 649–654. DOI: 10.1016/S0959-437X(98)80032-4.

DELONG, E. F., L. L. KING, R. MASSANA, H. CITTONE, A. MURRAY, C. SCHLEPER, and S. G. WAKEHAM (1998). Dibiphytanyl ether lipids in nonthermophilic crenarchaeotes. *Applied and Environmental Microbiology* **64** (3), 1133–1138.

DELONG, E. F., K. Y. WU, B. B. PRÉZELIN, and R. V. JOVINE (1994). High abundance of Archaea in Antarctic marine picoplankton. *Nature* **371** (6499), 695–697. DOI: 10.1038/371695a0.

DEMBITSKY, V. M. (1996). Betaine ether-linked glycerolipids: Chemistry and biology. *Progress in Lipid Research* **35** (1), 1–51. DOI: 10.1016/0163-7827(95)00009-7.

DEUSER, W. G. (1972). Late-Pleistocene and Holocene history of the Black Sea as indicated by stable-isotope studies. *Journal of Geophysical Research* **77** (6), 1071–1077. DOI: 10.1029/JC077i006p01071.

D'HONDT, S., B. JØRGENSEN, and D. MILLER (2003). *Proceedings of the Ocean Drilling Program, Initial Reports, 201*. Tech. rep. College Station, TX, USA: Ocean Drilling Program. DOI: 10.2973/odp.proc.ir.201.2003.

DIETRICH, L. E. P., M. M. TICE, and D. K. NEWMAN (2006). The co-evolution of life and Earth. *Current Biology* **16**, 395–400. DOI: 10.1016/j.cub.2006.05.017.

DIETRICH, W. and O. KLIMMEK (2002). The function of methyl-menaquinone-6 and polysulfide reductase membrane anchor (PsrC) in polysulfide respiration of *Wolinella succinogenes*. *European Journal of Biochemistry* **269** (4), 1086–1095. DOI: 10.1046/j.0014-2956.2001.02662.x.

DISPIRITO, A. A., W. H. T. LOH, and O. H. TUOVINEN (1983). A novel method for the isolation of bacterial quinones and its application to appraise the ubiquinone composition of *Thiobacillus ferrooxidans*. *Archives of Microbiology* **135** (1), 77–80. DOI: 10.1007/BF00419487.

DODSWORTH, J. A., B. A. HUNGATE, and B. P. HEDLUND (2011). Ammonia oxidation, denitrification and dissimilatory nitrate reduction to ammonium in two US Great Basin hot springs with abundant ammonia-oxidizing archaea. *Environmental Microbiology* **13** (8), 2371–2386. DOI: 10.1111/j.1462-2920.2011.02508.x.

DOWHAN, W. (1997). Molecular basis for membrane phospholipid diversity: why are there so many lipids? *Annual review of biochemistry* **66** (1), 199–232. DOI: 10.1146/annurev.biochem.66.1.199.

DOXEY, A. C., D. A. KURTZ, M. D. J. LYNCH, L. A. SAUDER, and J. D. NEUFELD (2015). Aquatic metagenomes implicate *Thaumarchaeota* in global cobalamin production. *The ISME Journal* **9** (2), 461–471. DOI: 10.1038/ismej.2014.142.

DUGDALE, R. C. and J. J. GOERING (1967). Uptake of new and regenerated forms of nitrogen in primary productivity. *Limnology and Oceanography* **12** (2), 196–206. DOI: 10.4319/lo.1967.12.2.0196.

DUNPHY, P. J., D. L. GUTNICK, P. G. PHILLIPS, and A. F. BRODIE (1968). A new natural naphthoquinone in *Mycobacterium phlei*. *Journal of Biological Chemistry* **243** (2), 398–407.

DURISCH-KAISER, E., L. KLAUSER, B. WEHRLI, and C. SCHUBERT (2005). Evidence of intense archaeal and bacterial methanotrophic activity in the Black Sea water column. *Applied and Environmental Microbiology* **71** (12), 8099–8106. DOI: 10.1128/AEM.71.12.8099-8106.2005.

ECKERT, S., H. J. BRUMSACK, S. SEVERMANN, B. SCHNETGER, C. MÄRZ, and H. FRÖLLJE (2013). Establishment of euxinic conditions in the Holocene Black Sea. *Geology* **41**, 431–434. DOI: 10.1130/G33826.1.

EKIEL, I. and G. D. SPROTT (1992). Identification of degradation artifacts formed upon treatment of hydroxydiether lipids from methanogens with methanolic HCl. *Canadian Journal of Microbiology* **38** (8), 764–768. DOI: 10.1139/m92-124.

ELKINS, J. G., M. PODAR, D. E. GRAHAM, K. S. MAKAROVA, Y. WOLF, L. RANDAU, B. P. HEDLUND, C. BROCHIER-ARMANET, V. KUNIN, I. ANDERSON, A. LAPIDUS, E. GOLTSMAN, K. BARRY, E. V. KOONIN, P. HUGENHOLTZ, N. KYRPIDES, G. WANNER, P. RICHARDSON, M. KELLER, and K. O. STETTER (2008). A korarchaeal genome reveals insights into the evolution of the Archaea. *Proceedings of the National Academy of Sciences of the United States of America* **105** (23), 8102–8107. DOI: 10.1073/pnas.0801980105.

ELLING, F. J., M. KÖNNEKE, J. S. LIPP, K. W. BECKER, E. J. GAGEN, and K.-U. HINRICHS (2014). Effects of growth phase on the membrane lipid composition of the thaumarchaeon *Nitrosopumilus maritimus* and their implications for archaeal lipid distributions in the marine environment. *Geochimica et Cosmochimica Acta* **141**, 579–597. DOI: 10.1016/j.gca.2014.07.005.

EMBLEY, T. M. and W. MARTIN (2006). Eukaryotic evolution, changes and challenges. *Nature* **440** (7084), 623–630. DOI: 10.1038/nature04546.

ENGELHARDT, H. (2007). Mechanism of osmoprotection by archaeal S-layers: A theoretical study. *Journal of Structural Biology* **160** (2), 190–199. DOI: 10.1016/j.jsb.2007.08.004.

ERGUDER, T. H., N. BOON, L. WITTEBOLLE, M. MARZORATI, and W. VERSTRAETE (2009). Environmental factors shaping the ecological niches of ammonia-oxidizing archaea. *FEMS Microbiology Reviews* **33** (5), 855–869. DOI: 10.1111/j.1574-6976.2009.00179.x.

ETTWIG, K. F., M. K. BUTLER, D. LE PASLIER, E. PELLETIER, S. MANGENOT, M. M. M. KUYPERS, F. SCHREIBER, B. E. DUTILH, J. ZEDELIUS, D. DE BEER, J. GLOERICH, H. J. C. T. WESSELS, T. VAN ALEN, F. LUESKEN, M. L. WU, K. T. VAN DE PAS-SCHOONEN, H. J. M. OP DEN CAMP, E. M. JANSSEN-MEGENS, K.-J. FRANCOIJS, H. STUNNENBERG, J. WEISSENBACH, M. S. M. JETTEN, and M. STROUS (2010). Nitrite-driven anaerobic methane oxidation by oxygenic bacteria. *Nature* **464** (7288), 543–548. DOI: 10.1038/nature08883.

FALKOWSKI, P. G. (1997). Evolution of the nitrogen cycle and its influence on the biological sequestration of CO_2 in the ocean. *Nature* **387** (6630), 272–275. DOI: 10.1038/387272a0.

FALKOWSKI, P. G., T. FENCHEL, and E. F. DELONG (2008). The microbial engines that drive Earth's biogeochemical cycles. *Science* **320** (3), 1034–1039. DOI: 10.1126/science.1153213.

FANG, J., M. J. BARCELONA, and J. D. SEMRAU (2000). Characterization of methanotrophic bacteria on the basis of intact phospholipid profiles. *FEMS Microbiology Letters* **189** (1), 67–72. DOI: 10.1111/j.1574-6968.2000.tb09207.x.

FERNÀNDEZ-GUERRA, A. and E. O. CASAMAYOR (2012). Habitat-associated phylogenetic community patterns of microbial ammonia oxidizers. *PloS One* **7** (10), e47330. DOI: 10.1371/journal.pone.0047330.

FERRANTE, G., I. EKIEL, G. B. PATEL, and G. D. SPROTT (1988). A novel core lipid isolated from the aceticlastic methanogen, *Methanothrix concilii* GP6. *Biochimica et Biophysica Acta* **963** (2), 173–182. DOI: 10.1016/0005-2760(88)90278-0.

FERRANTE, G., J. C. RICHARDS, and G. D. SPROTT (1990). Structures of polar lipids from the thermophilic, deep-sea archaeobacterium *Methanococcus jannaschii*. *Biochemistry and Cell Biology* **68** (1), 274–283. DOI: 10.1139/o90-038.

FORTERRE, P., C. BROCHIER, and H. PHILIPPE (2002). Evolution of the Archaea. *Theoretical Population Biology* **61** (4), 409–422. DOI: 10.1006/tpbi.2002.1592.

FRANCIS, C. A., J. M. BEMAN, and M. M. M. KUYPERS (2007). New processes and players in the nitrogen cycle: the microbial ecology of anaerobic and archaeal ammonia oxidation. *The ISME Journal* **1** (1), 19–27. DOI: 10.1038/ismej.2007.8.

FRANCIS, C. A., K. J. ROBERTS, J. M. BEMAN, A. E. SANTORO, and B. B. OAKLEY (2005). Ubiquity and diversity of ammonia-oxidizing archaea in water columns and sediments of the ocean. *Proceedings of the National Academy of Sciences of the United States of America* **102** (41), 14683–14688. DOI: 10.1073/pnas.0506625102.

FRENCH, E., J. A. KOZLOWSKI, M. MUKHERJEE, G. BULLERJAHN, and A. BOLLMANN (2012). Ecophysiological characterization of ammonia-oxidizing Archaea and Bacteria from freshwater. *Applied and Environmental Microbiology* **78** (16), 5773–5780. DOI: 10.1128/AEM.00432-12.

FRIGAARD, N. U., S. TAKAICHI, M. HIROTA, K. SHIMADA, and K. MATSUURA (1997). Quinones in chlorosomes of green sulfur bacteria and their role in the redox-dependent fluorescence studied in chlorosome-like bacteriochlorophyll c aggregates. *Archives of Microbiology* **167**, 343–349. DOI: 10.1007/s002030050453.

FRIGAARD, N.-U., A. MARTINEZ, T. J. MINCER, and E. F. DELONG (2006). Proteorhodopsin lateral gene transfer between marine planktonic Bacteria and Archaea. *Nature* **439** (7078), 847–850. DOI: 10.1038/nature04435.

FRYDMAN, B. and H. RAPOPORT (1963). Non-chlorophyllous pigments of *Chlorobium Thiosulfatophilum* chlorobiumquinone. *Journal of the American Chemical Society* **85** (6), 823–825. DOI: 10.1021/ja00889a044.

FUCHSMAN, C. A., J. B. KIRKPATRICK, W. J. BRAZELTON, J. W. MURRAY, and J. T. STALEY (2011). Metabolic strategies of free-living and aggregate-associated bacterial communities inferred from biologic and chemical profiles in the Black Sea suboxic zone. *FEMS Microbiology Ecology* **78**, 586–603. DOI: 10.1111/j.1574-6941.2011.01189.x.

FUHRMAN, J. A., K. MCCALLUM, and A. A. DAVIS (1992). Novel major archaebacterial group from marine plankton. *Nature* **356** (6365), 148–149. DOI: 10.1038/356148a0.

FUHRMAN, J. A. and A. A. DAVIS (1997). Widespread Archaea and novel Bacteria from the deep sea as shown by 16S rRNA gene sequences. *Marine Ecology Progress Series* **150** (1-3), 275–285. DOI: 10.3354/meps150275.

GABRIEL, J. L. and P. L. G. CHONG (2000). Molecular modeling of archaebacterial bipolar tetraether lipid membranes. *Chemistry and Physics of Lipids* **105** (2), 193–200. DOI: 10.1016/S0009-3084(00)00126-2.

GALAND, P. E., E. O. CASAMAYOR, D. L. KIRCHMAN, M. POTVIN, and C. LOVEJOY (2009a). Unique archaeal assemblages in the Arctic Ocean unveiled by massively parallel tag sequencing. *ISME Journal* **3** (7), 860–869. DOI: 10.1038/ismej.2009.23.

GALAND, P. E., C. LOVEJOY, A. K. HAMILTON, R. G. INGRAM, E. PEDNEAULT, and E. C. CARMACK (2009b). Archaeal diversity and a gene for ammonia oxidation are coupled to oceanic circulation. *Environmental Microbiology* **11** (4), 971–980. DOI: 10.1111/j.1462-2920.2008.01822.x.

GALLIKER, P., O. GRÄTHER, M. RÜMMLER, W. FITZ, and D. ARIGONI (1998). New structural and biosynthetic aspects of the unusual core lipids from *Archaebacteria*. In: *Vitamin B12 and B12-proteins*. Ed. by B. Krautler, D. Arigoni, and B. T. Golding. Hoboken, USA: Wiley-VCH, pp. 447–458. DOI: 10.1002/9783527612192.ch29.

GALLOWAY, J. N., F. J. DENTENER, D. G. CAPONE, E. W. BOYER, R. W. HOWARTH, S. P. SEITZINGER, G. P. ASNER, C. C. CLEVELAND, P. A. GREEN, E. A. HOLLAND, D. M. KARL, A. F. MICHAELS, J. H. PORTER, A. R. TOWNSEND, and C. J. VÖOSMARTY (2004). Nitrogen Cycles: Past, Present, and Future. *Biogeochemistry* **70**, 153–226. DOI: 10.1007/s10533-004-0370-0.

GEIGER, O., N. GONZÁLEZ-SILVA, I. M. LÓPEZ-LARA, and C. SOHLENKAMP (2010). Amino acid-containing membrane lipids in bacteria. *Progress in Lipid Research* **49** (1), 46–60. DOI: 10.1016/j.plipres.2009.08.002.

GEYER, R., A. D. PEACOCK, D. C. WHITE, C. LYTLE, and G. J. V. BERKEL (2004). Atmospheric pressure chemical ionization and atmospheric pressure photoionization for simultaneous mass spectrometric analysis of microbial respiratory ubiquinones and menaquinones. *Journal of Mass Spectrometry* **39**, 922–929. DOI: 10.1002/jms.670.

GIBSON, J. A. E., M. R. MILLER, N. W. DAVIES, G. P. NEILL, D. S. NICHOLS, and J. K. VOLKMAN (2005). Unsaturated diether lipids in the psychrotrophic archaeon *Halorubrum lacusprofundi*. *Systematic and Applied Microbiology* **28** (1), 19–26. DOI: 10.1016/j.syapm.2004.09.004.

GILMORE, S. F., A. I. YAO, Z. TIETEL, T. KIND, M. T. FACCIOTTI, and A. N. PARIKH (2013). Role of squalene in the organization of monolayers derived from lipid extracts of *Halobacterium salinarum*. *Langmuir* **29** (25), 7922–7930. DOI: 10.1021/la401412t.

GLIOZZI, A., G. PAOLI, M. DE ROSA, and A. GAMBACORTA (1983). Effect of isoprenoid cyclization on the transition temperature of lipids in thermophilic archaebacteria. *Biochimica et Biophysica Acta* **735**, 234–242.

GOLDFINE, H. and P.-O. HAGEN (1968). *N*-Methyl Groups in Bacterial Lipids. *Journal of Bacteriology* **95** (2), 367–375.

GOLDFINE, H. (1984). Bacterial membranes and lipid packing theory. *Journal of Lipid Research* **25** (13), 1501–1507.

GRAY, H. B. and W. R. ELLIS (1994). Electron transfer. In: *Bioinorganic Chemistry*. Ed. by I. Bertini, H. B. Gray, S. J. Lippard, and J. S. Valentine. Mill Valley, CA, USA: University Science Books, pp. 315–363.

GRUBER, N. (2008). The Marine Nitrogen Cycle: Overview and Challenges. In: *Nitrogen in the Marine Environment*. Ed. by D. G. Capone, D. A. Bronk, M. R. Mulholland, and E. J. Carpenter. San Diego, Academic Press, pp. 1–50. DOI: 10.1016/B978-0-12-372522-6.00001-3.

GUBRY-RANGIN, C., B. HAI, C. QUINCE, M. ENGEL, B. C. THOMSON, P. JAMES, M. SCHLOTER, R. I. GRIFFITHS, J. I. PROSSER, and G. W. NICOL (2011). Niche specialization of terrestrial archaeal ammonia oxidizers. *Proceedings of the National Academy of Sciences of the United States of America* **108** (52), 21206–21211. DOI: 10.1073/pnas.1109000108.

GUCKERT, J. B., M. a. HOOD, and D. C. WHITE (1986). Phospholipid ester-linked fatty acid profile changes during nutrient deprivation of *Vibrio Cholerae*: Increases in the *trans/cis* ratio and proportions of cyclopropyl fatty acids. *Applied and Environmental Microbiology* **52** (4), 794–801.

GUY, L., J. H. SAW, and T. J. G. ETTEMA (2014). The Archaeal Legacy of Eukaryotes: A Phylogenomic Perspective. *Cold Spring Harbor Perspectives in Biology* **6** (10), a016022. DOI: 10.1101/cshperspect.a016022.

HALL, P. O. J. and R. C. ALLER (1992). Rapid, Small-Volume, Flow Injection Analysis for CO_2 and NH_4^+ in Marine and Freshwaters. *Limnology and Oceanography* **37** (5), 1113–1119.

HAMERSLEY, M. R., G. LAVIK, D. WOEBKEN, J. E. RATTRAY, P. LAM, E. C. HOPMANS, J. S. S. DAMSTÉ, S. KRÜGER, M. GRACO, and D. GUTIÉRREZ (2007). Anaerobic ammonium oxidation in the Peruvian oxygen minimum zone. *Limnology and Oceanography* **52** (3), 923–933. DOI: 10.4319/lo.2007.52.3.0923.

HARVEY, H. R., R. D. FALLON, and J. S. PATTON (1986). The effect of organic matter and oxygen on the degradation of bacterial membrane lipids in marine sediments. *Geochimica et Cosmochimica Acta* **50** (5), 795–804. DOI: 10.1016/0016-7037(86)90355-8.

HARWOOD, J. L. (1998). Membrane Lipids in Algae. In: *Lipids in phothosynthesis: Structure, Function and Genetics*. Ed. by S. Paul-André and M. Norio. Vol. 6. Dordrecht, The Netherlands: Springer, pp. 53–64. DOI: 10.1007/0-306-48087-5.

HATZENPICHLER, R., E. V. LEBEDEVA, E. SPIECK, K. STOECKER, A. RICHTER, H. DAIMS, and M. WAGNER (2008). A moderately thermophilic ammonia-oxidizing crenarchaeote from a hot spring. *Proceedings of the National Academy of Sciences of the United States of America* **105** (6), 2134–2139. DOI: 10.1073/pnas.0708857105.

HAY, B. J., S. HONJO, S. KEMPE, V. A. ITTEKKOT, E. T. DEGENS, T. KONUK, and E. IZDAR (1990). Interannual variability in particle flux in the southwestern Black Sea. *Deep Sea Research Part A. Oceanographic Research Papers* **37** (6), 911–928. DOI: 10.1016/0198-0149(90)90103-3.

HEDRICK, D. B. and D. C. WHITE (1986). Microbial respiratory quinones in the environment. *Journal of Microbiological Methods* **5** (5-6), 243–254. DOI: 10.1016/0167-7012(86)90049-7.

HEINZ, V., E. GAGEN, S. DAXER, M. KÖNNEKE, K.-U. HINRICHS, M. THOMM, and R. RACHEL (2013). "*Nitrosopumilus maritimus* - analysis of its ultrastructure by electron microscopy". In: *Biospektrum: Sonderausgabe zur Jahrestagung der VAAM 2013*. Bremen, p. 61.

HEIPIEPER, H. J., R. DIEFENBACH, and H. KEWELOH (1992). Conversion of *cis* unsaturated fatty acids to *trans*, a possible mechanism for the protection of phenol-degrading *Pseudomonas putida* P8 from substrate toxicity. *Applied and Environmental Microbiology* **58** (6), 1847–1852.

HENSEL, R., K. MATUSSEK, K. MICHALKE, L. TACKE, B. J. TINDALL, M. KOHLHOFF, B. SIEBERS, and J. DIELENSCHNEIDER (1997). *Sulfophobococcus zilligii* gen. nov., spec. nov. a Novel Hyperthermophilic Archaeum Isolated from Hot Alkaline Springs of Iceland. *Systematic and Applied Microbiology* **20** (1), 102–110. DOI: 10.1016/S0723-2020(97)80054-9.

HERFORT, L., S. SCHOUTEN, B. ABBAS, M. J. W. VELDHUIS, M. J. L. COOLEN, C. WUCHTER, J. P. BOON, G. J. HERNDL, and J. S. SINNINGHE DAMSTÉ (2007). Variations in spatial and temporal distribution of Archaea in the North Sea in relation to environmental variables. *FEMS Microbiology Ecology* **62** (3), 242–257. DOI: 10.1111/j.1574-6941.2007.00397.x.

HERNÁNDEZ-SÁNCHEZ, M., E. WOODWARD, K. TAYLOR, G. M. HENDERSON, and R. PANCOST (2014). Variations in GDGT distributions through the water column in the South East Atlantic Ocean. *Geochimica et Cosmochimica Acta* **132**, 337–348. DOI: 10.1016/j.gca.2014.02.009.

HERNDL, G. J., T. REINTHALER, E. TEIRA, H. VAN AKEN, C. VETH, A. PERNTHALER, and J. PERNTHALER (2005). Contribution of Archaea to total prokaryotic production in the deep Atlantic Ocean. *Applied and Environmental Microbiology* **71** (5), 2303–2309. DOI: 10.1128/AEM.71.5.2303-2309.2005.

HINRICHS, K.-U., J. M. HAYES, S. P. SYLVA, P. G. BREWER, and E. F. DELONG (1999). Methane-consuming archaebacteria in marine sediments. *Nature* **398** (6730), 802–805. DOI: 10.1038/19751.

HIRAISHI, A. (1999). Isoprenoid quinones as biomarkers of microbial populations in the environment. *Journal of Bioscience and Bioengineering* **88** (5), 449–460. DOI: 10.1016/S1389-1723(00)87658-6.

HIRAISHI, A. and K. KATO (1999). Quinone profiles in lake sediments: Implications for microbial diversity and community structures. *The Journal of General and Applied Microbiology* **45** (5), 221–227. DOI: 10.2323/jgam.45.221.

HIRAISHI, A., M. IWASAKI, T. KAWAGISHI, N. YOSHIDA, T. NARIHIRO, and K. KATO (2003). Significance of lipoquinones as quantitative biomarkers of bacterial populations in the environment. *Microbes and Environments* **18** (2), 89–93. DOI: 10.1264/jsme2.18.89.

HIRATSUKA, T., K. FURIHATA, J. ISHIKAWA, H. YAMASHITA, N. ITOH, H. SETO, and T. DAIRI (2008). An alternative menaquinone biosynthetic pathway operating in microorganisms. *Science* **321** (5896), 1670–1673. DOI: 10.1126/science.1160446.

HO, S. L., G. MOLLENHAUER, S. FIETZ, A. MARTÍNEZ-GARCIA, F. LAMY, G. RUEDA, K. SCHIPPER, M. MÉHEUST, A. ROSELL-MELÉ, R. STEIN, and R. TIEDEMANN (2014). Appraisal of TEX_{86} and TEX_{86}^{L} thermometries in subpolar and polar regions. *Geochimica et Cosmochimica Acta* **131**, 213–226. DOI: 10.1016/j.gca.2014.01.001.

HOEFS, M., S. SCHOUTEN, J. W. DE LEEUW, L. L. KING, S. G. WAKEHAM, and J. S. SINNINGHE DAMSTÉ (1997). Ether lipids of planktonic archaea in the marine water column. *Applied and Environmental Microbiology* **63** (8), 3090–3095.

HOLLÄNDER, R. (1976). Correlation of the function of demethylmenaquinone in bacterial electron transport with its redox potential. *FEBS Letters* **72** (1), 98–100. DOI: 10.1016/0014-5793(76)80821-6.

HOLLIBAUGH, J. T., S. M. GIFFORD, M. A. MORAN, M. J. ROSS, S. SHARMA, and B. B. TOLAR (2014). Seasonal variation in the metatranscriptomes of a Thaumarchaeota population from SE USA coastal waters. *The ISME Journal* **8** (3), 685–698. DOI: 10.1038/ismej.2013.171.

HOLLIS, C. J., L. HANDLEY, E. M. CROUCH, H. E. G. MORGANS, J. A. BAKER, J. CREECH, K. S. COLLINS, S. J. GIBBS, M. HUBER, S. SCHOUTEN, J. C. ZACHOS, and R. D. PANCOST (2009). Tropical sea temperatures in the high-latitude South Pacific during the Eocene. *Geology* **37** (2), 99–102. DOI: 10.1130/G25200A.1.

HÖLZL, G. and P. DÖRMANN (2007). Structure and function of glycoglycerolipids in plants and bacteria. *Progress in Lipid Research* **46** (5), 225–243. DOI: 10.1016/j.plipres.2007.05.001.

HÖNISCH, B., A. RIDGWELL, D. N. SCHMIDT, E. THOMAS, S. J. GIBBS, A. SLUIJS, R. ZEEBE, L. KUMP, R. C. MARTINDALE, S. E. GREENE, W. KIESSLING, J. RIES, J. C. ZACHOS, D. L. ROYER, S. BARKER, T. M. MARCHITTO, R. MOYER, C. PELEJERO, P. ZIVERI, G. L. FOSTER, and B. WILLIAMS (2012). The Geological Record of Ocean Acidification. *Science* **335**, 1058–1063. DOI: 10.1126/science.1208277.

HONJO, S., B. J. HAY, S. MANGANINI, V. L. ASPER, E. T. DEGENS, V. ITTEKKOT, S. KEMPE, E. IZDAR, Y. T. KONUK, and H. A. BENLI (1987). Seasonal cyclicity of lithogenic particle fluxes at a Southern Black Sea sediment trap station. In: *Particle Flux in the Ocean*. Ed. by E. Degens, E. Izdar, and S. Honjo. Hamburg, Germany: Universität Hamburg, pp. 19–40.

HOOPER, A. B., R. H. ERICKSON, and K. R. TERRY (1972). Electron transport systems of Nitrosomonas: isolation of a membrane-envelope fraction. *Journal of Bacteriology* **110** (1), 430–438.

HUBER, H. and K. O. STETTER (2006). Thermoplasmatales. In: *The Prokaryotes, Volume 3: Archaea. Bacteria: Firmicutes, Actinomycetes*. Ed. by M. Dworkin, S. Falkow, E. Rosenberg, K.-H. Schleifer, and E. Stackebrandt, pp. 101–112. DOI: 10.1007/0-387-30743-5_7.

HUBER, H., M. J. HOHN, R. RACHEL, T. FUCHS, V. C. WIMMER, and K. O. STETTER (2002). A new phylum of Archaea represented by a nanosized hyperthermophilic symbiont. *Nature* **417** (6884), 63–67. DOI: 10.1038/417063a.

HUBER, H., M. THOMM, H. KÖNIG, G. THIES, and K. O. STETTER (1982). *Methanococcus thermolithotrophicus*, a novel thermophilic lithotrophic methanogen. *Archives of Microbiology* **132** (1), 47–50. DOI: 10.1007/BF00690816.

HUBER, M. and R. CABALLERO (2011). The early Eocene equable climate problem revisited. *Climate of the Past* **7**, 603–633. DOI: 10.5194/cp-7-603-2011.

HUGUET, C., E. C. HOPMANS, W. FEBO-AYALA, D. H. THOMPSON, J. S. SINNINGHE DAMSTÉ, and S. SCHOUTEN (2006). An improved method to determine the absolute abundance of glycerol dibiphytanyl glycerol tetraether lipids. *Organic Geochemistry* **37** (9), 1036–1041. DOI: 10.1016/j.orggeochem.2006.05.008.

HUGUET, C., A. SCHIMMELMANN, R. THUNELL, L. J. LOURENS, J. S. SINNINGHE DAMSTÉ, and S. SCHOUTEN (2007). A study of the TEX_{86} paleothermometer in the water column and sediments of the Santa Barbara Basin, California. *Paleoceanography* **22** (3), PA3203. DOI: 10.1029/2006PA001310.

HUGUET, C., H. URAKAWA, W. MARTENS-HABBENA, L. TRUXAL, D. A. STAHL, and A. E. INGALLS (2010). Changes in intact membrane lipid content of archaeal cells as an indication of metabolic status. *Organic Geochemistry* **41** (9), 930–934. DOI: 10.1016/j.orggeochem.2010.04.012.

IMHOFF, J. and U. BIAS-IMHOFF (1995). Lipids, quinones and fatty acids of anoxygenic phototrophic bacteria. In: *Anoxygenic Photosynthetic Bacteria*. Ed. by R. Blankenship, M. Madigan, and C. Bauer. Dordrecht, The Netherlands: Kluwer Academic Publishers, pp. 179–205.

INAGAKI, F., T. NUNOURA, S. NAKAGAWA, A. TESKE, M. LEVER, A. LAUER, M. SUZUKI, K. TAKAI, M. DELWICHE, F. S. COLWELL, K. H. NEALSON, K. HORIKOSHI, S. D'HONDT, and B. B. JØRGENSEN (2006). Biogeographical distribution and diversity of microbes in methane hydrate-bearing deep marine sediments on the Pacific Ocean Margin. *Proceedings of the National Academy of Sciences of the United States of America* **103** (8), 2815–2820. DOI: 10.1073/pnas.0511033103.

INGALLS, A. E., C. HUGUET, and L. T. TRUXAL (2012). Distribution of intact and core membrane lipids of archaeal glycerol dialkyl glycerol tetraethers among size-fractionated particulate organic matter in Hood Canal, Puget Sound. *Applied and Environmental Microbiology* **78** (5), 1480–1490. DOI: 10.1128/AEM.07016-11.

INGALLS, A. E., S. R. SHAH, R. L. HANSMAN, L. I. ALUWIHARE, G. M. SANTOS, E. R. M. DRUFFEL, and A. PEARSON (2006). Quantifying archaeal community autotrophy in the mesopelagic ocean using natural radiocarbon. *Proceedings of the National Academy of Sciences of the United States of America* **103** (17), 6442–6447. DOI: 10.1073/pnas.0510157103.

IONESCU, D., S. PENNO, M. HAIMOVICH, B. RIHTMAN, A. GOODWIN, D. SCHWARTZ, L. HAZANOV, M. CHERNIHOVSKY, A. F. POST, and A. OREN (2009). Archaea in the Gulf of Aqaba. *FEMS Microbiology Ecology* **69** (3), 425–438. DOI: 10.1111/j.1574-6941.2009.00721.x.

IVERSON, V., R. M. MORRIS, C. D. FRAZAR, C. T. BERTHIAUME, R. L. MORALES, and E. V. ARMBRUST (2012). Untangling genomes from metagenomes: revealing an uncultured class of marine Euryarchaeota. *Science* **335** (6068), 587–590. DOI: 10.1126/science.1212665.

IWASAKI, M. and A. HIRAISHI (1998). A New Approach to Numerical Analyses of Microbial Quinone Profiles in the Environment. *Microbes and Environments* **13** (2), 67–76. DOI: 10.1264/jsme2.13.67.

JAESCHKE, A., C. ROOKS, M. TRIMMER, J. C. NICHOLLS, E. C. HOPMANS, S. SCHOUTEN, and J. S. SINNINGHE DAMSTÉ (2009). Comparison of ladderane phospholipid and core lipids as indicators for anaerobic ammonium oxidation (anammox) in marine sediments. *Geochimica et Cosmochimica Acta* **73** (7), 2077–2088. DOI: 10.1016/j.gca.2009.01.013.

JAHN, U., R. SUMMONS, H. STURT, E. GROSJEAN, and H. HUBER (2004). Composition of the lipids of *Nanoarchaeum equitans* and their origin from its host *Ignicoccus* sp. strain KIN4/I. *Archives of Microbiology* **182** (5), 404–413. DOI: 10.1007/s00203-004-0725-x.

JANNASCH, H. W., C. O. WIRSEN, and S. J. MOLYNEAUX (1991). Chemoautotrophic sulfur-oxidizing bacteria from the Black Sea. *Deep Sea Research Part A. Oceanographic Research Papers* **38**, S1105–S1120. DOI: 10.1016/S0198-0149(10)80026-3.

JANNASCH, H. W. (1991). Microbial Processes in the Black Sea Water Column and Top Sediment: An Overview. In: *Black Sea Oceanography*. Ed. by E. Ä°zdar and J. W. Murray. Dordrecht, The Netherlands: Springer, pp. 271–286. DOI: 10.1007/978-94-011-2608-3.

JARRELL, K. F., A. D. WALTERS, C. BOCHIWAL, J. M. BORGIA, T. DICKINSON, and J. P. J. CHONG (2011). Major players on the microbial stage: why archaea are important. *Microbiology* **157**, 919–936. DOI: 10.1099/mic.0.047837-0.

JENKYNS, H. C., L. SCHOUTEN-HUIBERS, S. SCHOUTEN, and J. S. SINNINGHE DAMSTÉ (2012). Warm Middle Jurassic–Early Cretaceous high-latitude sea-surface temperatures from the Southern Ocean. *Climate of the Past* **8** (1), 215–226. DOI: 10.5194/cp-8-215-2012.

JENSEN, M. M., M. M. M. KUYPERS, G. LAVIK, and B. THAMDRUP (2008). Rates and regulation of anaerobic ammonium oxidation and denitrification in the Black Sea. *Limnology and Oceanography* **53** (1), 23–36. DOI: 10.4319/lo.2008.53.1.0023.

JIA, G., J. ZHANG, J. CHEN, and C. L. ZHANG (2012). Archaeal tetraether lipids record subsurface water temperature in the South China Sea. *Organic Geochemistry* **50**, 68–77. DOI: 10.1016/j.orggeochem.2012.07.002.

JØRGENSEN, B. B. (1990). A thiosulfate shunt in the sulfur cycle of marine sediments. *Science* **249** (4965), 152–154. DOI: 10.1126/science.249.4965.152.

JØRGENSEN, B. B., M. E. BÖTTCHER, H. LÜSCHEN, L. N. NERETIN, and I. I. VOLKOV (2004). Anaerobic methane oxidation and a deep H_2S sink generate isotopically heavy sulfides in Black Sea sediments. *Geochimica et Cosmochimica Acta* **68** (9), 2095–2118. DOI: 10.1016/j.gca.2003.07.017.

JØRGENSEN, B. B., H. FOSSING, C. O. WIRSEN, and H. W. JANNASCH (1991). Sulfide oxidation in the anoxic Black Sea chemocline. *Deep Sea Research Part A. Oceanographic Research Papers* **38**, S1083–S1103. DOI: 10.1016/S0198-0149(10)80025-1.

JØRGENSEN, B. B., A. WEBER, and J. ZOPFI (2001). Sulfate reduction and anaerobic methane oxidation in Black Sea sediments. *Deep Sea Research Part I: Oceanographic Research Papers* **48**, 2097–2120. DOI: 10.1016/S0967-0637(01)00007-3.

JORGENSEN, S. L., B. HANNISDAL, A. LANZÉN, T. BAUMBERGER, K. FLESLAND, R. FONSECA, L. ØVREÅS, I. H. STEEN, I. H. THORSETH, R. B. PEDERSEN, and C. SCHLEPER (2012). Correlating microbial community profiles with geochemical data in highly stratified sediments from the Arctic Mid-Ocean Ridge. *Proceedings of the National Academy of Sciences of the United States of America* **109** (42), 2846–2855. DOI: 10.1073/pnas.1207574109.

KAISER, P., R. GEYER, P. SURMANN, and H. FUHRMANN (2012). LC-MS method for screening unknown microbial carotenoids and isoprenoid quinones. *Journal of Microbiological Methods* **88** (1), 28–34. DOI: 10.1016/j.mimet.2011.10.001.

KALLMEYER, J., R. POCKALNY, R. R. ADHIKARI, D. C. SMITH, and S. D'HONDT (2012). Global distribution of microbial abundance and biomass in subseafloor sediment. *Proceedings of the National Academy of Sciences of the United States of America* **109** (40), 16213–16216. DOI: 10.1073/pnas.1203849109.

KALLMEYER, J., T. G. FERDELMAN, K.-H. JANSEN, and B. B. JØRGENSEN (2003). A high-pressure thermal gradient block for investigating microbial activity in multiple deep-sea samples. *Journal of Microbiological Methods* **55** (1), 165–172. DOI: 10.1016/S0167-7012(03)00138-6.

KAMEKURA, M., M. L. DYALL-SMITH, V. UPASANI, A. VENTOSA, and M. KATES (1997). Diversity of alkaliphilic halobacteria: proposals for transfer of *Natronobacterium vacuolatum*, *Natronobacterium magadii*, and *Natronobacterium pharaonis* to *Halorubrum*, *Natrialba*, and *Natronomonas* gen. nov., respect. *International Journal of Systematic Bacteriology* **47** (3), 853–857. DOI: 10.1099/00207713-47-3-853.

KAMEKURA, M. (1998). Diversity of extremely halophilic bacteria. *Extremophiles* **2** (3), 289–295.

KANE, M. D., L. K. POULSEN, and D. A. STAHL (1993). Monitoring the enrichment and isolation of sulfate-reducing bacteria by using oligonucleotide hybridization probes designed from environmentally derived 16S rRNA sequences. *Applied and Environmental Microbiology* **59** (3), 682–686.

KANESHIRO, S. M. and D. S. CLARK (1995). Pressure effects on the composition and thermal behavior of lipids from the deep-sea thermophile *Methanococcus jannaschii*. *Journal of Bacteriology* **177** (13), 3668–3672.

KARL, D. M. and G. A. KNAUER (1991). Microbial production and particle flux in the upper 350 m of the Black Sea. *Deep Sea Research Part A. Oceanographic Research Papers* **38**, S921–S942. DOI: 10.1016/S0198-0149(10)80017-2.

KARL, D. M., L. BEVERSDORF, K. M. BJÖRKMAN, M. J. CHURCH, A. MARTINEZ, and E. F. DELONG (2008). Aerobic production of methane in the sea. *Nature Geoscience* **1** (7), 473–478. DOI: 10.1038/ngeo234.

KARNER, M. B., E. F. DELONG, and D. M. KARL (2001). Archaeal dominance in the mesopelagic zone of the Pacific Ocean. *Nature* **409** (6819), 507–510. DOI: 10.1038/35054051.

KARTAL, B., M. M. M. KUYPERS, G. LAVIK, J. SCHALK, H. J. M. OP DEN CAMP, M. S. M. JETTEN, and M. STROUS (2007). Anammox bacteria disguised as denitrifiers: Nitrate reduction to dinitrogen gas via nitrite and ammonium. *Environmental Microbiology* **9** (3), 635–642. DOI: 10.1111/j.1462-2920.2006.01183.x.

KASHEFI, K. and D. R. LOVLEY (2003). Extending the upper temperature limit for life. *Science* **301** (5635), 934. DOI: 10.1126/science.1086823.

KATES, M. (1993). Membrane lipids of archaea. In: *The Biochemistry of Archaea (Archaebacteria)*. Ed. by M. Kates D. J. Kushner and A. T. Matheson. Amsterdam, The Netherlands: Elsevier Science, pp. 261–295.

KELLER, M., F. J. BRAUN, R. DIRMEIER, D. HAFENBRADL, S. BURGGRAF, R. RACHEL, and K. O. STETTER (1995). *Thermococcus alcaliphilus* sp. nov., a new hyperthermophilic archaeum growing on polysulfide at alkaline pH. *Archives of Microbiology* **164** (6), 390–395. DOI: 10.1007/BF02529736.

KELLERMANN, M. Y., G. WEGENER, M. ELVERT, M. Y. YOSHINAGA, Y.-S. LIN, T. HOLLER, X. P. MOLLAR, K. KNITTEL, K.-U. HINRICHS, and X. PRIETO MOLLAR (2012). Autotrophy as a predominant mode of carbon fixation in anaerobic methane-oxidizing microbial communities. *Proceedings of the National Academy of Sciences of the United States of America* **109** (47), 19321–19326. DOI: 10.1073/pnas.1208795109.

KENDALL, M. and D. BOONE (2006). The order Methanosarcinales. In: *The Prokaryotes, Volume 3: Archaea. Bacteria: Firmicutes, Actinomycetes*. Ed. by M. Dworkin, S. Falkow, E. Rosenberg, K.-H. Schleifer, and E. Stackebrandt. New York, USA: Springer, pp. 244–256.

KIM, J.-H., S. SCHOUTEN, E. C. HOPMANS, B. DONNER, and J. S. SINNINGHE DAMSTÉ (2008). Global sediment core-top calibration of the TEX_{86} paleothermometer in the ocean. *Geochimica et Cosmochimica Acta* **72** (4), 1154–1173. DOI: 10.1016/j.gca.2007.12.010.

KIM, J.-H., S. SCHOUTEN, M. RODRIGO-GA, S. RAMPEN, G. MARINO, C. HUGUET, P. HELMKE, R. BUSCAIL, E. C. HOPMANS, and F. SANGIORGI (2015). Influence of deep-water derived isoprenoid tetraether lipids on the TEX_{86}^{H} paleothermometer in the Mediterranean Sea. *Geochimica et Cosmochimica Acta* **150**, 125–141. DOI: 10.1016/j.gca.2014.11.017.

KIM, J.-H., J. VAN DER MEER, S. SCHOUTEN, P. HELMKE, V. WILLMOTT, F. SANGIORGI, N. KOÇ, E. C. HOPMANS, and J. S. SINNINGHE DAMSTÉ (2010). New indices and calibrations derived from the distribution of crenarchaeal isoprenoid tetraether lipids: Implications for past sea surface temperature reconstructions. *Geochimica et Cosmochimica Acta* **74** (16), 4639–4654. DOI: 10.1016/j.gca.2010.05.027.

KIM, K. C., Y. KAMIO, and H. TAKAHASHI (1970). Glyceryl ether phospholipid in anaerobic bacteria. *The Journal of General and Applied Microbiology* **16** (4), 321–325. DOI: 10.2323/jgam.16.4_321.

KJELLEBERG, S., M. HERMANSSON, P. MÅRDÉN, and G. W. JONES (1987). The transient phase between growth and nongrowth of heterotrophic bacteria, with emphasis on the marine environment. *Annual Review of Microbiology* **41**, 25–49. DOI: 10.1146/annurev.mi.41.100187.000325.

KNAB, N. J., B. A. CRAGG, E. R. C. HORNIBROOK, L. HOLMKVIST, R. D. PANCOST, C. BOROWSKI, R. J. PARKES, and B. B. JORGENSEN (2009). Regulation of anaerobic methane oxidation in sediments of the Black Sea. *Biogeosciences* **6**, 1505–1518. DOI: 10.5194/bgd-5-2305-2008.

KNAPPY, C. S. and B. J. KEELY (2012). Novel glycerol dialkanol triols in sediments: transformation products of glycerol dibiphytanyl glycerol tetraether lipids or biosynthetic intermediates? *Chemical Communications* **48** (6), 841–843. DOI: 10.1039/c1cc15841d.

KNAPPY, C. S., J. P. J. CHONG, and B. J. KEELY (2009). Rapid discrimination of archaeal tetraether lipid cores by liquid chromatography-tandem mass spectrometry. *Journal of the American Society for Mass Spectrometry* **20** (1), 51–59. DOI: 10.1016/j.jasms.2008.09.015.

KNAPPY, C., P. YAO, M. PICKERING, and B. KEELY (2014). Identification of homoglycerol- and dihomoglycerol-containing isoprenoid tetraether lipid cores in aquatic sediments and a soil. *Organic Geochemistry* **76**, 146–156. DOI: 10.1016/j.orggeochem.2014.06.003.

KNUDSEN, E., E. JANTZEN, K. BRYN, J. G. ORMEROD, and R. SIREVÅG (1982). Quantitative and structural characteristics of lipids in *Chlorobium* and *Chloroflexus*. *Archives of Microbiology* **132** (2), 149–154. DOI: 10.1007/BF00508721.

KOGA, Y. and H. MORII (2005). Recent advances in structural research on ether lipids from Archaea including comparative and physiological aspects. *Bioscience, Biotechnology, and Biochemistry* **69** (11), 2019–2034. DOI: 10.1271/bbb.69.2019.

KOGA, Y. (2011). Early evolution of membrane lipids: how did the lipid divide occur? *Journal of Molecular Evolution* **72** (3), 274–282. DOI: 10.1007/s00239-011-9428-5.

KOGA, Y. (2012). Thermal adaptation of the archaeal and bacterial lipid membranes. *Archaea* **2012**, 789652. DOI: 10.1155/2012/789652.

KOGA, Y. (2014). From promiscuity to the lipid divide: On the evolution of distinct membranes in Archaea and Bacteria. *Journal of Molecular Evolution* **78**, 234–242. DOI: 10.1007/s00239-014-9613-4.

KOGA, Y., M. NISHIHARA, H. MORII, and M. AKAGAWA-MATSUSHITA (1993). Ether polar lipids of methanogenic bacteria: structures, comparative aspects, and biosyntheses. *Microbiological Reviews* **57** (1), 164–182.

KONINGS, W. N., S.-V. ALBERS, S. KONING, and A. J. M. DRIESSEN (2002). The cell membrane plays a crucial role in survival of bacteria and archaea in extreme environments. *Antonie van Leeuwenhoek* **81**, 61–72. DOI: 10.1023/A:1020573408652.

KÖNNEKE, M., A. E. BERNHARD, J. R. DE LA TORRE, C. B. WALKER, J. B. WATERBURY, and D. A. STAHL (2005). Isolation of an autotrophic ammonia-oxidizing marine archaeon. *Nature* **437** (7058), 543–546. DOI: 10.1038/nature03911.

KÖNNEKE, M., J. S. LIPP, and K.-U. HINRICHS (2012). Carbon isotope fractionation by the marine ammonia-oxidizing archaeon *Nitrosopumilus maritimus*. *Organic Geochemistry* **48**, 21–24. DOI: 10.1016/j.orggeochem.2012.04.007.

KÖNNEKE, M., D. M. SCHUBERT, P. C. BROWN, M. HÜGLER, S. STANDFEST, T. SCHWANDER, L. SCHADA VON BORZYSKOWSKI, T. J. ERB, D. A. STAHL, and I. A. BERG (2014). Ammonia-oxidizing archaea use the most energy-efficient aerobic pathway for CO_2 fixation. *Proceedings of the National Academy of Sciences of the United States of America* **111** (22), 8239–8244. DOI: 10.1073/pnas.1402028111.

KONOVALOV, S. K., G. W. I. LUTHER, G. E. FRIEDERICH, D. B. NUZZIO, B. M. TEBO, J. W. MURRAY, T. OGUZ, B. GLAZER, and R. E. TROUWBORST (2003). Lateral injection of oxygen with the Bosporus plume-fingers of oxidizing potential in the Black Sea. *Limnology and Oceanography* **48** (6), 2369–2376. DOI: 10.4319/lo.2003.48.6.2369.

KONOVALOV, S., J. MURRAY, and G. LUTHER (2005). Basic Processes of Black Sea Biogeochemistry. *Oceanography* **18** (2), 24–35. DOI: 10.5670/oceanog.2005.39.

KONOVALOV, S., A. SAMODUROV, T. OGUZ, and L. IVANOV (2004). Parameterization of iron and manganese cycling in the Black Sea suboxic and anoxic environment. *Deep-Sea Research Part I: Oceanographic Research Papers* **51**, 2027–2045. DOI: 10.1016/j.dsr.2004.08.005.

KONSTANTINIDIS, K. T., J. BRAFF, D. M. KARL, and E. F. DELONG (2009). Comparative metagenomic analysis of a microbial community residing at a depth of 4,000 meters at station ALOHA in the North Pacific subtropical gyre. *Applied and Environmental Microbiology* **75** (16), 5345–5355. DOI: 10.1128/AEM.00473-09.

KOONIN, E. V., K. S. MAKAROVA, and L. ARAVIND (2001). Horizontal gene transfer in prokaryotes: quantification and classification. *Annual Review of Microbiology* **55**, 709–742. DOI: 10.1146/annurev.micro.55.1.709.

KOWALCHUK, G. A. and J. R. STEPHEN (2001). Ammonia-oxidizing bacteria: a model for molecular microbial ecology. *Annual Review of Microbiology* **55**, 485–529. DOI: 10.1146/annurev.micro.55.1.485.

KRÖGER, A. and V. DADÁK (1969). On the Role of Quinones in Bacterial Electron Transport. The Respiratory System of *Bacillus megaterium*. *European Journal of Biochemistry* **11** (2), 328–340. DOI: 10.1111/j.1432-1033.1969.tb00776.x.

KRUMHOLZ, L. R., J. P. MCKINLEY, G. A. ULRICH, and J. M. SUFLITA (1997). Confined subsurface microbial communities in Cretaceous rock. *Nature* **386** (6620), 64–66. DOI: 10.1038/386064a0.

KRÜMMEL, A. and H. HARMS (1982). Effect of organic matter on growth and cell yield of ammonia-oxidizing bacteria. *Archives of Microbiology* **133** (1), 50–54. DOI: 10.1007/BF00943769.

KULICHEVSKAYA, I. S., A. A. IVANOVA, E. N. DETKOVA, W. I. C. RIJPSTRA, J. S. SINNINGHE DAMSTÉ, and S. N. DEDYSH (2015). *Planctomicrobium piriforme* gen. nov., sp. nov., a Stalked Planctomycete from a Littoral Wetland of a Boreal Lake. *International Journal of Systematic and Evolutionary Microbiology*. DOI: 10.1099/ijs.0.000154.

KULICHEVSKAYA, I. S., A. O. IVANOVA, O. I. BAULINA, P. L. E. BODELIER, J. S. S. DAMSTÉ, and S. N. DEDYSH (2008). *Singulisphaera acidiphila* gen. nov., sp. nov., a non-filamentous, *Isosphaera*-like planctomycete from acidic northern wetlands. *International Journal of Systematic and Evolutionary Microbiology* **58** (5), 1186–1193. DOI: 10.1099/ijs.0.65593-0.

KULICHEVSKAYA, I. S., A. O. IVANOVA, S. E. BELOVA, O. I. BAULINA, P. L. E. BODELIER, W. I. C. RIJPSTRA, J. S. SINNINGHE DAMSTÉ, G. A. ZAVARZIN, and S. N. DEDYSH (2007). *Schlesneria paludicola* gen. nov., sp. nov., the first acidophilic member of the order Planctomycetales, from *Sphagnum*-dominated boreal wetlands. *International Journal of Systematic and Evolutionary Microbiology* **57** (11), 2680–2687. DOI: 10.1099/ijs.0.65157-0.

KUNIHIRO, T., B. VEUGER, D. VASQUEZ-CARDENAS, L. POZZATO, M. LE GUITTON, K. MORIYA, M. KUWAE, K. OMORI, H. T. S. BOSCHKER, and D. VAN OEVELEN (2014). Phospholipid-derived fatty acids and quinones as markers for bacterial biomass and community structure in marine sediments. *PloS One* **9** (4), e96219. DOI: 10.1371/journal.pone.0096219.

KUYPERS, M. M., P. BLOKKER, J. ERBACHER, H. KINKEL, R. D. PANCOST, S. SCHOUTEN, and J. S. SINNINGHE DAMSTÉ (2001). Massive expansion of marine archaea during a mid-Cretaceous oceanic anoxic event. *Science* **293** (5527), 92–95. DOI: 10.1126/science.1058424.

KUYPERS, M. M. M., G. LAVIK, D. WOEBKEN, M. SCHMID, B. M. FUCHS, R. AMANN, B. B. JØRGENSEN, and M. S. M. JETTEN (2005). Massive nitrogen loss from the Benguela upwelling system through anaerobic ammonium oxidation. *Proceedings of the National Academy of Sciences of the United States of America of the United States of America* **102** (18), 6478–6483. DOI: 10.1073/pnas.0502088102.

KUYPERS, M. M. M., A. O. SLIEKERS, G. LAVIK, M. SCHMID, B. B. JØRGENSEN, J. G. KUENEN, J. S. SINNINGHE DAMSTÉ, M. STROUS, and M. S. M. JETTEN (2003). Anaerobic ammonium oxidation by anammox bacteria in the Black Sea. *Nature* **422**, 608–611. DOI: 10.1038/nature01472.

KVENVOLDEN, K. A. and T. J. MCDONALD (1986). *Organic Geochemistry on JOIDES Resolution - An essay*. College Station, TX, United States: Ocean Drilling Program, Texas A&M University, p. 97. DOI: 10.2973/odp.tn.6.1986.

KWIECIEN, O., H. W. ARZ, F. LAMY, S. WULF, A. BAHR, U. RÖHL, and G. H. HAUG (2008). Estimated reservoir ages of the Black Sea since the last glacial. *Radiocarbon* **50** (1), 99–118.

LAI, D., J. R. SPRINGSTEAD, and H. G. MONBOUQUETTE (2008). Effect of growth temperature on ether lipid biochemistry in Archaeoglobus fulgidus. *Extremophiles* **12** (2), 271–278. DOI: 10.1007/s00792-007-0126-6.

LAM, P. and M. M. M. KUYPERS (2011). Microbial nitrogen cycling processes in oxygen minimum zones. *Annual Review of Marine Science* **3** (1), 317–345. DOI: 10.1146/annurev-marine-120709-142814.

LAM, P., M. M. JENSEN, G. LAVIK, D. F. MCGINNIS, B. MÜLLER, C. J. SCHUBERT, R. AMANN, B. THAMDRUP, and M. M. M. KUYPERS (2007). Linking crenarchaeal and bacterial nitrification to anammox in the Black Sea. *Proceedings of the National Academy of Sciences of the United States of America* **104** (17), 7104–7109. DOI: 10.1073/pnas.0611081104.

LAM, P., G. LAVIK, M. M. JENSEN, J. VAN DE VOSSENBERG, M. SCHMID, D. WOEBKEN, D. GUTIÉRREZ, R. AMANN, M. S. M. JETTEN, and M. M. M. KUYPERS (2009). Revising the nitrogen cycle in the Peruvian oxygen minimum zone. *Proceedings of the National Academy of Sciences of the United States of America* **106** (12), 4752–4757. DOI: 10.1073/pnas.0812444106.

LANGWORTHY, T. A., W. R. MAYBERRY, and P. F. SMITH (1974). Long-chain glycerol diether and polyol dialkyl glycerol triether lipids of *Sulfolobus acidocaldarius*. *Journal of Bacteriology* **119** (1), 106–116.

LANYI, J. K., W. Z. PLACHY, and M. KATES (1974). Lipid interactions in membranes of extremely halophilic bacteria. II. Modification of the bilayer structure by squalene. *Biochemistry* **13**, 4914–4920. DOI: 10.1021/bi00721a006.

LANYI, J. K. (1974). Irregular bilayer structure in vesicles prepared from *Halobacterium cutirubrum* lipids. *Biochimica et Biophysica Acta* **356**, 245–256.

LEBEDEVA, E. V., M. ALAWI, C. FIENCKE, B. NAMSARAEV, E. BOCK, and E. SPIECK (2005). Moderately thermophilic nitrifying bacteria from a hot spring of the Baikal rift zone. *FEMS Microbiology Ecology* **54** (2), 297–306. DOI: 10.1016/j.femsec.2005.04.010.

LEBEDEVA, E. V., R. HATZENPICHLER, E. PELLETIER, N. SCHUSTER, S. HAUZMAYER, A. BULAEV, N. V. GRIGOR'EVA, A. GALUSHKO, M. SCHMID, M. PALATINSZKY, D. LE PASLIER, H. DAIMS, and M. WAGNER (2013). Enrichment and genome sequence of the group I.1a ammonia-oxidizing archaeon "*Ca.* Nitrosotenuis uzonensis" representing a clade globally distributed in thermal habitats. *PloS One* **8** (11), e80835. DOI: 10.1371/journal.pone.0080835.

LEE, K. E., J.-H. KIM, I. WILKE, P. HELMKE, and S. SCHOUTEN (2008). A study of the alkenone, TEX_{86}, and planktonic foraminifera in the Benguela Upwelling System: Implications for past sea surface temperature estimates. *Geochemistry, Geophysics, Geosystems* **9** (10), Q10019. DOI: 10.1029/2008GC002056.

LEHTOVIRTA, L. E., J. I. PROSSER, and G. W. NICOL (2009). Soil pH regulates the abundance and diversity of Group 1.1c Crenarchaeota. *FEMS Microbiology Ecology* **70** (3), 367–376. DOI: 10.1111/j.1574-6941.2009.00748.x.

LEHTOVIRTA-MORLEY, L. E., K. STOECKER, A. VILCINSKAS, J. I. PROSSER, and G. W. NICOL (2011). Cultivation of an obligate acidophilic ammonia oxidizer from a nitrifying acid soil. *Proceedings of the National Academy of Sciences of the United States of America* **108** (38), 15892–15897. DOI: 10.1073/pnas.1107196108.

LEHTOVIRTA-MORLEY, L. E., D. T. VERHAMME, G. W. NICOL, and J. I. PROSSER (2013). Effect of nitrification inhibitors on the growth and activity of *Nitrosotalea devanaterra* in culture and soil. *Soil Biology and Biochemistry* **62**, 129–133. DOI: 10.1016/j.soilbio.2013.01.020.

LEIDER, A., K.-U. HINRICHS, G. MOLLENHAUER, and G. J. M. VERSTEEGH (2010). Core-top calibration of the lipid-based $U^{K'}_{37}$ and TEX_{86} temperature proxies on the southern Italian shelf (SW Adriatic Sea, Gulf of Taranto). *Earth and Planetary Science Letters* **300** (1-2), 112–124. DOI: 10.1016/j.epsl.2010.09.042.

LEININGER, S., T. URICH, M. SCHLOTER, L. SCHWARK, J. QI, G. W. NICOL, J. I. PROSSER, S. C. SCHUSTER, and C. SCHLEPER (2006). Archaea predominate among ammonia-oxidizing prokaryotes in soils. *Nature* **442** (7104), 806–809. DOI: 10.1038/nature04983.

LELOUP, J., A. LOY, N. J. KNAB, C. BOROWSKI, M. WAGNER, and B. B. JØRGENSEN (2007). Diversity and abundance of sulfate-reducing microorganisms in the sulfate and methane zones of a marine sediment, Black Sea. *Environmental Microbiology* **9**, 131–142. DOI: 10.1111/j.1462-2920.2006.01122.x.

LENAZ, G. (1987). Lipid fluidity and membrane protein dynamics. *Bioscience Reports* **7** (11), 823–837. DOI: 10.1007/BF01119473.

LENAZ, G., R. FATO, G. FORMIGGINI, and M. L. GENOVA (2007). The role of Coenzyme Q in mitochondrial electron transport. *Mitochondrion* **7S**, 8–33. DOI: 10.1016/j.mito.2007.03.009.

LENGGER, S. K., E. C. HOPMANS, G.-J. REICHART, K. G. J. NIEROP, J. S. SINNINGHE DAMSTÉ, and S. SCHOUTEN (2012). Intact polar and core glycerol dibiphytanyl glycerol tetraether lipids in the Arabian Sea oxygen minimum zone. Part II: Selective preservation and degradation in

sediments and consequences for the TEX_{86}. *Geochimica et Cosmochimica Acta* **98**, 244–258. DOI: 10.1016/j.gca.2012.05.003.

LENGGER, S. K., E. C. HOPMANS, J. S. SINNINGHE DAMSTÉ, and S. SCHOUTEN (2014). Impact of sedimentary degradation and deep water column production on GDGT abundance and distribution in surface sediments in the Arabian Sea: Implications for the TEX_{86} paleothermometer. *Geochimica et Cosmochimica Acta* **142**, 386–399. DOI: 10.1016/j.gca.2014.07.013.

LENGGER, S. K., M. KRAAIJ, R. TJALLINGII, M. BAAS, J.-B. STUUT, E. C. HOPMANS, J. S. SINNINGHE DAMSTÉ, and S. SCHOUTEN (2013). Differential degradation of intact polar and core glycerol dialkyl glycerol tetraether lipids upon post-depositional oxidation. *Organic Geochemistry* **65**, 83–93. DOI: 10.1016/j.orggeochem.2013.10.004.

LEVER, M. A. (2013). Functional gene surveys from ocean drilling expeditions - a review and perspective. *FEMS Microbiology Ecology* **84** (1), 1–23. DOI: 10.1111/1574-6941.12051.

LEWIS, B. and W. LANDING (1991). The biogeochemistry of manganese and iron in the Black Sea. *Deep Sea Research Part A. Oceanographic Research Papers* **38**, S773–S803. DOI: 10.1016/S0198-0149(10)80009-3.

LIN, X., S. G. WAKEHAM, I. F. PUTNAM, Y. M. ASTOR, M. I. SCRANTON, A. Y. CHISTOSERDOV, and G. T. TAYLOR (2006). Comparison of vertical distributions of prokaryotic assemblages in the anoxic Cariaco Basin and Black Sea by use of fluorescence in situ hybridization. *Applied and Environmental Microbiology* **72** (4), 2679–2690. DOI: 10.1128/AEM.72.4.2679-2690.2006.

LIN, Y.-S., V. B. HEUER, T. GOLDHAMMER, M. Y. KELLERMANN, M. ZABEL, and K.-U. HINRICHS (2012). Towards constraining H2 concentration in subseafloor sediment: A proposal for combined analysis by two distinct approaches. *Geochimica et Cosmochimica Acta* **77**, 186–201. DOI: 10.1016/j.gca.2011.11.008.

LINCOLN, S. A., B. WAI, J. M. EPPLEY, M. J. CHURCH, R. E. SUMMONS, and E. F. DELONG (2014a). Planktonic Euryarchaeota are a significant source of archaeal tetraether lipids in the ocean. *Proceedings of the National Academy of Sciences of the United States of America* **111** (27), 9858–9863. DOI: 10.1073/pnas.1409439111.

LINCOLN, S. A., B. WAI, J. M. EPPLEY, M. J. CHURCH, R. E. SUMMONS, and E. F. DELONG (2014b). Reply to Schouten et al.: Marine Group II planktonic Euryarchaeota are significant contributors to tetraether lipids in the ocean. *Proceedings of the National Academy of Sciences of the United States of America* **111** (41), 4286. DOI: 10.1073/pnas.1416736111.

LINDÅS, A.-C., E. A. KARLSSON, M. T. LINDGREN, T. J. G. ETTEMA, and R. BERNANDER (2008). A unique cell division machinery in the Archaea. *Proceedings of the National Academy of Sciences of the United States of America* **105** (48), 18942–18946. DOI: 10.1073/pnas.0809467105.

LINNERT, C., S. A. ROBINSON, J. A. LEES, P. R. BOWN, I. PÉREZ-RODRÍGUEZ, M. R. PETRIZZO, F. FALZONI, K. LITTLER, J. A. ARZ, and E. E. RUSSELL (2014). Evidence for global cooling in the Late Cretaceous. *Nature Communications* **5**, 4194. DOI: 10.1038/ncomms5194.

LIPP, J. S. and K.-U. HINRICHS (2009). Structural diversity and fate of intact polar lipids in marine sediments. *Geochimica et Cosmochimica Acta* **73** (22), 6816–6833. DOI: 10.1016/j.gca.2009.08.003.

LIPP, J. S., Y. MORONO, F. INAGAKI, and K.-U. HINRICHS (2008). Significant contribution of Archaea to extant biomass in marine subsurface sediments. *Nature* **454** (7207), 991–994. DOI: 10.1038/nature07174.

LIU, X.-L. (2011). "Glycerol ether lipids in sediments: sources, diversity and implications". PhD Thesis. University of Bremen.

LIU, X.-L., J. S. LIPP, J. M. SCHRÖDER, R. E. SUMMONS, and K.-U. HINRICHS (2012a). Isoprenoid glycerol dialkanol diethers: A series of novel archaeal lipids in marine sediments. *Organic Geochemistry* **43**, 50–55. DOI: 10.1016/j.orggeochem.2011.11.002.

LIU, X.-L., J. S. LIPP, J. H. SIMPSON, Y.-S. LIN, R. E. SUMMONS, and K.-U. HINRICHS (2012b). Mono- and dihydroxyl glycerol dibiphytanyl glycerol tetraethers in marine sediments: Identification of both core and intact polar lipid forms. *Geochimica et Cosmochimica Acta* **89**, 102–115. DOI: 10.1016/j.gca.2012.04.053.

LIU, X., J. S. LIPP, and K.-U. HINRICHS (2011). Distribution of intact and core GDGTs in marine sediments. *Organic Geochemistry* **42** (4), 368–375. DOI: 10.1016/j.orggeochem.2011.02.003.

LIU, X.-L., R. E. SUMMONS, and K.-U. HINRICHS (2012c). Extending the known range of glycerol ether lipids in the environment: structural assignments based on tandem mass spectral fragmentation patterns. *Rapid Communications in Mass Spectrometry* **26** (19), 2295–2302. DOI: 10.1002/rcm.6355.

LIU, X.-L., C. ZHU, S. G. WAKEHAM, and K.-U. HINRICHS (2014). In situ production of branched glycerol dialkyl glycerol tetraethers in anoxic marine water columns. *Marine Chemistry* **166**, 1–8. DOI: 10.1016/j.marchem.2014.08.008.

LIU, Y. and W. B. WHITMAN (2008). Metabolic, phylogenetic, and ecological diversity of the methanogenic archaea. *Annals of the New York Academy of Sciences* **1125**, 171–189. DOI: 10.1196/annals.1419.019.

LOCARNINI, R. A., A. V. MISHONOV, J. I. ANTONOV, T. P. BOYER, H. E. GARCIA, O. K. BARANOVA, M. M. ZWENG, and D. R. JOHNSON (2010). *World Ocean Atlas 2009, Volume 1: Temperature*. Ed. by S. Levitus. NOAA Atlas. Washington, D.C.: U.S. Government Printing Office, p. 184.

LODISH, H. F., A. BERK, S. L. ZIPURSKY, P. MATSUDAIRA, D. BALTIMORE, and J. DARNELL (2000). *Molecular Cell Biology*. New York, USA: WH Freeman, p. 1150.

LOFFELD, B. and H. KEWELOH (1996). *cis/trans* isomerization of unsaturated fatty acids as possible control mechanism of membrane fluidity in *Pseudomonas putida* P8. *Lipids* **31** (8), 811–815.

LOGEMANN, J., J. GRAUE, J. KÖSTER, B. ENGELEN, J. RULLKÖTTER, and H. CYPIONKA (2011). A laboratory experiment of intact polar lipid degradation in sandy sediments. *Biogeosciences* **8** (9), 2547–2560. DOI: 10.5194/bg-8-2547-2011.

LOMBARD, J., P. LÓPEZ-GARCÍA, and D. MOREIRA (2012). The early evolution of lipid membranes and the three domains of life. *Nature Reviews Microbiology* **10** (7), 507–515. DOI: 10.1038/nrmicro2815.

LÓPEZ, D. and R. KOLTER (2010). Functional microdomains in bacterial membranes. *Genes and Development* **24** (17), 1893–1902. DOI: 10.1101/gad.1945010.

LÓPEZ-GARCÍA, P., D. MOREIRA, a. LÓPEZ-LÓPEZ, and F. RODRÍGUEZ-VALERA (2001). A novel haloarchaeal-related lineage is widely distributed in deep oceanic regions. *Environmental Microbiology* **3** (1), 72–78. DOI: 10.1046/j.1462-2920.2001.00162.x.

LÖSCHER, C. R., A. KOCK, M. KÖNNEKE, J. LAROCHE, H. W. BANGE, and R. A. SCHMITZ (2012). Production of oceanic nitrous oxide by ammonia-oxidizing archaea. *Biogeosciences* **9** (7), 2419–2429. DOI: 10.5194/bg-9-2419-2012.

LU, L., W. HAN, J. ZHANG, Y. WU, B. WANG, X. LIN, J. ZHU, Z. CAI, and Z. JIA (2012). Nitrification of archaeal ammonia oxidizers in acid soils is supported by hydrolysis of urea. *The ISME Journal* **6** (10), 1978–1984. DOI: 10.1038/ismej.2012.45.

LUDWIG, W., O. STRUNK, R. WESTRAM, L. RICHTER, H. MEIER, a. YADHUKUMAR, A. BUCHNER, T. LAI, S. STEPPI, G. JACOB, W. FÖRSTER, I. BRETTSKE, S. GERBER, A. W. GINHART, O. GROSS, S. GRUMANN, S. HERMANN, R. JOST, A. KÖNIG, T. LISS, R. LÜSSBMANN, M. MAY, B. NONHOFF, B. REICHEL, R. STREHLOW, A. STAMATAKIS, N. STUCKMANN, A. VILBIG, M. LENKE, T. LUDWIG, A. BODE, and K. H. SCHLEIFER (2004). ARB: A software environment for sequence data. *Nucleic Acids Research* **32** (4), 1363–1371. DOI: 10.1093/nar/gkh293.

LUNAU, M., A. LEMKE, K. WALTHER, W. MARTENS-HABBENA, and M. SIMON (2005). An improved method for counting bacteria from sediments and turbid environments by epifluorescence microscopy. *Environmental Microbiology* **7** (7), 961–968. DOI: 10.1111/j.1462-2920.2005.00767.x.

LUO, H., B. B. TOLAR, B. K. SWAN, C. L. ZHANG, R. STEPANAUSKAS, M. A. MORAN, and J. T. HOLLIBAUGH (2014). Single-cell genomics shedding light on marine Thaumarchaeota diversification. *The ISME Journal* **8** (3), 732–736. DOI: 10.1038/ismej.2013.202.

MACALADY, J. L., M. M. VESTLING, D. BAUMLER, N. BOEKELHEIDE, C. W. KASPAR, and J. F. BANFIELD (2004). Tetraether-linked membrane monolayers in *Ferroplasma* spp: a key to survival in acid. *Extremophiles* **8** (5), 411–419. DOI: 10.1007/s00792-004-0404-5.

MADIGAN, M. T., J. M. MARTINKO, and J. PARKER (2011). *Brock Biology of Microorganisms*. Upper Saddle River, NJ: Pearson Education.

MAKULA, R. A. and W. R. FINNERTY (1975). Isolation and characterization of an ornithine-containing lipid from *Desulfovibrio gigas*. *Journal of Bacteriology* **123** (2), 523–529.

MAKULA, R. A. (1978). Phospholipid composition of methane-utilizing bacteria. *Journal of Bacteriology* **134** (3), 771–777.

MANSKE, A. K., J. GLAESER, M. M. M. KUYPERS, and J. OVERMANN (2005). Physiology and phylogeny of green sulfur bacteria forming a monospecific phototrophic assemblage at a depth of 100 meters in the Black Sea. *Applied and Environmental Microbiology* **71** (12), 8049–8060. DOI: 10.1128/AEM.71.12.8049-8060.2005.

MARSCHALL, E., M. JOGLER, U. HENSSGE, and J. OVERMANN (2010). Large-scale distribution and activity patterns of an extremely low-light-adapted population of green sulfur bacteria in the Black Sea. *Environmental Microbiology* **12** (5), 1348–1362. DOI: 10.1111/j.1462-2920.2010.02178.x.

MARTENS-HABBENA, W., P. M. BERUBE, H. URAKAWA, J. R. DE LA TORRE, and D. A. STAHL (2009). Ammonia oxidation kinetics determine niche separation of nitrifying Archaea and Bacteria. *Nature* **461** (7266), 976–979. DOI: 10.1038/nature08465.

MARTIN, W. F. (2012). Hydrogen, metals, bifurcating electrons, and proton gradients: the early evolution of biological energy conservation. *FEBS Letters* **586** (5), 485–493. DOI: 10.1016/j.febslet.2011.09.031.

MARTIN-CUADRADO, A.-B., F. RODRIGUEZ-VALERA, D. MOREIRA, J. C. ALBA, E. IVARS-MARTÍNEZ, M. R. HENN, E. TALLA, and P. LÓPEZ-GARCÍA (2008). Hindsight in the relative abundance, metabolic potential and genome dynamics of uncultivated marine archaea from comparative metagenomic analyses of bathypelagic plankton of different oceanic regions. *The ISME Journal* **2** (8), 865–886. DOI: 10.1038/ismej.2008.40.

MASSANA, R., E. F. DELONG, and C. PEDRÓS-ALIÓ (2000). A few cosmopolitan phylotypes dominate planktonic archaeal assemblages in widely different oceanic provinces. *Applied and Environmental Microbiology* **66** (5), 1777–1787.

MASSANA, R., A. E. MURRAY, C. M. PRESTON, and E. F. DELONG (1997). Vertical distribution and phylogenetic characterization of marine planktonic *Archaea* in the Santa Barbara Channel. *Applied and Environmental Microbiology* **63** (1), 50–56.

MASSANA, R., L. T. TAYLOR, A. E. MURRAY, K. Y. WU, W. H. JEFFREY, and E. F. DELONG (1998). Vertical distribution and temporal variation of marine planktonic archaea in the Gerlache Strait, Antarctica, during early spring. *Limnology and Oceanography* **43** (4), 607–617. DOI: 10.4319/lo.1998.43.4.0607.

MATHAI, J. C., G. D. SPROTT, and M. L. ZEIDEL (2001). Molecular mechanisms of water and solute transport across archaebacterial lipid membranes. *The Journal of Biological Chemistry* **276** (29), 27266–27271. DOI: 10.1074/jbc.M103265200.

MATSUNO, Y., A. SUGAI, H. HIGASHIBATA, W. FUKUDA, K. UEDA, I. UDA, I. SATO, T. ITOH, T. IMANAKA, and S. FUJIWARA (2009). Effect of growth temperature and growth phase on the lipid composition of the archaeal membrane from *Thermococcus kodakaraensis*. *Bioscience, Biotechnology, and Biochemistry* **73** (1), 104–108. DOI: 10.1271/bbb.80520.

MEADOR, T. B., E. J. GAGEN, M. E. LOSCAR, T. GOLDHAMMER, M. Y. YOSHINAGA, J. WENDT, M. THOMM, and K.-U. HINRICHS (2014a). *Thermococcus kodakarensis* modulates its polar membrane lipids and elemental composition according to growth stage and phosphate availability. *Frontiers in Microbiology* **5**, 10. DOI: 10.3389/fmicb.2014.00010.

MEADOR, T. B., C. ZHU, F. J. ELLING, M. KÖNNEKE, and K.-U. HINRICHS (2014b). Identification of isoprenoid glycosidic glycerol dibiphytanol diethers and indications for their biosynthetic origin. *Organic Geochemistry* **69**, 70–75. DOI: 10.1016/j.orggeochem.2014.02.005.

MEGONIGAL, J. P., M. E. HINES, and V. P. T. (2003). Anaerobic metabolism: Linkages to trace gases and aerobic processes. In: *Treatise on Geochemistry*. Ed. by H. D. Holland and K. K. Turekian. Oxford, UK: Pergamon, pp. 317–424.

MERBT, S. N., D. A. STAHL, E. O. CASAMAYOR, E. MARTÍ, G. W. NICOL, and J. I. PROSSER (2012). Differential photoinhibition of bacterial and archaeal ammonia oxidation. *FEMS Microbiology Letters* **327** (1), 41–46. DOI: 10.1111/j.1574-6968.2011.02457.x.

METCALF, W. W., B. M. GRIFFIN, R. M. CICCHILLO, J. GAO, S. C. JANGA, H. A. COOKE, B. T. CIRCELLO, B. S. EVANS, W. MARTENS-HABBENA, D. A. STAHL, and W. A. VAN DER DONK (2012). Synthesis of Methylphosphonic Acid by Marine Microbes: A Source for Methane in the Aerobic Ocean. *Science* **337** (6098), 1104–1107. DOI: 10.1126/science.1219875.

MILLERO, F. J. (2007). The marine inorganic carbon cycle. *Chemical Review* **107**, 308–341. DOI: 10.1021/cr0503557.

MINCER, T. J., M. J. CHURCH, L. T. TAYLOR, C. PRESTON, D. M. KARL, and E. F. DELONG (2007). Quantitative distribution of presumptive archaeal and bacterial nitrifiers in Monterey Bay and the North Pacific Subtropical Gyre. *Environmental Microbiology* **9** (5), 1162–1175. DOI: 10.1111/j.1462-2920.2007.01239.x.

MITCHELL, P. (1961). Coupling of phosphorylation to electron and hydrogen transfer by a chemi-osmotic type of mechanism. *Nature* **191**, 144–148. DOI: 10.1038/191144a0.

MOORE, E. K., E. C. HOPMANS, W. I. C. RIJPSTRA, L. VILLANUEVA, S. N. DEDYSH, I. S. KULICHEVSKAYA, H. WIENK, F. SCHOUTSEN, and J. S. SINNINGHE DAMSTÉ (2013). Novel mono-, di-, and trimethylornithine membrane lipids in northern wetland planctomycetes. *Applied and Environmental Microbiology* **79** (22), 6874–6884. DOI: 10.1128/AEM.02169-13.

MORII, H. and Y. KOGA (1994). Asymmetrical topology of diether- and tetraether-type polar lipids in membranes of *Methanobacterium thermoautotrophicum* cells. *The Journal of Biological Chemistry* **269** (14), 10492–10497.

MORII, H., H. YAGI, H. AKUTSU, N. NOMURA, Y. SAKO, and Y. KOGA (1999). A novel phosphoglycolipid archaetidyl(glucosyl)inositol with two sesterterpanyl chains from the aerobic hyperthermophilic archaeon *Aeropyrum pernix* K1. *Biochimica et Biophysica Acta* **1436** (3), 426–436. DOI: 10.1016/S0005-2760(98)00157-X.

MORII, H. and Y. KOGA (1993). Tetraether type polar lipids increase after logarithmic growth phase of *Methanobacterium thermoautotrophicum* in compensation for the decrease of diether lipids. *FEMS Microbiology Letters* **109** (2-3), 283–287.

MOSIER, A. C., M. B. LUND, and C. A. FRANCIS (2012). Ecophysiology of an ammonia-oxidizing archaeon adapted to low-salinity habitats. *Microbial Ecology* **64** (4), 955–963. DOI: 10.1007/s00248-012-0075-1.

MULDER, A., A. A. VAN DE GRAAF, L. A. ROBERTSON, and J. G. KUENEN (1995). Anaerobic ammonium oxidation discovered in a denitrifying fluidized bed reactor. *FEMS Microbiology Ecology* **16** (3), 177–184. DOI: 10.1016/0168-6496(94)00081-7.

MULLER, F., T. BRISSAC, N. LE BRIS, H. FELBECK, and O. GROS (2010). First description of giant *Archaea* (*Thaumarchaeota*) associated with putative bacterial ectosymbionts in a sulfidic marine habitat. *Environmental Microbiology* **12** (8), 2371–2383. DOI: 10.1111/j.1462-2920.2010.02309.x.

MUNSON, M. A. and D. B. NEDWELL (1997). Phylogenetic diversity of *Archaea* in sediment samples from a coastal salt marsh. *Applied and Environmental Microbiology* **63** (12), 4729–4733.

MURRAY, A. E., C. M. PRESTON, R. MASSANA, L. T. TAYLOR, A. BLAKIS, K. WU, and E. F. DELONG (1998). Seasonal and spatial variability of bacterial and archaeal assemblages in the coastal waters near Anvers Island, Antarctica. *Applied and Environmental Microbiology* **64** (7), 2585–2595.

MURRAY, J. W. and E. YAKUSHEV (2006). The suboxic transition zone in the Black Sea. In: *Past and Present Water Column Anoxia*. Ed. by L. N. Neretin. Springer, pp. 105–138.

MURRAY, J. W., H. W. JANNASCH, S. HONJO, R. F. ANDERSON, W. S. REEBURGH, Z. TOP, G. E. FRIEDERICH, L. A. CODISPOTI, and E. IZDAR (1989). Unexpected changes in the oxic/anoxic interface in the Black Sea. *Nature* **338**, 411–413. DOI: 10.1038/338411a0.

MUSSMANN, M., I. BRITO, A. PITCHER, J. S. SINNINGHE DAMSTÉ, R. HATZENPICHLER, A. RICHTER, J. L. NIELSEN, P. H. NIELSEN, A. MÜLLER, H. DAIMS, M. WAGNER, and I. M. HEAD (2011). Thaumarchaeotes abundant in refinery nitrifying sludges express *amoA* but are not obligate autotrophic ammonia oxidizers. *Proceedings of the National Academy of Sciences of the United States of America* **108** (40), 16771–16776. DOI: 10.1073/pnas.1106427108.

NAMWONG, S., S. TANASUPAWAT, T. KUDO, and T. ITOH (2011). *Haloarcula salaria* sp. nov. and *Haloarcula tradensis* sp. nov., isolated from salt in Thai fish sauce. *International Journal of Systematic and Evolutionary Microbiology* **61**, 231–236. DOI: 10.1099/ijs.0.021790-0.

NEALSON, K., C. MYERS, and B. WIMPEE (1991). Isolation and identification of manganese-reducing bacteria and estimates of microbial Mn(IV)-reducing potential in the Black Sea. *Deep Sea Research Part A. Oceanographic Research Papers* **38**, S907–S920. DOI: 10.1016/S0198-0149(10)80016-0.

NELSON, K. E., R. A. CLAYTON, S. R. GILL, M. L. GWINN, R. J. DODSON, D. H. HAFT, E. K. HICKEY, J. D. PETERSON, W. C. NELSON, K. A. KETCHUM, L. MCDONALD, T. R. UTTERBACK, J. A. MALEK, K. D. LINHER, M. M. GARRETT, A. M. STEWART, M. D. COTTON, M. S. PRATT, C. A. PHILLIPS, D. RICHARDSON, J. HEIDELBERG, G. G. SUTTON, R. D. FLEISCHMANN, J. A. EISEN, O. WHITE, S. L. SALZBERG, H. O. SMITH, J. C. VENTER, and C. M. FRASER (1999). Evidence for lateral gene transfer between Archaea and Bacteria from genome sequence of *Thermotoga maritima*. *Nature* **399** (6734), 323–329. DOI: 10.1038/20601.

NELSON-SATHI, S., T. DAGAN, G. LANDAN, A. JANSSEN, M. STEEL, J. O. MCINERNEY, U. DEPPENMEIER, and W. F. MARTIN (2012). Acquisition of 1,000 eubacterial genes physiologically transformed a methanogen at the origin of Haloarchaea. *Proceedings of the National Academy of Sciences of the United States of America* **109** (50), 20537–20542. DOI: 10.1073/pnas.1209119109.

NELSON-SATHI, S., F. L. SOUSA, M. ROETTGER, N. LOZADA-CHÁVEZ, T. THIERGART, A. JANSSEN, D. BRYANT, G. LANDAN, P. SCHÖNHEIT, B. SIEBERS, J. O. MCINERNEY, and W. F. MARTIN (2014). Origins of major archaeal clades correspond to gene acquisitions from bacteria. *Nature* **517**, 77–80. DOI: 10.1038/nature13805.

NEWMAN, D. K. and J. F. BANFIELD (2002). Geomicrobiology: how molecular-scale interactions underpin biogeochemical systems. *Science* **296**, 1071–1077. DOI: 10.1126/science.1010716.

NGUGI, D. K., J. BLOM, I. ALAM, M. RASHID, W. BA-ALAWI, G. ZHANG, T. HIKMAWAN, Y. GUAN, A. ANTUNES, R. SIAM, H. EL DORRY, V. BAJIC, and U. STINGL (2015). Comparative genomics reveals adaptations of a halotolerant thaumarchaeon in the interfaces of brine pools in the Red Sea. *The ISME Journal* **9** (2), 396–411. DOI: 10.1038/ismej.2014.137.

NICHOLS, D. S., M. R. MILLER, N. W. DAVIES, A. GOODCHILD, M. RAFTERY, and R. CAVICCHIOLI (2004). Cold adaptation in the antarctic archaeon *Methanococcoides burtonii* involves membrane lipid unsaturation. *Journal of Bacteriology* **186** (24), 8508–8515. DOI: 10.1128/JB.186.24.8508.

NICOL, G. W. and C. SCHLEPER (2006). Ammonia-oxidising Crenarchaeota: important players in the nitrogen cycle? *Trends in Microbiology* **14** (5), 207–212. DOI: 10.1016/j.tim.2006.03.004.

NICOL, G. W., S. LEININGER, C. SCHLEPER, and J. I. PROSSER (2008). The influence of soil pH on the diversity, abundance and transcriptional activity of ammonia oxidizing archaea and bacteria. *Environmental Microbiology* **10** (11), 2966–2978. DOI: 10.1111/j.1462-2920.2008.01701.x.

NICOLAUS, B., A. TRINCONE, L. LAMA, G. PALMIERI, and A. GAMBACORTA (1992). Quinone composition in *Sulfolobus solfataricus* grown under different conditions. *Systematic and Applied Microbiology* **15** (1), 18–20. DOI: 10.1016/S0723-2020(11)80131-1.

NICOLSON, G. L. (2014). The Fluid - Mosaic Model of Membrane Structure: Still relevant to understanding the structure, function and dynamics of biological membranes after more than 40 years. *Biochimica et Biophysica Acta - Biomembranes* **1838** (6), 1451–1466. DOI: 10.1016/j.bbamem.2013.10.019.

NISHIDA, F., M. NISHIJIMA, K. MOCHIDA, H. SANO, N. NOMURA, Y. SAKO, and T. MARUYAMA (1999). Isoprenoid quinones in an aerobic hyperthermophilic archaeon, *Aeropyrum pernix*. *FEMS Microbiology Letters* **174** (2), 339–346. DOI: 10.1111/j.1574-6968.1999.tb13588.x.

NITSCHKE, W., D. KRAMER, A. RIEDEL, and U. LIEBL (1995). From naphtho- to benzoquinones -(r)evolutionary reorganizations of electron transfer chains. In: *Photosynthesis: From Light to Biosphere*. Ed. by P. Mathis. Dordrecht, The Netherlands: Kluwer Academic, pp. 945–950.

NOWICKA, B. and J. KRUK (2010). Occurrence, biosynthesis and function of isoprenoid quinones. *Biochimica et Biophysica Acta* **1797** (9), 1587–1605. DOI: 10.1016/j.bbabio.2010.06.007.

NYSTRÖM, T. (2004). Stationary-phase physiology. *Annual Review of Microbiology* **58**, 161–181. DOI: 10.1146/annurev.micro.58.030603.123818.

OCHSENREITER, T., D. SELEZI, A. QUAISER, L. BONCH-OSMOLOVSKAYA, and C. SCHLEPER (2003). Diversity and abundance of Crenarchaeota in terrestrial habitats studied by 16S RNA surveys and real time PCR. *Environmental Microbiology* **5** (9), 787–797. DOI: 10.1046/j.1462-2920.2003.00476.x.

OFFRE, P., A. SPANG, and C. SCHLEPER (2013). Archaea in biogeochemical cycles. *Annual Review of Microbiology* **67**, 437–457. DOI: 10.1146/annurev-micro-092412-155614.

OGER, P. M. and A. CARIO (2013). Adaptation of the membrane in Archaea. *Biophysical Chemistry* **183**, 42–56. DOI: 10.1016/j.bpc.2013.06.020.

OGUZ, T., J. W. MURRAY, and A. E. CALLAHAN (2001). Modeling redox cycling across the suboxic-anoxic interface zone in the Black Sea. *Deep-Sea Research Part I: Oceanographic Research Papers* **48** (3), 761–787. DOI: 10.1016/S0967-0637(00)00054-6.

OKAYAMA, S. (1976). Redox potential of plastoquinone A in spinach chloroplasts. *Biochimica et Biophysica Acta* **440**, 331–336. DOI: 10.1016/0005-2728(76)90067-0.

OLSEN, I. and E. JANTZEN (2001). Sphingolipids in bacteria and fungi. *Anaerobe* **7** (2), 103–112. DOI: 10.1006/anae.2001.0376.

OREMLAND, R. S. and S. POLCIN (1982). Methanogenesis and Sulfate Reduction: Competitive and Noncompetitive Substrates in Estuarine Sediments. *Applied and Environmental Microbiology* **44** (6), 1270–1276.

OREMLAND, R. S., L. M. MARSH, and S. POLCIN (1982). Methane production and simultaneous sulphate reduction in anoxic, salt marsh sediments. *Nature* **296** (5853), 143–145. DOI: 10.1038/296143a0.

ORPHAN, V. J., C. H. HOUSE, K. U. HINRICHS, K. D. MCKEEGAN, and E. F. DELONG (2001). Methane-consuming archaea revealed by directly coupled isotopic and phylogenetic analysis. *Science* **293** (5529), 484–487. DOI: 10.1126/science.1061338.

OUVERNEY, C. C. and J. A. FUHRMAN (2000). Marine Planktonic Archaea Take Up Amino Acids. *Applied and Environmental Microbiology* **66** (11), 4829–4833. DOI: 10.1128/AEM.66.11.4829-4833.2000.

OVERMANN, J. (2006). The Family Chlorobiaceae. In: *The Prokaryotes. Volume 7: Proteobacteria: Delta, Epsilon Subclass*. Ed. by M. Dworkin, S. Falkow, E. Rosenberg, K.-H. Schleifer, and E. Stackebrandt. New York, USA: Springer, pp. 359–378. DOI: 10.1007/0-387-30747-8_13.

OVERMANN, J., H. CYPIONKA, and N. PFENNIG (1992). An extremely low-light adapted phototrophic sulfur bacterium from the Black Sea. *Limnology and Oceanography* **37** (1), 150–155. DOI: 10.4319/lo.1992.37.1.0150.

PACE, N. R. (1997). A molecular view of microbial diversity and the biosphere. *Science* **276** (5313), 734–740. DOI: 10.1126/science.276.5313.734.

PALMER, M. R., P. N. PEARSON, and S. J. COBB (1998). Reconstructing Past Ocean pH-Depth Profiles. *Science* **282**, 1468–1471. DOI: 10.1126/science.282.5393.1468.

PAPER, W., U. JAHN, M. J. HOHN, M. KRONNER, D. J. NÄTHER, T. BURGHARDT, R. RACHEL, K. O. STETTER, and H. HUBER (2007). *Ignicoccus hospitalis* sp. nov., the host of *'Nanoarchaeum equitans'*. *International Journal of Systematic and Evolutionary Microbiology* **57** (4), 803–808. DOI: 10.1099/ijs.0.64721-0.

PARK, S.-J., R. GHAI, A.-B. MARTÍN-CUADRADO, F. RODRÍGUEZ-VALERA, W.-H. CHUNG, K. KWON, J.-H. LEE, E. L. MADSEN, and S.-K. RHEE (2014). Genomes of two new ammonia-oxidizing archaea enriched from deep marine sediments. *PloS One* **9** (5), e96449. DOI: 10.1371/journal.pone.0096449.

PARKES, R. J., B. A. CRAGG, and P. WELLSBURY (2000). Recent studies on bacterial populations and processes in subseafloor sediments: A review. *Hydrogeology Journal* **8**, 11–28. DOI: 10.1007/PL00010971.

PEARSON, A., Z. HUANG, A. E. INGALLS, C. S. ROMANEK, J. WIEGEL, K. H. FREEMAN, R. H. SMITTENBERG, and C. L. ZHANG (2004). Nonmarine crenarchaeol in Nevada hot springs. *Applied and Environmental Microbiology* **70** (9), 5229–5237. DOI: 10.1128/AEM.70.9.5229-5237.2004.

PEARSON, A., A. P. MCNICHOL, B. C. BENITEZ-NELSON, J. M. HAYES, and T. I. EGLINTON (2001). Origins of lipid biomarkers in Santa Monica Basin surface sediment: a case study using compound-specific Δ^{14}C analysis. *Geochimica et Cosmochimica Acta* **65** (18), 3123–3137. DOI: 10.1016/S0016-7037(01)00657-3.

PEARSON, A. and A. E. INGALLS (2013). Assessing the Use of Archaeal Lipids as Marine Environmental Proxies. *Annual Review of Earth and Planetary Sciences* **41** (1), 359–384. DOI: 10.1146/annurev-earth-050212-123947.

PEDNEAULT, E., P. E. GALAND, M. POTVIN, J.-É. TREMBLAY, and C. LOVEJOY (2014). Archaeal *amoA* and *ureC* genes and their transcriptional activity in the Arctic Ocean. *Scientific Reports* **4**, 4661. DOI: 10.1038/srep04661.

PELVE, E. A., A.-C. LINDÅS, W. MARTENS-HABBENA, J. R. DE LA TORRE, D. A. STAHL, and R. BERNANDER (2011). Cdv-based cell division and cell cycle organization in the thaumarchaeon *Nitrosopumilus maritimus*. *Molecular Microbiology* **82** (3), 555–566. DOI: 10.1111/j.1365-2958.2011.07834.x.

PERRY, K. A., J. E. KOSTKA, G. W. LUTHER, and K. H. NEALSON (1993). Mediation of sulfur speciation by a Black Sea facultative anaerobe. *Science* **259** (1990), 801–803. DOI: 10.1126/science.259.5096.801.

PESTER, M., T. RATTEI, S. FLECHL, A. GRÖNGRÖFT, A. RICHTER, J. OVERMANN, B. REINHOLD-HUREK, A. LOY, and M. WAGNER (2012). *amoA*-based consensus phylogeny of ammonia-oxidizing archaea and deep sequencing of *amoA* genes from soils of four different geographic regions. *Environmental Microbiology* **14** (2), 525–539. DOI: 10.1111/j.1462-2920.2011.02666.x.

PESTER, M., C. SCHLEPER, and M. WAGNER (2011). The Thaumarchaeota: an emerging view of their phylogeny and ecophysiology. *Current Opinion in Microbiology* **14** (3), 300–306. DOI: 10.1016/j.mib.2011.04.007.

PIMENOV, N. and L. NERETIN (2006). Composition and activities of microbial communities involved in carbon, sulfur, nitrogen and manganese cycling in the oxic/anoxic interface of the Black Sea. In: *Past and Present Water Column Anoxia*. Ed. by L. N. Neretin. Berlin, Germany: Springer, pp. 501–521.

PITCHER, A., E. C. HOPMANS, A. C. MOSIER, S.-J. PARK, S.-K. RHEE, C. A. FRANCIS, S. SCHOUTEN, and J. S. SINNINGHE DAMSTÉ (2011a). Core and intact polar glycerol dibiphytanyl glycerol tetraether lipids of ammonia-oxidizing archaea enriched from marine and estuarine sediments. *Applied and Environmental Microbiology* **77** (10), 3468–3477. DOI: 10.1128/AEM.02758-10.

PITCHER, A., N. RYCHLIK, E. C. HOPMANS, E. SPIECK, W. I. C. RIJPSTRA, J. OSSEBAAR, S. SCHOUTEN, M. WAGNER, and J. S. SINNINGHE DAMSTÉ (2010). Crenarchaeol dominates the membrane lipids of *Candidatus* Nitrososphaera gargensis, a thermophilic group I.1b Archaeon. *The ISME Journal* **4** (4), 542–552. DOI: 10.1038/ismej.2009.138.

PITCHER, A., S. SCHOUTEN, and J. S. SINNINGHE DAMSTÉ (2009). In situ production of crenarchaeol in two California hot springs. *Applied and Environmental Microbiology* **75** (13), 4443–4451. DOI: 10.1128/AEM.02591-08.

PITCHER, A., L. VILLANUEVA, E. C. HOPMANS, S. SCHOUTEN, G.-J. REICHART, and J. S. SINNINGHE DAMSTÉ (2011b). Niche segregation of ammonia-oxidizing archaea and anammox bacteria in the Arabian Sea oxygen minimum zone. *The ISME Journal* **5** (12), 1896–1904. DOI: 10.1038/ismej.2011.60.

PITCHER, A., C. WUCHTER, K. SIEDENBERG, S. SCHOUTEN, and J. S. SINNINGHE DAMSTÉ (2011c). Crenarchaeol tracks winter blooms of ammonia-oxidizing Thaumarchaeota in the coastal North Sea. *Limnology and Oceanography* **56** (6), 2308–2318. DOI: 10.4319/lo.2011.56.6.2308.

PODLASKA, A., S. G. WAKEHAM, K. A. FANNING, and G. T. TAYLOR (2012). Microbial community structure and productivity in the oxygen minimum zone of the eastern tropical North Pacific. *Deep-Sea Research I* **66**, 77–89. DOI: 10.1016/j.dsr.2012.04.002.

POPENDORF, K. J., T. TANAKA, M. PUJO-PAY, A. LAGARIA, C. COURTIES, P. CONAN, L. ORIOL, L. E. SOFEN, T. MOUTIN, and B. A. S. VAN MOOY (2011). Gradients in intact polar diacylglycerolipids across the Mediterranean Sea are related to phosphate availability. *Biogeosciences* **8** (12), 3733–3745. DOI: 10.5194/bg-8-3733-2011.

POULIOT, J., P. E. GALAND, C. LOVEJOY, and W. F. VINCENT (2009). Vertical structure of archaeal communities and the distribution of ammonia monooxygenase A gene variants in two meromictic High Arctic lakes. *Environmental Microbiology* **11** (3), 687–699. DOI: 10.1111/j.1462-2920.2008.01846.x.

POWERS, L. A., J. P. WERNE, T. C. JOHNSON, E. C. HOPMANS, J. S. SINNINGHE DAMSTÉ, and S. SCHOUTEN (2004). Crenarchaeotal membrane lipids in lake sediments: A new paleotemperature proxy for continental paleoclimate reconstruction? *Geology* **32** (7), 613–615. DOI: 10.1130/G20434.1.

POWLS, R., E. REDFEARN, and S. TRIPPETT (1968). The structure of chlorobiumquinone. *Biochemical and Biophysical Research Communications* **33** (3), 408–411.

PRAHL, F. G. and S. G. WAKEHAM (1987). Calibration of unsaturation patterns in long-chain ketone compositions for palaeotemperature assessment. *Nature* **330** (6146), 367–369. DOI: 10.1038/330367a0.

PRESTON, C. M. (1996). A psychrophilic crenarchaeon inhabits a marine sponge: Cenarchaeum symbiosum gen. nov., sp. nov. *Proceedings of the National Academy of Sciences of the United States of America* **93** (13), 6241–6246. DOI: 10.1073/pnas.93.13.6241.

PROSSER, J. I. and G. W. NICOL (2008). Relative contributions of archaea and bacteria to aerobic ammonia oxidation in the environment. *Environmental Microbiology* **10** (11), 2931–2941. DOI: 10.1111/j.1462-2920.2008.01775.x.

QIN, W., S. A. AMIN, W. MARTENS-HABBENA, C. B. WALKER, H. URAKAWA, A. H. DEVOL, A. E. INGALLS, J. W. MOFFETT, E. V. ARMBRUST, and D. A. STAHL (2014). Marine ammonia-oxidizing archaeal isolates display obligate mixotrophy and wide ecotypic variation. *Proceedings of the National Academy of Sciences of the United States of America* **111** (34). DOI: 10.1073/pnas.1324115111.

RABUS, R., T. A. HANSEN, and F. WIDDEL (2006). Dissimilatory Sulfate and Sulfur-Reducing Prokaryotes. In: *The Prokaryotes. Volume 2: Ecophysiology and Biochemistry*. Ed. by M. Dworki, S. Falkow, E. Rosenberg, K.-H. Schleifer, and E. Stackebrandt. New York, USA: Springer, pp. 659–768. DOI: 10.1007/0-387-30742-7_22.

RECHKA, J. and J. MAXWELL (1988). Characterisation of alkenone temperature indicators in sediments and organisms. *Organic Geochemistry* **13** (4-6), 727–734. DOI: 10.1016/0146-6380(88)90094-0.

REDFEARN, E. and R. POWLS (1968). Quinones of green photosynthetic bacteria. *Bioochemical Journal* **106**, 50.

REEBURGH, W. S., B. B. WARD, S. C. WHALEN, K. A. SANDBECK, K. A. KILPATRICKT, and L. J. KERKHOF (1991). Black Sea methane geochemistry. *Deep Sea Research Part A. Oceanographic Research Papers* **38**, S1189–S1210. DOI: 10.1016/S0198-0149(10)80030-5.

REIGSTAD, L. J., A. RICHTER, H. DAIMS, T. URICH, L. SCHWARK, and C. SCHLEPER (2008). Nitrification in terrestrial hot springs of Iceland and Kamchatka. *FEMS Microbiology Ecology* **64** (2), 167–174. DOI: 10.1111/j.1574-6941.2008.00466.x.

RENO, M. L., N. L. HELD, C. J. FIELDS, P. V. BURKE, and R. W. WHITAKER (2009). Biogeography of the *Sulfolobus islandicus* pan-genome. *Proceedings of the National Academy of Sciences of the United States of America* **106** (44), 18873–18873. DOI: 10.1073/pnas.0911400106.

REPETA, D. J. and D. J. SIMPSON (1991). The distribution and recycling of chlorophyll, bacteriochlorophyll and carotenoids in the Black Sea. *Deep Sea Research Part A. Oceanographic Research Papers* **38**, S969–S984. DOI: 10.1016/S0198-0149(10)80019-6.

REPETA, D. J. (1993). A high resolution historical record of Holocene anoxygenic primary production in the Black Sea. *Geochimica et Cosmochimica Acta* **57** (17), 4337–4342. DOI: 10.1016/0016-7037(93)90334-S.

RIEDINGER, N., B. BRUNNER, Y.-S. LIN, A. VOSSMEYER, T. G. FERDELMAN, and B. B. JØRGENSEN (2010). Methane at the sediment–water transition in Black Sea sediments. *Chemical Geology* **274** (1-2), 29–37. DOI: 10.1016/j.chemgeo.2010.03.010.

ROSS, D. A., E. T. DEGENS, and J. MACILVAINE (1970). Black sea: Recent sedimentary history. *Science* **170** (3954), 163–165. DOI: 10.1126/science.170.3954.163.

ROSSEL, P. E., J. S. LIPP, H. F. FREDRICKS, J. ARNDS, A. BOETIUS, M. ELVERT, and K.-U. HINRICHS (2008). Intact polar lipids of anaerobic methanotrophic archaea and associated bacteria. *Organic Geochemistry* **39** (8), 992–999. DOI: 10.1016/j.orggeochem.2008.02.021.

ROUSSEL, E. G., A. L. SAUVADET, C. CHADUTEAU, Y. FOUQUET, J. L. CHARLOU, D. PRIEUR, and M. A. CAMBON BONAVITA (2009). Archaeal communities associated with shallow to deep subseafloor sediments of the New Caledonia Basin. *Environmental Microbiology* **11** (9), 2446–2462. DOI: 10.1111/j.1462-2920.2009.01976.x.

RUEPP, A., W. GRAML, M. L. SANTOS-MARTINEZ, K. K. KORETKE, C. VOLKER, H. W. MEWES, D. FRISHMAN, S. STOCKER, A. N. LUPAS, and W. BAUMEISTER (2000). The genome sequence of the thermoacidophilic scavenger *Thermoplasma acidophilum*. *Nature* **407** (6803), 508–513. DOI: 10.1038/35035069.

RÜTTERS, H., H. SASS, H. CYPIONKA, and J. RULLKÖTTER (2001). Monoalkylether phospholipids in the sulfate-reducing bacteria *Desulfosarcina variabilis* and *Desulforhabdus amnigenus*. *Archives of Microbiology* **176** (6), 435–442. DOI: 10.1007/s002030100343.

SÁENZ, J. P., E. SEZGIN, P. SCHWILLE, and K. SIMONS (2012). Functional convergence of hopanoids and sterols in membrane ordering. *Proceedings of the National Academy of Sciences of the United States of America* **109** (35), 14236–14240. DOI: 10.1073/pnas.1212141109.

SANINA, N. M., S. N. GONCHAROVA, and E. Y. KOSTETSKY (2004). Fatty acid composition of individual polar lipid classes from marine macrophytes. *Phytochemistry* **65** (6), 721–730. DOI: 10.1016/j.phytochem.2004.01.013.

SANTORO, A. E. and K. L. CASCIOTTI (2011). Enrichment and characterization of ammonia-oxidizing archaea from the open ocean: phylogeny, physiology and stable isotope fractionation. *The ISME Journal* **5** (11), 1796–1808. DOI: 10.1038/ismej.2011.58.

SANTORO, A. E., C. BUCHWALD, M. R. MCILVIN, and K. L. CASCIOTTI (2011). Isotopic signature of N_2O produced by marine ammonia-oxidizing archaea. *Science* **333** (6047), 1282–1285. DOI: 10.1126/science.1208239.

SANTORO, A. E., C. L. DUPONT, R. A. RICHTER, M. T. CRAIG, P. CARINI, M. R. MCILVIN, Y. YANG, W. D. ORSI, D. M. MORAN, and M. A. SAITO (2015). Genomic and proteomic characterization of "*Candidatus* Nitrosopelagicus brevis": An ammonia-oxidizing archaeon from the open ocean. *Proceedings of the National Academy of Sciences of the United States of America* **112** (4), 1173–1178. DOI: 10.1073/pnas.1416223112.

SCHÄFER, G., S. ANEMÜLLER, R. MOLL, M. GLEISSNER, and C. L. SCHMIDT (1993). Has *Sulfolobus* an Archaic Respiratory System? Structure, Function and Genes of its Components. *Systematic and Applied Microbiology* **16** (4), 544–555. DOI: 10.1016/S0723-2020(11)80324-3.

SCHÄFER, G., M. ENGELHARD, and V. MÜLLER (1999). Bioenergetics of the Archaea. *Microbiology and Molecular Biology Reviews* **63** (3), 570–620.

SCHATTENHOFER, M., B. M. FUCHS, R. AMANN, M. V. ZUBKOV, G. A. TARRAN, and J. PERNTHALER (2009). Latitudinal distribution of prokaryotic picoplankton populations in the Atlantic Ocean. *Environmental Microbiology* **11** (8), 2078–2093. DOI: 10.1111/j.1462-2920.2009.01929.x.

SCHIPPERS, A., L. N. NERETIN, J. KALLMEYER, T. G. FERDELMAN, B. A. CRAGG, R. J. PARKES, and B. B. JØRGENSEN (2005). Prokaryotic cells of the deep sub-seafloor biosphere identified as living bacteria. *Nature* **433** (7028), 861–864. DOI: 10.1038/nature03302.

SCHLEPER, C., G. PÜHLER, B. KÜHLMORGEN, and W. ZILLIG (1995). Life at extremely low pH. *Nature* **375** (6534), 741–742. DOI: 10.1038/375741b0.

SCHLEPER, C. and G. W. NICOL (2010). Ammonia-oxidising archaea - physiology, ecology and evolution. *Advances in Microbial Physiology* **57**, 1–41. DOI: 10.1016/B978-0-12-381045-8.00001-1.

SCHLEPER, C., G. JURGENS, and M. JONUSCHEIT (2005). Genomic studies of uncultivated archaea. *Nature Reviews Microbiology* **3** (6), 479–488. DOI: 10.1038/nrmicro1159.

SCHNORF, U. (1966). "Der Einfluss von Substituenten auf Redoxpotential und Wuchsstoffeigenschaften von Chinonen". PhD Thesis. Eidgenössische Technische Hochschule, Zürich. DOI: 10.3929/ethz-a-000090587.

SCHOEPP-COTHENET, B., C. LIEUTAUD, F. BAYMANN, A. VERMÉGLIO, T. FRIEDRICH, D. M. KRAMER, and W. NITSCHKE (2009). Menaquinone as pool quinone in a purple bacterium. *Proceedings of the National Academy of Sciences of the United States of America* **106** (21), 8549–8554. DOI: 10.1073/pnas.0813173106.

SCHOEPP-COTHENET, B., R. VAN LIS, A. ATTEIA, F. BAYMANN, L. CAPOWIEZ, A.-L. DUCLUZEAU, S. DUVAL, F. TEN BRINK, M. J. RUSSELL, and W. NITSCHKE (2013). On the universal core of bioenergetics. *Biochimica et Biophysica Acta* **1827** (2), 79–93. DOI: 10.1016/j.bbabio.2012.09.005.

SCHOUTEN, S., A. FORSTER, F. E. PANOTO, and J. S. SINNINGHE DAMSTÉ (2007a). Towards calibration of the TEX_{86} palaeothermometer for tropical sea surface temperatures in ancient greenhouse worlds. *Organic Geochemistry* **38** (9), 1537–1546. DOI: 10.1016/j.orggeochem.2007.05.014.

SCHOUTEN, S., E. C. HOPMANS, and J. S. SINNINGHE DAMSTÉ (2013). The organic geochemistry of glycerol dialkyl glycerol tetraether lipids: A review. *Organic Geochemistry* **54**, 19–61. DOI: 10.1016/j.orggeochem.2012.09.006.

SCHOUTEN, S., E. C. HOPMANS, M. BAAS, H. BOUMANN, S. STANDFEST, M. KÖNNEKE, D. A. STAHL, and J. S. SINNINGHE DAMSTÉ (2008). Intact Membrane Lipids of "*Candidatus* Nitrosopumilus maritimus," a Cultivated Representative of the Cosmopolitan Mesophilic Group I Crenarchaeota. *Applied and Environmental Microbiology* **74** (8), 2433–2440. DOI: 10.1128/AEM.01709-07.

SCHOUTEN, S., E. C. HOPMANS, R. D. PANCOST, and J. S. SINNINGHE DAMSTÉ (2000). Widespread occurrence of structurally diverse tetraether membrane lipids: evidence for the ubiquitous presence of low-temperature relatives of hyperthermophiles. *Proceedings of the National Academy of Sciences of the United States of America* **97** (26), 14421–14426. DOI: 10.1073/pnas.97.26.14421.

SCHOUTEN, S., E. C. HOPMANS, E. SCHEFUSS, and J. S. SINNINGHE DAMSTÉ (2002). Distributional variations in marine crenarchaeotal membrane lipids: a new tool for reconstructing ancient sea water temperatures? *Earth and Planetary Science Letters* **204** (1-2), 265–274. DOI: 10.1016/S0012-821X(02)00979-2.

SCHOUTEN, S., C. HUGUET, E. C. HOPMANS, M. V. M. KIENHUIS, and J. S. S. DAMSTÉ (2007b). Analytical methodology for TEX_{86} paleothermometry by high-performance liquid chromatography/atmospheric pressure chemical ionization-mass spectrometry. *Analytical Chemistry* **79** (7), 2940–2944. DOI: 10.1021/ac062339v.

SCHOUTEN, S., J. J. MIDDELBURG, E. C. HOPMANS, and J. S. SINNINGHE DAMSTÉ (2010). Fossilization and degradation of intact polar lipids in deep subsurface sediments: A theoretical approach. *Geochimica et Cosmochimica Acta* **74** (13), 3806–3814. DOI: 10.1016/j.gca.2010.03.029.

SCHOUTEN, S., A. PITCHER, E. C. HOPMANS, L. VILLANUEVA, J. VAN BLEIJSWIJK, and J. S. SINNINGHE DAMSTÉ (2012). Intact polar and core glycerol dibiphytanyl glycerol tetraether lipids in the Arabian Sea oxygen minimum zone: I. Selective preservation and degradation in the water column and consequences for the TEX_{86}. *Geochimica et Cosmochimica Acta* **98**, 228–243. DOI: 10.1016/j.gca.2012.05.002.

SCHOUTEN, S., L. VILLANUEVA, E. C. HOPMANS, M. T. J. VAN DER MEER, and J. S. SINNINGHE DAMSTÉ (2014). Are Marine Group II Euryarchaeota significant contributors to tetraether lipids in the ocean? *Proceedings of the National Academy of Sciences of the United States of America* **111** (41), 4285. DOI: 10.1073/pnas.1416176111.

SCHRÖDER, J. M. (2015). "Intact polar lipids in marine sediments: improving analytical protocols and assessing planktonic and benthic sources". PhD Thesis. University of Bremen.

SCHUBERT, C. J., M. J. L. COOLEN, L. N. NERETIN, A. SCHIPPERS, B. ABBAS, E. DURISCH-KAISER, B. WEHRLI, E. C. HOPMANS, J. S. S. DAMSTÉ, S. WAKEHAM, and M. M. M. KUYPERS (2006). Aerobic and anaerobic methanotrophs in the Black Sea water column. *Environmental Microbiology* **8** (10), 1844–1856. DOI: 10.1111/j.1462-2920.2006.01079.x.

SCHUBOTZ, F., D. R. MEYER-DOMBARD, A. S. BRADLEY, H. F. FREDRICKS, K.-U. HINRICHS, E. L. SHOCK, and R. E. SUMMONS (2013). Spatial and temporal variability of biomarkers and microbial diversity reveal metabolic and community flexibility in streamer biofilm communities in the Lower Geyser Basin, Yellowstone National Park. *Geobiology* **11** (6), 549–569. DOI: 10.1111/gbi.12051.

SCHUBOTZ, F., J. S. LIPP, M. ELVERT, and K.-U. HINRICHS (2011). Stable carbon isotopic compositions of intact polar lipids reveal complex carbon flow patterns among hydrocarbon degrading microbial communities at the Chapopote asphalt volcano. *Geochimica et Cosmochimica Acta* **75** (16), 4399–4415. DOI: 10.1016/j.gca.2011.05.018.

SCHUBOTZ, F., S. G. WAKEHAM, J. S. LIPP, H. F. FREDRICKS, and K.-U. HINRICHS (2009). Detection of microbial biomass by intact polar membrane lipid analysis in the water column and surface sediments of the Black Sea. *Environmental Microbiology* **11** (10), 2720–2734. DOI: 10.1111/j.1462-2920.2009.01999.x.

SCHUT, F., R. A. PRINS, and J. C. GOTTSCHAL (1997). Oligotrophy and pelagic marine bacteria: facts and fiction. *Aquatic Microbial Ecology* **12**, 177–202. DOI: 10.3354/ame012177.

SCHÜTZ, M., M. BRUGNA, E. LEBRUN, F. BAYMANN, R. HUBER, K. O. STETTER, G. HAUSKA, R. TOCI, D. LEMESLE-MEUNIER, P. TRON, C. SCHMIDT, and W. NITSCHKE (2000). Early evolution of cytochrome *bc* complexes. *Journal of Molecular Biology* **300** (4), 663–675. DOI: 10.1006/jmbi.2000.3915.

SEIDEL, M., H. RÜTTERS, J. RULLKÖTTER, and H. SASS (2013). Phosphate-free ornithine lipid contents in *Desulfovibrio* spp. respond to growth temperature. *Organic Geochemistry* **59**, 133–142. DOI: 10.1016/j.orggeochem.2013.04.004.

SEKI, O., J. A. BENDLE, N. HARADA, M. KOBAYASHI, K. SAWADA, H. MOOSSEN, G. N. INGLIS, S. NAGAO, and T. SAKAMOTO (2014). Assessment and calibration of TEX_{86} paleothermometry in the Sea of Okhotsk and sub-polar North Pacific region: Implications for paleoceanography. *Progress in Oceanography* **126**, 254–266. DOI: 10.1016/j.pocean.2014.04.013.

SÉVIN, D. C. and U. SAUER (2014). Ubiquinone accumulation improves osmotic-stress tolerance in *Escherichia coli*. *Nature Chemical Biology* **10** (4), 266–272. DOI: 10.1038/nchembio.1437.

SHAH, S. R., G. MOLLENHAUER, N. OHKOUCHI, T. I. EGLINTON, and A. PEARSON (2008). Origins of archaeal tetraether lipids in sediments: Insights from radiocarbon analysis. *Geochimica et Cosmochimica Acta* **72** (18), 4577–4594. DOI: 10.1016/j.gca.2008.06.021.

SHIMADA, H., N. NEMOTO, Y. SHIDA, T. OSHIMA, and A. YAMAGISHI (2002). Complete Polar Lipid Composition of *Thermoplasma acidophilum* HO-62 Determined by High-Performance Liquid Chromatography with Evaporative Light-Scattering Detection. *Journal of Bacteriology* **184** (2), 556–563. DOI: 10.1128/JB.184.2.556-563.2002.

SHIMADA, H., N. NEMOTO, Y. SHIDA, T. OSHIMA, and A. YAMAGISHI (2008). Effects of pH and temperature on the composition of polar lipids in *Thermoplasma acidophilum* HO-62. *Journal of Bacteriology* **190** (15), 5404–5411. DOI: 10.1128/JB.00415-08.

SHIMADA, H., Y. SHIDA, N. NEMOTO, T. OSHIMA, and A. YAMAGISHI (2001). Quinone profiles of *Thermoplasma acidophilum* HO-62. *Journal of Bacteriology* **183** (4), 1462–1465. DOI: 10.1128/JB.183.4.1462-1465.2001.

SHIVELY, J. M. and A. A. BENSON (1967). Phospholipids of *Thiobacillus thiooxidans*. *Journal of Bacteriology* **94** (5), 1679–1683.

SHORT, S. A., D. C. WHITE, and M. I. ALEEM (1969). Phospholipid metabolism in *Ferrobacillus ferrooxidans*. *Journal of Bacteriology* **99** (1), 142–150.

SIMON, J. (2002). Enzymology and bioenergetics of respiratory nitrite ammonification. *FEMS Microbiology Reviews* **26** (3), 285–309. DOI: 10.1111/j.1574-6976.2002.tb00616.x.

SIMON, M. and F. AZAM (1989). Protein content and protein synthesis rates of planktonic marine bacteria. *Marine Ecology Progress Series* **51**, 201–213.

SIMONS, K. and E. IKONEN (1997). Functional rafts in cell membranes. *Nature* **387** (6633), 569–572. DOI: 10.1038/42408.

SINGER, S. J. and G. L. NICOLSON (1972). The fluid mosaic model of the structure of cell membranes. *Science* **175** (23), 720–731. DOI: 10.1126/science.175.4023.720.

SINNINGHE DAMSTÉ, J. S., S. G. WAKEHAM, M. E. KOHNEN, J. M. HAYES, and J. W. DE LEEUW (1993). A 6,000-year sedimentary molecular record of chemocline excursions in the Black Sea. *Nature* **362** (6423), 827–829. DOI: 10.1038/362827a0.

SINNINGHE DAMSTÉ, J. S., E. C. HOPMANS, R. D. PANCOST, S. SCHOUTEN, and J. A. J. GEENEVASEN (2000). Newly discovered non-isoprenoid glycerol dialkyl glycerol tetraether lipids in sediments. *Chemical Communications* (17), 1683–1684. DOI: 10.1039/b004517i.

SINNINGHE DAMSTÉ, J. S., W. I. C. RIJPSTRA, E. C. HOPMANS, M.-Y. JUNG, J.-G. KIM, S.-K. RHEE, M. STIEGLMEIER, and C. SCHLEPER (2012). Intact polar and core glycerol dibiphytanyl glycerol tetraether lipids of group I.1a and I.1b *Thaumarchaeota* in soil. *Applied and Environmental Microbiology* **78** (19), 6866–6874. DOI: 10.1128/AEM.01681-12.

SINNINGHE DAMSTÉ, J. S., W. I. C. RIJPSTRA, E. C. HOPMANS, F. G. PRAHL, S. G. WAKEHAM, and S. SCHOUTEN (2002a). Distribution of membrane lipids of planktonic *Crenarchaeota* in the Arabian Sea. *Applied and Environmental Microbiology* **68** (6), 2997–3002. DOI: 10.1128/AEM.68.6.2997-3002.2002.

SINNINGHE DAMSTÉ, J. S., W. I. C. RIJPSTRA, E. C. HOPMANS, S. SCHOUTEN, M. BALK, and A. J. M. STAMS (2007). Structural characterization of diabolic acid-based tetraester, tetraether and mixed ether/ester, membrane-spanning lipids of bacteria from the order *Thermotogales*. *Archives of Microbiology* **188** (6), 629–641. DOI: 10.1007/s00203-007-0284-z.

SINNINGHE DAMSTÉ, J. S., S. SCHOUTEN, E. C. HOPMANS, A. C. T. VAN DUIN, and J. A. J. GEENEVASEN (2002b). Crenarchaeol: the characteristic core glycerol dibiphytanyl glycerol tetraether membrane lipid of cosmopolitan pelagic crenarchaeota. *The Journal of Lipid Research* **43** (10), 1641–1651. DOI: 10.1194/jlr.M200148-JLR200.

SINTES, E., K. BERGAUER, D. DE CORTE, T. YOKOKAWA, and G. J. HERNDL (2013). Archaeal *amoA* gene diversity points to distinct biogeography of ammonia-oxidizing *Crenarchaeota* in the ocean. *Environmental Microbiology* **15** (5), 1647–1658. DOI: 10.1111/j.1462-2920.2012.02801.x.

SITTIG, M. and H. SCHLESNER (1993). Chemotaxonomic Investigation of Various Prosthecate and/or Budding Bacteria. *Systematic and Applied Microbiology* **16** (1), 92–103. DOI: 10.1016/S0723-2020(11)80253-5.

SØRENSEN, K. B. and A. TESKE (2006). Stratified communities of active Archaea in deep marine subsurface sediments. *Applied and Environmental Microbiology* **72** (7), 4596–4603. DOI: 10.1128/AEM.00562-06.

SØRENSEN, P. G., R. P. COX, and M. MILLER (2008). Chlorosome lipids from *Chlorobium tepidum*: Characterization and quantification of polar lipids and wax esters. *Photosynthesis Research* **95** (2-3), 191–196. DOI: 10.1007/s11120-007-9242-5.

SOROKIN, Y. I. (2002). *The Black Sea: Ecology and Oceanography*. Leiden, The Netherlands: Backhuys Publishers, p. 875.

SOROKIN, Y. I., P. Y. SOROKIN, V. A. AVDEEV, D. Y. SOROKIN, and S. V. ILCHENKO (1995). Biomass, production and activity of bacteria in the Black Sea, with special reference to chemosynthesis and the sulfur cycle. *Hydrobiologia* **308**, 61–76. DOI: 10.1007/BF00037788.

SOUSA, F. L., T. THIERGART, G. LANDAN, S. NELSON-SATHI, I. A. C. PEREIRA, J. F. ALLEN, N. LANE, and W. F. MARTIN (2013). Early bioenergetic evolution. *Philosophical Transactions of the Royal Society of London. Series B, Biological Sciences* **368** (1622), 20130088. DOI: 10.1098/rstb.2013.0088.

SPANG, A., R. HATZENPICHLER, C. BROCHIER-ARMANET, T. RATTEI, P. TISCHLER, E. SPIECK, W. STREIT, D. A. STAHL, M. WAGNER, and C. SCHLEPER (2010). Distinct gene set in two different lineages of ammonia-oxidizing archaea supports the phylum Thaumarchaeota. *Trends in Microbiology* **18** (8), 331–340. DOI: 10.1016/j.tim.2010.06.003.

SPIECK, E. and A. LIPSKI (2010). Cultivation, growth physiology, and chemotaxonomy of nitrite-oxidizing bacteria. In: *Methods in Enzymology*. Ed. by M. G. Klotz. Vol. 486. San Diego, USA: Academic Press, pp. 109–130. DOI: 10.1016/B978-0-12-381294-0.00005-5.

SPROTT, G. D., B. J. AGNEW, and G. B. PATEL (1997). Structural features of ether lipids in the archaeobacterial thermophiles *Pyrococcus furiosus*, *Methanopyrus kandleri*, *Methanothermus fervidus*, and *Sulfolobus acidocaldarius*. en. *Canadian Journal of Microbiology* **43** (5), 467–476. DOI: 10.1139/m97-066.

SPROTT, G. D., I. EKIEL, and C. DICAIRE (1990). Novel, acid-labile, hydroxydiether lipid cores in methanogenic bacteria. *The Journal of Biological Chemistry* **265** (23), 13735–13740.

STAHL, D. A. and J. R. DE LA TORRE (2012). Physiology and Diversity of Ammonia-Oxidizing Archaea. *Annual Review of Microbiology* **66** (1), 83–101. DOI: 10.1146/annurev-micro-092611-150128.

STAMS, A. J. M. and C. M. PLUGGE (2009). Electron transfer in syntrophic communities of anaerobic bacteria and archaea. *Nature Reviews Microbiology* **7** (8), 568–577. DOI: 10.1038/nrmicro2166.

STETTER, K. O., G. FIALA, G. HUBER, R. HUBER, and A. SEGERER (1990). Hyperthermophilic microorganisms. *FEMS Microbiology Reviews* **75**, 117–124. DOI: 10.1111/j.1574-6968.1990.tb04089.x.

STEWART, F. J., O. ULLOA, and E. F. DELONG (2012). Microbial metatranscriptomics in a permanent marine oxygen minimum zone. *Environmental Microbiology* **14** (1), 23–40. DOI: 10.1111/j.1462-2920.2010.02400.x.

STICKLAND, J. D. H. and T. R. A. PARSONS (1972). *A Practical Handbook of Seawater Analysis*. Ottawa: Fisheries Research Board of Canada.

STIEGLMEIER, M., R. J. E. ALVES, and C. SCHLEPER (2014a). The Phylum Thaumarchaeota. In: *The Prokaryotes, Other Major Lineages of Bacteria and The Archaea*. Ed. by E. Rosenberg, E. F. DeLong, S. Lory, E. Stackebrandt, and F. Thompson. Berlin, Germany: Springer, pp. 347–362. DOI: 10.1007/978-3-642-30194-0.

STIEGLMEIER, M., A. KLINGL, R. J. E. ALVES, S. K.-M. R. RITTMANN, M. MELCHER, N. LEISCH, and C. SCHLEPER (2014b). *Nitrososphaera viennensis* gen. nov., sp. nov., an aerobic and mesophilic, ammonia-oxidizing archaeon from soil and a member of the archaeal phylum *Thaumarchaeota*. *International Journal of Systematic and Evolutionary Microbiology* **64**, 2738–2752. DOI: 10.1099/ijs.0.063172-0.

STIEHL, T., J. RULLKÖTTER, and A. NISSENBAUM (2005). Molecular and isotopic characterization of lipids in cultured halophilic microorganisms from the Dead Sea and comparison with the sediment record of this hypersaline lake. *Organic Geochemistry* **36** (9), 1242–1251. DOI: 10.1016/j.orggeochem.2005.05.002.

STROUS, M., J. A. FUERST, E. H. KRAMER, S. LOGEMANN, G. MUYZER, K. T. VAN DE PAS-SCHOONEN, R. WEBB, J. G. KUENEN, and M. S. JETTEN (1999). Missing lithotroph identified as new planctomycete. *Nature* **400** (6743), 446–449. DOI: 10.1038/22749.

STURT, H. F., R. E. SUMMONS, K. SMITH, M. ELVERT, and K.-U. HINRICHS (2004). Intact polar membrane lipids in prokaryotes and sediments deciphered by high-performance liquid chromatography/electrospray ionization multistage mass spectrometry - new biomarkers for biogeochemistry and microbial ecology. *Rapid Communications in Mass Spectrometry* **18** (6), 617–628. DOI: 10.1002/rcm.1378.

SUZUMURA, M. (2005). Phospholipids in marine environments: A review. *Talanta* **66** (2 SPEC. ISS.), 422–434. DOI: 10.1016/j.talanta.2004.12.008.

TAKAI, K. E. N., D. P. MOSER, M. D. E. FLAUN, T. C. ONSTOTT, and J. K. FREDRICKSON (2001). Archaeal Diversity in Waters from Deep South African Gold Mines. *Applied and Environmental Microbiology* **67** (12), 5750–5760. DOI: 10.1128/AEM.67.21.5750.

TAKAI, K., K. NAKAMURA, T. TOKI, U. TSUNOGAI, M. MIYAZAKI, J. MIYAZAKI, H. HIRAYAMA, S. NAKAGAWA, T. NUNOURA, and K. HORIKOSHI (2008). Cell proliferation at 122Â°C and isotopically heavy CH_4 production by a hyperthermophilic methanogen under high-pressure cultivation. *Proceedings of the National Academy of Sciences of the United States of America* **105** (31), 10949–10954. DOI: 10.1073/pnas.0712334105.

TARUI, M., N. TANAKA, K. TOMURA, M. OHGA, H. MORII, and Y. KOGA (2007). Lipid component parts analysis of the hyperthermophilic sulfate-reducing archaeon *Archaeoglobus fulgidus*. *Journal of UOEH* **29** (2), 131–139.

TAYLOR, K. W. R., M. HUBER, C. J. HOLLIS, M. T. HERNANDEZ-SANCHEZ, and R. D. PANCOST (2013). Re-evaluating modern and Palaeogene GDGT distributions: Implications for SST reconstructions. *Global and Planetary Change* **108**, 158–174. DOI: 10.1016/j.gloplacha.2013.06.011.

TEBO, B. M. (1991). Manganese(II) oxidation in the suboxic zone of the Black Sea. *Deep Sea Research Part A. Oceanographic Research Papers* **38** (1), S883–S905. DOI: 10.1016/S0198-0149(10)80015-9.

TEIRA, E., P. LEBARON, H. V. AKEN, and G. J. HERNDL (2006). Distribution and activity of Bacteria and Archaea in the deep water masses of the North Atlantic. *Limnology and Oceanography* **51** (5), 2131–2144. DOI: 10.4319/lo.2006.51.5.2131.

TEIRA, E., T. REINTHALER, A. PERNTHALER, J. PERNTHALER, and G. J. HERNDL (2004). Combining catalyzed reporter deposition-fluorescence in situ hybridization and microautoradiography to detect substrate utilization by bacteria and Archaea in the deep ocean. *Applied and Environmental Microbiology* **70** (7), 4411–4414. DOI: 10.1128/AEM.70.7.4411-4414.2004.

TEIXIDOR, P., J. O. GRIMALT, J. J. PUEYO, and F. RODRIGUEZ-VALERA (1993). Isopranylglycerol diethers in non-alkaline evaporitic environments. *Geochimica et Cosmochimica Acta* **57** (18), 4479–4489. DOI: 10.1016/0016-7037(93)90497-K.

TENCHOV, B., E. M. VESCIO, G. D. SPROTT, M. L. ZEIDEL, and J. C. MATHAI (2006). Salt tolerance of archaeal extremely halophilic lipid membranes. *The Journal of Biological Chemistry* **281** (15), 10016–10023. DOI: 10.1074/jbc.M600369200.

TESKE, A. and K. B. SØRENSEN (2008). Uncultured archaea in deep marine subsurface sediments: have we caught them all? *The ISME journal* **2** (1), 3–18. DOI: 10.1038/ismej.2007.90.

THAMDRUP, B. (2012). New Pathways and Processes in the Global Nitrogen Cycle. *Annual Review of Ecology, Evolution, and Systematics* **43** (1), 407–428. DOI: 10.1146/annurev-ecolsys-102710-145048.

THAUER, R. K., A.-K. KASTER, H. SEEDORF, W. BUCKEL, and R. HEDDERICH (2008). Methanogenic archaea: ecologically relevant differences in energy conservation. *Nature Reviews Microbiology* **6** (8), 579–591. DOI: 10.1038/nrmicro1931.

THURL, S., W. WITKE, I. BUHROW, and W. SCHÄFER (1986). Different types of quinones from sulphur-dependent archaebacteria. *Biological Chemistry Hoppe-Seyler* **367** (3), 191–197. DOI: 10.1515/bchm3.1986.367.1.191.

THURL, S. and W. SCHÄFER (1988). Lipids from the sulphur-dependent archaebacterium *Thermoproteus tenax*. *Biochimica et Biophysica Acta* **961** (2), 253–261. DOI: 10.1016/0005-2760(88)90120-8.

THURL, S., I. BUHROW, and W. SCHÄFER (1985). New types of menaquinones from the thermophilic archaebacterium *Thermoproteus tenax*. *Biological Chemistry Hoppe-Seyler* **366** (2), 1079–1084. DOI: 10.1515/bchm3.1985.366.2.1079.

TIERNEY, J. E. and M. P. TINGLEY (2014). A Bayesian, spatially-varying calibration model for the TEX_{86} proxy. *Geochimica et Cosmochimica Acta* **127**, 83–106. DOI: 10.1016/j.gca.2013.11.026.

TIETZE, M., A. BEUCHLE, I. LAMLA, N. ORTH, M. DEHLER, G. GREINER, and U. BEIFUSS (2003). Redox potentials of methanophenazine and CoB-S-S-CoM, factors involved in electron transport in Methanogenic archaea. *Chembiochem* **4** (4), 333–335. DOI: 10.1002/cbic.200390053.

TINDALL, B. J., K. O. STETTER, and M. D. COLLINS (1989). A novel, fully saturated menaquinone from the thermophilic, sulphate-reducing archaebacterium *Archaeoglobus fulgidus*. *Microbiology* **135** (3), 693–696. DOI: 10.1099/00221287-135-3-693.

TINDALL, B. J., V. WRAY, R. HUBER, and M. D. COLLINS (1991). A novel, fully saturated cyclic menaquinone in the archaebacterium *Pyrobaculum organotrophum*. *Systematic and Applied Microbiology* **14** (3), 218–221. DOI: 10.1016/S0723-2020(11)80371-1.

TORNABENE, T. G., T. A. LANGWORTHY, G. HOLZER, and J. ORÓ (1979). Squalenes, phytanes and other isoprenoids as major neutral lipids of methanogenic and thermoacidophilic "archaebacteria". *Journal of Molecular Evolution* **13** (1), 73–83. DOI: 10.1007/BF01732755.

TOURNA, M., M. STIEGLMEIER, A. SPANG, M. KÖNNEKE, A. SCHINTLMEISTER, T. URICH, M. ENGEL, M. SCHLOTER, M. WAGNER, A. RICHTER, and C. SCHLEPER (2011). *Nitrososphaera viennensis*, an ammonia oxidizing archaeon from soil. *Proceedings of the National Academy of Sciences of the United States of America* **108** (20), 8420–8425. DOI: 10.1073/pnas.1013488108.

TREUSCH, A. H., S. LEININGER, A. KLETZIN, S. C. SCHUSTER, H.-P. KLENK, and C. SCHLEPER (2005). Novel genes for nitrite reductase and Amo-related proteins indicate a role of uncultivated mesophilic crenarchaeota in nitrogen cycling. *Environmental Microbiology* **7** (12), 1985–1995. DOI: 10.1111/j.1462-2920.2005.00906.x.

TRINCONE, A., V. LANZOTTI, B. NICOLAUS, W. ZILLIG, M. DE ROSA, and A. GAMBACORTA (1989). Comparative Lipid Composition of Aerobically and Anaerobically Grown *Desulfurolobus ambivalens*, an Autotrophic Thermophilic Archaeobacterium. *Microbiology* **135** (10), 2751–2757. DOI: 10.1099/00221287-135-10-2751.

TRINCONE, A., B. NICOLAUS, G. PALMIERI, M. DE ROSA, R. HUBER, G. HUBER, K. O. STETTER, and A. GAMBACORTA (1992). Distribution of complex and core lipids within new hyperthermophilic members of the *Archaea* domain. *Systematic and Applied Microbiology* **15** (1), 11–17. DOI: 10.1016/S0723-2020(11)80130-X.

TROMMER, G., M. SICCHA, M. T. J. VAN DER MEER, S. SCHOUTEN, J. S. SINNINGHE DAMSTÉ, H. SCHULZ, C. HEMLEBEN, and M. KUCERA (2009). Distribution of Crenarchaeota tetraether membrane lipids in surface sediments from the Red Sea. *Organic Geochemistry* **40** (6), 724–731. DOI: 10.1016/j.orggeochem.2009.03.001.

TULLY, B. J., W. C. NELSON, and J. F. HEIDELBERG (2012). Metagenomic analysis of a complex marine planktonic thaumarchaeal community from the Gulf of Maine. *Environmental Microbiology* **14** (1), 254–267. DOI: 10.1111/j.1462-2920.2011.02628.x.

TURICH, C., K. H. FREEMAN, M. A. BRUNS, M. CONTE, A. D. JONES, and S. G. WAKEHAM (2007). Lipids of marine Archaea: Patterns and provenance in the water-column and sediments. *Geochimica et Cosmochimica Acta* **71** (13), 3272–3291. DOI: 10.1016/j.gca.2007.04.013.

TURICH, C., S. SCHOUTEN, R. C. THUNELL, R. VARELA, Y. ASTOR, and S. G. WAKEHAM (2013). Comparison of TEX_{86} and temperature proxies in sinking particles in the Cariaco Basin. *Deep Sea Research Part I: Oceanographic Research Papers* **78**, 115–133. DOI: 10.1016/j.dsr.2013.02.008.

UDA, I., A. SUGAI, Y. H. ITOH, and T. ITOH (2001). Variation in molecular species of polar lipids from Thermoplasma acidophilum depends on growth temperature. *Lipids* **36** (1), 103–105. DOI: 10.1007/s11745-001-0914-2.

UDA, I., A. SUGAI, Y. H. ITOH, and T. ITOH (2004). Variation in molecular species of core lipids from the order Thermoplasmales strains depends on the growth temperature. *Journal of Oleo Science* **53** (8), 399–404.

ULLOA, O., D. E. CANFIELD, E. F. DELONG, R. M. LETELIER, and F. J. STEWART (2012). Microbial oceanography of anoxic oxygen minimum zones. *Proceedings of the National Academy of Sciences of the United States of America* **109** (40), 15996–16003. DOI: 10.1073/pnas.1205009109.

ULLOA, O., J. J. WRIGHT, L. BELMAR, and S. J. HALLAM (2013). Pelagic Oxygen Minimum Zone Microbial Communities. In: *The Prokaryotes. Prokaryotic Communities and Ecophysiology*. Ed. by E. Rosenberg, E. F. Delong, S. Lory, E. Stackebrandt, and F. Thompson. Berlin, Germany: Springer, pp. 113–122. DOI: 10.1007/978-3-642-30123-0_45.

ULRIH, N. P., D. GMAJNER, and P. RASPOR (2009). Structural and physicochemical properties of polar lipids from thermophilic archaea. *Applied Microbiology and Biotechnology* **84** (2), 249–260. DOI: 10.1007/s00253-009-2102-9.

URAKAWA, H., T. YOSHIDA, M. NISHIMURA, and K. OHWADA (2000). Characterization of depth-related population variation in microbial communities of a coastal marine sediment using 16S rDNA-based approaches and quinone profiling. *Environmental Microbiology* **2** (5), 542–554. DOI: 10.1046/j.1462-2920.2000.00137.x.

URAKAWA, H., T. YOSHIDA, M. NISHIMURA, and K. OHWADA (2001). Characterization of microbial communities in marine surface sediments by terminal-restriction fragment length polymorphism (T-RFLP) analysis and quinone profiling. *Marine Ecology Progress Series* **220**, 47–57. DOI: 10.3354/meps220047.

URAKAWA, H., T. YOSHIDA, M. NISHIMURA, and K. OHWADA (2005). Characterization of depth-related changes and site-specific differences of microbial communities in marine sediments using quinone profiles. *Fisheries Science* **71** (1), 174–182. DOI: 10.1111/j.1444-2906.2005.00945.x.

VAJRALA, N., W. MARTENS-HABBENA, L. A. SAYAVEDRA-SOTO, A. SCHAUER, P. J. BOTTOMLEY, D. A. STAHL, and D. J. ARP (2013). Hydroxylamine as an intermediate in ammonia oxidation by globally abundant marine archaea. *Proceedings of the National Academy of Sciences of the United States of America* **110** (3), 1006–1011. DOI: 10.1073/pnas.1214272110.

VALENTINE, D. L. (2007). Adaptations to energy stress dictate the ecology and evolution of the Archaea. *Nature Reviews Microbiology* **5** (4), 316–323. DOI: 10.1038/nrmicro1619.

VAN DE VOSSENBERG, J. L. C. M., A. J. M. DRIESSEN, and W. N. KONINGS (1998). The essence of being extremophilic: the role of the unique archaeal membrane lipids. *Extremophiles* **2** (3), 163–170. DOI: 10.1007/s007920050056.

VAN DEN DOOL, H. and P. D. KRATZ (1963). A generalization of the retention index system including linear temperature programmed gas-liquid partition chromatography. *Journal of Chromatography A* **11**, 463–471. DOI: 10.1016/S0021-9673(01)80947-X.

VAN MOOY, B. A. S. and H. F. FREDRICKS (2010). Bacterial and eukaryotic intact polar lipids in the eastern subtropical South Pacific: Water-column distribution, planktonic sources, and fatty acid composition. *Geochimica et Cosmochimica Acta* **74** (22), 6499–6516. DOI: 10.1016/j.gca.2010.08.026.

VAN MOOY, B. A. S., H. F. FREDRICKS, B. E. PEDLER, S. T. DYHRMAN, D. M. KARL, M. KOBLÍZEK, M. W. LOMAS, T. J. MINCER, L. R. MOORE, T. MOUTIN, M. S. RAPPÉ, and E. A. WEBB (2009). Phytoplankton in the ocean use non-phosphorus lipids in response to phosphorus scarcity. *Nature* **458** (7234), 69–72. DOI: 10.1038/nature07659.

VAN VLEET, E. S. and J. G. QUINN (1979). Early diagenesis of fatty acids and isoprenoid alcohols in estuarine and coastal sediments. *Geochimica et Cosmochimica Acta* **43** (3), 289–303. DOI: 10.1016/0016-7037(79)90195-9.

VAN MEER, G., D. R. VOELKER, and G. W. FEIGENSON (2008). Membrane lipids: where they are and how they behave. *Nature Reviews Molecular Cell Biology* **9** (2), 112–124. DOI: 10.1038/nrm2330.

VENTER, J. C., K. REMINGTON, J. F. HEIDELBERG, A. L. HALPERN, D. RUSCH, J. A. EISEN, D. WU, I. PAULSEN, K. E. NELSON, W. NELSON, D. E. FOUTS, S. LEVY, A. H. KNAP, M. W. LOMAS, K. NEALSON, O. WHITE, J. PETERSON, J. HOFFMAN, R. PARSONS, H. BADEN-TILLSON, C. PFANNKOCH, Y.-H. ROGERS, and H. O. SMITH (2004). Environmental genome shotgun sequencing of the Sargasso Sea. *Science* **304** (5667), 66–74. DOI: 10.1126/science.1093857.

VETRIANI, C., H. V. TRAN, and L. J. KERKHOF (2003). Fingerprinting microbial assemblages from the oxic/anoxic chemocline of the Black Sea. *Applied and Environmental Microbiology* **69** (11), 6481–6488. DOI: 10.1128/AEM.69.11.6481.

VILLANUEVA, L., J. DEL CAMPO, R. GUERRERO, and R. GEYER (2010). Intact phospholipid and quinone biomarkers to assess microbial diversity and redox state in microbial mats. *Microbial Ecology* **60** (1), 226–238. DOI: 10.1007/s00248-010-9645-2.

VILLANUEVA, L., S. SCHOUTEN, and J. S. SINNINGHE DAMSTÉ (2014a). Depth-related distribution of a key gene of the tetraether lipid biosynthetic pathway in marine Thaumarchaeota. *Environmental Microbiology*. DOI: 10.1111/1462-2920.12508.

VILLANUEVA, L., J. S. SINNINGHE DAMSTÉ, and S. SCHOUTEN (2014b). A re-evaluation of the archaeal membrane lipid biosynthetic pathway. *Nature Reviews Microbiology* **12** (6), 438–448. DOI: 10.1038/nrmicro3260.

VÖLKL, P., R. HUBER, E. DROBNER, R. RACHEL, S. BURGGRAF, A. TRINCONE, and K. O. STETTER (1993). *Pyrobaculum aerophilum* sp. nov., a novel nitrate-reducing hyperthermophilic archaeum. *Applied and Environmental Microbiology* **59** (9), 2918–2926.

WAGNER, G. C., R. J. KASSNER, and M. D. KAMEN (1974). Redox Potentials of Certain Vitamins K: Implications for a Role in Sulfite Reduction by Obligately Anaerobic Bacteria. *Proceedings of the National Academy of Sciences of the United States of America* **71** (2), 253–256. DOI: 10.1073/pnas.71.2.253.

WAKEHAM, S. G., R. AMANN, K. H. FREEMAN, E. C. HOPMANS, B. B. JØRGENSEN, I. F. PUTNAM, S. SCHOUTEN, J. S. SINNINGHE DAMSTÉ, H. M. TALBOT, and D. WOEBKEN (2007). Microbial ecology of the stratified water column of the Black Sea as revealed by a comprehensive biomarker study. *Organic Geochemistry* **38** (12), 2070–2097. DOI: 10.1016/j.orggeochem.2007.08.003.

WAKEHAM, S. G., C. TURICH, F. SCHUBOTZ, A. PODLASKA, X. N. LI, R. VARELA, Y. ASTOR, J. P. SÁENZ, D. RUSH, J. S. SINNINGHE DAMSTÉ, R. E. SUMMONS, M. I. SCRANTON, G. T. TAYLOR, and K.-U. HINRICHS (2012). Biomarkers, chemistry and microbiology show chemoautotrophy in a multilayer chemocline in the Cariaco Basin. *Deep Sea Research Part I: Oceanographic Research Papers* **63**, 133–156. DOI: 10.1016/j.dsr.2012.01.005.

WALKER, C. B., J. R. DE LA TORRE, M. G. KLOTZ, H. URAKAWA, N. PINEL, D. J. ARP, C. BROCHIER-ARMANET, P. S. G. CHAIN, P. P. CHAN, A. GOLLABGIR, J. HEMP, M. HÜGLER, E. A. KARR, M. KÖNNEKE, M. SHIN, T. J. LAWTON, T. LOWE, W. MARTENS-HABBENA, L. A. SAYAVEDRA-SOTO, D. LANG, S. M. SIEVERT, A. C. ROSENZWEIG, G. MANNING, and D. A. STAHL (2010). *Nitrosopumilus maritimus* genome reveals unique mechanisms for nitrification and autotrophy in globally distributed marine crenarchaea. *Proceedings of the National Academy of Sciences of the United States of America* **107** (19), 8818–8823. DOI: 10.1073/pnas.0913533107.

WARD, B. B., A. H. DEVOL, J. J. RICH, B. X. CHANG, S. E. BULOW, H. NAIK, A. PRATIHARY, and A. JAYAKUMAR (2009). Denitrification as the dominant nitrogen loss process in the Arabian Sea. *Nature* **461** (7260), 78–81. DOI: 10.1038/nature08276.

WARD, N., J. T. STALEY, J. A. FUERST, S. GIOVANNONI, and E. SCHLESNER, H. STACKEBRANDT (2006). The order Planctomycetales, including the genera Planctomyces, Pirellula, Gemmata and Isosphaera and the Candidatus genera Brocadia, Kuenenia and Scalindua. In: *The*

Prokaryotes, Volume 3: Archaea. Bacteria: Firmicutes, Actinomycetes. Ed. by M. Dworkin, S. Falkow, E. Rosenberg, K.-H. Schleifer, and E. Stackebrandt. New York, USA: Springer, pp. 757–793.

WEBER, E. B., L. E. LEHTOVIRTA-MORLEY, J. I. PROSSER, and C. GUBRY-RANGIN (2015). Ammonia oxidation is not required for growth of Group 1.1c soil Thaumarchaeota. *FEMS Microbiology Ecology* **91** (3). DOI: 10.1093/femsec/fiv001.

WEI, Y., J. WANG, J. LIU, L. DONG, L. LI, H. WANG, P. WANG, M. ZHAO, and C. L. ZHANG (2011). Spatial variations in archaeal lipids of surface water and core-top sediments in the South china sea and their implications for paleoclimate studies. *Applied and Environmental Microbiology* **77** (21), 7479–7489. DOI: 10.1128/AEM.00580-11.

WHITE, D. C., W. M. DAVIS, J. S. NICKELS, J. D. KING, and R. J. BOBBIE (1979). Determination of the sedimentary microbial biomass by extractible lipid phosphate. *Oecologia* **40** (1), 51–62. DOI: 10.1007/BF00388810.

WHITICAR, M. J., E. FABER, and M. SCHOELL (1986). Biogenic methane formation in marine and freshwater environments: CO_2 reduction vs. acetate fermentation–Isotope evidence. *Geochimica et Cosmochimica Acta* **50** (5), 693–709. DOI: 10.1016/0016-7037(86)90346-7.

WHITICAR, M. J. (1999). Carbon and hydrogen isotope systematics of bacterial formation and oxidation of methane. *Chemical Geology* **161** (1-3), 291–314. DOI: 10.1016/S0009-2541(99)00092-3.

WHITMAN, W. B., D. C. COLEMAN, and W. J. WIEBE (1998). Prokaryotes: the unseen majority. *Proceedings of the National Academy of Sciences of the United States of America* **95** (12), 6578–6583. DOI: 10.1073/pnas.95.12.6578.

WHITTAKER, M., D. BERGMANN, D. ARCIERO, and A. B. HOOPER (2000). Electron transfer during the oxidation of ammonia by the chemolithotrophic bacterium *Nitrosomonas europaea*. *Biochimica et Biophysica Acta* **1459** (2-3), 346–355. DOI: 10.1016/S0005-2728(00)00171-7.

WIDDEL, F. and F. BAK (1992). Gram-negative mesophilic sulfate-reducing bacteria. In: *The Prokaryotes. A Handbook on the Biology of Bacteria: Ecophysiology, Isolation, Identification, Application*. Ed. by A. Ballows, H. G. Trüper, M. Dworkin, W. Harder, and K.-H. Schleifer. 2nd ed. New York: Springer, pp. 3352–3378.

WILLIAMS, T. A., P. G. FOSTER, C. J. COX, and T. M. EMBLEY (2013). An archaeal origin of eukaryotes supports only two primary domains of life. *Nature* **504** (7479), 231–236. DOI: 10.1038/nature12779.

WINOGRADSKY, S. (1890). Recherches sur les Organismes des la Nitrification (Parts 1-3). *Annales de l'Institut Pasteur* **4**, 213–311.

WINOGRADSKY, S. (1891). Recherches sur les Organismes des la Nitrification (Parts 4-5). *Annales de l'Institut Pasteur* **5**, 92–100.

WISSENBACH, U., A. KRÖGER, and G. UNDEN (1990). The specific functions of menaquinone and demethylmenaquinone in anaerobic respiration with fumarate, dimethylsulfoxide, trimethylamine N-oxide and nitrate by *Escherichia coli*. *Archives of Microbiology* **154** (1), 60–66. DOI: 10.1007/BF00249179.

WOEBKEN, D., B. M. FUCHS, M. M. M. KUYPERS, and R. AMANN (2007). Potential interactions of particle-associated anammox bacteria with bacterial and archaeal partners in the Namibian upwelling system. *Applied and Environmental Microbiology* **73** (14), 4648–57. DOI: 10.1128/AEM.02774-06.

WOESE, C. R. and G. E. FOX (1977). Phylogenetic structure of the prokaryotic domain: the primary kingdoms. *Proceedings of the National Academy of Sciences of the United States of America* **74** (11), 5088–5090. DOI: 10.1073/pnas.74.11.5088.

WOESE, C. R., O. KANDLER, and M. L. WHEELIS (1990). Towards a natural system of organisms: proposal for the domains Archaea, Bacteria, and Eucarya. *Proceedings of the National Academy*

of Sciences of the United States of America **87** (12), 4576–4579. DOI: 10.1073/pnas.87.12.4576.

WOESE, C. R., L. J. MAGRUM, and G. E. FOX (1978). Archaebacteria. *Journal of Molecular Evolution* **11** (3), 245–252. DOI: 10.1007/BF01734485.

WÖRMER, L., J. S. LIPP, J. M. SCHRÖDER, and K.-U. HINRICHS (2013). Application of two new LC–ESI–MS methods for improved detection of intact polar lipids (IPLs) in environmental samples. *Organic Geochemistry* **59**, 10–21. DOI: 10.1016/j.orggeochem.2013.03.004.

WUCHTER, C. (2006). "Ecology and membrane lipid distribution of marine Crenarchaeota: Implications for TEX_{86} paleothermometry". PhD Thesis. University of Utrecht, The Netherlands.

WUCHTER, C., B. ABBAS, M. J. L. COOLEN, L. HERFORT, J. VAN BLEIJSWIJK, P. TIMMERS, M. STROUS, E. TEIRA, G. J. HERNDL, J. J. MIDDELBURG, S. SCHOUTEN, and J. S. SINNINGHE DAMSTÉ (2006). Archaeal nitrification in the ocean. *Proceedings of the National Academy of Sciences of the United States of America* **103** (33), 12317–12322. DOI: 10.1073/pnas.0600756103.

WUCHTER, C., S. SCHOUTEN, H. T. S. BOSCHKER, and J. S. SINNINGHE DAMSTÉ (2003). Bicarbonate uptake by marine Crenarchaeota. *FEMS Microbiology Letters* **219** (2), 203–207. DOI: 10.1016/S0378-1097(03)00060-0.

WUCHTER, C., S. SCHOUTEN, M. J. L. COOLEN, and J. S. SINNINGHE DAMSTÉ (2004). Temperature-dependent variation in the distribution of tetraether membrane lipids of marine Crenarchaeota: Implications for TEX_{86} paleothermometry. *Paleoceanography* **19** (4), PA4028. DOI: 10.1029/2004PA001041.

WUCHTER, C., S. SCHOUTEN, S. G. WAKEHAM, and J. S. SINNINGHE DAMSTÉ (2005). Temporal and spatial variation in tetraether membrane lipids of marine Crenarchaeota in particulate organic matter: implications for TEX_{86} paleothermometry. *Paleoceanography* **20**, PA3013. DOI: 10.1029/2004PA001110.

XIE, S., J. S. LIPP, G. WEGENER, T. G. FERDELMAN, and K.-U. HINRICHS (2013). Turnover of microbial lipids in the deep biosphere and growth of benthic archaeal populations. *Proceedings of the National Academy of Sciences of the United States of America* **110** (15), 6010–6014. DOI: 10.1073/pnas.1218569110.

XIE, S., X.-L. LIU, F. SCHUBOTZ, S. G. WAKEHAM, and K.-U. HINRICHS (2014). Distribution of glycerol ether lipids in the oxygen minimum zone of the Eastern Tropical North Pacific Ocean. *Organic Geochemistry* **71**, 60–71. DOI: 10.1016/j.orggeochem.2014.04.006.

YAKIMOV, M. M., V. LA CONO, F. SMEDILE, T. H. DELUCA, S. JUÁREZ, S. CIORDIA, M. FERNÁNDEZ, J. P. ALBAR, M. FERRER, P. N. GOLYSHIN, and L. GIULIANO (2011). Contribution of crenarchaeal autotrophic ammonia oxidizers to the dark primary production in Tyrrhenian deep waters (Central Mediterranean Sea). *The ISME Journal* **5** (6), 945–961. DOI: 10.1038/ismej.2010.197.

YAMAUCHI, K., K. DOI, Y. YOSHIDA, and M. KINOSHITA (1993). Archaebacterial lipids: highly proton-impermeable membranes from 1,2-diphytanyl-sn-glycero-3-phosphocoline. *Biochimica et Biophysica Acta* **1146** (2), 178–182. DOI: 10.1016/0005-2736(93)90353-2.

YAN, J., S. C. M. HAAIJER, H. J. M. OP DEN CAMP, L. VAN NIFTRIK, D. A. STAHL, M. KÖNNEKE, D. RUSH, J. S. SINNINGHE DAMSTÉ, Y. Y. HU, and M. S. M. JETTEN (2012). Mimicking the oxygen minimum zones: stimulating interaction of aerobic archaeal and anaerobic bacterial ammonia oxidizers in a laboratory-scale model system. *Environmental Microbiology* **14**, 3146–3158. DOI: 10.1111/j.1462-2920.2012.02894.x.

YANG, H., R. D. PANCOST, C. TANG, W. DING, X. DANG, and S. XIE (2014). Distributions of isoprenoid and branched glycerol dialkanol diethers in Chinese surface soils and a loess–paleosol sequence: Implications for the degradation of tetraether lipids. *Organic Geochemistry* **66**, 70–79. DOI: 10.1016/j.orggeochem.2013.11.003.

YOOL, A., A. P. MARTIN, C. FERNÁNDEZ, and D. R. CLARK (2007). The significance of nitrification for oceanic new production. *Nature* **447** (7147), 999–1002. DOI: 10.1038/nature05885.

YOSHINAGA, M. Y., E. J. GAGEN, L. WÖRMER, N. K. BRODA, T. B. MEADOR, J. WENDT, M. THOMM, and K.-U. HINRICHS (2015). *Methanothermobacter thermautotrophicus* modulates its membrane lipids in response to hydrogen and nutrient availability. *Frontiers in Microbiology* **6**, 5. DOI: 10.3389/fmicb.2015.00005.

YOSHINAGA, M. Y., T. HOLLER, T. GOLDHAMMER, G. WEGENER, J. W. POHLMAN, B. BRUNNER, M. M. M. KUYPERS, K.-U. HINRICHS, and M. ELVERT (2014). Carbon isotope equilibration during sulphate-limited anaerobic oxidation of methane. *Nature Geoscience* **7** (3), 190–194. DOI: 10.1038/ngeo2069.

YOSHINAGA, M. Y., M. Y. KELLERMANN, P. E. ROSSEL, F. SCHUBOTZ, J. S. LIPP, and K.-U. HINRICHS (2011). Systematic fragmentation patterns of archaeal intact polar lipids by high-performance liquid chromatography/electrospray ionization ion-trap mass spectrometry. *Rapid communications in mass spectrometry* **25** (23), 3563–3574. DOI: 10.1002/rcm.5251.

ZABEL, M. and CRUISE PARTICIPANTS (2011). *RV METEOR, Cruise Report M84/L1, Biogeochemistry and methane hydrates of the Black Sea; Oceanography of the Mediterranean; Shelf sedimentation and cold water carbonates*. DFG Senatskommission für Ozeanographie. DOI: 10.2312/cr_m84_1.

ZABEL, M., A. BOETIUS, K.-C. EMEIS, T. G. FERDELMAN, and V. SPIESS (2008). *Cruise Report M76/L1, M76/L2, M76/L3a+b, PROSA Process studies in the eastern South Atlantic*. DFG Senatskommission für Ozeanographie. DOI: 10.2312/cr_m76.

ZACHOS, J. C., G. R. DICKENS, and R. E. ZEEBE (2008). An early Cenozoic perspective on greenhouse warming and carbon-cycle dynamics. *Nature* **451** (7176), 279–283. DOI: 10.1038/nature06588.

ZEHR, J. P. and R. M. KUDELA (2011). Nitrogen cycle of the open ocean: from genes to ecosystems. *Annual Review of Marine Science* **3**, 197–225. DOI: 10.1146/annurev-marine-120709-142819.

ZEHR, J. P. (2011). Nitrogen fixation by marine cyanobacteria. *Trends in Microbiology* **19** (4), 162–173. DOI: 10.1016/j.tim.2010.12.004.

ZEIKUS, J. G. (1977). The Biology of Methanogenic Bacteria. *Bacteriological Reviews* **41** (2), 514–541.

ZHAI, Y., P. LEE-GAU CHONG, L. J. A. TAYLOR, M. ERLKAMP, S. GROBELNY, C. CZESLIK, E. WATKINS, and R. WINTER (2012). Physical properties of archaeal tetraether lipid membranes as revealed by differential scanning and pressure perturbation calorimetry, molecular acoustics, and neutron reflectometry: Effects of pressure and cell growth temperature. *Langmuir* **28**, 5211–5217. DOI: 10.1021/la300142r.

ZHANG, C. L., A. PEARSON, Y.-L. LI, G. MILLS, and J. WIEGEL (2006). Thermophilic temperature optimum for crenarchaeol synthesis and its implication for archaeal evolution. *Applied and Environmental Microbiology* **72** (6), 4419–4422. DOI: 10.1128/AEM.00191-06.

ZHANG, C. L., Q. YE, Z. HUANG, W. LI, J. CHEN, Z. SONG, W. ZHAO, C. BAGWELL, W. P. INSKEEP, C. ROSS, L. GAO, J. WIEGEL, C. S. ROMANEK, E. L. SHOCK, and B. P. HEDLUND (2008). Global occurrence of archaeal *amoA* genes in terrestrial hot springs. *Applied and Environmental Microbiology* **74** (20), 6417–6426. DOI: 10.1128/AEM.00843-08.

ZHI, X.-Y. Y., J.-C. C. YAO, S.-K. K. TANG, Y. HUANG, H.-W. W. LI, and W.-J. J. LI (2014). The futalosine pathway played an important role in menaquinone biosynthesis during early prokaryote evolution. *Genome Biology and Evolution* **6** (1), 149–160. DOI: 10.1093/gbe/evu007.

ZHU, C., J. S. LIPP, L. WÖRMER, K. W. BECKER, J. SCHRÖDER, and K.-U. HINRICHS (2013). Comprehensive glycerol ether lipid fingerprints through a novel reversed phase liquid

chromatography-mass spectrometry protocol. *Organic Geochemistry* **65**, 53–62. DOI: 10.1016/j.orggeochem.2013.09.012.

ZHU, C., T. B. MEADOR, W. DUMMANN, and K.-U. HINRICHS (2014a). Identification of unusual butanetriol dialkyl glycerol tetraether and pentanetriol dialkyl glycerol tetraether lipids in marine sediments. *Rapid Communications in Mass Spectrometry* **28** (4), 332–338. DOI: 10.1002/rcm.6792.

ZHU, C., M. Y. YOSHINAGA, C. A. PETERS, X.-L. LIU, M. ELVERT, and K.-U. HINRICHS (2014b). Identification and significance of unsaturated archaeal tetraether lipids in marine sediments. *Rapid Communications in Mass Spectrometry* **28** (10), 1144–1152. DOI: 10.1002/rcm.6887.

ZINK, K.-G., K. MANGELSDORF, L. GRANINA, and B. HORSFIELD (2008). Estimation of bacterial biomass in subsurface sediments by quantifying intact membrane phospholipids. *Analytical and Bioanalytical Chemistry* **390** (3), 885–896. DOI: 10.1007/s00216-007-1732-y.

N a m e : ..... Datum .....

Anschrift : .....

E r k l ä r u n g

Hiermit versichere ich, dass ich

1. die Arbeit ohne unerlaubte fremde Hilfe angefertigt habe,
2. keine anderen als die von mir angegebenen Quellen und Hilfsmittel benutzt habe und
3. die den benutzten Werken wörtlich oder inhaltlich entnommenen Stellen als solche kenntlich gemacht habe.

_____, den .....

(Unterschrift)